TD

Nanotechnology Approaches for the Delivery of Antitumor Drugs
The case of doxorubicin

DOCTORAL THESIS

Mara Isabel Jesus Gonçalves
DOCTORATE IN CHEMISTRY
SPECIALTY IN MATERIALS CHEMISTRY

UNIVERSIDADE da MADEIRA
A Nossa Universidade
www.uma.pt

March | 2018

Nanotechnology Approaches for the Delivery of Antitumor Drugs

The case of doxorubicin

DOCTORAL THESIS

Mara Isabel Jesus Gonçalves
DOCTORATE IN CHEMISTRY
SPECIALTY IN MATERIALS CHEMISTRY

SUPERVISOR
Helena Maria Pires Gaspar Tomás

CO-SUPERVISOR
João Manuel Cunha Rodrigues
Yulin Li

Acknowledgments

This thesis represents a set of results achieved over several years of work and obstacles. All this work was only possible due to the contribution of several people, who during this journey stayed always on my side to support me, in the good and also in the bad moments.

First of all, I would like to express my sincere gratitude to my supervisor Prof. Helena Tomás for all the support and encouragement during my Ph.D study and related research. Her patience, motivation and knowledge were essential during the period of research and at the time of writing the thesis. Her immense guidance helped me to grow as a researcher and also as a person.

Besides my supervisor, I would like to thank my co-supervisor Prof. João Rodrigues for providing me the opportunity to join his team, and for all the knowledge and constructive observations to pursue this research field.

I would like to express my appreciation to my co-supervisor Prof. Yulin Li, for giving me the opportunity to work in such interesting area, and also for providing all the knowledge in the polymer field.

My sincere thanks to all the members of the Molecular Materials Research Group who directly or indirectly contributed to this thesis. A special thanks to my fellow labmates for all the stimulating discussions, for working together as a group and for all the fun during the last years. A very special gratitude goes out to all the persons who were always present for helping and supporting me all these years. My dear friends, Alireza Nouri, Cláudia Camacho, Carla Alves, Dina Maciel, João Figueira, Luís Santos, Manuel Jardim and Nilsa Oliveira, I owe you all a deep and sincere thank you for all the strength and for the amusing moments.

I wish to express a special mention to Dina Maciel and Nilsa Oliveira who introduced me to the synthesis field.

A real special thanks to my friend Rita Castro who was always there to support me. Her endless patience, friendship, and encouragement were crucial for the achievement of this goal.

A special gratitude to my friend Carla Alves for her readiness and immense support. Her concern and friendship were essential to accomplish this long pursue.

Moreover, I would also like to thank the technician staff (Paula Andrade and Paula Vieira) from the Chemistry Department of the *Universidade da Madeira* (UMa) for their help and assistance.

I am also grateful to all the institutions or entities that provided the funding and the laboratory facilities to support and conduct this research.

To the *Fundação para a Ciência e Tecnologia (FCT), I.P.*, for the Ph.D. scholarship (ref. SFRH/BD/88721/2012), the CQM Strategic Project UID/QUI/00674/2013 (Portuguese Government Funds), the NMR Network PTNMR-2015/2016 and the research project PTDC/CTM-NAN/116788/2010. The project *PROEQUIPRAM – Reforço do Investimento em Equipamentos e Infraestruturas Científicas na RAM* (M1420-01-0145-FEDER-000008) and *Centro de Química da Madeira – CQM+* (M1420-01-0145-FEDER-000005, ARDITI), funded by Madeira Regional Operational Programme (Madeira 1420), are also acknowledged.

Last but not the least, I would like to thank my family: my parents for all the unconditional love, endless support, and concern. Their strength and tough work were crucial to achieve this goal. To my brother, for the affection, enthusiasm and for all the relaxed moments. To my love, João Brito, for the endless patience, concern, and affect. His extraordinary humour and unconditional support were essential during the last years.

Abstract

Over the years, nanotechnology had a huge evolution and gathered the attention of many scientists, including those involved in medical sciences. Nanomedicine thus appeared, trying to overcome obstacles that still exist in conventional medicine, by providing innovative approaches for the diagnosis and treatment of diseases.

Nowadays, cancer is considered one of the major causes of worldwide death. Doxorubicin (DOX) is a chemotherapeutic drug which is routinely used for cancer treatment. Due to its broad spectrum of activity, DOX is used as a first-line treatment combined with other drugs and procedures. However, this drug has several associated side effects, being the injury of the cardiac muscle tissue and myelosuppression the most reported. Cancer nanomedicine stands up as an alternative to conventional cancer therapy by using nanomaterials as drug carriers which, potentially, make the treatment more efficient and safe. Polymer-based nanomaterials are very promising vehicles for drug delivery, due to the easiness in modelling their properties. Over the years, polymers have proven to be capable of encapsulating and releasing drugs in a sustained manner, improving their biodistribution and accumulation in tumours.

The main goal of this thesis was to find new drug delivery systems that could be able to encapsulate DOX and successfully deliver it inside cancer cells. Hopefully, using nanomaterials for DOX delivery, it will be possible to overcome the side effects which are frequently associated to this antitumor drug.

Thesis Content

- Chapter I provides an overview over DOX-based nanotherapeutics, from the ones which are still under study in the laboratory, to those that are commercially available. Furthermore, the science underneath these nanotherapeutics are explored and the state of art on DOX-based clinical trials is presented.

- Chapter II and III report the synthesis, characterization and biological evaluation of two different hydrogel systems as DOX delivery vehicles. Indeed, one important problem in cancer treatment using DOX is its low uptake by cells due to ion-trapping in the acidic extracellular environment of solid tumours. Also because of this effect, once inside cells, DOX can be retained in the endo-lysosomal cell compartments. Having these in mind, new systems based on a clay mineral (Laponite®) and alginate were developed for DOX delivery. Laponite® is a synthetic clay mineral with

disk shape that has a high tendency to adsorb host molecules. Furthermore, it is biocompatible, presenting a negative charge in the faces and a pH-sensitive charge in the edge surface. Alginate is a natural polymer, more specifically, an anionic polysaccharide. This polymer is non-toxic, biocompatible and biodegradable. In addition, alginate is known for its easy gelation process, which is usually achieved by the presence of divalent cations. So, in Chapter II, macroscopic hybrid hydrogels based on Laponite® and alginate were prepared which were designed to suffer *in situ* degradation giving rise to nanohybrid vehicles that were very efficient in carrying DOX through the cell membrane. In Chapter III, materials also based on Laponite® and alginate were specifically developed at the nanoscale that were also capable of carrying a high load of DOX across the cell membrane. In addition, the results suggested that these nanohybrids can use the acidic environment of the endolysosomes to release the drug, while helping to break down these organelles and thereby avoid DOX ion-trapping.

- Finally, in Chapter IV, a new dendrimer family was studied for the cellular delivery of doxorubicin. Over the years, dendrimers have been widely exploited for biomedical applications. Their well-defined architecture, monodispersity, and multivalency are attractive characteristics which make them almost perfect drug nanocarrier candidates. 2,2-bis(hydroxymethyl)propionic acid (bis-MPA)-based dendrimers are biodegradable, biocompatible, and present a high water solubility. Due to these features, bis-MPA dendrimers are very interesting materials to be used in the biomedical field. In this chapter, bis-MPA dendrimers were evaluated as DOX nanocarriers. Their capability to encapsulate and release DOX was studied and compared with that of poly(amidoamine) (PAMAM) dendrimers which are non-biodegradable.

In summary, three different types of DOX delivery systems were studied. These materials were shown to be suitable platforms for drug delivery, presenting high drug encapsulation efficiencies, a sustainable drug release and, finally, a high biocompatibility.

Key-words: Doxorubicin; Alginate; Laponite®; Nanogels; Dendrimers; Drug delivery.

Resumo

Ao longo dos anos, a área da nanotecnologia passou por uma grande evolução, atraindo a atenção de muitos cientistas, incluindo os relacionados com as ciências médicas. Surgiu assim a nanomedicina que tenta ultrapassar os obstáculos ainda existentes na medicina convencional ao fornecer abordagens inovadoras para o diagnóstico e tratamento de doenças.

Atualmente, o cancro é considerado uma das principais causas de morte a nível mundial. A doxorubicina (DOX) é um fármaco antitumoral que é frequentemente utilizado para o tratamento do cancro. Devido ao seu amplo espectro de ação, a doxorubicina é usada como tratamento de primeira linha combinada com outros fármacos ou procedimentos. No entanto, este fármaco tem sido associado a diversos efeitos secundários, sendo os mais reportados a lesão ao nível do tecido muscular cardíaco e a mielosupressão. Na área do cancro, entre outras vantagens, a nanomedicina pode conferir aos fármacos tradicionais (já em uso) elevados níveis de eficácia e segurança ao usar nanomateriais como veículos para o seu transporte. Os nanomateriais constituídos à base de polímeros são veículos muito promissores para a entrega de fármacos, devido à facilidade em modular as suas propriedades. Ao longo dos anos, os polímeros demonstraram ser capazes de encapsular e libertar os fármacos de uma forma sustentada, melhorando assim a sua biodistribuição e acumulação nos tumores.

O objetivo principal desta tese foi desenvolver novos nano-sistemas de entrega de fármacos que fossem capazes de encapsular a doxorubicina e de a libertar com sucesso dentro das células cancerígenas. Desejavelmente, usando nanomateriais para entrega de DOX, será possível superar os efeitos colaterais que frequentemente estão associados a este fármaco.

Conteúdo da Tese

- O Capítulo I apresenta uma visão geral sobre os nanomateriais que atualmente são explorados para a entrega de doxorubicina, desde os que se encontram em estudo no laboratório, até aqueles que já estão comercialmente disponíveis. Adicionalmente, é abordada a ciência subjacente a estes nanomateriais e é feito o ponto da situação relativamente aos ensaios clínicos em curso.

- Os Capítulos II e III relatam a síntese, caracterização e avaliação biológica de dois sistemas diferentes à base de um hidrogel como veículos de entrega de DOX. De facto, um problema importante no tratamento do cancro usando a DOX é a sua baixa internalização celular devido à sua retenção no ambiente extracelular ácido (“ion-trapping”) apresentado pelos tumores sólidos. Também por causa desse efeito, uma vez dentro das células, a DOX pode ser retida nos endolisossomas. Tendo isto em

mente, foram desenvolvidos novos sistemas baseados em Laponite® e alginato para a entrega de DOX. A Laponite® é uma argila sintética com formato de disco que tem uma alta tendência a adsorver moléculas. Além disso, é biocompatível, apresentando uma carga negativa nas faces e uma carga sensível ao pH na borda. O alginato é um polímero natural, mais especificamente, um polissacárido aniónico. Este polímero não é tóxico, e é biocompatível e biodegradável. Além disso, o alginato é conhecido pelo seu fácil processo de gelificação, que geralmente é obtido na presença de catiões divalentes. Assim, no Capítulo II, foram preparados hidrogéis híbridos macroscópicos baseados em Laponite® e alginato com capacidade para sofrer degradação *in situ*, dando origem a nanohíbridos que foram muito eficientes em transportar DOX através da membrana celular. No Capítulo III, foram desenvolvidos materiais também baseados em Laponite® e alginato, desta vez especificamente à nano-escala, os quais também mostraram ser capazes de transportar uma alta carga de DOX através da membrana celular. Além disso, os resultados sugerem que estes nano-híbridos podem usar o ambiente ácido dos endolisossomas para libertar o fármaco, ajudando simultaneamente a romper estes organelos e, assim, aí evitando o aprisionamento da DOX.

- Por fim, no capítulo IV, foi estudada uma nova família de dendrímeros para a entrega de DOX em células cancerígenas. Ao longo dos anos, os dendrímeros têm sido muito estudados para aplicações biomédicas. A sua arquitetura bem definida, monodispersividade e multivalência são características atrativas que os tornam candidatos perfeitos para entrega de fármacos. Os dendrímeros constituídos com base no ácido 2,2-bis(hidroximetil) propiónico (bis-MPA) são biodegradáveis, biocompatíveis e apresentam elevada solubilidade em água. Devido a estas propriedades, os dendrímeros bis-MPA são materiais muito interessantes para serem usados na área biomédica. Neste capítulo, os dendrímeros bis-MPA foram avaliados como transportadores de DOX. A sua capacidade para encapsular e libertar o fármaco foi estudada e comparada com a dos dendrímeros de poli(amidoamine) (PAMAM) que são não-biodegradáveis.

Em suma, foram estudados três tipos diferentes de sistemas para a entrega de DOX. Estes materiais mostraram ser plataformas adequadas para a entrega do fármaco, apresentando uma elevada eficiência de encapsulamento, uma libertação de fármaco controlada e uma elevada biocompatibilidade.

Palavras-Chaves: Doxorubicina; Alginato; Laponite®; Nanogéis; Dendrímeros; Entrega de fármacos.

Abbreviations

3D	Three-dimensional
A2780	Ovarian cancer cell line
A549	Lung cancer cell line
AA	Antibiotic/antimycotic
AG	Alginate
AgNPs	Silver nanoparticles
AR	Aspect ratio
ASP	Polyaspartic acid
AuNPs	Gold nanoparticles
BBB	Blood-brain barrier
Bis-MPA	2,2-bis(hydroxymethyl)propionic acid
BOC-Gly-OH	N-(tert-Butoxycarbonyl) glycine
CAL-72	Osteosarcoma cancer cell line
CMC	Critical micelle concentration
CNS	Central nervous system
CNTs	Carbon nanotubes
CPP	Cyclophosphamide
CT	Computed Tomography
DAPI	4’,6-diamidino-2-phenylindole
DCC	N, N'-dicyclohexylcarbodiimide
DCM	Dichloromethane
DLS	Dynamic light scattering
DLTs	Dose-limiting toxicities
DMAP	4-(Dimethylamino)pyridine
DMF	Dimethylformamide
DNA	Deoxyribonucleic acid
DOX	Doxorubicin
DOX.HCl	Doxorubicin hydrochloride salt
DPPC	1,2-dihexadecanoyl-sn-glycero-3-phosphocholine
DPTS	4-(dimethylamino) pyridinium 4-toluene sulfonate
DSMB	Data and Safety Monitoring Board
DSPE	1,2-distearoyl-sn-glycero-3-phosphoethanolamine
EE	Encapsulation efficiency
EGFR	Epidermal growth factor receptor
EMA	European Medicines Agency
EPR	Enhanced Permeation and Retention
ESF	European Science Foundation
EtOAc	Ethyl acetate
FBS	Fetal bovine serum
FDA	Food and Drug Administration
GBM	Glioblastoma multiform
GSH	Glutathione
HCC	Hepatocellular carcinoma
HER-2	Human epidermal growth factor receptor-2
HL-60	Promyelocytic leukaemia cancer cell line
hMSCs	Human mesenchymal stem cells
HPMA	N-(2-hydroxypropyl) methacrylamide
HSPC	Hydrogenated soy phosphatidylcholine
I.V.	Intravenous

ILs	Immunoliposomes
ITS	Insulin-transferrin-selenium
L.C.	Loading capacity
L.E.	Loading efficiency
LP	Laponite®
LPS	Lipopolysaccharide
LTSL	Low temperature-sensitive liposomes
mAb	Monoclonal antibody fragments
MB	Methylene blue
MCF-7	Breast cancer cell line
MDA-MB-468	Breast cancer cell line
MRI	Magnetic Resonance Imaging
MTD	Maximum-tolerated dose
MW	Molecular weight
NCI	American National Cancer Institute
NEAA	Nonessential amino acids
NHL	Non-Hodgkin's lymphoma
NMR	Nuclear Magnetic Resonance Spectroscopy
NPs	Nanoparticles
NSCLC	Non-small cell lung cancer
OS	Overall survival
PAMAM	Poly(amidoamine)
PBS	Phosphate-buffered saline solution
PC	Phosphatidylcholine
PEG	Polyethylene glycol
PEO	Poly(ethylene oxide)
PFS	Progression-free survival
PIHCA	Polyisohexylcyanoacrylate
PLGA	Poly(lactic-co-glycolic acid)
PPO	Poly(propylene oxide)
PTSA	p-Toluenesulfonic acid monohydrate
PVA	Polyvinyl alcohol
RFA	Radiofrequency ablation
RNA	Ribonucleic acid
ROS	Reactive oxygen species
RT	Room temperature
scFv	Single-chain antibody fragment
SKOV-3	Ovarian cancer cell line
SLNs	Solid-lipid nanoparticles
STS	Soft tissue sarcoma
TE	Trypsin-ethylenediaminetetraacetic acid solution
TEA	Triethylamine
TEM	Transmission electron microscopy
THF	Tetrahydrofuran
Tm	Phase transition temperature
TNBS	2,4,6-trinitrobenzenesulfonic acid
TOP2	Topoisomerase II enzyme
U87MG	Glioblastoma cell line
UV-Vis	Ultraviolet-visible
V	Vectibix

Table of contents

List of figures

List of tables

Short *curriculum vitae*

Mara Gonçalves was born in 1988, in Funchal, Portugal. She got her graduation in Biomedical Sciences at *Universidade da Beira Interior* (UBI) in 2009. She continued the studies in UBI developing her master thesis in collaboration with the Materials Molecular Research Group – Centro de Química da Madeira (MMRG-CQM), under the supervision of Helena Tomás (Ph.D.) at the *Universidade da Madeira* (UMa). The purpose of the work was to evaluate the effect of dendrimers on mesenchymal stem cells differentiation, thereby obtaining, in 2011, the Master degree in Biomedical Sciences. This investigation led to a publication in an international journal, as well as a poster presentation. In 2012, she was awarded with a Ph.D. research grant by *Fundação para a Ciência e Tecnologia* (FCT) and, since then, she is a Ph.D. student at UMa, developing the experimental work at CQM. Her Ph.D. work was done under the supervision of Helena Tomás (Ph.D.) and co-supervision of Yulin Li (Ph.D.) and João Rodrigues (Ph.D). During the Ph.D. period, she participated in several advanced courses and scientific meetings. She has also contributed for several research projects and activities developed at CQM and UMa that are described in more detail below.

As a result of her scientific activity, she is author/co-author of 1 Thesis and 10 papers in international peer-reviewed journals (8 published and 2 still in preparation). Also, her work resulted in 16 oral communications (4 international and 12 in CQM meetings) and 9 posters presentations (all international) in scientific meetings.

PARTICIPATION IN RESEARCH PROJECTS

Project SELF-ASSEMBLED NANOPARTICLES BASED ON PEG-PLA-DENDRIMER BUILDING BLOCKS FOR DUAL GENE/DRUG DELIVERY (Ref. PTDC/CTM-NAN/116788/2010). Research grant (BI-Master) in the period April **2012**- September **2013**.

PARTICIPATION IN ADVANCED COURSES

- ✓ Gordon Research Conference on Cancer Nanotechnology. Mount Snow in West Dover, VT, United States of America: June 18-23, **2017**.
- ✓ Nanoschool 2016: "Principles and Applications of Fluorescence Spectroscopy" (8h, October **2016**). Lecturer: Prof. Fernando Lahoz, University of La Laguna (Spain).
- ✓ Nanoschool 2015: "Bionanotechnology: From Bio to Nano & From Nano to Bio" (8h, October **2015**). Lecturer: Prof. Hiroshi Matsui, City University of New York (USA).

- ✓ Nanoschool 2014: "Nanomedicines: Considerations for Design and Transfer into Clinical Use" (8h, October **2014**). Lecturer: Prof. Ruth Duncan, Cardiff University (UK).
- ✓ Nanoschool 2013: “Nanomedicines: the Next Generation of Pharmaceuticals” (8h, October **2013**). Lecturer: Prof. Serge Mignani, University of Paris Descartes (France).
- ✓ Nanoschool 2012: “Design, synthesis and biofunctionalization of magnetic nanoparticles: current and prospective *in vivo* applications” (8h, October **2012**). Lecturer: Prof. Etienne Duguet, University of Bordeaux (France).
- ✓ Nanoschool 2010: “Inorganic nanoparticles: from synthesis to applications” (8h, October **2010**). Lecturer: Prof. Mathias Epple, University of Duisburg-Essen (Germany).

OTHER COURSES

- ✓ "Introdução à Gestão de Resíduos Perigosos": 19 of January 2016.
- ✓ "Science Communication Short Course": 17 and 18 of April 2015 – Hernani Zão (CQM).
- ✓ Level 1 Competency on IZON's Tunable Resistive Pulse Sensing (TRPS) System – 2nd April 2013 Certified by Dr. Rebecca Warr, IZON Science Limited.
- ✓ 2nd NMR Course – PTNMR – “Short Theoretical and Practical Introduction in the NMR Technique” – 13 and 14 of December 2012 – João Figueira (CQM).
- ✓ 1st Course on “Fundamentals and Applications of Electrospinning Technology” – 15 of June 2012 – Shili Xiao (CQM).
- ✓ 2nd MS Course “Introduction to the Fundamentals of Mass Spectrometry and Basic Training on Electrospray Ion Trap Multistage Mass Spectrometer”: 11 and 12 of November 2011.
- ✓ 1st MS Course “Basic Training on Operation of an Electrospray Ion Trap Multistage Mass Spectrometer”: 21 and 22 February 2011.
- ✓ "LC-MS techniques: fundamentals and applications": 4 and 5 of November 2010.

PUBLICATIONS

Master Thesis

Gonçalves M. Avaliação do efeito de dendrímeros com diferentes grupos funcionais à superfície na diferenciação de células estaminais mesenquimais. Master Thesis. Covilhã, Universidade da Beira Interior, **2012**.

Papers in international scientific periodicals with referees

1. Gonçalves M, Mignani S, Rodrigues J, Tomás H. A glance over doxorubicin based-nanotherapeutics: from proof-of-concept studies to solutions in the market (in preparation).

2. Gonçalves M, Rodrigues J, Tomás H. Polyester dendrimers based on bis-MPA for doxorubicin delivery (in preparation).
3. Zhan Y, Gonçalves M, Yi P, Capelo D, Zhang Y, Rodrigues J, Liu C, Tomás H, Li Y, He P. Thermo/Redox/pH-stimulative Nanogel Delivery Systems. *Nanomedicine: Nanotechnology, Biology, and Medicine*. **2016**; 12:567.
4. Gonçalves M, Olival A, Rodrigues J, Li Y, Tomás H. Polyester Dendrimers for Dual Gene and Drug Delivery – Preliminary Results. *Journal of Materials Nanoscience*. **2016**; 3:S7-S8.
5. Xiao S, Castro R, Maciel D, Gonçalves M, Shi X, Rodrigues J, Tomás H. Fine tuning of the pH-sensitivity of laponite-doxorubicin nanohybrids by polyelectrolyte multilayer coating. *Materials Science and Engineering C*. **2016**; 60:348-356.
6. Zhan Y*, Gonçalves M*, Yi P, Capelo D, Zhang Y, Rodrigues J, Liu C, Tomás H, Li Y, He P. Thermo/redox/pH- triple sensitive Poly(N-isopropylacrylamide-co-acrylic acid) Nanogels for Anticancer Drug Delivery. *Journal of Materials Chemistry B*. **2015**; 3:4221-4230. (*Equal contribution)
7. Gonçalves M*, Maciel D*, Capelo D, Xiao S, Sun W, Shi X, Rodrigues J, Tomás H, Li Y. Dendrimer-Assisted Formation of Fluorescent Nanogels for Drug Delivery and Intracellular Tracking Imaging. *Biomacromolecules*. **2014**; 15:492-499. (*Equal contribution)
8. Gonçalves M, Figueira P, Maciel D, Rodrigues J, Qu X, Liu C, Tomás H, Li Y. pH Sensitive Laponite®/Doxorubicin/Alginate Nanohybrids With Improved Anticancer Efficacy. *Acta Biomaterialia*. **2014**; 10:300-307.
9. Gonçalves M, Figueira P, Maciel D, Rodrigues J, Shi X, Tomás H, Li Y. Antitumor Efficacy of Doxorubicin-loaded Laponite/Alginate Hybrid Hydrogels. *Macromolecular. Bioscience*. **2014**; 14:110-20.
10. Gonçalves M, Castro R, Rodrigues J, Tomás H. The Effect of PAMAM Dendrimers on Mesenchymal Stem Cell Viability and Differentiation. *Current Medicinal Chemistry*. **2012**; 19:4969-4975.

ORAL COMMUNICATIONS IN INTERNATIONAL MEETINGS

1. Gonçalves M, Rodrigues J, Li Y, Tomás H. Laponite®/alginate based materials: evaluation of two different strategies for doxorubicin delivery. Madeira International Conference on Emerging Trends and Future of Nanomaterials for Human Health - MAD-NANO16. Funchal, Portugal: November 17-20, **2016**.
2. Gonçalves M, Figueira P, Maciel D, Rodrigues J,Qu X, Liu C, Tomás H, Li Y; Doxorubicin Loaded pH-sensitive Laponite/Alginate Nanohybrids: a Sustainable Release with Improved Anticancer Efficiency; 1st International Conference on Emerging Trends of Nanotechnology in Drug Discovery - INDD-2014. New Delhi, India: May 26-27, **2014** (invited speaker).

3. Li Y, Gonçalves M, Figueira P, Maciel D, Rodrigues J, Shi X, Tomás H. pH Sensitive Laponite/Doxorubicin/Alginate Nanohybrids With Improved Anticancer Efficacy; International Conference on Nanoparticles and Nanotechnologies in Medicine. Milan, Italy: June 19-21, **2013**.
4. Li Y, Gonçalves M, Figueira P, Maciel D, Rodrigues J, Tomás H. pH Sensitive Laponite/Alginate Nanogels for Release of Doxorubicin; International Symposium on Nanomaterials and Nanodevices. Suzhou, China: September 5-12, **2012**.

ORAL COMMUNICATIONS IN CQM MEETINGS

1. Gonçalves M, Rodrigues J, Tomás H. Doxorubicin nanoformulations overview: from bench to bedside. 5th CQM Annual Meeting. Funchal, Portugal: February 01-03, **2018**.
2. Gonçalves M, Rodrigues J, Li Y, Tomás H. Dendritic systems as delivery vehicles for doxorubicin: poly(amidoamine) vs polyester dendrimers. 4th CQM Annual Meeting. Funchal, Portugal: February 03 & 04, **2017**.
3. Gonçalves M, Rodrigues J, Li Y, Tomás H. Biodegradable Amine-modified Dendrimers as Drug/Gene Nanocarriers – Preliminary Results. 3rd CQM Annual Meeting. Funchal, Portugal: April 1 & 2, **2016**.
4. Gonçalves M, Rodrigues J, Tomás H, Li Y. Self-Assembled Nanoparticles for Dual Gene and Drug Delivery. 2nd CQM Annual Meeting. Funchal, Portugal: January 30 & 31, **2015**.
5. Alves CS, Gonçalves M, Tomás H, Rodrigues J, Li Y, Shi X. Dendrimers in Bioimaging and Therapeutics. 2nd CQM Annual Meeting. Funchal, Portugal: January 30 & 31, **2015.**
6. Maciel D, Gonçalves M, Alves CS, Rodrigues J, Shi X, Tomás H, Li Y. Multi-Responsive Nanogels for Anticancer Drug Delivery. 2nd CQM Annual Meeting. Funchal, Portugal: January 30 & 31, **2015.**
7. Gonçalves M, Maciel D, Capelo D, Sun W, Shi X, Rodrigues J, Tomás H, Li Y. Dendrimer-Assisted Formation of Self-Fluorescent Nanogels for Simultaneous Drug Delivery and Intracellular Tracking Imaging. 1st CQM Annual Meeting & 9th Materials Line Meeting. Funchal, Portugal: January 31 & February 1, **2014**.
8. Maciel D, Gonçalves M, Rodrigues J, Tomás H, Li Y. Alginate/Laponite Hybrid Nanogels for Anticancer Drug Delivery. 1st CQM Annual Meeting & 9th Materials Line Meeting. Funchal, Portugal: January 31 & February 1, **2014**.
9. Gonçalves M, Figueira P, Maciel D, Rodrigues J, Tomás H, Li Y. pH Sensitive Laponite/Alginate nanohybrids with improved anticancer efficacy. 8th Materials Line Meeting. Funchal, Portugal: January 25, **2013**.
10. Alves CS, Gonçalves M, Castro R, Rodrigues J, Tomás H, Li Y. Dendrimer/Gold Nanoparticles for Gene Delivery. 8th Materials Line Meeting. Funchal, Portugal: January 25, **2013.**

11. Maciel D, Gonçalves M, Rodrigues J, Tomás H, Li Y. pH Sensitive HaP/PEI/AG Nanocarriers for Controlled Delivery of Anticancer Drugs. 8th Materials Line Meeting. Funchal, Portugal: January 25, **2013.**
12. Gonçalves M, Castro R, Shi X, Rodrigues J, Tomás H. Evaluation of the effect of dendrimers with different surface functionalities on the differentiation of Mesenchymal Stem Cells. 6th Materials Line Meeting. Funchal, Portugal: January 28, **2011**.

POSTER COMMUNICATIONS IN INTERNATIONAL SCIENTIFIC MEETINGS

1. Gonçalves M, Rodrigues J, Li Y, Tomás H. Poly(amidoamine) vs bis-MPA Dendrimers: A comparative Study for Doxorubicin Encapsulation. Gordon Research Center on Cancer Nanotechnology. Mount Snow in West Dover, VT, United States of America: June 18-23, **2017**.
2. Gonçalves M, Olival A, Rodrigues J, Li Y, Tomás H. Polyester Dendrimers for Dual Gene and Drug Delivery - Preliminary Results. Indo-Portuguese Workshop on Emerging Trends of Nanotechnology in Chemistry and Biology – INCB-2016. New Delhi, India: February 12-13, **2016**.
3. Zhan Y, Gonçalves M, Yi P, Capelo D, Zhang Y, Rodrigues J, Liu C, Tomás H, Li Y, He P. Thermo/Redox/pH-stimulative Nanogel Delivery Systems. International Conference on Nanomedicine and NanoBiotechnology - ChinaNanomedicine 2015. Hangzhou, China: April 6-9, **2015**.
4. Gonçalves M, Maciel D, Capelo D, Xiao S, Sun W, Shi X, Rodrigues J, Tomás H, Li Y. Poly(amidoamine) dendrimer-mediated nanogels for drug delivery and intracellular tracking. 1st International Conference on Emerging Trends of Nanotechnology in Drug Discovery - INDD-2014. New Delhi, India: May 26-27, **2014**.
5. Gonçalves M, Maciel D, Xiao S, Shi X, Rodrigues J, Tomás H, Li Y. Dendrimer-Assisted Formation Of Self-Fluorescent Nanogels For Simultaneous Drug Delivery and Intracellular Tracking Imaging. Chinese Medicinal Chemistry Symposium (CMCS). Jinan Shandong, China: November 01-03, **2013**.
6. Maciel D, Gonçalves M, Alves CS, Shi X, Rodrigues J, Tomás H, Li Y. Triple Cell-Responsive Nanogels For Drug Delivery Into Cancer Cells. Chinese Pharmaceutical Conference. Wuhan, China: October 26-27, **2013**.
7. Castro R, Santos JL, Gonçalves M, Rodrigues J, Tomás H. Fatty-acid Functionalized PAMAM Dendrimers for Gene Silencing. 8th International Dendrimer Symposium. Madrid, Spain: June 23-27, **2013**.
8. Gonçalves M, Castro R, Rodrigues J, Tomás H. PAMAM Dendrimers do Not Affect Mesenchymal Stem Cells Differentiation. 8th International Dendrimer Symposium. Madrid, Spain: June 23-27, **2013** (with Flash Presentation).

9. Gonçalves M, Castro R, Rodrigues J, Tomás H. Effect of PAMAM Dendrimers with Different Surface Functionalities on Mesenchymal Stem Cells Differentiation. 7th International Meeting of the Portuguese Society for Stem Cells & Cell Therapies. Porto, Portugal: April 26-27, **2012**.

OTHER ACTIVITIES

- ✓ Participation in several science dissemination activities carried out in the scope of CQM, of which should be highlighted *A Química é Divertida* ("Chemistry is fun"). Collaborator in the period **2010-2016**.
- ✓ Member of the Organizing Committee of MAD-Nano16: Madeira International conference on Emerging Trends and Future of Nanomaterials for Human Health, Funchal, Madeira Island, Portugal (17 - 20 November **2016**).

Chapter I.

A Glance Over Doxorubicin Based-Nanotherapeutics: from proof-of-concept studies to solutions in the market

Abstract

Cancer is one of the leading causes of death worldwide and, as such, efforts are being done to find new chemotherapeutic drugs or novel approaches for the delivery of old ones. Doxorubicin (DOX) is one of the most commonly used chemotherapeutic drugs as first-line treatment. This drug is used for a variety of cancer types due to its broad spectrum of activity. However, DOX use presents a few drawbacks, being cardiovascular toxicity and dose-dependent myelosuppression the most relevant. To help overcoming these issues, over time, several DOX-based nanotherapeutics appear, some of which are already being used in the clinical scenario. In fact, it is recognized that nanomedicine may present advantages over the conventional administration of drugs, that is, the use of the chemotherapeutic agents alone. The focus of this review is to give an overview over DOX-based nanotherapeutics, from the ones that are still under study in the laboratory, to those existent in the market, thus contributing for a better understanding of the underneath nanoscience. Furthermore, a state of art of DOX-based clinical trials and commercially available products will be presented.

1. Introduction

The problem of cancer is continuously increasing and quickly becoming a global epidemic mostly due to population ageing, environmental problems and adopted lifestyle. According to estimates of the World Health Organization, in 2012 there was about 14 million new cancer cases and 8.8 million cancer deaths occurred in 2015.[1] The American National Cancer Institute (NCI) defines cancer as being a collection of related diseases.[2] In all cancer types, cells start to divide indefinitely and may spread to other organs. The cancer focus can be anywhere in the human body. Normally, cells grow and divide just when they are needed and, when this equilibrium is destabilized, cancer can take place. Depending on multiple factors, cancer development can be fast or slow. Sometimes, it can take several decades since the initial cell mutation until cancer detection. Usually, at this point, cancer is already at a late stage with low treatment hypothesis.

Chemotherapeutic drugs can act against cancer through different mechanisms which are often not unique. For example, alkylating agents directly damage deoxyribonucleic acid (DNA) by covalent binding via their alkyl group, thus preventing tumour cells to divide. Antimetabolites interfere with the DNA and ribonucleic acid (RNA) synthesis through the substitution of the standard building blocks used for replication and transcription. Anti-microtubule agents, on the other hand, can block cell division by preventing microtubule function. Also, topoisomerase inhibitors interfere with topoisomerase enzymes which are responsible for cutting the phosphate backbone of either one or both DNA strands, allowing DNA to be untangled and then resealed again, during DNA replication and transcription. Anthracyclines (antitumor antibiotics) are amongst the most common and effective antitumor drugs, being able to exert their action independently of the cell cycle stage.[3] As will be explained later, this is due to the existence of multiple molecular targets for anthracyclines which turn them powerful anticancer drugs. In the course of a cancer treatment, at some point, the patient will receive systemic anthracycline chemotherapy.[4]

The long pursuit for antibiotics has begun a few decades ago. Waksman and co-workers[5] discovered in 1942 the first antibiotic with antitumor activity, actinomycin A, an antibacterial material extracted from *Actinomyces antibioticus*. In the 1950s, daunorubicin was isolated from a strain of the soil-based microorganism *Streptomyces peucetius*.[6] A few years later, daunorubicin entered in clinical trials and proved to be successful for the treatment of lymphoma and acute leukaemia, however having been associated to fatal cardiac toxicity.[7] Later on, in the 1960s, Arcamone and colleagues[8] promoted a genetic mutation in the *Streptomyces peucetius* strain while continuing their studies. The surviving colonies of *Streptomyces peucetius var. caesius* started to produce a reddish compound, Adriamycin®, later renamed to doxorubicin (DOX). This compound presented a better anticancer activity than daunorubicin and, during the last decades, a great effort has been done to understand

the exact mechanism of its action. Nowadays, DOX is one of the most used chemotherapeutic drugs amongst those approved by the Food and Drug Administration (FDA).[9] Despite the broad range of activity, DOX also presents side effects, from which the most important are cardiotoxicity and myelosuppression, that limit its clinical use.[10] Indeed, since the beginning of the initial research on this class of antitumor antibiotics, doxorubicin has shown a high potential, being applied for treatment of both solid and liquid tumours.[11] It can be synthesized through two different approaches: by fermentation using *Streptomyces peucetius var. caesius* followed by solvent extraction and chromatographic purification or by chemical synthesis from daunorubicin.[12]

This review is about doxorubicin (DOX) which is considered one of the most frequently used anthracycline drugs. Especially, focus will be on DOX-based nanoscale systems that constitute a new approach for delivering the drug, trying to improve its efficiency and, simultaneously, to minimize its side effects.

2. Doxorubicin physicochemical properties and toxicity mechanisms

DOX is a non-selective anthracycline whose structure is based on a water-insoluble aglycone (adriamycinone, with lipophilic character) and a water-soluble amino-sugar moiety (daunosamine, with hydrophilic character). The adriamycinone consists in a tetracyclic ring with a quinine-hydroquinone group nearby. The amino-sugar moiety is linked to one of the rings through a glycosidic bond (Figure 1).[12]

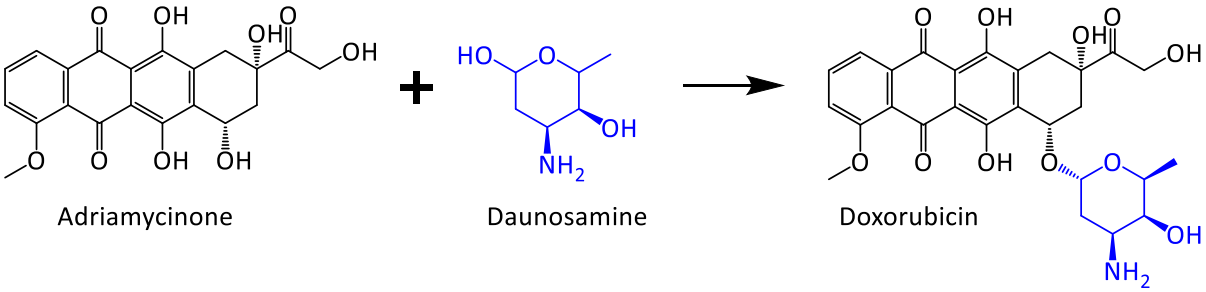

Figure 1. Chemical structure of DOX.

DOX is an amphoteric molecule with acidic and basic functions. It exhibits three ionizable groups with pK_a values of 8.2, 10.2 and 13.2, correspondent to the amino group at daunosamine, the hydroxyl group at C_{11}, and the hydroxyl group at C_6, respectively.[13] The soluble form of DOX is the hydrochloride salt (DOX.HCl), a crystalline orange-red powder with needle-like appearance and hygroscopic behaviour. DOX is soluble in water, methanol and biological saline solutions, and nearly insoluble in organic solvents. DOX aqueous solutions can be used as an indicator of pH as they show a transition from orange-red at neutral pH to blue-violet at a pH value of 9 (Figure 2). The presence of a chromophore in the DOX molecule (dihydroxyanthraquinone) is responsible for this colour change.

Drug concentration, ionic strength, type of solvent and pH are among the variables that strongly influence the absorption spectrum of DOX. Figure 2 shows the ultraviolet-visible (UV-Vis) absorption spectrum of DOX.HCl in methanol where several absorption peaks are evident (at 233, 253, 290, 477, 495 and 530 nm). When in an alkaline environment, the spectrum is shifted for longer wavelengths.[12] Additionally, the DOX molecule presents intrinsic fluorescence. This fluorescence is recurrently used to monitor the uptake and localization of DOX inside cells. However, the interaction with the cell membrane, proteins and/or DNA can lead to an increase or decrease of the signal intensity.[14–16] Bearing this in mind, some studies have been performed to evaluate the correlation between the fluorescence intensity and the solvent.[17,18] According with the work developed by Karukstis *et al*[17], the fluorescence of DOX decreases with an increase in concentration and with a decrease in the environmental pH. They also found two emission characteristic peaks for DOX in aqueous solutions (λ_1 = 560 nm and λ_2 = 593 nm).

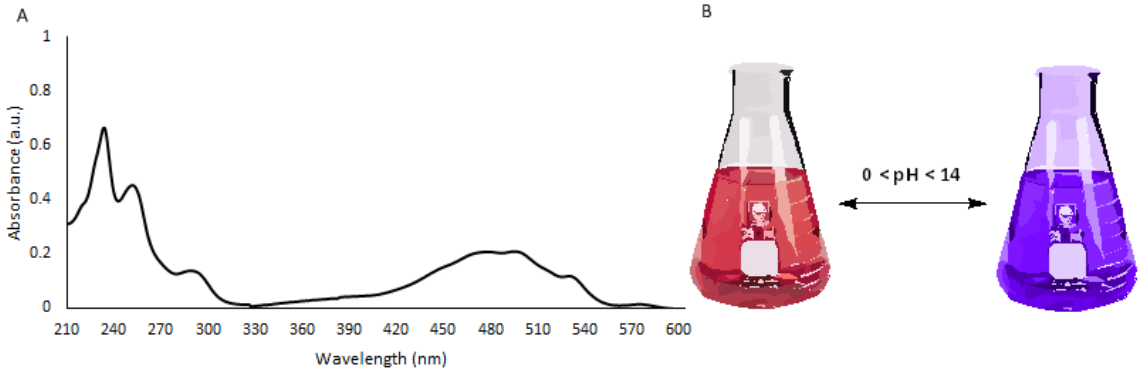

Figure 2. A) UV-Vis absorption spectrum of DOX.HCl in methanol (10 µg/mL) and B) Colour transition of DOX solution in an acidic and basic environment.

Although DOX is routinely used as an effective anticancer drug, its exact mechanism of action is complex and still not completely clear. According to literature, DOX has multiple molecular targets but its cytotoxic effects are essentially based on two phenomena: (a) first, one should consider the intercalation of the planar adriamycinone moiety of DOX between adjacent DNA base pairs; this intercalation interferes with the action of the enzyme topoisomerase II (TOP2), preventing the DNA double helix from being resealed and, as a consequence, stopping DNA replication and RNA transcription[4,19]; and (b) second, by producing reactive oxygen species (ROS), thus, disrupting the cell membrane, proteins and DNA[4,10,11,13]; briefly, several cellular enzymes can oxidize the quinone form of DOX to a semiquinone free radical, an harmful metabolite that can damage DNA; since this metabolite is unstable, it can also be transformed back to the quinone form, giving rise to ROS which can further induce lipid peroxidation, DNA and membrane damage, oxidative stress and activation of the apoptotic cascade (Figure 3).[4,11] In fact, most of the side effects of DOX are associated with ROS, as is the case of

cardiotoxicity. Many body tissues possess enzymes responsible for the combat of free radicals that prevent or limit tissue damage. Since the cardiac tissue has a relatively low number of these enzymes, it will be more susceptible to these reactive species.[4]

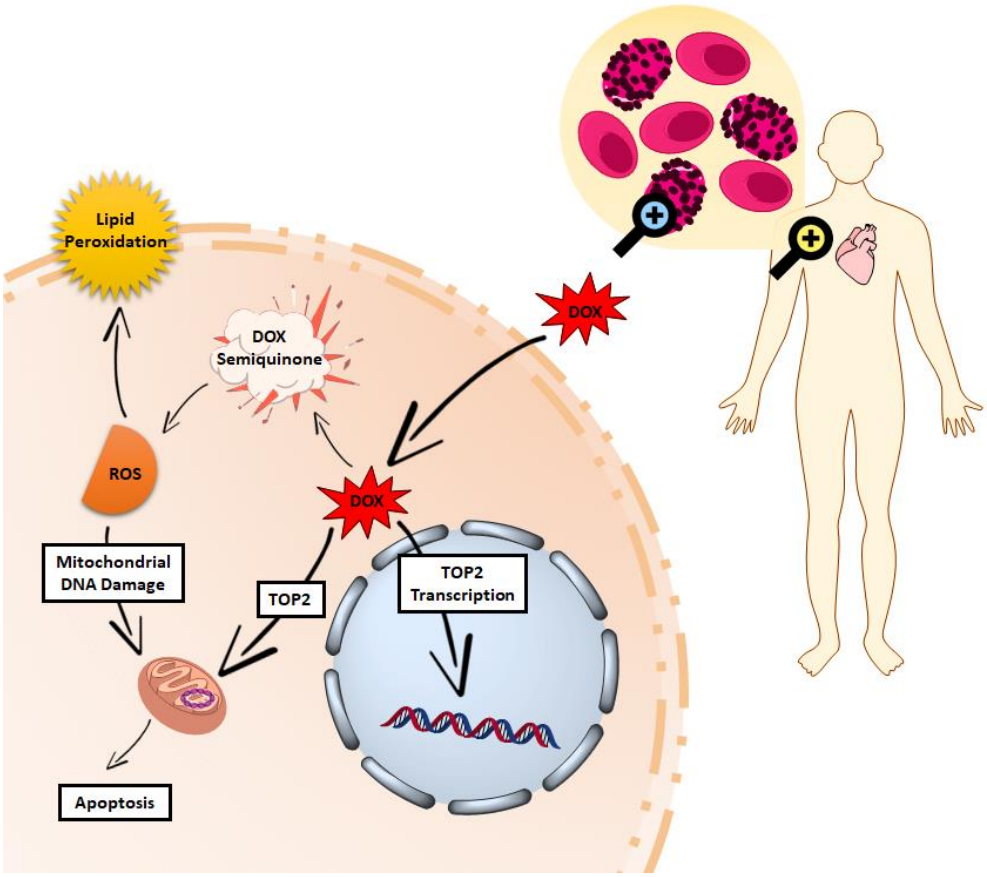

Figure 3. Doxorubicin's mechanism of action.

3. Nanomedicine, nanomaterials and cancer

The European Science Foundation (ESF), in the document "Scientific Forward Look on Nanomedicine" that resulted from discussions of experts in the field, says that nanomedicine "uses nano-sized tools for the diagnosis, prevention and treatment of disease and to gain an increased understanding of the complex underlying pathophysiology of the disease.[20,21] The ultimate goal is improved quality of life". In this context, there is a especial interest in using nanotechnology in the case of cancer too, since it can provide solutions for well-known problems associated with conventional anticancer therapy.[22] Nanomaterials offer the possibility to carry poorly soluble drugs, providing them protection and modifying their biodistribution.[23] Ideally, nanomaterials should be designed to specifically target cancer cells (targeted nanomaterials), thus helping to diminish drug side effects, and should be able to deliver more than one drug at the same place and at the same time, allowing a more effective treatment when using drug combinations. Additionally, they may help to

overcome drug resistance which is a big problem in cancer therapy and a well-document subject regarding doxorubicin.

Nanomaterials, by definition, present properties that are different from the ones shown by their bulk counterparts. These properties are related with their nanoscale size, like high surface-to-volume ratio, and high surface energy, and can also include unique mechanical, magnetic, optical, thermal and electrical behaviours.[24] Nanomaterials also possess the right size to circulate inside the human body and to interact with biological targets, like macromolecules, cells and cell organelles, being perfect tools for the delivery of therapeutic agents. These nanoscale carriers may be prepared in a diversity of different materials and shapes[25–27], and exhibit special chemical and physical properties that are dependent on their size, shape/architecture, chemical composition and surface functionalization. They can be designed to transport drugs (small molecules, proteins and nucleic acids) and, simultaneously, to serve as contrast agents for medical imaging techniques, thus working as theranostic materials (for simultaneous therapy and diagnostic purposes).[25,26] Some nanomaterials can even act as drugs and/or contrast agents by themselves. In the present review, we will start to give an overview over the research on DOX-based nanotherapeutics (the combination of DOX with carrier nanomaterials) that is being conducted in the laboratories resulting in proof-of-concept work. For this, five main classes of nanomaterials will be highlighted: polymeric systems (dendrimers, hydrogels, polymer conjugates and polymeric micelles), lipid-based structures (solid-lipid nanoparticles, liposomes and lipid micelles), metallic nanoparticles (iron oxide, gold and silver nanoparticles), carbon-based structures (from fullerenes to carbon dots), and clay-based nanomaterials (Figure 4). Actually some nanomaterials do not exactly fall into only one of these categories due to their hybrid nature.

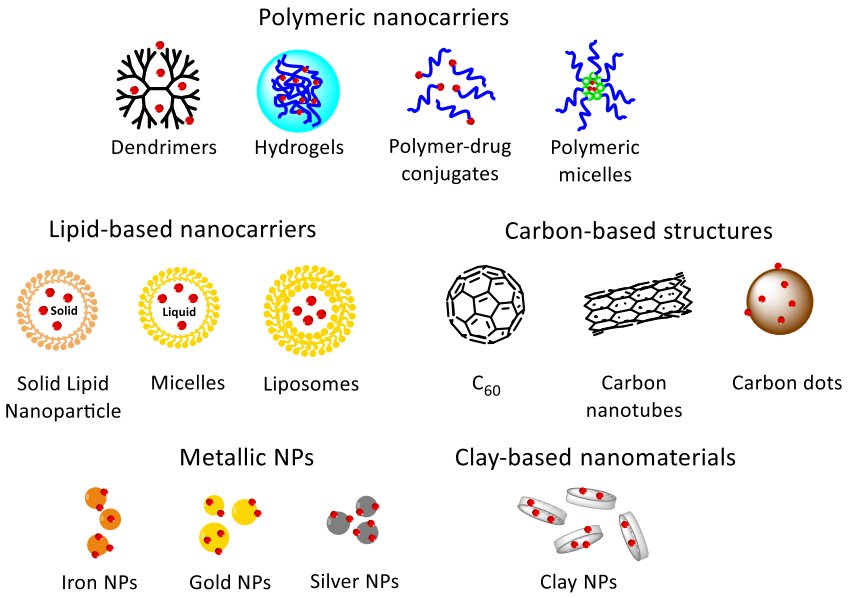

Figure 4. Representation of different classes of nanocarrier systems.

4. Physiological barriers and nanomaterial's design

To be successful, nanomaterials should be designed to surpass several biological barriers that may appear along their route inside the body. Depending on the nanomaterial's method of administration and the localization of the cells/tissues to be treated or imaged, these may include the mononuclear phagocyte system, cellular barriers, stromal barriers and cell/organelle membranes. Beyond surpassing these difficulties, targeted nanomaterials must find their molecular targets and interact with them in an effective manner, thus being even more challenging in terms of design.

4.1. The mononuclear phagocyte system

The mononuclear phagocyte system (or reticuloendothelial system) makes part of our immune system and mainly consists of phagocytic cells, of which the most important are the macrophages. Once inside the body, nanomaterials may suffer opsonization (Figure 5, B) by interaction with opsonins in the blood and/or tissues, thus triggering an immune response, that is, resulting in phagocytosis and clearance from the body (or, in alternative, accumulation in organs such as the lymph nodes and the spleen). The surface charge of a nanomaterial can favour protein adsorption. It is reported that negatively charged nanomaterials are less prone to opsonization and are consequently less recognized by the phagocytic cells, thus spending more time in blood circulation. On the contrary, other reports reveal that neutral nanomaterials, as well as positively charged ones, attract phagocytic cells attention.[28–31] In addition, a common strategy to diminish opsonization is to cover the nanomaterial's surface with a hydrophilic polymer like polyethylene glycol (PEG). Beyond preventing phagocytosis, PEG also confers a higher biocompatibility to the nanocarrier and helps to improve its solubility in aqueous environment. Moreover, PEG prevents the *in vitro* aggregation of nanomaterials and increases the hydrodynamic diameter of very small nanomaterials, increasing their circulation half-time.[32]

4.2. Cellular barriers and the EPR effect

DOX is usually administrated intravenously, being able to cross the vascular-endothelium cell lining and reach most of the body tissues. However, if the idea is to use nanomaterials to avoid side effects and target specific tissues/cells, then one should have in mind that they need to go through this cellular barrier. In fact, in respect to solid tumours, this is facilitated due to a phenomenon baptized as "Enhanced Permeation and Retention effect" (EPR effect, Figure 5, A). The EPR effect results from a combination of two main factors: the presence of fenestrations in the tumour blood vessels and deficient lymphatic drainage.[23] Essentially, when a solid tumour achieves a certain size, its normal vasculature becomes an insufficient oxygen supplier for cell proliferation. In the meantime, cells start

to produce growth factors that trigger angiogenesis.[33] This process is responsible for the quick-growing of new and irregular blood vessels with a deficient epithelium and lacking a basal membrane. The vessel walls then offer little resistance to extravasation, becoming leaky and hyperpermeable. Also, the vessels can collapse due to stress and compression coming from the proliferating tumour cells and/or stromal cells. Depending on the tumour type, location and environment, the size of the fenestrations in the capillaries can range from 200 to 2000 nm. Since the lymphatic drainage is abnormal, this results in a reduced re-absorption of the solutes and other materials present in the interstitial fluid.[23] Whereas small molecules (~4 nm) can be re-absorbed by diffusion to the blood circulation, macromolecules or nanomaterials cannot due to their size.[34] For this reason, macromolecules and nanomaterials accumulate in the tumour site. The EPR effect is, in fact, a passive form of targeting. This means that the targeting process depends on the characteristics of the biological system (the tumour and the new blood vessels, in this case) and not on especial properties of the nanomaterial. However, all the factors that are comprised in the EPR effect are not universal and can be different interpatient and dependent on the tumour type.[23] In fact, the EPR effect has only been routinely studied *in vivo* in animal models (murine models) and, recently, its occurrence in humans is being contested. Some researchers contribute for this controversy pointing out that murine and human tumour microenvironments are quite distinct. When using murine models, the EPR effect is relatively higher than in humans due to the rapid growth of rodent tumours. For instance, a tumour in a mice undergoes an exponential growth of 1 cm (~0.5 g) within 2 to 4 weeks, this is comparable to a ~20 cm (~1 to 2 kg) tumour size in humans which could take years to develop.[35,36] As consequence of this rapid growth, the newly blood vessels present defective and leaky vessels and a vast number of fenestrations.

Beyond extravasation due to the EPR effect, there are several possible mechanisms of transport across the vascular endothelium: a) lipophilic molecules are able to diffuse across the endothelial cell membrane; b) small hydrophilic molecules can diffuse through the tight intercellular junctions; c) receptor-mediated endocytosis and d) vesicular endocytosis.[37] Considering that the diffusion process varies according with the molecule, the transport across the vascular endothelium will strongly depend on nanomaterial's physiochemical properties like size, shape, flexibility and charge. Another important cellular barrier is the blood-brain barrier (BBB) that separates the circulating blood from the central nervous system and that is highly selective. DOX, for example, cannot cross the BBB which is a limitation for its use in the treatment of brain cancers.[10] In this case, the use of nanomaterials especially designed to serve as shuttles for DOX delivery into the brain would certainly extend the possibility of benefiting from the therapeutic properties of this drug.

4.3. Stromal barriers

After crossing the cellular barriers that separate the blood from the tissues, nanomaterials may further find stromal barriers, that is, they must be transported through the interstitial space between cells to reach their target. The easiness with which the nanomaterial follows its path towards the target cells will depend on the characteristics of the biological tissue but also on their own properties, like size, charge, flexibility, etc. Stromal barriers in solid tumours can be even more difficult to be crossed. For example, the abnormal architecture of the blood vessels in tumours and the lack of lymphatic drainage leading to a lack of perfusion can result in an increase of the fluid pressure inside the tumour that, ultimately, will retard the movement of nanomaterials.[38] In part, this phenomenon counterbalances the EPR effect.

4.4. Cell/organelle membranes

DOX, like other drugs, can be internalized by cells through passive diffusion and accumulates intracellularly at high concentrations which is attributed to its lipophilic properties and easy DNA intercalation.[39] On the other side, the tumour microenvironment is often characterized by a privation of oxygen and low pH due to the change of cell metabolism towards fermentative processes.[40,41] This low pH can affect the cellular uptake of drugs that are weak-bases, as is the case of doxorubicin. The acid environment will retain the drug outside the cells in a great extent by a process called “ion-trapping”. In this context, the use of nanomaterials can help to surpass this problem, that is, to increase the cellular uptake of doxorubicin.

Notwithstanding, the cell membrane as well as organelle membranes also constitute barriers for the nanomaterials themselves (loaded, or not, with a drug). Depending on the type of cells and on their own properties, nanomaterials can enter cells by phagocytosis (a process triggered by opsonization) or by pinocytosis. The later can further be classified in four mechanisms: clathrin-mediated endocytosis, caveolin-mediated endocytosis, macropinocytosis and another class where all the other mechanisms different from the previous ones fall.[42] Then, once inside cells, nanomaterials should be able to release their therapeutic cargo near its molecular target. This means that, possibly, it will have to cross other biological membranes, such as the nuclear, lysosomal, or mitochondrial membranes. The design of a nanomaterial should, then, take all these issues into account which, by turn, are related with its specific application.

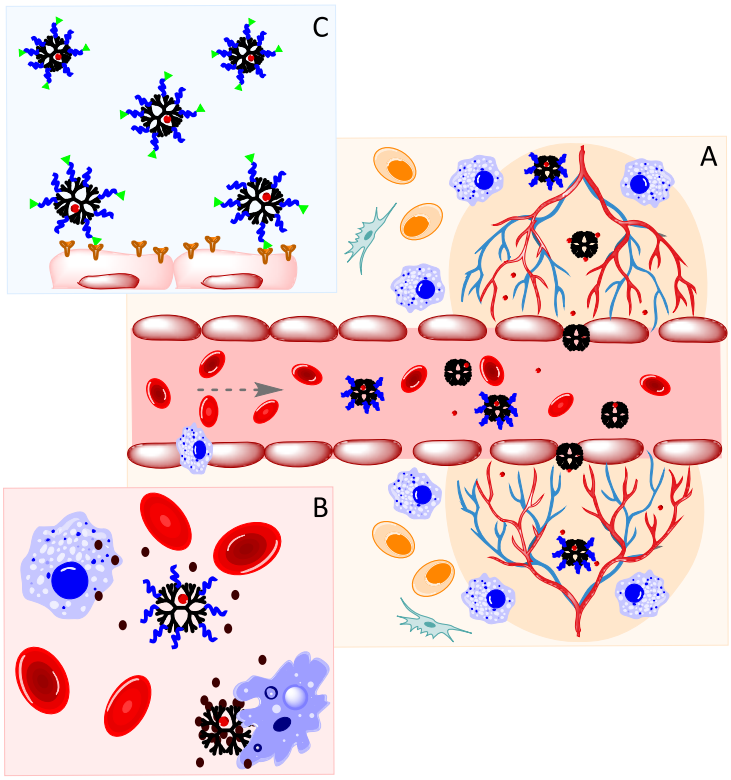

Figure 5. A) EPR effect: extravasation to tumour microenvironment through the leaky vessels and diffusion within the tumour tissue, B) Mononuclear phagocyte system recognition: opsonisation and phagocytosis and C) Active targeting: selective recognition of tumour cells through specific ligand-receptor interaction.

5. Nanomaterials and active targeting

Nanomaterials can actively be targeted towards biological entities. Active targeting, also known as ligand-mediated targeting, relies on the use of ligands (*e.g.* small molecules, carbohydrates, hormones, antibodies, peptides) with specific affinity for a molecular receptor that can, for example, be localized in the surface of the cells to be treated (Figure 5, C). This recognition between the ligand and the receptor may lead to a receptor-mediated mechanism for the cellular internalization of the nanomaterial, improving its efficacy as a delivery system.[23] In fact, the success of the process is dependent on several factors, the most important being the level of overexpression of the receptor in the target cells, and the affinity and selectivity of the ligand for the receptor. In cancer therapy, active targeting has the important objective of overcoming drugs' side effects. When allied with the EPR effect (increased accumulation), active targeting approaches (increased specificity) can greatly improve the performance of nanomaterials as anticancer drug delivery vehicles.

6. Proof-of-concept studies on DOX-based nanotherapeutics

The importance of DOX in the context of anticancer drugs justifies the large number of scientific studies that have been made in this area, as well as the variety of nanoscale systems that have been studied for its delivery in cancer cells and in tumours. The following sections will review the research on DOX-based nanotherapeutics, highlighting the characteristics, advantages and disadvantages of the different classes of nanomaterials. Representative examples will be given for each class which are organized in the form of tables.

6.1. Polymer-based nanocarriers

In nanomedicine, polymer-based systems are amongst the most successful nanocarriers. Polymeric nanomaterials gathered researchers' attention due to the easiness in modelling their features, such as chemical composition, size, morphology/architecture, solubility, functionalization, mechanical properties and biodegradability.[43] In this sense, they seem to be the perfect drug carriers for a variety of applications, being versatility their main advantage. Polymers have proven that are capable to maintain a sustained drug release of encapsulated drugs, protecting them from the surrounding environment, and of targeting cancer tissues both in passive (through the EPR effect) and active forms. Importantly, they can provide shelter to hydrophobic drugs, improving their aqueous solubility.[44] Often, they are used in combination with other classes of nanomaterials to improve their properties, as is the case of PEG that, as mentioned before, among other objectives, is usually used to camouflage nanoscale systems and avoid opsonization. Also, especially by varying the chemical composition, it is possible to tune polymer's toxicity and biodegradability, both relevant aspects for nanomaterials used in medicine. For instance, poly(lactic-co-glycolic acid) (PLGA) is one of the most known biodegradable and biocompatible polymer. When exposed to normal physiological conditions, PLGA is hydrolysed producing the original monomers, lactic acid and glycolic acid. These by-products are later metabolized through the normal metabolic pathways. PLGA is considered safe and is approved by FDA and European Medicines Agency (EMA, in Europe) for human use.[45] Possibly, the bigger disadvantage associated with polymers, that may limit their use in nanomedicine, is the difficulty in preparing molecules with well-defined sizes (they usually present a high polydispersity) and to assure homogeneity among product batches. Even so, chemical synthesis methodologies are continuously evolving and allowing, more and more, a better control over this problem.

6.1.1. Dendrimers

Dendrimers constitute a special group of polymers. Dendrimers were first synthesized by the group of Vögtle in 1978.[46] In 1985, Newkome *et al.*[47] published the synthesis of poly(amide) dendrimers

and Tomalia *et al.*[48] described the synthesis of poly(amidoamine) (PAMAM) dendrimers which are the dendrimers most studied until now due to their early commercial availability. Since then, many other families of dendrimers appeared. Dendrimers possess a regular and well-defined architecture, narrow polydispersity (especially when comparing them with the classical polymers) and a high number of terminal surface groups (multivalency) which allows further modification. Typically, the basic dendrimer structure consists of three main parts: a) the core; b) the branched shells (their number defines the dendrimer generation); and c) the outer functional groups that can be used for further conjugation.[49] Dendrimers can carry drugs by electrostatic interaction, by chemical conjugation to their surface functional groups or by encapsulation inside their inner voids. Not only by their intrinsic chemical nature, but also by the modification of their peripheral groups, it is possible to control the drug release rate, both in case of drug encapsulation or conjugation.[50]

Table 1 presents examples of nanotherapeutics based on dendrimers and evaluated for the cellular/tumour delivery of DOX. There, one can observe that dendrimers are ideal scaffolds for the simultaneous conjugation of different chemical entities, each one serving a distinct objective. In fact, due to dendrimer's multivalency, it is possible to congregate in the same structure ligands for targeting, PEG arms, other nanomaterials for bioimaging purposes (imaging contrast agents) or additional therapy (like those used for cancer hyperthermia), as well as the drug itself. Indeed, dendrimers are being studied for the development of theranostic materials as they can act as vehicles for drug delivery and, also, have a role in the diagnosis of diseases, and especially of cancer. For instance, several studies showed that theranostic nanomaterials based on dendrimers are able to serve as contrast agents for Magnetic Resonance Imaging (MRI) or/and for Computed Tomography (CT) imaging. Apart from the advantages, dendrimers also present weaknesses. In particular, those dendrimers that have terminal groups with a positive charge at physiological pH can present a high toxicity that grows with increasing generation.[51] Also, some works reveal that dendrimers can have a great affinity for metal ions, lipids, proteins, salts and nucleic acids, leading to disruption of biological processes and, consequently, presenting a toxicity higher than desired.[52] Naturally, the possibility of constructing dendrimers with different chemical nature also opens new routes to surpass these difficulties, as is the case of biodegradable dendrimers which are expected to offer a better performance in terms of biocompatibility.

Table 1. Examples of dendrimer-based nanomaterials for DOX delivery*.

Dendrimer Family	Nanocarrier description	Payload	Tumour model	Refs	Year
PAMAM	PEGylated PAMAM-G4-cis-aconityl-DOX conjugates	DOX	Skin cancer (*in vitro* & *in vivo*)	Zhu *et al*[28]	2010
	Peptide T7-modified PEGylated PAMAM-G5	DOX and TRAIL-encoded plasmid	Liver cancer cell line (*in vitro*)	Han *et al*[53]	2011
	Oligonucleotides-PAMAM-G4 bioconjugates	DOX and oligonucleotides	Breast cancer (*in vivo*)	Lee *et al*[54]	2011
	PSMA-targeted aptamer-oligonucleotide PAMAM-G4 bioconjugates	DOX and CpG oligonucleotides	Prostate cancer (*in vitro* & *in vivo*)	Lee *et al*[55]	2011
	Wheat germ agglutinin and transferrin-targeted PEG-PAMAM-G4	DOX	Brain cancer (*in vitro* & *in vivo*)	He *et al*[56]	2011
	PEG-PAMAM-Au nanorod dendrimer conjugate	DOX	Colon cancer (*in vitro* & *in vivo*)	Li *et al*[57]	2014
	FA and RGD-modified PEG-PAMAM-G5 conjugates	DOX	Brain cancer (*in vitro*)	He *et al*[58]	2015
	Hyperbranched PAMAM-PEG-cis-aconityl-DOX conjugates	DOX	Gastric cancer (*in vitro* & *in vivo*)	Nie *et al*[59]	2016
	PAMAM-SS-PEG conjugates	DOX	Skin cancer (*in vitro* & *in vivo*)	Hu *et al*[60]	2016
	FA and borneol-targeted PAMAM-G5 dendrimer conjugates	DOX	Brain cancer (*in vitro* & *in vivo*)	Xu *et al*[61]	2016
	$NAcGal_{\beta}$-targeted PEG-cis-aconityl-PAMAM-G5 dendrimer conjugates	DOX	Hepatic cancer (*in vitro* & *in vivo*)	Kuruvilla *et al*[62]	2017
Polyglutamic	Biotin-targeted poly(L-glutamic acid)-G3 dendrimer	DOX	Breast cancer (*in vitro* & *in vivo*)	Pu *et al*[63]	2013
Polylysine	DOX-HSBA-PEG-poly-lysine-G5 dendrimer conjugate	DOX	Breast cancer (*in vitro* & *in vivo*)	Kaminskas *et al*[64]	2011
	Cationic poly-lysine-G6 dendrimers	DOX	Prostate cancer (*in vitro*) Lung cancer (*in vivo*)	Al-Jamal *et al*[30]	2013
PPI	Dextran-conjugated PPI dendrimers	DOX	Lung cancer (*in vitro* & *in vivo*)	Agarwal *et al*[65]	2009
	Acetylated PPI dendrimers	DOX	Breast cancer cell line (*in vitro*) Lung cancer cell line (*in vitro*)	Wang *et al*[66]	2012

*T7: a transferrin receptor-specific peptide; RGD: arginine-glycine-aspartic acid; PSMA: prostate-specific membrane antigen; FA: Folic acid; $NAcGal_{\beta}$: N-acetylgalactosamine; HSBA: 4-(hydrazinosulfonyl) benzoic acid; PPI: poly(propylene)

6.1.2. Hydrogels

Research on hydrogels has become very popular since the 1960s with the interesting work of Wichterle and Lim.[67] Hydrogels are defined as three-dimensional (3D) networks made of cross-linked polymers that can absorb large amounts of water (or biological fluids) and swell still maintaining their 3D structure. Since hydrogels exhibit a high water content, soft consistency, flexibility and porosity, they resemble the microenvironment of the natural living tissues.[68,69] Furthermore, hydrogels can

result from physical or chemical crosslinking of natural and/or synthetic polymers, resulting in chemical stable systems, or eventually unstable by disintegration or dissolution.[70] There are different hydrogel materials that take into consideration the size of the physical network. For instance, macrohydrogels present a macroscopic network; microgels are discrete hydrogel particles with diameters above 1 μm; and nanogels are hydrogel particles at the submicrometer range.[71] The hydrogel porosity can simply be regulated by adjusting the cross-linking density in the gel matrix and, at the same time, the water affinity of the hydrogel. This feature allows drug loading into the hydrogel and further release with different diffusion rates depending on the molecule size.[72] The high biocompatibility degree and biodegradability of most hydrogels makes them special candidates for introduction in the clinical scenario. In the meantime, many nanotherapeutics based on hydrogels and used for the cellular/tumour delivery of DOX are being developed (Table 2). Smart hydrogels that respond to environmental changes (such as pH, redox conditions and temperature, among other stimuli) have been the focus of diverse works performed both *in vitro* and *in vivo*.

Table 2. Examples of hydrogel-based nanomaterials for DOX delivery*.

Nanocarrier description	**Payload**	**Tumour model**	**Refs**	**Year**
Poly(Vinyl Amine)-PEG-DOX hydrogels	DOX	N/A	Saito *et al*[73]	2007
Star-shaped PLGA-PEG Block copolymer hydrogel	DOX	Mice bearing tumours from KB cell line (*in vitro* & *in vivo*)	Lee *et al*[74]	2008
CHI–DOX conjugates and pluronic hydrogels	DOX	Lung cancer (*in vitro* & *in vivo*)	Cho *et al*[75]	2009
Poly(organophosphazene)–DOX conjugate hydrogels bearing IleOEt and α-amino-ω-methoxy-PEG	DOX	Gastric cancer (*in vitro* & *in vivo*)	Chun *et al*[76]	2009
CHI/dipotassium orthophosphate hydrogel	DOX	Bone cancer (*in vitro* & *in vivo*)	Ta *et al*[77]	2009
Poly(organophosphazene) hydrogels bearing IleOEt and α-amino-ω-methoxy-PEG and ethyl-2-(O-glycyl) lactate	DOX	Gastric cancer (*in vitro* & *in vivo*)	Kwak *et al*[78]	2010
Acetylated hyaluronic acid with low molecular weight	DOX	HeLa cell line (*in vitro*)	Park *et al*[79]	2010
Disulfide-core-crosslinked PEG-poly(amino acid)s	DOX	HeLa cell line (*in vitro*)	Ding *et al*[80]	2011
Silk-based hydrogels	DOX	Breast cancer (*in vitro* & *in vivo*)	Seib *et al*[81]	2013
Polyacrylic acid and gelatin hydrogel crosslinked with polycaprolactone diacrylate	DOX	Ehrlich's Ascites Tumor murine breast carcinoma cell lines (*in vitro* & *in vivo*)	Jaiswal *et al*[82]	2013
Alginate (AG) hydrogel crosslinked with cystamine	DOX	Bone cancer cell line (*in vitro*)	Maciel *et al*[83]	2013
Oxidized AG hydrogel formed by reaction with DOX-succinic acid conjugates crosslinked by Schiff bases	DOX	Breast cancer (*in vitro* & *in vivo*)	Shi *et al*[84]	2014
Hybrid AG/LP hydrogels crosslinked with calcium cations	DOX	Bone cancer cell line (*in vitro*)	Gonçalves *et al*[85]	2014
Dendrimer/AG nanogels using calcium cations as crosslinker and PAMAM-G5 amine terminated as a co-crosslinker	DOX	Bone cancer cell line and mouse fibroblasts (*in vitro*)	Gonçalves *et al*[86]	2014

Hyperbranched polyglycerol derivative and α-cyclodextrin hydrogel system	DOX and camptothecin	HNE-1 epithelial cancer cell line (*in vitro* & *in vivo*)	Zhang *et al*[87]	2015
Peptide–graphene oxide hybrid hydrogel	DOX	Hepatic cancer (*in vitro* & *in vivo*)	Wu *et al*[88]	2015
Poly(N-isopropylacrylamide-co-acrylic acid) nanogels crosslinked with N,N'-bis(acryloyl) cystamine or with N,N'-methylene bisacrylamide	DOX	Bone cancer cell line (*in vitro*)	Zhan *et al*[89]	2015
HA modified with adamantane and β-cyclodextrin	DOX and doxycycline	N/A	Mealy *et al*[90]	2015
Dextrin nanogels crosslinked with formaldehyde or glyoxal	DOX	Colon cancer (*in vitro* & *in vivo*)	Manchun *et al*[91]	2015
PMAA-ChCHl-P_2W_{15} POM hydrogel	DOX	Breast and HeLa cancer cell line Vero cell line (*in vitro*)	Azizullah *et al*[92]	2017
PELG-PEG-PELG hydrogel	DOX, IL-2 and IFN-γ cytokines	Skin cancer (*in vitro* & *in vivo*)	Lv *et al*[93]	2017

*CHI: chitosan; IleOEt: L-isoleucine ethyl ester; AG: alginate; LP: Laponite®; HA: hyaluronic acid; PMMA: poly(methacrylic acid); ChCHI: chitosan hydrochloride; P_2W_{15} POM: 15-tungsto-2-phosphate polyoxometalates; PELG-PEG-PELG: Poly(g-ethyl-L- glutamate)-PEG-poly(g-ethyl-L-glutamate)

6.2. Polymer-drug conjugates and resultant polymeric micelles

Drugs can be covalently linked to polymers that will then act as carriers for their delivery inside the body. Usually, the conjugated drugs are hydrophobic and the polymer provides to the system the required solubility in aqueous environments. Often, due to their amphiphilic nature, when in aqueous solution, conjugates tend to organize and self-assemble as micelles.[94,95]

The first model suggested for a polymer-drug conjugate was introduced by Helmut Ringsdorf.[96] This model is represented by a polymer backbone linked to: a "solubilizer" motif to increase the water solubility; a drug which can be linked directly to the backbone or to a polymeric arm; and a targeting ligand for biological recognition. Polymer-drug conjugates enhance drug stability (due to the covalent conjugation), allow a higher lifespan in blood circulation, improve water-solubility and provide superior target-specificity.[97] As previously mentioned, polymeric micelles are formed by the self-assembling of amphiphilic polymers. The traditional structure consists of a spherical core-shell structure. Usually, the core is hydrophobic and can accommodate hydrophobic drugs, while the shell is hydrophilic conferring solubility in water and preventing aggregation.[98] Drugs can be conjugated to the hydrophobic moiety of the polymer or simply be encapsulated in the core. When present at low concentrations in water, the amphiphiles exist as discrete entities. When concentration increases, the conjugates start to self-assemble into supramolecular structures (micelles) to maintain the hydrophobic core protected from the polar surroundings. This turning concentration point is known as the "critical micelle concentration" (CMC). The CMC depends on the type of polymer, polymer chain-length, temperature, pressure and concentration.[99] The main advantage of polymeric micelles is their facility of production. Considering that anticancer drugs are usually associated with poor aqueous solubility, low stability and

low affinity for specific molecular targets, the use of polymer drug conjugates, alone or in the form micelles, can represent an important step in anticancer therapy. Table 3 shows several examples of these systems that can be found in the literature for the specific delivery of DOX. Only by the examples presented, it is already possible to see that these systems can be very diverse in terms of chemical composition and versatile in terms of the strategy followed for drug delivery.

Table 3. Examples of drug conjugates/polymer-based micelles for DOX delivery*.

Nanocarrier description	**Payload**	**Tumour model**	**Refs**	**Year**
PEG-poly(β-amino ester) block copolymers	DOX	Skin cancer (*in vitro* & *in vivo*)	Ko *et al*[100]	2007
PEG-GPLGV or GPLGVRG peptide-DOX conjugates	DOX	Lung cancer (*in vitro* &*in vivo*)	Lee *et al*[101]	2007
HPMA-based copolymer-DOX conjugates	DOX	Lymphoma (*in vitro* & *in vivo*)	Chytil *et al*[102]	2008
DOX-CHI oligosaccharide-stearic acid conjugates	DOX	Lung cancer (*in vitro* & *in vivo*)	Hu *et al*[103]	2009
PEG-poly(allyl glycidyl ether)-DOX block copolymers	DOX	Lymphoma (*in vitro* & *in vivo*)	Vetvicka *et al*[104]	2009
Multi-functionalized PEG-poly(3-caprolactone) (PCL) micelles with αvβ3 integrin and conjugated DOX	DOX	Breast cancer (*in vitro* & *in vivo*)	Xiong *et al*[105]	2010
PEO-PHB-PEO triblock copolymers	DOX	Cervical cancer (*in vitro* & *in vivo*)	Kim *et al*[106]	2010
Folic acid (FA)-maleilated pullulan-DOX conjugate	DOX	Ovarian cancer cell line (*in vitro*)	Zhang *et al*[107]	2011
Monoclonal antibody-targeted PEG-phosphatidylethanolamine (PE) micelles	DOX	Ovarian cancer cell line (*in v*itro)	Perche *et al*[108]	2012
HPMA copolymer-DOX conjugates with linear and star architectures	DOX	Lymphoma (*in vitro* & *in vivo*)	Etrych *et al*[109]	2012
FA-PEG-b-PLA, PEG-b-P(LA-co-2-Mercaptoethanol (ME)/ Rhodamine B), and PEG-b-P(LA-co-ME/Dox) micelles	DOX	Hepatic cancer (*in vitro* & *in vivo*)	Hu *et al*[110]	2012
PEG-PE micelles	DOX and vinorelbine	Breast cancer (*in vitro* & *in vivo*)	Qin *et al*[111]	2013
Octreotide-Modified N-Octyl-O, N-Carboxymethyl CHI Micelles	DOX	Breast cancer (*in vitro* & *in vivo*)	Zou *et al*[112]	2013
HPMA copolymer-DOX conjugates	DOX	Ovarian cancer (*in vitro* & *in vivo*)	Pan *et al*[113]	2013
DOX-glucuronide prodrug linked to mPEG-b-p(HPMAmLac$_2$-co-AzEMA) copolymers	DOX	Lung cancer (*in vitro* & *in vivo*)	Ruiz-Hernández *et al*[114]	2014
PEG-PCL micelles with different linked moieties	DOX	Breast cancer (*in vitro* & *in vivo*)	Liang *et al*[115]	2015
PEG-block-PCL micelles containing Rhenium-188 (^{188}Re)	DOX and ^{188}Re	Lung cancer (*in vitro* & *in vivo*)	Shih *et al*[116]	2015
cRGD-functionalized PEG-SS-PCL micelles	DOX	Brain cancer (*in vitro* & *in vivo*)	Zhu *et al*[117]	2016
cis-aconityl-DOX conjugate prodrug linked to Pluronic F127-CHI conjugates	DOX and paclitaxel	Pharmacokinetic studies in rats	Ma *et al*[118]	2016
Polymer PCP-DOX prodrug PMCP$_{40}$-PMEMA$_{12}$-Hydrazide-DOX	DOX	Liver, breast and lung cancer cell line (*in vitro*)	Wang *et al*[119]	2016
HA-2-(octadecyloxy)-1,3-dioxane-5-amine conjugates	DOX	Breast cancer (*in vitro* & *in vivo*)	Qiu *et al*[120]	2017
Chondroitin sulphate/poly (lactide-co-glycolide) block copolymer	DOX	Breast cancer cell line (*in vitro*)	Zhang *et al*[121]	2017

solanesyl PEG-dithiodipropionate and solanesyl PEG-succinate micelles	DOX	Hepatic cancer (*in vitro* & *in vivo*)	Qin *et al*[122]	2017
DOX-cis-aconityl-N,N,N-trimethyl CHI-FA	DOX and interleukin2	Hepatic cancer (*in vitro* & *in vivo*)	Wu *et al*[123]	2017

*PEG: poly(ethylene glycol); Peptide GPLGV: Gly-Pro-Leu-Gly-Val; Peptide GPLGVRG: Gly-Pro-Leu-Gly-Val-Arg-Gly; HPMA: N-(2-hydroxypropyl) methacrylamide; CHI: chitosan; PCL: poly(3-caprolactone); PEO-PHB-PEO: poly(ethylene oxide)-poly[(R)-3-hydroxybutyrate]-poly(ethylene oxide); FA: folic acid; PE: phosphatidylethanolamine; ^{188}Re: Rhenium-188; PCP: Poly(choline phosphate); PMCP: Poly(2-(methacryloyloxy) ethyl choline phosphate; PMEMA: Poly(2-methoxy-2-oxoethyl methacrylate)

6.3. Lipid-based nanocarriers

Since the 1960s, lipid-based nanomaterials have been deeply studied as potential systems for chemical and biomedical applications.[124–126] This kind of nanomaterials became popular due to their "natural" lipid composition and therefore low toxicity.[127] There are three major lipid-based nanomaterials: solid-lipid nanoparticles (SLNs), liposomes, and micelles. SLNs are usually spherical, and possess a solid lipid core matrix and an outer layer of a surfactant. Lipophilic drugs can be transported in the core. Lipid components of SLNs should be solid at both body and ambient temperature and can be prepared from triglycerides, complex glyceride mixtures or even waxes. The other two systems are mainly prepared from naturally occurring and/or synthetic phospholipids by self-assembly. Micelles are considered the smallest and simplest self-assembled lipid structures formed by one layer of polar lipids in aqueous solutions, forming spheres. Liposomes also consist of spherical assemblies of phospholipids that, in this case, are organized in bilayers (sometimes multiple bilayers) with a diameter size typically in the 50-200 nm range. In aqueous solutions, the formed micelles possess a hydrophobic core, whereas liposomes possess a hydrophilic core. Hydrophobic drugs can be incorporated into micelles. Since liposomes have an aqueous core and a lipid bilayer, they can accommodate both hydrophilic and hydrophobic molecules.[128] Cholesterol is generally added to the formulations of liposomes to stabilize the lipid bilayers.

The main advantages of lipid-based nanocarriers are that they can transport lipophilic drugs and are able to protect them from severe environmental conditions, both *in vitro* and *in vivo*. Additional advantages are the easiness of production, functionalization and control over the drug release process.[50,129] Over the last years, lipid-based nanocarriers have been used as delivery vehicles for a diversity of molecules, like chemotherapeutics, enzymes, peptides, nucleic acids, antigens, antifungals and imaging agents.[129,130] Table 4 presents recent examples of research studies on lipid-based systems for the release of DOX.

Table 4. Examples of lipid-based nanomaterials with DOX*.

Lipid family	Nanocarrier description	Payload	Tumour model	Refs	Year
Solid lipid NP	Transferrin-PEG-PE	DOX and EGFP-encoded plasmid	Lung cancer (*in vitro* & *in vivo*)	Han *et al*[131]	2014
Micelle	Labrafac WL 1349® and Solutol HS 15® micelles	DOX and docetaxel	N/A	Vrignaud *et al*[132]	2011
	DSPE-PEG_{2000}-CRGDK micelle	DOX	Breast cancer (*in vitro* & *in vivo*)	Wei *et al*[133]	2013
	FA-CMCHI-DSP-DOX	DOX and cisplatin	HeLa cancer cell line (*in vitro*)	Zhang *et al*[134]	2017
	HA-vitamin E succinate grafted polymer	DOX and curcumin	Breast cancer (*in vitro* & *in vivo*)	Ma *et al*[135]	2017
Liposome	Immunoliposome with $Fab'_{222\text{-}1D8}$ antibody fragment	DOX	Fibrosarcoma (*in vitro* & *in vivo*)	Hatakeyama *et al*[136]	2007
	Immunoliposomes with HER2-antibody	DOX and hollow gold nanospheres	Carcinoma and lung cancer (*in vitro* & *in vivo*)	Li *et al*[137]	2015
	HSPC/CH liposomes modified with sialic acid-octadecylamine	DOX and dexamethasone palmitate	Sarcoma cancer (*in vitro* & *in vivo*)	Sun *et al*[138]	2016
	Immunoliposomes with GE11 peptide and cetuximab Fab' antibody fragment	DOX	Breast cancer cell line (*in vitro*)	Haeri *et al*[139]	2016
	DPPC/DSPC/CH/DSPE-PEG liposomes	DOX and gadoteridol	Breast cancer (*in vitro* & *in vivo*)	Rizzitelli *et al*[140]	2016
	DSPC/CH; DSPC/DOTAP/CH and DSPC/PEG-DSPE/ DOTAP/CH micelles	DOX and 5-Flurouracil	Breast cancer (*in vitro* & *in vivo*)	Camacho *et al*[141]	2016
	$H_7K(R_2)_2$-modified peptide DSPE-PEG liposomes	DOX	Brain cancer (*in vitro* & *in vivo*)	Zhao *et al*[142]	2016
	DPPC/DSPC/$DPPG_2$ liposome	DOX and gadoteridol	Sarcoma cancer (*in vitro* & *in vivo*)	Peller *et al*[143]	2016
	PEG-DSPE/DOTAP/CH liposomes	DOX and micro-RNA	Hepatic cancer (*in vitro* & *in vivo*)	Fan *et al*[144]	2017
	PEG-DSPE/DPPC/CH liposomes	DOX and curcumin	Colon cancer cell line (*in vitro*)	Sesarman *et al*[145]	2017
	DOTAP/DSPE-PEG and POPC/CH/DSPE-PEG liposomes	DOX, tobramycin and DNA aptamer	HeLa cancer cell line (*in vitro*)	Plourde *et al*[146]	2017
	Selenium-functionalized lecithin S100/DOTAP/CH liposomes	DOX	Lung cancer (*in vitro* & *in vivo*)	Xie *et al*[147]	2018

*Labrafac WL 1349®: Caprylic-capric acid triglycerides; Solutol HS 15®: mixture of free PEG660 and PEG660 hydroxystearate; DSPE: 1,2-Distearoyl-sn-glycero-3-phosphoethanolamine; CMCHI: carboxymethyl chitosan; DSP: 3,3'-Dithiobis (N-hydroxysuccinimidyl propionate); HER2: Human epidermal growth factor receptor-2; HSPC: Hydrogenated soy phosphatidylcholine; CH: Cholesterol; DPPC: 1.2-Dipalmitoyl-sn-glycero-3-phosphocoline; DSPC: 1.2-Distearoyl-sn-glycero-3-phosphocoline; DSPE: Distearoyl-sn-glycero-3-phosphoethanolamine; DOTAP: 1,2-dioleoyl-3- trimethylammonium-propane; $H_7K(R_2)_2$ peptide: Ac-RRK(HHHHHHH)RR-NH_2 peptide; $DPPG_2$: 1,2-dipalmitoyl-sn-glycero-3-phosphodiglycerol; POPC: 1-palmitoyl-2- oleoyl-sn-glycero-3-phosphocholine

6.4. Metallic nanoparticles

Nanoparticles made of metals and metallic oxides present special properties, such as electronic, magnetic and optical, that can be tuned by adjusting their size, shape and composition.[148]

Numerous types of metallic NPs are under study for the purposes of therapy, medical imaging contrast enhancing or both (theranostic applications). Indeed, they can transport drugs adsorbed into their surface and, simultaneously, act as contrast agents in imaging techniques, like MRI (this is the case of iron oxide nanoparticles) or CT imaging (like gold nanoparticles). These nanoparticles are also promising due to their robustness, stability, and resistance to enzymatic degradation.[149] Also, as is well-known, some metals possess antimicrobial and anti-inflammatory properties, for instance gold, silver and platinum.[150] Table 5 shows representative examples of the possible use of metallic nanoparticles for DOX delivery.

6.4.1. Iron oxide nanoparticles

Usually, it is not difficult to functionalize metallic NPs with different surface groups, keeping the inner properties for imaging applications. Amongst metallic NPs, those of iron oxide are quite well studied and explored due to their magnetic properties. Their size ranges from 5 to 50 nm and they can be easily synthesized , being possible to control their size, shape and solubility.[151] However, to achieve such stability, they need to be stabilized which is achieved by surface modification with different ligands, such as carboxylates, phosphates, and also with polymers, like polyethylene glycol and polyvinyl alcohol (PVA).[152,153] Interestingly, iron oxide nanoparticles can be used as drug delivery systems, contrast agents in medical imaging and, in addition, by applying an adequate magnetic field, for the thermal ablation of cancer (cancer hyperthermia treatment). As naked iron oxide nanoparticles are toxic, they are usually coated, for example with polysaccharides, PEG, inorganic materials, etc.. Also in this case, the coating can confer stealth properties to the nanoparticles so that they can avoid recognition by the immune system and phagocytosis.

6.4.2. Gold nanoparticles

Gold nanoparticles (AuNPs) are unique amongst nanomaterials because of their inherent inert chemical properties, low toxicity, controllable size, shape and ease functionalization. The most usual method to synthesize AuNPs is through citrate reduction of chloroauric acid in water.[154] Their typical diameter is between 10-50 nm, being their colour shape/size-dependent. The colour shifts from red to blue which can be detected in the visible part of the electromagnetic spectra.[155] The role of AuNPs in the biomedical field include labelling (for example, they can be used as contrast agents in transmission electron microscopy), drug delivery (by adsorbing drugs at their surface), heating (like iron oxide NPs, they can be used for cancer hyperthermia treatment) and sensing (due to their optoelectronic properties). Furthermore, AuNPs can attenuate X-rays and, so, are being investigated to be used as contrast agents in CT imaging. Very important is also the fact that they are very easily functionalized

at the surface through the reaction of gold with sulfhydryl (R–SH) groups present in organic or biological molecules.

6.4.3. Silver nanoparticles

Silver nanoparticles (AgNPs) are being used in our daily life in a wide range of fields, including food, healthcare, medicine and industry.[156] AgNPs exhibit special features such as optical, thermal, electrical and biological properties. One important characteristic is their strong antimicrobial and antifungicidal activity. Due to this property, they have been employed in several materials for medical care, namely in silicon catheters, sterilizing filters, sutures and, also, as medicines for dermatitis. Recently, AgNPs have also been studied as anticancer agents themselves, beyond the possibility of being used as drug carriers. Like AuNPs, they may be applied as diagnostic or probing mediators.[157,158]

Table 5. Examples of metallic-based NPs with DOX*.

Metal Family	Nanocarrier description	Payload	Tumour model	Refs	Year
Iron Oxide	Gelatin-coated magnetic iron oxide NPs	DOX	N/A	Gaihre *et al*[159]	2009
	PNIPAM-coated magnetic iron oxide NPs	DOX	Liver cancer (*in vitro* & *in vivo*)	Purushotham *et al*[160]	2009
	PVA-coated iron oxide NPs	DOX	N/A	Kayal *et al*[161]	2010
	Multifunctional PEG-trimellitic anhydride chloride-folate superparamagnetic iron oxide NPs	DOX	Liver cancer (*in vitro* & *in vivo*)	Maeng *et al*[162]	2010
	PEG-coated superparamagnetic vs citrate-stabilized iron oxide NPs	DOX	Stealthiness evaluation in rats (*in vivo*)	Allard-Vannier *et al*[29]	2012
	PEGylated iron-platinum@iron oxide core-shell NPs	DOX	Breast cancer (*in vitro* & *in vivo*)	Liu *et al*[163]	2013
	PEG-b-PVBP-coated iron oxide NPs	DOX	Colon cancer (*in vitro* & *in vivo*)	Hałupka-Bryl *et al*[164]	2014
	Mesoporous silica-coated superparamagnetic iron oxide NPs	DOX	N/A	Pourjavadi *et al*[165]	2015
	Hydroxyapatite coated-superparamagnetic iron oxide NPs	DOX	Breast cancer cell line (*in vitro*)	Aval *et al*[166]	2016
	Superparamagnetic iron oxide-chondroitin sulphate-CHI microparticles	DOX	Liver cancer (*in vitro* & *in vivo*)	Tang *et al*[167]	2017
Gold	AuNPs stabilized with P(LA-DOX)-b-PEG-OH/FA	DOX	Breast cancer cell line (*in vitro*)	Prabaharam *et al*[168]	2009
	FA-modified gold nanoclusters	DOX and a NIR fluorescent dye ICG-Der-02	Lung, liver, breast and colon cancer cells (*in vitro* & *in vivo*)	Chen *et al*[169]	2012
	Multifunctional gold nanorods	DOX, cRGD and a ^{64}Cu chelator	Brain cancer (*in vitro* & *in vivo*)	Xiao *et al*[170]	2012
	DOX-CPLGLAGG peptide AuNPs conjugate	DOX	Mouse head and neck carcinoma cell line (*in vitro* & *in vivo*)	Chen *et al*[171]	2013

	PEG-coated hollow gold nanoshells	DOX	Breast cancer (*in vitro* & *in vivo*)	Lee *et al*[172]	2013
	DOX-PEG-AuNPs conjugate	DOX	Breast cancer (*in vitro* & *in vivo*)	Sun *et al*[173]	2014
	Human serum albumin/indocyanine green/FA-coated gold nanoshells	DOX	Breast cancer (*in vitro* & *in vivo*)	Topete *et al*[174]	2014
	PEGylated magnetic AuNPs	DOX	Breast cancer (*in vitro* & *in vivo*)	Elbialy *et al*[175]	2015
	AuNPs crosslinked with PCL-b-PDMAEMA-b-PEG	DOX	Mouse head and neck carcinoma cell line (*in vitro* & *in vivo*)	Jeon *et al*[176]	2015
	PEGylated PDPH-AuNP complex	DOX	Human head and neck squamous carcinoma cell line (*in vitro*)	Lee *et al*[177]	2015
	AuNPs-DOX conjugate	DOX	Skin cancer (*in vitro* & *in vivo*)	Zhang *et al*[178]	2015
	Oligonucleotide-conjugated AuNPs	DOX	Colon cancer (*in vitro* & *in vivo*)	Lee *et al*[179]	2017
Silver	Alendronate-coated AgNPs	DOX and alendronate	HeLa cancer cell line (*in vitro*)	Benyettou *et al*[180]	2015

*PNIPAM: poly-n-isopropylacrylamide; PVA: polyvinyl alcohol; PEG: poly(ethylene glycol); PVBP: poly(4-vinylbenzylphosphonate); CHI: chitosan; P(LA): poly(L-aspartate); FA: folic acid; PCL: poly(3-caprolactone); PDMAEMA: poly(2-(dimethylamino) ethyl methacrylate); PDPH: 3-[2-pyridyldithio]propionyl hydrazide;

6.5. Carbon-based nanomaterials

The existence of multiple carbon-based nanomaterials is associated with the vast and varied chemistry of this element. They have notable chemical and physical properties (e.g., electrical and thermal conductivity, high mechanical strength and optical properties), thus being used in many different applications. Carbon-based nanomaterials such as graphene, carbon nanotubes (CNTs) and fullerenes, stem from graphite as "starting material".[181] Graphite structure is a combination of stacked layers of carbon atoms arranged in a honeycomb lattice. Graphene is single layer sheet structure with a thickness of a carbon atom and can be prepared from graphite. Its robust structure and, at the same time, its high flexibility makes it attractive for biomedical applications. CNTs are cylindrical hollow structures with the walls made of sheets of carbon, also with a thickness of a carbon atom. Graphene and CNTs present similar electrical, optical and thermal properties.[182] Another interesting carbon structure is the popular C_{60}, also known as buckyball. Like CNTs, C_{60} belongs to the fullerene family of carbon materials. Fullerenes were discovered in 1985 and resulted in a Nobel Prize in 1996.[183] Currently, other carbon nanomaterials appeared like carbon nanohorns, derived from CNTs but having a conical cap, and carbon dots which are fluorescent nanomaterials. Curiously, many of the mentioned carbon structures were tested for drug delivery applications and, particularly, for the delivery of DOX as can be seen in the examples listed in Table 6.

Table 6. Examples of carbon-based nanomaterials with DOX*.

Nanocarrier description	Payload	Tumour model	Refs	Year
PEGylated Oxidized Carbon Single-Walled Nanohorns	DOX	Lung cancer cell line (*in vitro*)	Murakami *et al*[184]	2006
Multi-walled CNTs	DOX	Breast cancer cell line (*in vitro*)	Ali-Boucetta *et al*[185]	2008
AG, CHI and FA-modified Single-walled CNTs	DOX	HeLa cancer cell line (*in vitro*)	Zhang *et al*[186]	2009
PEGylated Single-walled CNTs	DOX	Lymphoma (*in vitro* & *in vivo*)	Liu *et al*[187]	2009
C_{60}	DOX	Breast cancer cell line (*in vitro*)	Liu *et al*[188]	2010
PEGylated Single-Walled CNTs with hydrazone linkage	DOX	Lung cancer cell line (*in vitro*)	Gu *et al*[189]	2011
FA-modified Multi-Walled CNTs functionalized with iron NPs	DOX	HeLa cancer cell line (*in vitro*)	Li *et al* [190]	2011
PEGylated oxidized Multi-Walled CNTs modified with angiopep-2	DOX	Brain cancer (*in vitro* & *in vivo*)	Ren *et al*[191]	2012
C_{60}	DOX	Chicken embryo (*in vitro* & *in vivo*)	Blazkova *et al*[192]	2014
FA-PEG-Multi-Walled CNTs	DOX	HeLa cancer cell line (*in vitro*) Liver perfusion study (*in vivo*)	Dinan *et al*[193]	2014
FA-modified carbon dots functionalized with bovine serum albumin	DOX	Vero cell line and HeLa cancer cell line (*in vitro*)	Mewada *et al*[194]	2014
C_{60}	DOX	Lung cancer (*in vitro* & *in vivo*)	Prylutska *et al*[195]	2014
PEI-derivatized fullerene	DOX	Skin cancer (*in vitro* and *in vivo*)	Shi *et al*[196]	2014
PEGylated fullerene	DOX	Breast cancer cell line (*in vitro*)	Magoulas *et al*[197]	2015
C_{60}	DOX	Lung cancer (*in vitro* & *in vivo*)	Panchuk *et al*[198]	2015
C_{60}	DOX	Lung cancer (*in vitro* & *in vivo*)	Prylutska *et al*[199]	2015
Galactosylated CHI-oxidized Multi-Walled CTNs	DOX	Liver cancer (*in vitro* & *in vivo*)	Qi *et al*[200]	2015
Nuclear localization signal peptide-targeted carbon dots	DOX	Lung cancer (*in vitro* & *in vivo*)	Yang *et al*[201]	2016
Transferrin-modified carbon dots	DOX	Brain cancer cell line (*in vitro*)	Li *et al*[202]	2016
Carbon dots	DOX	HeLa cancer cell line (*in vitro*)	Wang *et al*[203]	2016
Heparin-modified carbon dots	DOX	Breast and lung cancer cell line (*in vitro*) HeLa cancer cell line (*in vitro*)	Zhang *et al*[204]	2017
Polydopamine-coated carbon dots	DOX	HeLa cancer cell line (*in vitro*)	Sun *et al*[205]	2017
Carbon dots	DOX	Mouse fibroblast cell line (*in vitro*) Adenoid cystic carcinoma cell line (*in vitro*)	Yuan *et al*[206]	2017
PEI-modified carbon dots	DOX	Mouse fibroblast cell line (*in vitro*) HeLa cancer cell line (*in vitro*)	Gao *et al*[207]	2017

*AG: alginate; CHI: chitosan; FA: folic acid; PEI: Polyethylenimine;

6.6. Clay-based nanomaterials

Other drug delivery systems that are now being explored in the biomedical field are clay-based nanomaterials. These clays are already being used for cosmetic and pharmaceutic applications and, so, researchers are now trying to take advantage of their properties for further application in tissue engineering, regenerative medicine, medical imaging and cancer treatment. Especial attention is being given to the synthetic clay Laponite® ($Na^{+}_{0.7}[(Si_8Mg_{5.5}Li_{0.3})O_{20}(OH)_4]^{-0.7}$, LP) that can be produced with a controllable composition at a large scale and low cost. Although there are several different LP grades commercially available, for medical applications, the grades having high purity and low heavy metals content should be used.[208] LP is composed of nanoscale crystals with a disk shape (about 25 nm in diameter and 0.92 nm in thickness). In these disks, the faces are negatively charged whereas the edges possess pH-dependent charge.[209] Like other clays, LP presents a high swelling capacity and tendency to adsorb many types of molecules at its surface. Furthermore, by reaction of the silanol groups present at its edges with alkoxysilanes with additional reactive groups, the clay can also be covalently linked to molecules of interest. Also, although this clay degrades when exposed to acidic environments, it gives rise to non-toxic products such as aqueous silica, and magnesium, sodium and lithium ions.[210] For these reasons, LP is now being evaluated as a nanocarrier for diverse biological and therapeutic molecules, including for the transport of DOX.

The first work on the use of LP for DOX delivery, was authored by Wang and colleagues[211] that used naked LP for that purpose. Their study showed promising results since LP was loaded with a high content of DOX, being the drug released in a sustainable and pH-dependent manner. These *in vitro* results revealed that the DOX-LP platform was more efficient in diminishing the viability of cancer cells than DOX alone. As can be seen in Table 7, several other LP-based nanoscale systems (nanohybrid materials) were meanwhile assayed for DOX delivery. All these platforms were developed having in view the improvement of the behaviour of LP as a drug delivery system, namely in what concerns the drug release profiles and stability in the physiological environment.

Table 7. Examples of clay-based nanomaterials with DOX*.

Nanocarrier description	Payload	Tumour model	Refs	Year
DOX-loaded LP disks	DOX	Liver cancer (*in vivo*)	Li *et al*[212]	2014
PEG-PLA-modified LP disks	DOX	Bone cancer (*in vitro*)	Wang *et al*[213]	2014
Alginate-coated LP nanodisks	DOX	Bone cancer (*in vitro)*	Gonçalves *et al*[214]	2014
PEG-Lactobionic acid-modified LP nanodisks	DOX	Liver cancer (*in vitro*)	Chen *et al*[215]	2015
Polyelectrolyte multilayer (PAH/PSS)-coated DOX/LP nanohybrids	DOX	Breast cancer (*in vitro)*	Xiao *et al*[216]	2016

Hyaluronic acid functionalized PLA-PEG-PEI-AuNPs-modified LP disks	DOX	HeLa cancer cell line (*in vitro* & *in vivo*)	Zhuang *et al*[217]	2017

*LP: Laponite®; PEG: PEG: poly(ethylene glycol); PAH: poly(allylamine) hydrochloride; PSS: poly(sodiumstyrene sulfonate); PLA: poly(lactic acid)

7. DOX-based nanotherapeutics in the clinical scenario

As will be detailed in the following sections, several DOX-based nanotherapeutics are already in clinical use or under clinical trials. It is known that, despite the extensive research work on drug delivery, only very few nanocarriers achieved preclinical and clinical study phases. Some of the DOX-based nanotherapeutics were however successful in this process since they met the needed requirements, like increasing DOX solubility and efficacy and, simultaneously, decreasing its clearance rate and systemic toxicity.

In fact, from the discovery phase and before reaching the market, drugs (and nanodrugs too) must go through a selection process which is closely followed by regulatory agencies (like FDA in the United States or the EMA, in Europe) to assure their safety and effectiveness (Figure 6).[218] Along this path, the number of drug candidates decreases and few are considered promising for further evaluation. First, researchers should perform experiments in *in vitro* and *in vivo* models (only animal studies) to obtain systematic data regarding the drug's pharmacodynamics (what the drug does to the body), and pharmacokinetics (what the body does to the drug) which is considered a preclinical phase of drug development. The preclinical phase main objective is, then, to provide knowledge concerning the safety of the drug and establish the safe dose for the first-in-man study. Then, experiments can start in humans, step by step, from Phase I to Phase III clinical studies. For these, specific protocols should be followed that clearly establish who is qualified to participate, number of persons, study duration, administration method, dosage and how data will be collected and analysed (Figure 6). Still, even after the drug reaching the market, it is important to gather information from the drug's performance while it is in active medical use.

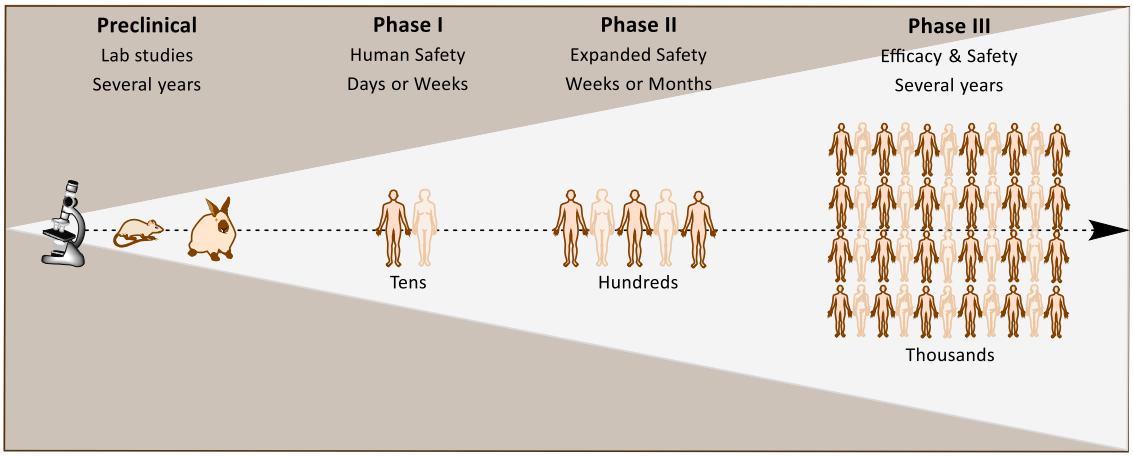

Figure 6. Stages of clinical trials.[219]

Many years may pass since the beginning of the preclinical studies until the end of clinical trials. Often, the results do not match the expectations and the studies fall apart. Nowadays, there are several nanotherapeutics in the market and at clinical stage, being the main effort headed by the oncology field. Figure 7 presents a timeline relative to DOX-based nanotherapeutics highlighting the most important landmarks in this area. Information regarding these nanotherapeutics, such as their generic name, formulation type, therapeutic indications and clinical phase status is also summarized in Table 8. These nanotherapeutics cover different nanoplatform types, including liposomes, nanoparticles, polymer-drug conjugates, polymeric micelles, or even biological derivatives (Table 8).[220–226] It must be mention that Table 8 does not include generic versions or very similar variants of the listed DOX-based nanotherapeutics that meanwhile appeared in the market.

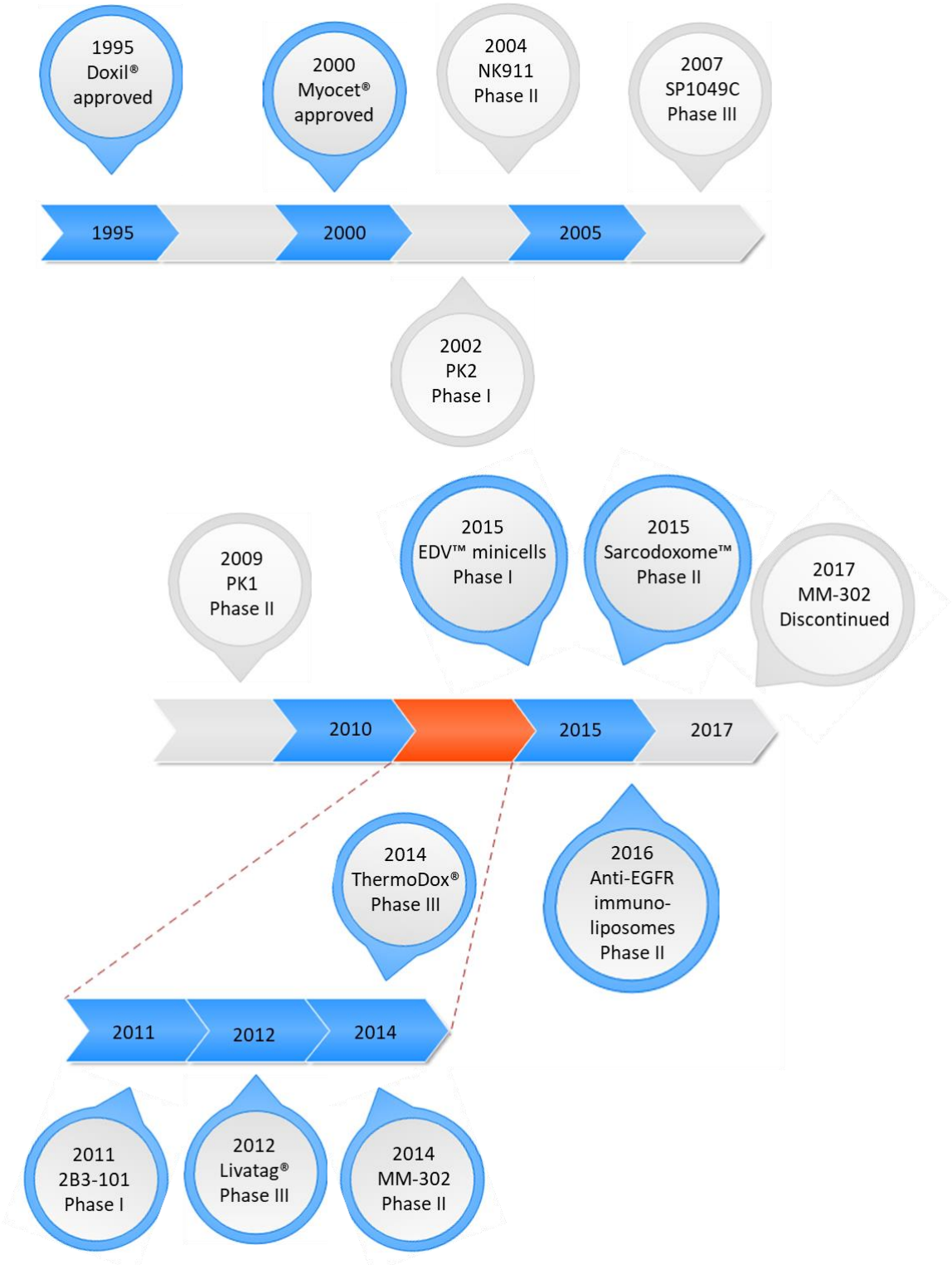

Figure 7. Timeline based for the DOX-based nanotherapeutics in clinical stages or already in the market.

Table 8. DOX-based nanotherapeutics in the market and in clinical stages.

Nanocarrier platform	Generic name	Formulation type	Therapeutic indication	Phase status	Refs
Liposomes	Doxil®/Caelyx®	PEGylated liposomal DOX	Kaposi's sarcoma Breast cancer Ovarian cancer Multiple myeloma	Approved	Stewart et al[227] Northfelt et al[228] O'Brien et al[229] Gordon et al[230] Rifkin et al[231]
	Myocet®	Liposomal DOX	Breast cancer	Approved	Batist et al[232,233] Harris et al[234] Chan et al[235]
	ThermoDox®	Thermosensitive liposomal DOX	Non-resectable hepatocellular carcinoma Non-resectable hepatocellular carcinoma Breast cancer	Phase III Phase III Phase I/II	NCT02112656[236] NCT00617981[237] NCT00826085[238]
	Sarcodoxome™	Liposomal DOX containing lipochroman 6	Small cell lung cancer	Phase II	Lopez-Pousa et al[239]
	2B3-101	Glutathione PEGylated liposomal DOX	Meningeal carcinomatosis Brain metastases	Phase II Phase I	NCT01818713[240] Kerklaan et al[241]
	anti-EGFR ILs-DOX	EGFR targeted liposomal DOX	Solid tumours	Phase II	Mamot et al[242]
	MM-302	HER2 targeted liposomal DOX	HER2 positive breast cancer	Phase II*	Miller et al[243] ADCreview Website[244]
NPs	Livatag®	DOX-loaded poly(isohexyl-cyanoacrylate) NPs	Hepatocellular carcinoma	Phase III**	Onxeo company[245,246]
Polymer-drug conjugates	FCE28068/PK1	N-(2-Hydroxypropyl) methacrylamide-DOX copolymer	Breast cancer Non-small cell lung cancer Colorectal cancer	Phase II	Leonard et al[247]
	FCE28069/PK2	N-(2-Hydroxypropyl) methacrylamide-DOX-Galactosamine	Primary/metastatic liver cancer	Phase II	Seymour et al[248]
Polymeric micelles	SP1049C	DOX block copolymer micelle	Non-resectable stage IVb adenocarcinoma	Phase III	Valle et al[249]
	NK911	mPEG-DOX-poly-aspartic acid conjugates	Solid tumours	Phase II	Matsumura et al[250]
Bacteria-derived	EDV™ minicells	DOX-loaded EDV nanocells	Glioblastoma multiform	Phase I	Whittle et al[251]

*MM-302 Phase II clinical trial was discontinued in March 2017.

**Livatag Phase III clinical trial was discontinued in September 2017.

7.1. Doxil®/Caelyx®

Liposomes are experiencing an exponential evolution since almost 50 years ago.[252] Doxil®, currently commercialized by Johnson & Johnson, was the first nanotherapeutic approved by FDA in 1995.[253] Doxil® was pioneer in the field of drug carriers in the US market and, in Europe, is commercialized under the name Caelyx®.[254] At the beginning, Doxil® was approved for the treatment of AIDS-related Kaposi's sarcoma[255] and, later on, for recurrent ovarian cancer (1998)[256], metastatic breast cancer (2003)[257] and multiple myeloma (2007)[258]. This system is based on a PEGylated liposome containing DOX in the internal cavity and has a mean diameter of about 80 to 90 nm.[259] Doxil® liposome is composed of three main lipid components: the hydrogenated soy phosphatidylcholine (HSPC); cholesterol and 1,2-distearoyl-*sn*-glycero-3-phosphoethanolamine-N-(methoxy-PEG) (DSPE-PEG) (Figure 8). These lipids are considered safe once they do part of the diet and they are present on the cell membrane. The molar ratios (56: 38: 5) among them are responsible for maintaining the liposome structure.[259,260] The rigid bilayer at physiological temperature is achieved by the ratio between HSPC and cholesterol. DSPE is incorporated in the liposome bilayer and works as a docking point for PEG conjugation. Doxil® was conceived considering three objectives: to avoid the retention by the mononuclear phagocyte system and, as consequence, to prolong the circulation time; to achieve a high and stable loading of DOX; and to have the lipid bilayer in a "liquid order" phase. All of these requirements were achieved using: PEGylation to improve the biodistribution; the transmembrane ammonium-sulphate ($(NH_4)_2SO_4$) gradient driven force for DOX encapsulation; and the use of HSPC which exhibits a high phase transition temperature (melting temperature, Tm).[259]

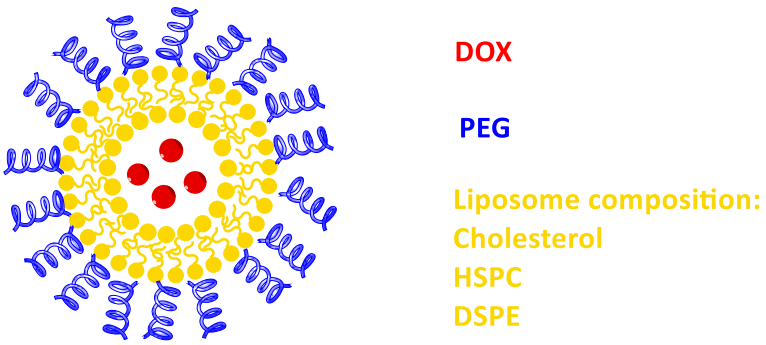

Figure 8. Illustration of a PEGylated Doxil® liposome.

Interestingly, Barenholz and co-workers[259] developed a remote drug loading approach which was responsible for the high efficiency and stable drug loading. This method relies on a transmembrane gradient of $(NH_4)_2SO_4$, which involves a higher concentration of $(NH_4)_2SO_4$ inside the liposome when compared with the outside. This difference between the concentration in both compartments works as a driving force for the loading of DOX. With this loading technique, it was possible to reach a very high accumulation of DOX in the core (around 15 000 DOX molecules/liposome).

According to literature, more than ten Phase I/II clinical trials were performed in patients suffering from AIDS-related Kaposi's sarcoma. Overall, patients treated with Doxil® formulation presented improved responses when compared with conventional chemotherapy.[261] Passing to the Phase III clinical trials, two independent randomized studies were performed.[227,228] Stewart and colleagues[227] evaluated if Doxil® could be an effective approach when compared with the traditional bleomycin and vincristine treatment. They studied 241 patients in a randomized study where 20 mg/m^2 of Doxil® was administered against the combination of 15 IU/m^2 bleomycin with 1.4 mg/m^2 vincristine. In another study performed by Northfelt *et al.*[228], Doxil® efficacy was accessed versus the conventional treatment with DOX, bleomycin and vincristine. A total of 258 patients with AIDS-related Kaposi's sarcoma participated in the study. The treatment consisted in the administration of 20 mg/m^2 Doxil® versus the combination of 20 mg/m^2 DOX, 10 mg/m^2 bleomycin and 1 mg vincristine. In both studies, Doxil® improved the treatment, being more effective and less toxic than traditional chemotherapy. Regarding ovarian cancer treatment, Gordon and colleagues[230] performed a Phase III clinical trial with the purpose of evaluating the long-term survival. The study was performed with a total of 481 patients randomly distributed in two groups. In the first group, 50 mg/m^2 Doxil® was administered every 4th week; in the second group, 1.5 mg/m^2/day of topotecan was administered during 5 days, repeating the dose at every 3 weeks. This follow-up study demonstrated that treating patients suffering from recurrent and refractory ovarian cancer with Doxil® significantly improved the overall survival (OS) (from 70.1 weeks for topotecan to 108 weeks for Doxil® patients). Therefore, these results proved that Doxil® could be used as first-line treatment for this type of cancer. Also, O'Brien *et al.* [229] showed that Doxil® has higher efficacy and less cardiotoxicity than conventional DOX and that could be used as first-line treatment for metastatic breast cancer. In this Phase III clinical study, around 509 women received 50 mg/m^2 of Doxil® every 4 weeks or 60 mg/m^2 of DOX every 3 weeks. The results showed that Doxil® led to an overall reduction in cardiotoxicity and myelosuppression, and had an efficacy equivalent to that of DOX. Rifkin and co-workers[231] conducted a Phase III clinical trial in patients newly diagnosed with active multiple myeloma. The patients (n = 192) were split and exposed to two different treatment methodologies. In the first method, the treatment consisted in the combination of 40 mg/m^2 Doxil® with 1.4 mg/m^2 vincristine plus the reduction in the oral dose of dexamethasone (40 mg) in the first 4 days. The second methodology was based on 0.4 mg/day vincristine, 9 mg/m^2/day DOX and, also, a reduction in the dexamethasone dose for 4 days. At the end, both approaches gave a similar response, less toxicity and improved overall survival when compared with conventional treatment with DOX.

Doxil® approval was the primary step to launch other nanomedicines. Following Doxil®, several other lipid-based systems were created, either based on stealth liposomes with a cocktail of loaded drugs or on liposomes with loaded drugs and targeted moieties conjugated at the surface.

7.2. Myocet®

Five years after Doxil® approval, Myocet® (Teva Pharma), a non-PEGylated liposomal DOX, was approved in Europe by the EMA and in Canada.[233] Myocet® liposome presents a diameter size around 150-250 nm and is composed by cholesterol, egg phosphatidylcholine (PC) and, in the interior, a DOX citrate complex (Figure 9).[262]

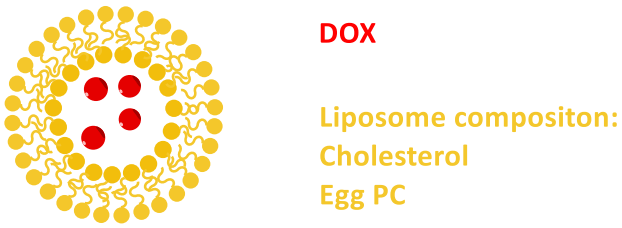

Figure 9. Representation of the Myocet® liposome.

This formulation was approved as first-line treatment for metastatic breast cancer in combination with cyclophosphamide (CPP).[235,263] Bearing in mind the results from preclinical stage[264], a Phase I clinical trial[265] was conducted in 38 patients with refractory solid tumours. The study was made using two different approaches. The first consisted in intravenous (*i.v.*) administration of a dosage of 20 mg/m^2 escalating to 30, 45, 60, 75 and 90 mg/m^2 every 3 weeks. The second involved a consecutive administration for three days, starting with 20, then 25 and then 30 mg/m^2/day. The maximum-tolerated dose (MTD) was achieved by detection of leukopenia. In the first approach, the maximum dose was 90 mg/m^2 and for the second was 25 mg/m^2/day. In general, Myocet® was well tolerated and revealed fewer symptoms (nausea, vomiting and stomatitis) than free DOX. Cardiotoxicity wasn't detected in any of the patients. Phase III clinical trials were carried on by different research groups.[232,234,235] In the first study accomplished by Batist *et al.*[232], the purpose was to evaluate if the combination of Myocet® and CPP could significantly reduce DOX cardiotoxicity and, at the same time, the improvement of the antitumor efficacy as first-line therapy for metastatic breast cancer. In this study, 297 patients received conventional DOX or Myocet® (60 mg/m^2, *i.v.*) and, additionally, a 600 mg/m^2 dose of CPP every 3 weeks. Both groups revealed a similar response, but the Myocet® group demonstrated less cardiac toxicity. Another Phase III clinical trial developed by Harris *et al.*[234] consisted in the i.v. administration of 75 mg/m^2 Myocet® or DOX each 3rd week for the treatment of metastatic breast cancer. The obtained results revealed a comparable reaction for both groups, being more satisfactory the cardiotoxicity results of the Myocet® group. A few years later, one more Phase III clinical trial was carried on by Chan *et al.*.[235] In this study, they compared the combined effect of 75 mg/m^2 Myocet® and CPP against 75 mg/m^2 epirubicin and CPP (600 mg/m^2 for both approaches) as first-line treatment for metastatic breast cancer. A total of 160 patients were randomized either to receive the first combined approach, either the second, every 3 weeks. At the end, the combination of

Myocet® and CPP revealed to be a more promising approach as first-line treatment since it gathers the dose-effect dependability of DOX with the safety of epirubicin. All the previous clinical trials demonstrated that Myocet® could be a good candidate for substitution of the traditional DOX.

7.3. ThermoDox®

ThermoDox® was developed by Celsion Corporation and consists of thermosensitive liposomes with DOX that have a mean diameter size of 100 nm.[266] The liposomes are composed of 1,2-dihexadecanoyl-sn-glycero-3-phosphocholine (DPPC), 1-stearoyl-2-hydroxy-sn-glycero-3-phosphocholine (MSPC) and DSPE-PEG, at molar ratios of 86: 10: 4, respectively. These systems are described as low temperature-sensitive liposomes (LTSL) since, when exposed to a relatively high temperatures (≈42°C), become leaky and release the encapsulated drug.[267,268] The phase transition temperature (Tm) of phospholipids is very important. In LTSL systems, the transition temperature of lipids is usually around 40 to 45°C and it is for this reason that they are used.[269,270] Phospholipids can exist in a fluid state (when the temperature is higher than their Tm) or in a gel state (when the temperature is lower than their Tm). Temperature sensitive liposomes should exist in the gel state at body temperature to retain the drug while they are circulating in the bloodstream. If the temperature rises and reaches the Tm value, then the liposome changes to the fluid state and the drug is released.

ThermoDox® formulation was conceived for the treatment of primary liver cancer (hepatocellular carcinoma, HCC) and also for recurring chest wall breast cancer. Part of the typical treatment for these pathologies is based on the use of radiofrequency ablation combined with chemotherapy.[267,271] In this context, ThermoDox® liposomes are delivered by *i.v*. administration and, due to defective vasculature, they accumulate in the tumour site. Afterwards, a source of heat is applied and in response to that stimuli, the drug is released nearby and inside of the tumour tissue (Figure 10). The key goal of ThermoDox® is to achieve the micro-metastases which are the main responsible for cancer recurrence.

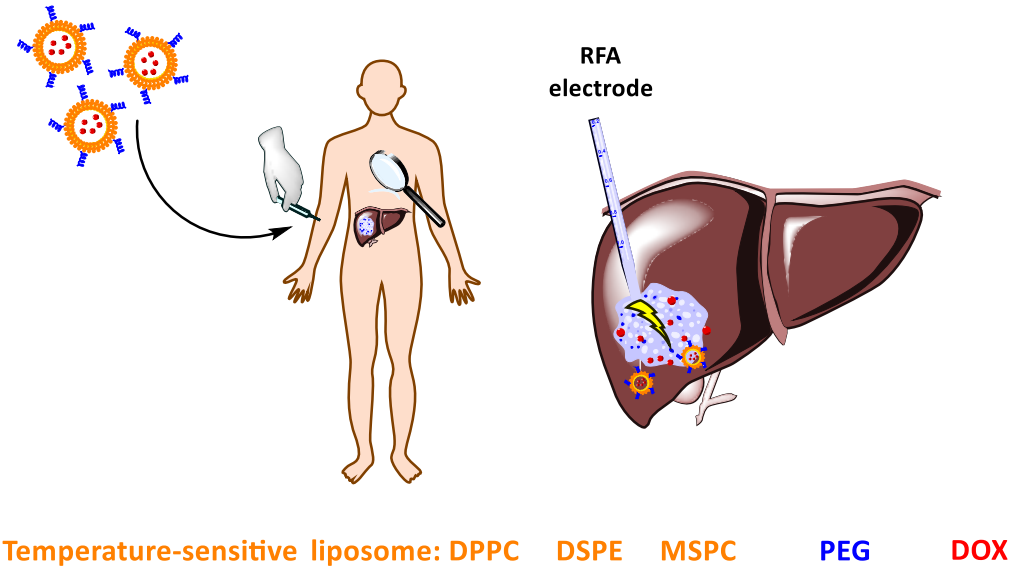

Figure 10. Illustrative mechanism to trigger ThermoDox®.

In 2009, FDA gave the status of Orphan drug (a drug developed to treat a rare medical condition) to ThermoDox® for treatment of HCC. Several clinical studies with ThermoDox® are currently ongoing, although the results have not yet been disclosed. The Phase I/II DIGNITY study (NCT00826085)[238] involved ThermoDox® and microwave hyperthermia for the treatment of breast cancer recurrence at the chest wall. Another study which is ongoing is Phase III OPTIMA study (NCT02112656)[236] which is using ThermoDox® and radiofrequency ablation (RFA) for treatment of HCC. Still another study, the Phase I HEAT study (NCT00617981)[237], started with 24 patients suffering from HCC and metastatic liver tumours. The data from this study was not published but according to Poon and Borys[266], the MTD was achieved at 50 mg/m^2. Due to the outstanding Phase I results, this project jumped directly to Phase III. Phase III study has just been completed but the result are not yet known. The study was conducted in 600 patients aiming at treating non-resectable HCC using ThermoDox® and RFA. If ThermoDox® and RFA had synergistic effects in the treatment, then maybe this approach can be used as front-line treatment.

7.4. Sarcodoxome™

GP Pharma has developed a new liposomal formulation containing DOX, Sarcodoxome™, for treating soft tissue sarcoma (STS). These liposomes are not PEGylated and contain lipochroman 6 to improve their stability. In this system, DOX is loaded in the walls of the liposome. In 2006, Sarcodoxome™ received the Orphan drug status by EMA and later on the same status was approved by FDA (2007). Phase I/II clinical trials were launched by GP Pharma in Spain.[272] A Phase II clinical trial[239] was performed in 37 patients with advanced or metastatic STS and with 65 years or older. In general,

Sarcodoxome™ revealed a safe and acceptable toxicity profile, an MTD of 80 mg/m^2 and no cardiotoxicity associated. However, further studies are needed with younger patients.

7.5. 2B3-101

Brain tumours are considered devastating diseases, only starting to reveal symptoms already at a late stage. As mentioned before, the BBB is a protective shield of the central nervous system (CNS), being responsible for blocking the passage into the CNS of strange and potentially harmful molecules. As a consequence, treating brain malignancies is a very big challenge.[273] As a way to overcome this issue, to-BBB Technologies is developing the 2B3-101 system which consists of a PEGylated liposomal DOX formulation conjugated to glutathione (GSH) as targeting ligand. It has an average diameter of 95 nm (Figure 11).[274,275] The technology behind 2B3-101 is entitled "G-technology" and explores existing GSH-transport mechanisms across the BBB.[274] This system was designed for targeting glioma brain and metastases.

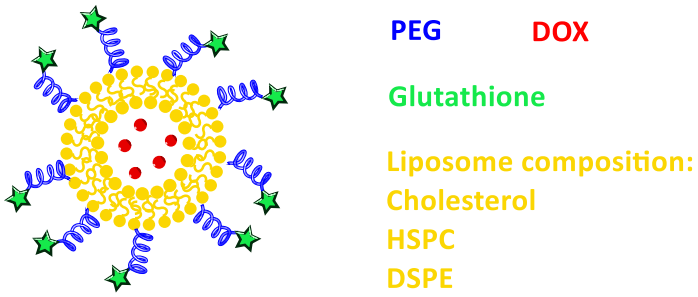

Figure 11. Schematic structure of GSH-PEG liposomal DOX.

The performance (affinity and uptake) of 2B3-101 was evaluated *in vitro* using human brain capillary endothelial cells.[275] Results suggested that the uptake of 2B3-101 is time-, temperature- and concentration-dependent. Overall, the presence of GSH really improved the efficacy of the 2B3-101 system, increasing the efficacy of DOX delivery. Further pharmacokinetic and brain uptake studies were performed *in vivo* with concentrations comparable to those tested *in vitro*. Moreover, the efficacy of 2B3-101 was studied *in vivo* in mice using a brain tumour model of glioblastoma multiform (GBM). Basically, U87MG cells (human glioblastoma cell line) were injected directly into the brain of athymic FVB mice, originating a high vascularized brain tumour. In this study the efficacy of free DOX, PEGylated liposomal DOX and 2B3-101 were compared. At the end, no neurological indicators were seen and both systems were well tolerated. However, the presence of GSH in 2B3-101 resulted in a superior efficacy. The aim of this study was not to determine the toxicity and, thus, no MTD was determined.[275] However, these promising results were the initial impulse for the beginning of the clinical trials. A phase I/IIa clinical trial[241] was performed in patients with solid tumours and brain metastases or recurrent malignant glioma. The patients received 40-70 mg/m^2 or 60 mg/m^2 dosages.

In general, 2B3-101 was considered safe and it was well tolerated. For phase IIa trial, the recommended doses were based on the tolerability of the previous results. The 2B3-101 system is also being studied for the treatment of meningeal carcinomatosis (NCT01818713).[240] In this Phase II clinical trial, the aim is to evaluate the primary efficacy of 2B3-101 in patients suffering from leptomeningeal metastases of breast cancer. According to the clinical trials website, just a few patients received the treatment (n = 6). A single-dose of 50 mg/m^2 was administered intravenously every 3 weeks. Up to date, no results were published.

7.6. Anti-EGFR immunoliposomes-DOX

The conjugation of monoclonal antibody fragments (mAb) to liposomes result in immunoliposomes (ILs). These anti-EGFR immunoliposomes-DOX, now in phase II clinical trial, are based on liposomes made of cholesterol and PC conjugated to a monoclonal antibody (mAb) against the epidermal growth factor receptor (EGFR) (Figure 12).[276] These liposomes present an average diameter of 100-120 nm.[277] They can target the EGFR overexpressing tumours and, at the same time, they can be used as drug carriers.[278]

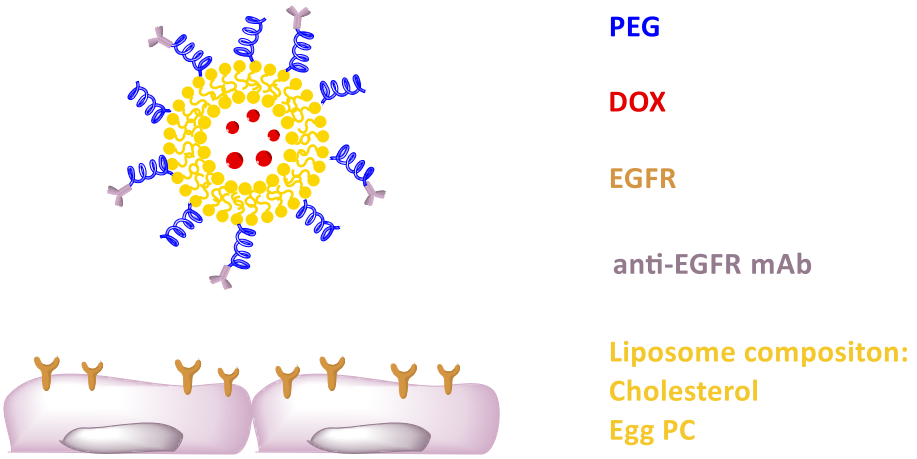

Figure 12. Scheme showing the interaction of anti-EGFR ILs-DOX with cells.

Mamot *et al.* studied the delivery of DOX from the anti-EGFR ILs-DOX system (Hermes Bioscience). According to these *in vitro* studies[278], a higher DOX internalization (about 29- fold more) was achieved in the presence of the EGFR ligand in EGFR-overexpressing cell lines (MDA-MB-468 human breast cancer and U87MG human GBM). In the *in vivo* studies[279], healthy rats revealed similar pharmacokinetic profiles between the liposomal DOX with and without EGFR ligand, suggesting that the mAb fragment was not crucial for biodistribution stability. The therapeutic efficacy of the anti-EGFR ILs-DOX was evaluated by using the cancer cell lines previously used, but this time as xenograft models. The results clearly showed that anti-EGFR ILs-DOX could significantly inhibit the tumour size and overcome the problem of multidrug resistance.[280] Considering the positive results, this anti-EGFR

ILs-DOX system proceeded for Phase I clinical trial.[242] The main goal of this study was to determine the MTD in patients with EGFR-overexpressing advanced solid tumours. In this trial, 26 patients were treated with *i.v.* administration of anti-EGFR ILs-DOX. The concentration was scaled up (5-60 mg/m^2 DOX equivalents) over the six cycles. Interestingly, was the absence of cardiotoxicity, cumulative toxicity or alopecia. The suggested anti-EGFR ILs-DOX concentration for Phase II clinical trial was 50 mg/m^2, which corresponds to the MTD.

7.7. MM-302

Merrimack Pharmaceuticals™ designed a new drug delivery system, MM-302. This system displays an average size of 75-110 nm and is a HER2-targeted antibody-liposomal doxorubicin conjugate. HER2 is the human epidermal growth factor receptor-2 that may be overexpressed in breast cancer (Figure 13).[281] The targeting is accomplished by attaching a single-chain antibody fragment (scFv) of HER2 via a polyethylene glycol spacer (PEG-DSPE) to the DOX-loaded ILs surface.[276]

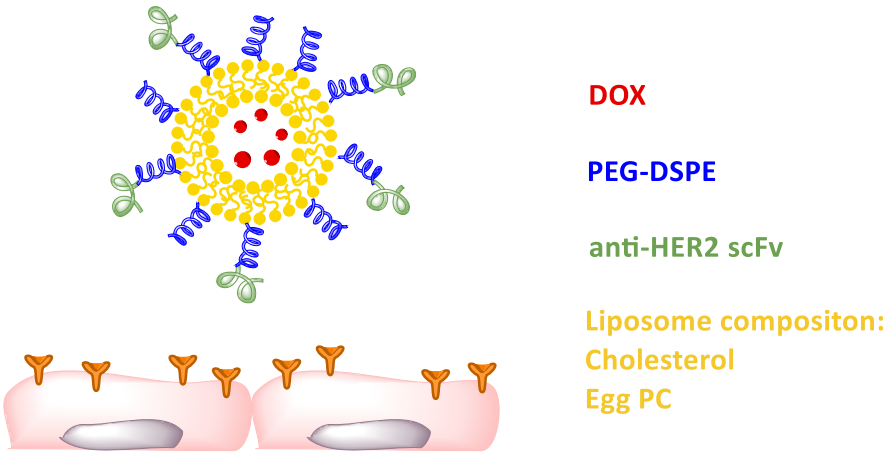

Figure 13. Illustration of the interaction of MM-302 with HER2 overexpressing cells.

In vitro studies revealed that the MM-302 liposomes were bind and internalized by HER2 overexpressing cells in a greater extent than the control.[282,283] According to the pharmacokinetic results in rats, there was no difference between the clearance rates of MM-302 and the control. Furthermore, the targeting capacity of MM-302 liposomes was extensively studied in four different human HER2-positive breast cancer xenograft models. These studies confirmed the selectivity for HER2 positive cells and, as a result, in some cases, a significant decrease in tumour growth.[282,283] According to Phase I trial[284] results reported at the San Antonio Breast Cancer Symposium in 2012, it was found that MTD was 40 mg/m^2. In this trial, 14 patients with positive HER2 advanced breast cancer received the MM-302. The administered dosage was 8, 16, 30 and 40 mg/m^2 every 4 weeks. In general, the results obtained suggested no cardiotoxicity associated up to the maximum dose administered.

Phase II clinical trial[243] (HERMIONE study) consisted in the random administration of MM-302 plus trastuzumab in patients with locally advanced/metastatic HER2-positive breast cancer. The main key points of this study were to assess the progression-free survival (PFS), the OS and also the safety, tolerability, quality of life and pharmacokinetic profile. For MM-302, the selected dose was 30 mg/m^2 every 3 weeks, and the combination with trastuzumab was also administered every 3 weeks. At the end, results demonstrated that the combination of both novel MM-302 and trastuzumab therapy could be well-tolerated and more effective. Unfortunately, the latest news were that "MM-302 misses endpoint in Phase II HERMIONE trial" according to the ADCreview website.[244] In this website, the article reports that after a recommendation of the independent monitoring panel "Data and Safety Monitoring Board" (DSMB), the Merrimack Pharmaceuticals decided to stop the Phase II HERMIONE clinical trial. The decision was taken considering that there were no improved safety signals after the treatment.

7.8. Livatag®

The translational process of nanoparticles (NPs) for clinical studies is still not so straightforward. So far, few nanoparticle formulations achieved clinical trials. Livatag® is a NP formulation of DOX (Transdrug™ technology) developed by BioAlliance Pharma S.A. (later on Onxeo Company) that consists in DOX-loaded polyisohexylcyanoacrylate (PIHCA) NPs with 300 nm size (Figure 14).[285] The Transdrug™ technology relies on the use of NPs to overcome drug resistance, facilitating cell penetration and cell-drug contact.

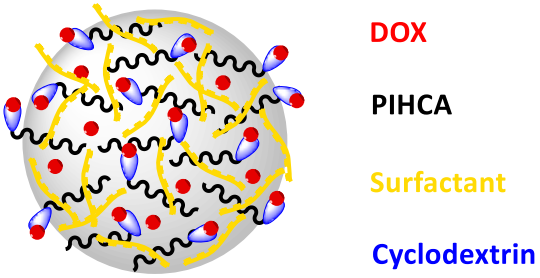

Figure 14. Representative scheme of PIHCA NPs loaded with DOX.

Livatag® received the status of Orphan drug in Europe in 2004 and in the US in 2011. This NP formulation was developed with the aim to treat patients with primary liver cancer.[286] In Phase I clinical trial (ReLive study), Kattan and colleagues[285] have studied the effect of Livatag® in patients with refractory solid tumours. A total of 21 patients have received the formulation by *i.v.* administration with an initial dose of 15 mg/m^2 (30, 45, 60, 75 and 90 mg/m^2) every 4 weeks. The MTD revealed neutropenia at 90 mg/m^2. Consequently, for further Phase II trial, it was suggested a dose of 75 mg/m^2. According to the Onxeo website[287], the results from Phase II showed an increase in the survival time

of patients with HCC. After that, a Phase III clinical trial was launched in 2012, in the US and Europe. This trial was designed to study the efficacy of Livatag® in 400 patients with HCC at advanced stage. At an early stage, Phase III results exhibit good results and tolerance. Unfortunately, in September 11, 2017, Onxeo Company announced that ReLive study did not met the principal purposes which were to improve the overall patient's survival when compared to the control group.[245] The final results from ReLive study were presented at the 11th Annual Conference of the International Liver Cancer Association in Seoul, South Korea (ILCA 2017).[246]

7.9. PK1

Currently, few anticancer-drug conjugates achieved the clinical phase. A few years back, Kopeček[288] and co-workers started the investigation on (N-(2-hydroxypropyl) methacrylamide) (HPMA) synthesis. Later on, fruit of collaborations with Duncan *et al*., a patent application arise (1985).[289] Until now, two types of HPMA copolymers conjugates were developed and reach the clinical trial stage. PK1 (Pfizer Inc.) was the first to be designed and consists in a HPMA backbone in which DOX is conjugated through a peptide linker (Gly-Phe-Leu-Gly) (Figure 15). This linker is stable at physiological pH but can be cleaved in the lysosomes by the lysosomal enzymes. PK1 presents a molecular weight (MW) ~ 30,000 g/mol and DOX content around 8.5 wt%.[290] At preclinical stage[291], this nanotherapeutic revealed to be promising when compared to the conventional drug. In a Phase I clinical trial[290], PK1 was administered to 36 patients with refractory or resistant cancer by *i.v.* administration with an interval of 3 weeks between cycles. The object of study was to determine the pharmacokinetic profile of PK1 and the toxicity associated with the determination of the MTD and dose-limiting toxicities (DLTs). At the beginning of the treatment, 20 mg/m^2 of PK1 were administered and increased until reaching 320 mg/m^2. At this step, few toxic effects were registered namely, mucositis and febrile neutropenia. Interestingly is that no cardiotoxicity was observed even at 1680 mg/m^2. Based on these results, the recommended dose to Phase II was 280 mg/m^2, to be implemented in patients with colorectal, non-small cell lung cancer (NSCLC) and breast cancer patients. In Phase II clinical trials[247], this recommendation was considered and 62 patients were divided into the three cancer types: breast (n = 17), NSCLC (n = 29) and colorectal (n = 16) cancer. The response was favourable in few cases (3 for breast and 3 for NSCLC) and no response for colorectal patients. In contrast, these studies demonstrated that the administration of high doses of PK1 (>20 g/m^2) did not triggered any toxicity related to the polymer or even immunogenicity.

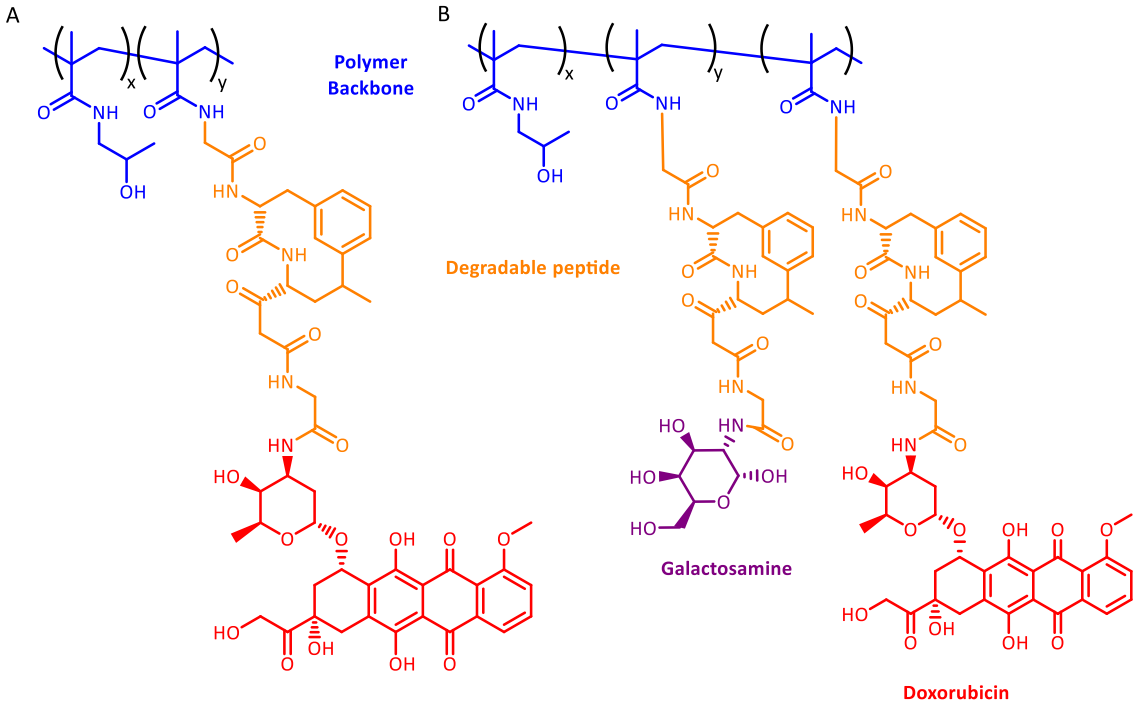

Figure 15. A) HPMA copolymer–DOX (PK1) structure; B) HPMA copolymer–DOX structure containing galactosamine (PK2) to promote liver targeting.

7.10. PK2

Bearing in mind the PK1 system and the positive results achieved, PK2 (Pfizer Inc.) was developed, being structurally similar to PK1 but with an additional galactosamine residue (Figure 15). This residue introduction is supposed to facilitate and improve the efficacy of the system by targeting the hepatocyte asialoglycoprotein receptors for hepatic cancer treatment. The MW of PK2 is about 25,000 g/mol with a DOX content of ≈7.5% and 1.5-2.5 mol% of galactosamine content.[248] PK2 is the first drug conjugate which was designed for active targeting. In preclinical studies with mice, reduced cardiotoxicity was observed when using PK2.[292] In a Phase I study[248], the pharmacokinetic profile, toxicity and the targeting specificity were evaluated in 31 patients with primary or metastatic liver cancer. PK2 was administered by *i.v.* with an initial concentration of 20 mg/m^2 (DOX equivalents) every 3 weeks. Consequently, with the escalation of the concentration (160 mg/m^2, further MTD) some side effects started to appear, such as severe fatigue, neutropenia and mucositis. Moreover, after 24 h injection, the biodistribution revealed that approximately 16.9% of the PK2 drug was targeting the liver, while the untargeted control did not. For further Phase II trials, a 120 mg/m^2 dosage was recommended to be administered every 3 weeks.

7.11. SP1049C

Nowadays, the number of copolymers used to produce micelles is increasing tremendously. The translational process from the laboratory to the clinical trial must be meticulously assessed due to the correlation between the risks and benefits[293]. Unfortunately, not all the nanomaterials exhibit the requested features for further clinical application. Alakhov and co-workers[294] developed a new micellar DOX formulation termed SP1049C that was manufactured by Supratek Pharma Inc.. This system consisted in the combination of two different Pluronic® copolymers, i.e., Pluronic® L61 and Pluronic® F127. Fundamentally, pluronics consist in ternary copolymers of poly(ethylene oxide) (PEO) and poly(propylene oxide) (PPO). Each of these segments is responsible for one part of the micelle formation. The PPO segment is hydrophobic and will assemble forming the hydrophobic core, whereas the PEO segment is hydrophilic and will be responsible for the corona formation (Figure 16).[295] The ratio Pluronic® L61:Pluronic® F127 used to obtain the desired polymeric micelle was 1:8 (w/w). Afterwards, DOX was loaded into the hydrophobic core by noncovalent interactions achieving a diameter of 22-27 nm.[294]

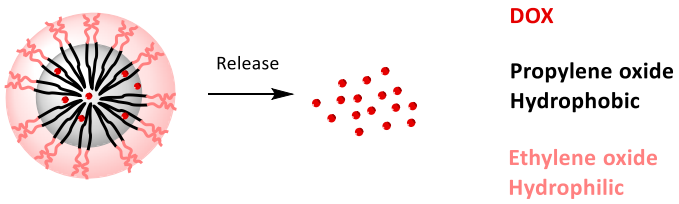

Figure 16. Schematic representation of drug-loaded polymeric micelle.

In vitro assays demonstrated that SP1049C had an improved efficacy when compared to free DOX.[296] Furthermore, the preclinical *in vivo* studies showed that the antitumor efficacy improved with SP1049C usage.[294,297] SP1049C had antitumor potential especially for treating adenocarcinoma in the oesophagus and gastroesophageal junction. In Phase I clinical trials[298] the goal was to assess all the pharmacokinetics and toxicity profiles, specifically, the DLTs and MTD. The study started with 28 patients with refractory tumours and a 5 mg/m^2 (DOX equivalents) dose every 3 weeks till reaching the 6th cycle. When the maximum dose was administered (90 mg/m^2), some toxic effects were observed, such as myelosuppression. Considering these results, a Phase II clinical trial was proposed but with a DLT around 70 mg/m^2. The Phase II clinical trials[249] included 21 patients with adenocarcinoma in the oesophagus and gastroesophageal junction. In this study, a 75 mg/m^2 (DOX equivalents) dose was injected every 3 weeks. Despite neutropenia manifestation, this Phase II revealed that SP1049C was really effective as monotherapy for the previously mentioned types of cancer. A Phase III clinical trial is currently under way for metastatic adenocarcinoma of the oesophagus, gastroesophageal junction and stomach. In the meantime, FDA approved SP1049C as an orphan drug for gastric cancer.

7.12. NK911

The NK911 (Nikon Kayaku Co. Ltd.) is a polymeric micellar formulation of DOX. This system is made of a copolymer of PEG (MW ~ 5000 g/mol) and polyaspartic acid (ASP) (Figure 17). To achieve a higher hydrophobicity, DOX was partially conjugated in the side chains of ASP (~ 45%). Therefore, when the copolymer is dissolved in water, it will assemble as a micelle with a high hydrophobic inner core. The hydrophobicity of the core will provide additional accommodation to encapsulate free DOX. As a result, the DOX which will be responsible for the antitumor activity is the loaded one, since the conjugated one does not reveal any activity. This lack of response is probably due to the stable coupling of DOX to the backbone of the polymer. NK911 exhibits a small size, nearby 40 nm in diameter, which is within the NPs size for passive targeting by the EPR effect.[299]

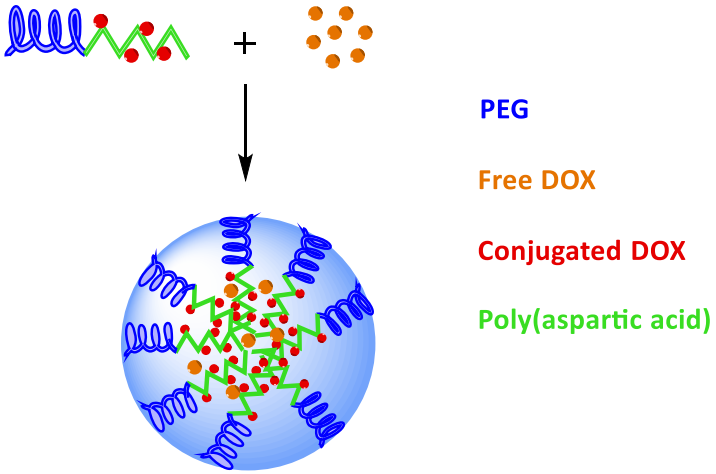

Figure 17. Schematic representation showing the structure of NK911.

This NK911 system successfully accumulated in solid tumours in mice. Bearing this in mind, this formulation was considered for Phase I clinical trial. In this study, a total of 23 patients with metastatic or recurrent solid tumours were followed. The aim was to analyse the pharmacokinetic profile of NK911 nanotherapeutics through the MTD and the DLTs. The treatment consisted in *i.v.* administration of the NK911 formulation, starting with 6 mg/m^2 DOX equivalent every 3 weeks. The haematological side effect most common was neutropenia when the doses were increased till 50 to 67 mg/m^2 DOX equivalents. Other associated effects were mild alopecia, anorexia and stomatitis. In general, NK911 was well tolerated and presented a good safety profile. A Phase II clinical trial was proposed with a recommended dosage of 50 mg/m^2 every 3 weeks, however, it is uncertain if the clinical trials proceeded.[250]

7.13. Bacterially-derived EDV™ minicells

Over the years, a huge effort has been done towards the development of new nanocarrier systems. MacDiarmid and colleagues[300] accomplished a novel technology based on a bacterially-derived nanoplatform (EDV™ minicells, EnGeneIC) for drug/gene encapsulation with specific targeting ability (Figure 18). These systems are obtained through a genetically *min*CDE-chromosomal deletion mutant from: *Salmonella enterica serovar Typhimurium* (S. Typhimurium); *Escherichia coli*; *Shigella flexneri*; *Pseudomonas aeruginosa* (Gram-negative) and *Listeria monocytes* (Gram-positive) strains. Essentially, bacterial minicells are anucleate NPs that present a uniform diameter (~400 nm), acquired by the inactivation of the genes that control normal bacterial cell division, therefore depressing the polar sites of cell fission. They are produced with high yields from both Gram-positive and Gram-negative bacteria. After the production and purification process, the minicells can be lyophilized and stored for about 4 months. They can be used as vectors for a wide range of chemotherapeutics with different charge, structure, solubility and hydrophobicity. The encapsulation process occurs by unilateral diffusion and shows to be dependent on concentration and time of incubation with the drug.

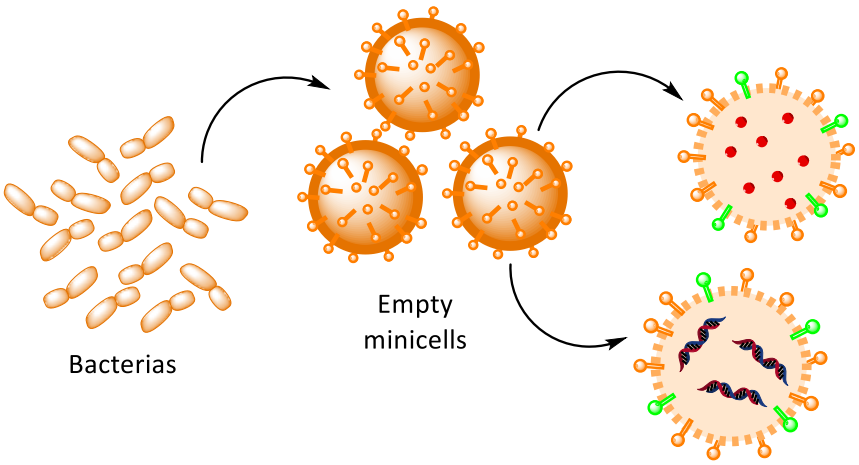

Figure 18. Scheme showing bispecific antibody-targeted, drug/siRNA-packaged minicells.

The targetability of these systems is accomplished by using bispecific antibodies, in which one arm will recognize the surface lipopolysaccharide (LPS), and the other will recognize a cell-surface receptor specific for the targeted cell, such as EGFR.[301] A single minicell can accommodate approximately 1 million molecules of DOX.[300] Once in the tumour microenvironment, the endocytosis process is triggered by the binding of the targeted-minicell to the specific antibody receptor present on the tumour cell surface. According to the *in vitro* studies (MDA-MB-468 breast, SKOV-3 ovarian, A549 lung, and HL-60 promyelocytic leukaemia cancer cell lines), minicells are internalized and degraded by the endosomes/lysosomes and, as a result, the cargo is released into the cytosol.[300,302] *In vivo* studies were performed with targeted DOX-loaded minicells to evaluate the antitumor potential. These experiments resulted in a huge inhibition and regression of the tumour growth either for mice

with cancer xenografts (breast, lung, ovarian and breast) and for dogs with Non-Hodgkin's lymphoma (NHL).[300] Besides cancer models, healthy pigs were also used to evaluate the safety of the *i.v.* administration of minicells. Despite the five consecutive *i.v.* administrations, pigs tolerate well and didn't reveal side effects for all haematological indices, serum chemistries, growth and food intake. The same was verified for the NHL dogs. Furthermore, there is the need to highlight that more exhaustive toxicology and stability studies are necessary for using this bacterial minicell in humans. The previous *in vitro* and *in vivo* results were responsible for the achievement of the "first-in-man" clinical trial. This study was based on EDV with the anti-human EGFR Erbitux and paclitaxel ($^{Erbitux}EDV_{Paclitaxel}$).[303] Another Phase I clinical trial which is currently under progress is the CerebralEDV study (NCT02766699).[251] The purpose of this research is to study the safety and tolerability of the EDV minicell (EGFR(V)-EDV-DOX ($^{V}EDV_{DOX}$)) packaged with DOX and coupled to panitumumab/Vectibix (V) to target the EGFR protein on the tumour cell membrane. The choice of the EGFR as target moiety and the Vectibix as the antibody are based on the literature, where EGFR seems to be important for GBM.[304,305] In this study, the patients with recurrent or progressive GBM randomly received one of two $^{V}EDV_{DOX}$ doses ($5x10^9$ or $8x10^9$) by *i.v.* administration, once a week for a period of 8 weeks. In general, $^{V}EDV_{DOX}$ was well tolerated and no severe side effects were reported, being the most common, fever, nausea and chills. However, MTD was not achieved. In summary, this Phase I trial revealed that $^{V}EDV_{DOX}$ can be administered to the patients with no severe risks.[251] Nevertheless, further research is needed to validate the safety of this novel technology. Meanwhile, in 2017, FDA approved the $^{EGFR}EDV_{DOX}$ minicells as an orphan drug status for the treatment of GBM.

8. Conclusions and future perspectives

Nanomedicine stands up as a novel and revolutionary area able to offer new opportunities for patient treatment. In the context of cancer, the introduction of nanomaterials as carriers for conventional drugs is extending the possibility of their use, by improving their efficacy and safety. This is the case of doxorubicin, an anthracycline widely applied in cancer treatment which has been associated to the occurrence of severe side effects. Although there is a long road to pursue until a nanotherapeutic reaches the market, a few DOX-based nanotherapeutics are now in the clinical scenario and others are currently under different phases of clinical trials. While liposomes are clearly ahead in the field of DOX-based nanotherapeutics, other nanoscale formulations are also now showing their applicability and specific advantages, such as nanoparticles, polymer-drug conjugates, micelles and nanocapsules from biological origin. Interestingly, one can notice that these DOX-nanotherapeutics are evolving, not only exploring the EPR effect to accumulate and exert their action in the tumour site, but they are getting smarter over time and equipped with new tools that allow them to overcome physiological barriers, respond to environmental stimuli and reach specific cells/molecular targets.

Meanwhile, research on the area of DOX-based nanotherapeutics is still very active and results are exciting. Given the number of publications that can be found in the literature, of which only representative examples are presented in this review, new and better solutions for the delivery of doxorubicin in cancer cells may be expected in the future, which will also possible be extended for the delivery of other drugs. Hopefully, in a medium/long-term, the future of cancer therapy will rely on personalized nanomedicine approaches, custom-made for each patient, and capable of treating not only primary tumours but also their metastases.

References

1 World Health Organization - Fact Sheets by Cancer, http://globocan.iarc.fr/Pages/fact_sheets_cancer.aspx, (accessed 6 March 2018).

2 National Cancer Institute, What Is Cancer?, https://www.cancer.gov/about-cancer/understanding/what-is-cancer, (accessed 31 July 2017).

3 I. D. González, R. S. Saez, E. M. Rodilla, E. L. Yges and F. L. Toledano, *Alergol Immunol Clin*, 2000, **15**, 161–181.

4 G. N. Hortobágyi, *Drugs*, 1997, **54**, 1–7.

5 S. A. Waksman and M. Tishler, *J. Biol. Chem.*, 1942, **142**, 519–528.

6 A. Di Marco, G. Cassinelli and F. Arcamone, *Cancer Treat. Rep.*, 1981, **65 Suppl 4**, 3–8.

7 C. Tan, H. Tasaka, K.-P. Yu, M. L. Murphy and D. A. Karnofsky, *Cancer*, 1967, **20**, 333–353.

8 F. Arcamone, G. Cassinelli, G. Fantini, A. Grein, P. Orezzi, C. Pol and C. Spalla, *Biotechnol. Bioeng.*, 1969, **11**, 1101–1110.

9 C. Carvalho, R. X. Santos, S. Cardoso, S. Correia, P. J. Oliveira, M. S. Santos and P. I. Moreira, *Curr. Med. Chem.*, 2009, **16**, 3267–3285.

10 O. Tacar, P. Sriamornsak and C. R. Dass, *J. Pharm. Pharmacol.*, 2013, **65**, 157–170.

11 C. F. Thorn, C. Oshiro, S. Marsh, T. Hernandez-Boussard, H. McLeod, T. E. Klein and R. B. Altman, *Pharmacogenet. Genomics*, 2011, **21**, 440–446.

12 F. Arcamone, G. Cassinelli, G. Franceschi, S. Penco, C. Pol, S. Redaelli and A. Selva, *Int. Symp. Adriamycin*, 1972, 9–22.

13 M. Cagel, E. Grotz, E. Bernabeu, M. A. Moretton and D. A. Chiappetta, *Drug Discov. Today*, 2017, **22**, 270–281.

14 T. G. Burke and T. R. Tritton, *Biochemistry*, 1985, **24**, 1768–1776.

15 F. Barcelo, I. Barcelo, F. Gavilanes, J. A. Ferragut, S. Yanovich and J. M. Gonzales-Ros, *Biochim. Biophys. Acta*, 1986, **884**, 172–181.

16 V. Rizzo, N. Sacchi and M. Menozzi, *Biochemistry*, 1989, **28**, 274–282.

17 K. K. Karukstis, E. H. Z. Thompson, J. A. Whiles and R. J. Rosenfeld, *Biophys. Chem.*, 1998, **73**, 249–263.

18 S. Shah, A. Chandra, A. Kaur, N. Sabnis, A. Lacko, Z. Gryczynski, R. Fudala and I. Gryczynski, *J. Photochem. Photobiol. B Biol.*, 2017, **170**, 65–69.

19 F. Yang, S. S. Teves, C. J. Kemp and S. Henikoff, *Biochim. Biophys. Acta*, 2014, **1845**, 84–89.

20 B. Andersson, *ESF Scientific Forward Look on Nanomedicine*, 2005.

21 R. A. Freitas, *Nanomedicine Nanotechnology, Biol. Med.*, 2005, **1**, 2–9.

22 T. Sun, Y. S. Zhang, B. Pang, D. C. Hyun, M. Yang and Y. Xia, *Angew. Chemie - Int. Ed.*, 2014, **53**, 12320–12364.

23 N. Bertrand, J. Wu, X. Xu, N. Kamaly and O. C. Farokhzad, *Adv. Drug Deliv. Rev.*, 2014, **66**, 2–25.

24 C. Burda, X. Chen, R. Narayanan and M. A. El-Sayed, *Chem. Rev.*, 2005, **105**, 1025–1102.

25 P. T. Wong and S. K. Choi, *Chem. Rev.*, 2015, **115**, 3388–3432.

26 E. K.-H. Chow and D. Ho, *Sci. Transl. Med.*, 2013, **5**, 216rv4.

27 G. Chen, I. Roy, C. Yang and P. N. Prasad, *Chem. Rev.*, 2016, **116**, 2826–2885.

28 S. Zhu, M. Hong, G. Tang, L. Qian, J. Lin, Y. Jiang and Y. Pei, *Biomaterials*, 2010, **31**, 1360–1371.

29 E. Allard-Vannier, S. Cohen-Jonathan, J. Gautier, K. Hervé-Aubert, E. Munnier, M. Soucé, P. Legras, C. Passirani and I. Chourpa, *Eur. J. Pharm. Biopharm.*, 2012, **81**, 498–505.

30 K. T. Al-Jamal, W. T. Al-Jamal, J. T.-W. Wang, N. Rubio, J. Buddle, D. Gathercole, M. Zloh and K. Kostarelos, *ACS Nano*, 2013, **7**, 1905–1917.

31 N. G. Yabbarov, E. D. Nikolskaya, O. A. Zhunina, I. G. Kondrasheva, I. A. Zamulaeva and E. S. Severin, *Russ. J. Bioorganic Chem.*, 2017, **43**, 155–162.

32 O. Gamucci, A. Bertero, M. Gagliardi and G. Bardi, *Coatings*, 2014, **4**, 139–159.

33 W. G. Roberts and G. E. Palade, *Cancer Res.*, 1997, **57**, 765–772.

34 R. K. Jain, *Cancer Metastasis Rev.*, 1987, **6**, 559–593.

35 T. Lammers, F. Kiessling, W. E. Hennink and G. Storm, *J. Control. Release*, 2012, **161**, 175–187.

36 S. Taurin, H. Nehoff and K. Greish, *J. Control. Release*, 2012, **164**, 265–275.

37 E. M. Renkin, *Am. Rev. Respir. Dis.*, 1992, **146**, S28-31.

38 L. Miao, C. M. Lin and L. Huang, *J. Control. Release*, 2015, **219**, 192–204.

39 F. Arcamone, *Med. Res. Rev.*, 1984, **4**, 153–188.

40 S. K. Hobbs, W. L. Monsky, F. Yuan, W. . G. Roberts, L. Griffith, V. ladimir P. Torchilin and R. K. Jain, *Proc. Natl. Acad. Sci. U. S. A.*, 1998, **95**, 4607–4612.

41 R. K. Jain and T. Stylianopoulos, *Nat. Rev. Clin. Oncol.*, 2010, **7**, 653–664.

42 L. M. Bareford and P. W. Swaan, *Adv. Drug Deliv. Rev.*, 2007, **59**, 748–758.

43 K. E. Uhrich, S. M. Cannizzaro, R. S. Langer and K. M. Shakesheff, *Chem. Rev.*, 1999, **99**, 3181–3198.

44 X. Li, Z. Yang, K. Yang, Y. Zhou, X. Chen, Y. Zhang, F. Wang, Y. Liu and L. Ren, *Nanoscale Res. Lett.*, 2009, **4**, 1502–1511.

45 F. Danhier, E. Ansorena, J. M. Silva, R. Coco, A. Le Breton and V. Préat, *J. Control. Release*, 2012, **161**, 505–522.

46 E. Buhleier, W. Wehner and F. Vöglte, *J. Chem. Inf. Model.*, 1978, **53**, 155–158.

47 G. R. Newkome, Z. Yao, G. R. Baker and V. K. Gupta, *J. Org. Chem.*, 1985, **50**, 2003–2004.

48 D. A. Tomalia, H. Baker, J. Dewald, M. Hall, G. Kallos, S. Martin, J. Roeck, J. Ryder and P. Smith, *Polym. J.*, 1985, **17**, 117–132.

49 R. Esfand and D. A. Tomalia, *Drug Discov. Today*, 2001, **6**, 427–436.

50 K. E. Sapsford, W. R. Algar, L. Berti, K. B. Gemmill, B. J. Casey, E. Oh, M. H. Stewart and I. L. Medintz, *Chem. Rev.*, 2013, **113**, 1904−2074.

51 J. B. Wolinsky and M. W. Grinstaff, *Adv. Drug Deliv. Rev.*, 2008, **60**, 1037–1055.

52 Y. Cheng, L. Zhao, Y. Li and T. Xu, *Chem. Soc. Rev.*, 2011, **40**, 2673–2703.

53 L. Han, R. Huang, J. Li, S. Liu, S. Huang and C. Jiang, *Biomaterials*, 2011, **32**, 1242–1252.

54 I.-H. Lee, M. K. Yu, I. H. Kim, J.-H. Lee, T. G. Park and S. Jon, *J. Control. Release*, 2011, **155**, 88–95.

55 I.-H. Lee, S. An, M. K. Yu, H.-K. Kwon, S.-H. Im and S. Jon, *J. Control. Release*, 2011, **155**, 435–441.

56 H. He, Y. Li, X.-R. Jia, J. Du, X. Ying, W.-L. Lu, J.-N. Lou and Y. Wei, *Biomaterials*, 2011, **32**, 478–487.

57 X. Li, M. Takashima, E. Yuba, A. Harada and K. Kono, *Biomaterials*, 2014, **35**, 6576–6584.

58 X. He, C. S. Alves, N. Oliveira, J. Rodrigues, J. Zhu, I. Bányai, H. Tomás and X. Shi, *Colloids Surf B Biointerfaces*, 2015, **125**, 82–89.

59 J. Nie, Y. Wang and W. Wang, *Int. J. Pharm.*, 2016, **509**, 168–177.

60 W. Hu, L. Qiu, L. Cheng, Q. Hu, Y. Liu, Z. Hu, D. Chen and L. Cheng, *Acta Biomater.*, 2016, **36**, 241–253.

61 X. Xu, J. Li, S. Han, C. Tao, L. Fang, Y. Sun, J. Zhu, Z. Liang and F. Li, *Eur. J. Pharm. Sci.*, 2016, **88**, 178–190.

62 S. P. Kuruvilla, G. Tiruchinapally, A. C. Crouch, M. E. H. ElSayed and J. M. Greve, *PLoS One*, 2017, **12**, e0181944.

63 Y. Pu, S. Chang, H. Yuan, G. Wang, B. He and Z. Gu, *Biomaterials*, 2013, **34**, 3658–3666.

64 L. M. Kaminskas, B. D. Kelly, V. M. McLeod, G. Sberna, D. J. Owen, B. J. Boyd and C. J. H. Porter, *J. Control. Release*, 2011, **152**, 241–248.

65 A. Agarwal, U. Gupta, A. Asthana and N. K. Jain, *Biomaterials*, 2009, **30**, 3588–3596.

66 F. Wang, X. Cai, Y. Su, J. Hu, Q. Wu, H. Zhang, J. Xiao and Y. Cheng, *Acta Biomater.*, 2012, **8**, 4304–4313.

67 O. Wichterle and D. Lím, *Nature*, 1960, **185**, 117–118.

68 T. R. Hoare and D. S. Kohane, *Polymer*, 2008, **49**, 1993–2007.

69 Y. Li, D. Maciel, J. Rodrigues, X. Shi and H. Tomás, *Chem. Rev.*, 2015, **115**, 8564–8608.

70 N. A. Peppas, P. Bures, W. Leobandung and H. Ichikawa, *Eur. J. Pharm. Biopharm.*, 2000, **50**, 27–46.

71 J. K. Oh, R. Drumright, D. J. Siegwart and K. Matyjaszewski, *Prog. Polym. Sci.*, 2008, **33**, 448–477.

72 E. Caló and V. V. Khutoryanskiy, *Eur. Polym. J.*, 2015, **65**, 252–267.

73 H. Saito, A. S. Hoffman and H. I. Ogawa, *J. Bioact. Compat. Polym.*, 2007, **22**, 589–601.

74 S. J. Lee, Y. Bae, K. Kataoka, D. Kim, D. S. Lee and S. C. Kim, *Polym. J.*, 2008, **40**, 171–176.

75 Y. Il Cho, S. Park, S. Y. Jeong and H. S. Yoo, *Eur. J. Pharm. Biopharm.*, 2009, **73**, 59–65.

76 C. Chun, S. M. Lee, C. W. Kim, K. Hong, S. Y. Kim, H. K. Yang and S.-C. Song, *Biomaterials*, 2009, **30**, 4752–4762.

77 H. T. Ta, C. R. Dass, I. Larson, P. F. M. Choong and D. E. Dunstan, *Biomaterials*, 2009, **30**, 3605–3613.

78 M. K. Kwak, K. Hur, J. E. Yu, T. S. Han, K. Yanagihara, W. H. Kim, S. M. Lee, S.-C. Song and H.-K. Yang, *Invest. New Drugs*, 2010, **28**, 284–290.

79 W. Park, K. S. Kim, B. Bae, Y. Kim and K. Na, *Eur. J. Pharm. Sci.*, 2010, **40**, 367–375.

80 J. Ding, F. Shi, C. Xiao, L. Lin, L. Chen, C. He, X. Zhuang and X. Chen, *Polym. Chem.*, 2011, **2**, 2857–2864.

81 F. P. Seib, E. M. Pritchard and D. L. Kaplan, *Adv. Funct. Mater.*, 2013, **23**, 58–65.

82 M. Jaiswal, F. Naz, A. K. Dinda and V. Koul, *Biomed. Mater.*, 2013, **8**, 045004.

83 D. Maciel, P. Figueira, S. Xiao, D. Hu, X. Shi, J. Rodrigues, H. Tomás and Y. Li, *Biomacromolecules*, 2013, **14**, 3140–3146.

84 J. Shi, W. Guobao, H. Chen, W. Zhong, X. Qiu and M. M. Q. Xing, *Polym. Chem.*, 2014, **5**, 6180–6189.

85 M. Gonçalves, P. Figueira, D. Maciel, J. Rodrigues, X. Shi, H. Tomás and Y. Li, *Macromol. Biosci.*, 2014, **14**, 110–120.

86 M. Gonçalves, D. Maciel, D. Capelo, S. Xiao, W. Sun, X. Shi, J. Rodrigues, H. Tomás and Y. Li, *Biomacromolecules*, 2014, **15**, 492–499.

87 W. Zhang, X. Zhou, T. Liu, D. Ma and W. Xue, *J. Mater. Chem. B*, 2015, **3**, 2127–2136.

88 J. Wu, A. Chen, M. Qin, R. Huang, G. Zhang, B. Xue, J. Wei, Y. Li, Y. Cao and W. Wang, *Nanoscale*, 2015, **7**, 1655–1660.

89 Y. Zhan, M. Gonçalves, P. Yi, D. Capelo, Y. Zhang, J. Rodrigues, C. Liu, H. Tomás, Y. Li and P. He, *J. Mater. Chem. B*, 2015, **3**, 4221–4230.

90 J. E. Mealy, C. B. Rodell and J. A. Burdick, *J. Mater. Chem. B*, 2015, **3**, 8010–8019.

91 S. Manchun, C. R. Dass, K. Cheewatanakornkool and P. Sriamornsak, *Carbohydr. Polym.*, 2015, **126**, 222–230.

92 Azizullah, Nisar-ur-Rehman, A. Haider, U. Kortz, S. Afridi, M. Sohail, S. A. Joshi and J. Iqbal, *Int. J. Pharm.*, 2017, **533**, 125–137.

93 Q. Lv, C. He, F. Quan, S. Yu and X. Chen, *Bioact. Mater.*, 2017, **3**, 118–128.

94 R. Duncan, *Nat. Rev. Drug Discov.*, 2003, **2**, 347–360.

95 R. Duncan, *Nat. Rev. Cancer*, 2006, **6**, 688–701.

96 H. Ringsdorf, *J. Polym. Sci. Polym. Symp.*, 1975, **51**, 135–153.

97 S. Wadhwa and R. J. Mumper, *Crit. Rev. Ther. Drug Carrier Syst.*, 2015, **32**, 215–45.

98 N. Larson and H. Ghandehari, *Chem. Mater.*, 2012, **24**, 840–853.

99 A. Domínguez, A. Fernández, N. González, E. Iglesias and L. Montenegro, *J. Chem. Educ.*, 1997, **74**, 1227–1231.

100 J. Ko, K. Park, Y.-S. Kim, M. S. Kim, J. K. Han, K. Kim, R.-W. Park, I.-S. Kim, H. K. Song, D. S. Lee and I. C. Kwon, *J. Control. Release*, 2007, **123**, 109–115.

101 G. Y. Lee, K. Park, S. Y. Kim and Y. Byun, *Eur. J. Pharm. Biopharm.*, 2007, **67**, 646–654.

102 P. Chytil, T. Etrych, Č. Koňák, M. Šírová, T. Mrkvan, J. Bouček, B. Říhová and K. Ulbrich, *J. Control. Release*, 2008, **127**, 121–130.

103 F.-Q. Hu, L.-N. Liu, Y.-Z. Du and H. Yuan, *Biomaterials*, 2009, **30**, 6955–6963.

104 D. Vetvicka, M. Hruby, O. Hovorka, T. Etrych, M. Vetrik, L. Kovar, M. Kovar, K. Ulbrich and B. Rihova, *Bioconjug. Chem.*, 2009, **20**, 2090–2097.

105 X.-B. Xiong, Z. Ma, R. Lai and A. Lavasanifar, *Biomaterials*, 2010, **31**, 757–768.

106 T.-H. Kim, C. W. Mount, W. R. Gombotz and S. H. Pun, *Biomaterials*, 2010, **31**, 7386–7397.

107 H. Zhang, F. Li, J. Yi, C. Gu, L. Fan, Y. Qiao, Y. Tao, C. Cheng and H. Wu, *Eur. J. Pharm. Sci.*, 2011, **42**, 517–526.

108 F. Perche, N. R. Patel and V. P. Torchilin, *J. Control. Release*, 2012, **164**, 95–102.

109 T. Etrych, V. Šubr, J. Strohalm, M. Šírová, B. Říhová and K. Ulbrich, *J. Control. Release*, 2012, **164**, 346–354.

110 X. Hu, R. Wang, J. Yue, S. Liu, Z. Xie and X. Jing, *J. Mater. Chem.*, 2012, **22**, 13303–13310.

111 L. Qin, F. Zhang, X. Lu, X. Wei, J. Wang, X. Fang, D. Si, Y. Wang, C. Zhang, R. Yang, C. Liu and W. Liang, *J. Control. Release*, 2013, **171**, 133–142.

112 A. Zou, Y. Chen, M. Huo, J. Wang, Y. Zhang, J. Zhou and Q. Zhang, *J. Pharm. Sci.*, 2013, **102**, 126–135.

113 H. Pan, M. Sima, J. Yang and J. Kopeček, *Macromol. Biosci.*, 2013, **13**, 155–160.

114 E. Ruiz-Hernández, M. Hess, G. J. Melen, B. Theek, M. Talelli, Y. Shi, B. Ozbakir, E. A. Teunissen, M. Ramírez, D. Moeckel, F. Kiessling, G. Storm, H. W. Scheeren, W. E. Hennink, A. A. Szalay, J. Stritzker and T. Lammers, *Polym. Chem.*, 2014, **5**, 1674–1681.

115 Y. Liang, X. Deng, L. Zhang, X. Peng, W. Gao, J. Cao, Z. Gu and B. He, *Biomaterials*, 2015, **71**, 1–10.

116 Y.-H. Shih, C.-L. Peng, P.-F. Chiang, W.-J. Lin, T.-Y. Luo and M.-J. Shieh, *Int. J. Nanomedicine*, 2015, **10**, 7443–7454.

117 Y. Zhu, J. Zhang, F. Meng, C. Deng, R. Cheng, J. Feijen and Z. Zhong, *J. Control. Release*, 2016, **233**, 29–38.

118 Y. Ma, X. Fan and L. Li, *Carbohydr. Polym.*, 2016, **137**, 19–29.

119 W. Wang, B. Wang, X. Ma, S. Liu, X. Shang and X. Yu, *Biomacromolecules*, 2016, **17**, 2223–2232.

120 L. Qiu, M. Zhu, K. Gong, H. Peng, L. Ge, L. Zhao and J. Chen, *Mater. Sci. Eng. C*, 2017, **78**, 912–922.

121 H. Zhang, J. Xu, L. Xing, J. Ji, A. Yu and G. Zhai, *J. Colloid Interface Sci.*, 2017, **492**, 101–111.

122 B. Qin, L. Liu, X. Wu, F. Liang, T. Hou, Y. Pan and S. Song, *Acta Biomater.*, 2017, **64**, 211–222.

123 J. Wu, C. Tang and C. Yin, *Acta Biomater.*, 2017, **47**, 81–90.

124 A. D. Bangham, *Nature*, 1961, **192**, 1197–1198.

125 A. D. Bangham and R. W. Horne, *J. Mol. Biol.*, 1964, **8**, 660–668.

126 T. P. Hoar and J. H. Schulman, *Nature*, 1943, **152**, 102–103.

127 R. Duncan and R. Gaspar, *Mol. Pharm.*, 2011, **8**, 2101–2141.

128 G. Verma and P. A. Hassan, *Phys. Chem. Chem. Phys.*, 2013, **15**, 17016–17028.

129 W. J. M. Mulder, G. J. Strijkers, G. A. F. Van Tilborg, D. P. Cormode, Z. A. Fayad and K. Nicolay, *Acc. Chem. Res.*, 2009, **42**, 904–914.

130 J. L. Arias, B. Clares, M. E. Morales, V. Gallardo and M. A. Ruiz, *Curr. Drug Targets*, 2011, **12**, 1151–1165.

131 Y. Han, Y. Zhang, D. Li, Y. Chen, J. Sun and F. Kong, *Int. J. Nanomedicine*, 2014, **9**, 4107–4116.

132 S. Vrignaud, N. Anton, P. Gayet, J.-P. Benoit and P. Saulnier, *Eur. J. Pharm. Biopharm.*, 2011, **79**, 197–204.

133 T. Wei, J. Liu, H. Ma, Q. Cheng, Y. Huang, J. Zhao, S. Huo, X. Xue, Z. Liang and X. J. Liang, *Nano Lett.*, 2013, **13**, 2528–2534.

134 X. Zhang, L. Li, C. Li, H. Zheng, H. Song, F. Xiong, T. Qiu and J. Yang, *Carbohydr. Polym.*, 2017, **155**, 407–415.

135 W. Ma, Q. Guo, Y. Li, X. Wang, J. Wang and P. Tu, *Eur. J. Pharm. Biopharm.*, 2017, **112**, 209–223.

136 H. Hatakeyama, H. Akita, E. Ishida, K. Hashimoto, H. Kobayashi, T. Aoki, J. Yasuda, K. Obata, H. Kikuchi, T. Ishida, H. Kiwada and H. Harashima, *Int. J. Pharm.*, 2007, **342**, 194–200.

137 Q. Li, Q. Tang, P. Zhang, Z. Wang, T. Zhao, J. Zhou, H. Li, Q. Ding, W. Li, F. Hu, Y. Du, H. Yuan, S. Chen, J. Gao, J. Zhan and J. You, *Biomaterials*, 2015, **57**, 1–11.

138 J. Sun, Y. Song, M. Lu, X. Lin, Y. Liu, S. Zhou, Y. Su and Y. Deng, *Eur. J. Pharm. Sci.*, 2016, **93**, 177–183.

139 A. Haeri, S. Zalba, T. L. M. ten Hagen, S. Dadashzadeh and G. A. Koning, *Colloids Surf B Biointerfaces*, 2016, **146**, 657–669.

140 S. Rizzitelli, P. Giustetto, D. Faletto, D. Delli Castelli, S. Aime and E. Terreno, *J. Control. Release*, 2016,

230, 57–63.

141 K. M. Camacho, S. Menegatti, D. R. Vogus, A. Pusuluri, Z. Fuchs, M. Jarvis, M. Zakrewsky, M. A. Evans, R. Chen and S. Mitragotri, *J. Control. Release*, 2016, **229**, 154–162.

142 Y. Zhao, W. Ren, T. Zhong, S. Zhang, D. Huang, Y. Guo, X. Yao, C. Wang, W.-Q. Zhang, X. Zhang and Q. Zhang, *J. Control. Release*, 2016, **222**, 56–66.

143 M. Peller, L. Willerding, S. Limmer, M. Hossann, O. Dietrich, M. Ingrisch, R. Sroka and L. H. Lindner, *J. Control. Release*, 2016, **237**, 138–146.

144 Y.-P. Fan, J.-Z. Liao, Y.-Q. Lu, D.-A. Tian, F. Ye, P.-X. Zhao, G.-Y. Xiang, W.-X. Tang and X.-X. He, *Mol. Ther. - Nucleic Acids*, 2017, **7**, 181–189.

145 A. Sesarman, L. Tefas, B. Sylvester, E. Licarete, V. Rauca, L. Luput, L. Patras, M. Banciu and A. Porfire, *Pharmacol. Reports*, 2017, **70**, 331–339.

146 K. Plourde, R. M. Derbali, A. Desrosiers, C. Dubath, A. Vallée-Bélisle and J. Leblond, *J. Control. Release*, 2017, **251**, 82–91.

147 Q. Xie, W. Deng, X. Yuan, H. Wang, Z. Ma, B. Wu and X. Zhang, *Eur. J. Pharm. Biopharm.*, 2018, **122**, 87–95.

148 J. Nam, N. Won, J. Bang, H. Jin, J. Park, S. Jung, S. Jung, Y. Park and S. Kim, *Adv. Drug Deliv. Rev.*, 2013, **65**, 622–648.

149 D. Chen, N. A. Monteiro-Riviere and L. W. Zhang, *Wiley Interdiscip. Rev. Nanomedicine Nanobiotechnology*, , DOI:10.1002/wnan.1419.

150 M. Yamada, M. Foote and T. W. Prow, *Wiley Interdiscip. Rev. Nanomedicine Nanobiotechnology*, 2015, **7**, 428–445.

151 V. I. Shubayev, T. R. Pisanic and S. Jin, *Adv. Drug Deliv. Rev.*, 2009, **61**, 467–477.

152 S. Laurent, D. Forge, M. Port, A. Roch, C. Robic, L. Vander Elst and R. N. Muller, *Chem. Rev.*, 2008, **108**, 2064–2110.

153 A. K. Gupta and M. Gupta, *Biomaterials*, 2005, **26**, 3995–4021.

154 M.-C. Daniel and D. Astruc, *Chem. Rev.*, 2004, **104**, 293–346.

155 W. Haiss, N. T. K. Thanh, J. Aveyard and D. G. Fernig, *Anal. Chem.*, 2007, **79**, 4215–4221.

156 X.-F. Zhang, Z.-G. Liu, W. Shen and S. Gurunathan, *Int. J. Mol. Sci.*, 2016, **17**, 1534–1568.

157 M. Ahamed, M. S. AlSalhi and M. K. J. Siddiqui, *Clin. Chim. Acta*, 2010, **411**, 1841–1848.

158 S. Chernousova and M. Epple, *Angew. Chemie - Int. Ed.*, 2013, **52**, 1636–1653.

159 B. Gaihre, M. S. Khil, D. R. Lee and H. Y. Kim, *Int. J. Pharm.*, 2009, **365**, 180–189.

160 S. Purushotham, P. E. J. Chang, H. Rumpel, I. H. C. Kee, R. T. H. Ng, P. K. H. Chow, C. K. Tan and R. V. Ramanujan, *Nanotechnology*, 2009, **20**, 305101.

161 S. Kayal and R. V. Ramanujan, *Mater. Sci. Eng. C*, 2010, **30**, 484–490.

162 J. H. Maeng, D.-H. Lee, K. H. Jung, Y.-H. Bae, I.-S. Park, S. Jeong, Y.-S. Jeon, C.-K. Shim, W. Kim, J. Kim, J. Lee, Y.-M. Lee, J.-H. Kim, W.-H. Kim and S.-S. Hong, *Biomaterials*, 2010, **31**, 4995–5006.

163 Y. Liu, K. Yang, L. Cheng, J. Zhu, X. Ma, H. Xu, Y. Li, L. Guo, H. Gu and Z. Liu, *Nanomedicine Nanotechnology, Biol. Med.*, 2013, **9**, 1077–1088.

164 M. Hałupka-Bryl, K. Asai, S. Thangavel, M. Bednarowicz, R. Krzyminiewski and Y. Nagasaki, *Colloids Surf B Biointerfaces*, 2014, **118**, 140–147.

165 A. Pourjavadi, Z. M. Tehrani and N. Mahmoudi, *J. Nanoparticle Res.*, 2015, **17**, 197.

166 N. Abbasi Aval, J. Pirayesh Islamian, M. Hatamian, M. Arabfirouzjaei, J. Javadpour and M.-R. Rashidi, *Int. J. Pharm.*, 2016, **509**, 159–167.

167 S.-L. Tang, M.-Y. Bai, J.-Y. Wang and P.-D. Hong, *Colloids Surf B Biointerfaces*, 2017, **151**, 304–313.

168 M. Prabaharan, J. J. Grailer, S. Pilla, D. A. Steeber and S. Gong, *Biomaterials*, 2009, **30**, 6065–6075.

169 H. Chen, S. Li, B. Li, X. Ren, S. Li, D. M. Mahounga, S. Cui, Y. Gu and S. Achilefu, *Nanoscale*, 2012, **4**, 6050–6064.

170 Y. Xiao, H. Hong, V. Z. Matson, A. Javadi, W. Xu, Y. Yang, Y. Zhang, J. W. Engle, R. J. Nickles, W. Cai, D. A. Steeber and S. Gong, *Theranostics*, 2012, **2**, 757–768.

171 W.-H. Chen, X.-D. Xu, H.-Z. Jia, Q. Lei, G.-F. Luo, S.-X. Cheng, R.-X. Zhuo and X.-Z. Zhang, *Biomaterials*, 2013, **34**, 8798–8807.

172 H. J. Lee, Y. Liu, J. Zhao, M. Zhou, R. R. Bouchard, T. Mitcham, M. Wallace, R. J. Stafford, C. Li, S. Gupta and M. P. Melancon, *J. Control. Release*, 2013, **172**, 152–158.

173 T.-M. Sun, Y.-C. Wang, F. Wang, J.-Z. Du, C.-Q. Mao, C.-Y. Sun, R.-Z. Tang, Y. Liu, J. Zhu, Y.-H. Zhu, X.-Z. Yang and J. Wang, *Biomaterials*, 2014, **35**, 836–845.

174 A. Topete, M. Alatorre-Meda, P. Iglesias, E. M. Villar-Alvarez, S. Barbosa, J. A. Costoya, P. Taboada and V. Mosquera, *ACS Nano*, 2014, **8**, 2725–2738.

175 N. S. Elbialy, M. M. Fathy and W. M. Khalil, *Int. J. Pharm.*, 2015, **490**, 190–199.

176 S. Jeon, H. Ko, N. Vijayakameswara Rao, H. Y. Yoon, D. G. You, H. S. Han, W. Um, G. Saravanakumar and J. H. Park, *R. Soc. Chem. Adv.*, 2015, **5**, 70352–70360.

177 K. Y. J. Lee, Y. Wang and S. Nie, *R. Soc. Chem. Adv.*, 2015, **5**, 65651–65659.

178 X. Zhang, J. G. Teodoro and J. L. Nadeau, *Nanomedicine Nanotechnology, Biol. Med.*, 2015, **11**, 1365–1375.

179 C.-S. Lee, H. Kim, J. Yu, S. H. Yu, S. Ban, S. Oh, D. Jeong, J. Im, M. J. Baek and T. H. Kim, *Eur. J. Med. Chem.*, 2017, **142**, 416–423.

180 F. Benyettou, R. Rezgui, F. Ravaux, T. Jaber, K. Blumer, M. Jouiad, L. Motte, J.-C. Olsen, C. Platas-Iglesias, M. Magzoub and A. Trabolsi, *J. Mater. Chem. B*, 2015, **3**, 7237–7245.

181 C. Cha, S. R. Shin, N. Annabi, M. R. Dokmeci and A. Khademhosseini, *ACS Nano*, 2013, **7**, 2891–2897.

182 K. S. Novoselov, V. I. Fal'ko, L. Colombo, P. R. Gellert, M. G. Schwab and K. Kim, *Nature*, 2013, **490**, 192–200.

183 Nobelprize.org, The Nobel Prize in Chemistry 1996, http://www.nobelprize.org/nobel_prizes/chemistry/laureates/1996/, (accessed 25 July 2017).

184 T. Murakami, J. Fan, M. Yudasaka, S. Iijima and K. Shiba, *Mol. Pharm.*, 2006, **3**, 407–414.

185 H. Ali-Boucetta, K. T. Al-Jamal, D. McCarthy, M. Prato, A. Bianco and K. Kostarelos, *Chem. Commun.*, 2008, **0**, 459–461.

186 X. Zhang, L. Meng, Q. Lu, Z. Fei and P. J. Dyson, *Biomaterials*, 2009, **30**, 6041–6047.

187 Z. Liu, A. C. Fan, K. Rakhra, S. Sherlock, A. Goodwin, X. Chen, Q. Yang, D. W. Felsher and H. Dai, *Angew. Chemie - Int. Ed.*, 2009, **48**, 7668–7672.

188 J.-H. Liu, L. Cao, P. G. Luo, S.-T. Yang, F. Lu, H. Wang, M. J. Meziani, S. A. Haque, Y. Liu, S. Lacher and Y.-P. Sun, *ACS Appl. Mater. Interfaces*, 2010, **2**, 1384–1389.

189 Y.-J. Gu, J. Cheng, J. Jin, S. H. Cheng and W.-T. Wong, *Int. J. Nanomedicine*, 2011, **6**, 2889–2898.

190 R. Li, R. Wu, L. Zhao, Z. Hu, S. Guo, X. Pan and H. Zou, *Carbon N. Y.*, 2011, **49**, 1797–1805.

191 J. Ren, S. Shen, D. Wang, Z. Xi, L. Guo, Z. Pang, Y. Qian, X. Sun and X. Jiang, *Biomaterials*, 2012, **33**, 3324–3333.

192 I. Blazkova, H. Viet Nguyen, M. Kominkova, R. Konecna, D. Chudobova, L. Krejcova, P. Kopel, D. Hynek, O. Zitka, M. Beklova, V. Adam and R. Kizek, *Electrophoresis*, 2014, **35**, 1040–1049.

193 N. M. Dinan, F. Atyabi, M.-R. Rouini, M. Amini, A.-A. Golabchifar and R. Dinarvand, *Mater. Sci. Eng. C*, 2014, **39**, 47–55.

194 A. Mewada, S. Pandey, M. Thakur, D. Jadhav and M. Sharon, *J. Mater. Chem. B*, 2014, **2**, 698–705.

195 S. V. Prylutska, V. F. Korolovych, Y. I. Prylutskyy, M. P. Evstigneev, U. Ritter and P. Scharff, *Nanomedicine and Nanobiology*, 2015, **2**, 49–53.

196 J. Shi, Y. Liu, L. Wang, J. Gao, J. Zhang, X. Yu, R. Ma, R. Liu and Z. Zhang, *Acta Biomater.*, 2014, **10**, 1280–1291.

197 G. E. Magoulas, M. Bantzi, D. Messari, E. Voulgari, C. Gialeli, D. Barbouri, A. Giannis, N. K. Karamanos, D. Papaioannou and K. Avgoustakis, *Pharm. Res.*, 2015, **32**, 1676–1693.

198 R. R. Panchuk, S. V. Prylutska, V. V. Chumak, N. R. Skorokhyd, L. V. Lehka, M. P. Evstigneev, Y. I. Prylutskyy, W. Berger, P. Heffeter, P. Scharff, U. Ritter and R. S. Stoika, *J. Biomed. Nanotechnol.*, 2015, **11**, 1139–1152.

199 S. V. Prylutska, L. M. Skivka, G. V. Didenko, Y. I. Prylutskyy, M. P. Evstigneev, G. P. Potebnya, R. R. Panchuk, R. S. Stoika, U. Ritter and P. Scharff, *Nanoscale Res. Lett.*, 2015, **10**, 499.

200 X. Qi, Y. Rui, Y. Fan, H. Chen, N. Ma and Z. Wu, *Colloids Surf B Biointerfaces*, 2015, **133**, 314–322.

201 L. Yang, Z. Wang, J. Wang, W. Jiang, X. Jiang, Z. Bai, Y. He, J. Jiang, D. Wang and L. Yang, *Nanoscale*, 2016, **8**, 6801–6809.

202 S. Li, D. Amat, Z. Peng, S. Vanni, S. Raskin, G. De Angulo, A. M. Othman, R. M. Graham and R. M. Leblanc, *Nanoscale*, 2016, **8**, 16662–16669.

203 B. Wang, S. Wang, Y. Wang, Y. Lv, H. Wu, X. Ma and M. Tan, *Biotechnol. Lett.*, 2016, **38**, 191–201.

204 M. Zhang, P. Yuan, N. Zhou, Y. Su, M. Shao and C. Chi, *R. Soc. Chem. Adv.*, 2017, **7**, 9347–9356.

205 T. Sun, M. Zheng, Z. Xie and X. Jing, *Mater. Chem. Front.*, 2017, **1**, 354–360.

206 Y. Yuan, B. Guo, L. Hao, N. Liu, Y. Lin, W. Guo, X. Li and B. Gu, *Colloids Surf B Biointerfaces*, 2017, **159**, 349–359.

207 N. Gao, W. Yang, H. Nie, Y. Gong, J. Jing, L. Gao and X. Zhang, *Biosens. Bioelectron.*, 2017, **96**, 300–307.

208 BYK Additives & Instruments, *LAPONITE Perform. Addit.*, 2014, 1–23.

209 D. Bonn, H. Kellay, H. Tanaka, G. Wegdam and J. Meunier, *Langmuir*, 1999, **15**, 7534–7536.

210 D. W. Thompson and J. T. Butterworth, *J. Colloid Interface Sci.*, 1992, **151**, 236–243.

211 S. Wang, Y. Wu, R. Guo, Y. Huang, S. Wen, M. Shen, J. Wang and X. Shi, *Langmuir*, 2013, **29**, 5030–5036.

212 K. Li, S. Wang, S. Wen, Y. Tang, J. Li, X. Shi and Q. Zhao, *ACS Appl. Mater. Interfaces*, 2014, **6**, 12328–12334.

213 G. Wang, D. Maciel, Y. Wu, J. Rodrigues, X. Shi, Y. Yuan, C. Liu, H. Tomás and Y. Li, *ACS Appl. Mater. Interfaces*, 2014, **6**, 16687–16695.

214 M. Gonçalves, P. Figueira, D. Maciel, J. Rodrigues, X. Qu, C. Liu, H. Tomás and Y. Li, *Acta Biomater.*, 2014, **10**, 300–307.

215 G. Chen, D. Li, J. Li, X. Cao, J. Wang, X. Shi and R. Guo, *New J. Chem.*, 2015, **39**, 2847–2855.

216 S. Xiao, R. Castro, D. Maciel, M. Gonçalves, X. Shi, J. Rodrigues and H. Tomás, *Mater. Sci. Eng. C*, 2016, **60**, 348–356.

217 Y. Zhuang, L. Zhao, L. Zheng, Y. Hu, L. Ding, X. Li, C. Liu, J. Zhao, X. Shi and R. Guo, *ACS Biomater. Sci. Eng.*, 2017, **3**, 431–442.

218 O. of the Commissioner, The Drug Development Process, https://www.fda.gov/ForPatients/Approvals/Drugs/default.htm, (accessed 9 October 2017).

219 Clinical Studies Explained, https://neurosciences.ucsd.edu/centers/huntingtons-disease/research/Pages/clinical-observational-trials.aspx, (accessed 27 March 2018).

220 J. M. Caster, A. N. Patel, T. Zhang and A. Wang, *Wiley Interdiscip. Rev. Nanomedicine Nanobiotechnology*, , DOI:10.1002/wnan.1416.

221 Y. Min, J. M. Caster, M. J. Eblan and A. Z. Wang, *Chem. Rev.*, 2015, **115**, 11147–11190.

222 S. Svenson, *Curr. Opin. Solid State Mater. Sci.*, 2012, **16**, 287–294.

223 H. Havel, G. Finch, P. Strode, M. Wolfgang, S. Zale, I. Bobe, H. Youssoufian, M. Peterson and M. Liu, *Am. Assoc. Pharm. Sci. J.*, 2016, **18**, 1373–1378.

224 J. I. Hare, T. Lammers, M. B. Ashford, S. Puri, G. Storm and S. T. Barry, *Adv. Drug Deliv. Rev.*, 2017, **108**, 25–38.

225 S. Hassan, G. Prakasha, A. Bal Ozturk, S. Saghazadeh, M. Farhan Sohail, J. Seo, M. Remzi Dokmeci, Y. S. Zhang and A. Khademhosseini, *Nano Today*, 2017, **15**, 91–106.

226 C. von Roemeling, W. Jiang, C. K. Chan, I. L. Weissman and B. Y. S. Kim, *Trends Biotechnol.*, 2017, **35**, 159–171.

227 S. Stewart, H. Jablonowski, F. D. Goebel, K. Arasteh, M. Spittle, A. Rios, D. Aboulafia, J. Galleshaw and B. J. Dezube, *J. Clin. Oncol.*, 1998, **16**, 683–691.

228 D. W. Northfelt, B. J. Dezube, J. A. Thommes, B. J. Miller, M. A. Fischl, A. Friedman-Kien, L. D. Kaplan, C. Du Mond, R. D. Mamelok and D. H. Henry, *J. Clin. Oncol*, 1998, **16**, 2445–2451.

229 M. E. R. O'Brien, N. Wigler, M. Inbar, R. Rosso, E. Grischke, A. Santoro, R. Catane, D. G. Kieback, P. Tomczak, S. P. Ackland, F. Orlandi, L. Mellars, L. Alland and C. Tendler, *Ann. Oncol.*, 2004, **15**, 440–449.

230 A. N. Gordon, M. Tonda, S. Sun and W. Rackoff, *Gynecol. Oncol.*, 2004, **95**, 1–8.

231 R. M. Rifkin, S. A. Gregory, A. Mohrbacher and M. A. Hussein, *Cancer*, 2006, **106**, 848–858.

232 G. Batist, G. Ramakrishnan, C. S. Rao, A. Chandrasekharan, J. Gutheil, T. Guthrie, P. Shah, A. Khojasteh, M. K. Nair, K. Hoelzer, K. Tkaczuk, Y. C. Park and L. W. Lee, *J. Clin. Oncol.*, 2001, **19**, 1444–1454.

233 G. Batist, J. Barton, P. Chaikin, C. Swenson and L. Welles, *Expert Opin Pharmacother*, 2002, **3**, 1739–1751.

234 L. Harris, G. Batist, R. Belt, D. Rovira, R. Navari, N. Azarnia, L. Welles and E. Winer, *Cancer*, 2002, **94**, 25–36.

235 S. Chan, N. Davidson, E. Juozaityte, F. Erdkamp, A. Pluzanska, N. Azarnia and L. W. Lee, *Ann. Oncol.*, 2004, **15**, 1527–1534.

236 Study of ThermoDox With Standardized Radiofrequency Ablation (RFA) for Treatment of Hepatocellular Carcinoma (HCC) (OPTIMA), https://www.clinicaltrials.gov/ct2/show/NCT02112656?term=NCT02112656&rank=1, (accessed 16 October 2017).

237 Phase 3 Study of ThermoDox With Radiofrequency Ablation (RFA) in Treatment of Hepatocellular Carcinoma (HCC), https://www.clinicaltrials.gov/ct2/show/NCT00617981?term=NCT00617981&rank=1, (accessed 16 October 2017).

238 T. M. Zagar, Z. Vujaskovic, S. Formenti, H. Rugo, F. Muggia, B. O'Connor, R. Myerson, P. Stauffer, I.-C. Hsu, C. Diederich, W. Straube, M.-K. Boss, A. Boico, O. Craciunescu, P. Maccarini, D. Needham, N. Borys, K. L. Blackwell and M. W. Dewhirst, *Int. J. Hyperth.*, 2014, **30**, 285–294.

239 A. Lopez-Pousa, B. B. Nguyen, X. G. del Muro, J. M. Broto, C. Balañá, J. Lavernia, J. Cruz, J. Maurel, R. Andres, C. M. Valverde, J. Fra, J. Martinez-Trufero, J. A. Lopez-Martin, I. Sevilla, R. Cubedo and J. Blay, *J. Clin. Oncol.*, 2011, **29**, 10072.

240 Clinical and Pharmacological Study With 2B3-101 in Patients With Breast Cancer and Leptomeningeal Metastases, https://www.clinicaltrials.gov/ct2/show/NCT01818713?term=2B3-101&rank=1, (accessed 13 October 2017).

241 B. M. Kerklaan, A. Jager, P. Aftimos, V. Dieras, S. Altintas, C. Anders, M. Arnedos, H. Gelderblom, P. Soetekouw, W. Gladdines, P. Gaillard, C. de Sousa, A. Awada, J. Schellens, M. van Linde and D. Brandsma, *Neuro. Oncol.*, 2014, **16**, v163–v163.

242 C. Mamot, R. Ritschard, A. Wicki, G. Stehle, T. Dieterle, L. Bubendorf, C. Hilker, S. Deuster, R. Herrmann and C. Rochlitz, *Lancet Oncol.*, 2012, **13**, 1234–1241.

243 K. Miller, J. Cortes, S. A. Hurvitz, I. E. Krop, D. Tripathy, S. Verma, K. Riahi, J. G. Reynolds, T. J. Wickham, I. Molnar and D. A. Yardley, *BioMed Cent. cancer*, 2016, **16**, 352.

244 MM-302 Misses Endpoint in Phase II Hermione Trial – ADC Review ADC Review, https://adcreview.com/news/mm-302-misses-endpoint-phase-ii-hermione-trial/, (accessed 25 September 2017).

245 Onxeo Announces Top-Line Results from ReLive Phase III Study of Livatag® in Advanced Hepatocellular Carcinoma, https://www.onxeo.com/onxeo-announces-top-line-results-relive-phase-iii-study-livatag-advanced-hepatocellular-carcinoma/, (accessed 28 September 2017).

246 Onxeo to host a Conference Call today to comment on the main findings from ReLive Phase III Study of Livatag®, https://www.onxeo.com/onxeo-host-conference-call-today-comment-main-findings-relive-phase-iii-study-livatag/, (accessed 28 September 2017).

247 L. W. Seymour, D. R. Ferry, D. J. Kerr, D. Rea, M. Whitlock, R. Poyner, C. Boivin, S. Hesslewood, C. Twelves, R. Blackie, A. Schatzlein, D. Jodrell, D. Bissett, H. Calvert, M. Lind, A. Robbins, S. Burtles, R. Duncan and J. Cassidy, *Int. J. Oncol.*, 2009, **34**, 1629–1636.

248 L. W. Seymour, D. R. Ferry, D. Anderson, S. Hesslewood, P. J. Julyan, R. Poyner, J. Doran, A. M. Young, S. Burtles and D. J. Kerr, *J. Clin. Oncol.*, 2002, **20**, 1668–1676.

249 J. W. Valle, J. Lawrance, J. Brewer, A. Clayton, P. Corrie, V. Alakhov and M. Ranson, *J. Clin. Oncol.*, 2004, **22**, 4195–4195.

250 Y. Matsumura, T. Hamaguchi, T. Ura, K. Muro, Y. Yamada, Y. Shimada, K. Shirao, T. Okusaka, H. Ueno, M. Ikeda and N. Watanabe, *Br. J. Cancer*, 2004, **91**, 1775–1781.

251 J. R. Whittle, J. D. Lickliter, H. K. Gan, A. M. Scott, J. Simes, B. J. Solomon, J. A. MacDiarmid, H. Brahmbhatt and M. A. Rosenthal, *J. Clin. Neurosci.*, 2015, **22**, 1889–1894.

252 G. Sessa and G. Weissmann, *J. Lipid Res.*, 1968, **9**, 310–318.

253 4,898,735, 1990.

254 Y. Barenholz, *J. Control. Release*, 2012, **160**, 117–134.

255 N. D. James, R. J. Coker, D. Tomlinson, J. R. W. Harris, M. Gompels, A. J. Pinching and J. S. W. Stewart, *Clin. Oncol.*, 1994, **6**, 294–296.

256 F. M. Muggia, J. D. Hainsworth, S. Jeffers, P. Miller, S. Groshen, M. Tan, L. Roman, B. Uziely, L. Muderspach, A. Garcia, A. Burnett, F. A. Greco, C. P. Morrow, L. J. Paradiso and L.-J. Liang, *J. Clin. Oncol.*, 1997, **15**, 987–993.

257 Z. Symon, A. Peyser, D. Tzemach, O. Lyass, E. Sucher, E. Shezen and A. Gabizon, *Cancer*, 1999, **86**, 72–78.

258 R. Z. Orlowski, A. Nagler, P. Sonneveld, J. Bladé, R. Hajek, A. Spencer, J. San Miguel, T. Robak, A. Dmoszynska, N. Horvath, I. Spicka, H. J. Sutherland, A. N. Suvorov, S. H. Zhuang, T. Parekh, L. Xiu, Z. Yuan, W. Rackoff and J.-L. Harousseau, *J. Clin. Oncol.*, 2007, **25**, 3892–3901.

259 A. Gabizon, H. Shmeeda and Y. Barenholz, *Clin. Pharmacokinet.*, 2003, **42**, 419–436.

260 P. K. Working and A. D. Dayan, *Hum. Exp. Toxicol.*, 1996, **15**, 751–85.

261 S. E. Krown, D. W. Northfelt, D. Osoba and J. S. Stewart, *Semin. Oncol.*, 2004, **31**, 36–52.

262 U. Bulbake, S. Doppalapudi, N. Kommineni and W. Khan, *Pharmaceutics*, 2017, **9**, 1–33.

263 R. C. F. Leonard, S. Williams, A. Tulpule, A. M. Levine and S. Oliveros, *The Breast*, 2009, **18**, 218–224.

264 P. M. Kanter, G. Klaich, G. A. Bullard, J. M. King and Z. P. Pavelic, *In Vivo*, 1994, **8**, 975–982.

265 J. W. Cowens, P. J. Creaven, W. R. Greco, D. E. Brenner, M. Ostro, F. Pilkiewicz and R. Ginsberg, *Cancer Res.*, 1993, **99**, 2796–2802.

266 R. T. Poon and N. Borys, *Futur. Oncol.*, 2011, **7**, 937–945.

267 R. T. Poon and N. Borys, *Expert Opin Pharmacother*, 2009, **10**, 333–343.

268 J. Chen, C.-Q. He, A.-H. Lin, W. Gu, Z.-P. Chen, W. Li and B.-C. Cai, *Int. J. Pharm.*, 2014, **475**, 408–415.

269 B. Kneidl, M. Peller, G. Winter, L. H. Lindner and M. Hossann, *Int. J. Nanomedicine*, 2014, **9**, 4387–4398.

270 A. Puri, *Pharmaceutics*, 2014, **6**, 1–25.

271 S. N. Goldberg, I. R. Kamel, J. B. Kruskal, K. Reynolds, W. L. Monsky, K. E. Stuart, M. Ahmed and V.

Raptopoulos, *Am. J. Roentgenol.*, 2002, **179**, 93–101.

272 V. Patravale, P. Dandekar and R. Jain, in *Nanoparticulate Drug Delivery*, Elsevier, 2012, pp. 191–207.

273 W. M. Pardridge, *Expert Opin. Drug Deliv.*, 2016, **13**, 963–975.

274 P. J. Gaillard, C. C. Visser, C. C. M. Appeldoorn and J. Rip, *Drug Discov. Today Technol.*, 2012, **9**, e155–e160.

275 P. J. Gaillard, C. C. M. Appeldoorn, R. Dorland, J. Van Kregten, F. Manca, D. J. Vugts, B. Windhorst, G. A. M. S. Van Dongen, H. E. De Vries, D. Maussang and O. Van Tellingen, *PLoS One*, 2014, **9**, e82331.

276 J. W. Park, K. Hong, D. B. Kirpotin, D. Papahadjopoulos and C. C. Benz, in *Advances in Pharmacology*, 1997, vol. 40, pp. 399–435.

277 US 2010/0239652 A1, 2010.

278 C. Mamot, D. C. Drummond, U. Greiser, K. Hong, D. B. Kirpotin, J. D. Marks and J. W. Park, *Cancer Res.*, 2003, **63**, 3154–3161.

279 C. Mamot, D. C. Drummond, C. O. Noble, V. Kallab, Z. Guo, K. Hong, D. B. Kirpotin and J. W. Park, *Cancer Res.*, 2005, **65**, 11631–11638.

280 C. Mamot, R. Ritschard, A. Wicki, W. Küng, J. Schuller, R. Herrmann and C. Rochlitz, *J. Drug Target.*, 2012, **20**, 422–432.

281 US20160038416A1, 2012.

282 J. W. Park, D. B. Kirpotin, K. Hong, R. Shalaby, Y. Shao, U. B. Nielsen, J. D. Marks, D. Papahadjopoulos and C. C. Benz, *J. Control. Release*, 2001, **74**, 95–113.

283 J. W. Park, K. Hong, D. B. Kirpotin, G. Colbern, R. Shalaby, J. Baselga, Y. Shao, U. B. Nielsen, J. D. Marks, D. Moore, D. Papahadjopoulos and C. C. Benz, *Clin. Cancer Res.*, 2002, **8**, 1172–1181.

284 P. Munster, K. Miller, I. E. Krop, C. Niyikiza, U. Nielsen, A. Odueyungbo, A. Rajarethinmam, K. Campbell, E. Geretti, J. Reynolds, J. Kim, B. Hendricks, K. Futch, T. Wickham, V. Moyo and P. LoRusso, in *Cancer Research*, 2012, vol. 72, pp. P5-18-09.

285 J. Kattan, J.-P. Droz, P. Couvreur, J.-P. Marino, A. Boutan-Laroze, P. Rougier, P. Brault, H. Vranckx, J.-M. Grognet, X. Morge and H. Sancho-Garnier, *Invest. New Drugs*, 1992, **10**, 191–199.

286 Orphan oncology products: Produits orphelins en oncologie, http://www.onxeo.com/en/nos-produits/orphelins-oncologie/#tabs-1-3, (accessed 28 September 2017).

287 B. Pharma, *Livatag® (Doxorubicin Transdrug™) follow up demonstrates significant survival increase in advanced hepatocellular carcinoma patients*, 2011.

288 J. Kopeček and H. Bažilová, *Eur. Polym. J.*, 1973, **9**, 7–14.

289 5,037,883, 1991.

290 P. A. Vasey, S. B. Kaye, R. Morrison, C. Twelves, P. Wilson, R. Duncan, A. H. Thomson, L. S. Murray, T. E. Hilditch, T. Murray, S. Burtles, D. Fraier, E. Frigerio and J. Cassidy, *Clin. Cancer Res.*, 1999, **5**, 83–94.

291 R. Duncan, J. K. Coatsworth and S. Burtles, *Hum. Exp. Toxicol.*, 1998, **17**, 93–104.

292 J. W. Hopewel, R. Duncan, D. Wilding and K. Chakrabarti, *Hum. Exp. Toxicol.*, 2001, **20**, 461–70.

293 R. Gaspar and R. Duncan, *Adv. Drug Deliv. Rev.*, 2009, **61**, 1220–1231.

294 V. Alakhov, E. Klinski, S. Li, G. Pietrzynski, A. Venne, E. Batrakova, T. Bronitch and A. Kabanov, *Colloids*

Surf B Biointerfaces, 1999, **16**, 113–134.

295 E. V. Batrakova and A. V. Kabanov, *J. Control. Release*, 2008, **130**, 98–106.

296 A. Venne, S. Li, R. Mandeville, A. Kabanov and V. Alakhov, *Cancer Res.*, 1996, **56**, 3626–3629.

297 E. V. Batrakova, T. Y. Dorodnych, E. Y. Klinskii, E. N. Kliushnenkova, O. B. Shemchukova, O. N. Goncharova, S. A. Arjakov, V. Y. Alakhov and A. V. Kabanov, *Br. J. Cancer*, 1996, **74**, 1545–1552.

298 S. Danson, D. Ferry, V. Alakhov, J. Margison, D. Kerr, D. Jowle, M. Brampton, G. Halbert and M. Ranson, *Br. J. Cancer*, 2004, **90**, 2085–2091.

299 T. Nakanishi, S. Fukushima, K. Okamoto, M. Suzuki, Y. Matsumura, M. Yokoyama, T. Okano, Y. Sakurai and K. Kataoka, *J. Control. Release*, 2001, **74**, 295–302.

300 J. A. MacDiarmid, N. B. Mugridge, J. C. Weiss, L. Phillips, A. L. Burn, R. P. Paulin, J. E. Haasdyk, K.-A. Dickson, V. N. Brahmbhatt, S. T. Pattison, A. C. James, G. Al Bakri, R. C. Straw, B. Stillman, R. M. Graham and H. Brahmbhatt, *Cancer Cell*, 2007, **11**, 431–445.

301 B. F. El-Rayes and P. M. LoRusso, *Br. J. Cancer*, 2004, **91**, 418–424.

302 J. A. MacDiarmid, N. B. Amaro-Mugridge, J. Madrid-Weiss, I. Sedliarou, S. Wetzel, K. Kochar, V. N. Brahmbhatt, L. Phillips, S. T. Pattison, C. Petti, B. Stillman, R. M. Graham and H. Brahmbhatt, *Nat. Biotechnol.*, 2009, **27**, 643–651.

303 B. J. Solomon, J. Desai, M. Rosenthal, G. A. McArthur, S. T. Pattison, S. L. Pattison, J. MacDiarmid, H. Brahmbhatt and A. M. Scott, *PLoS One*, 2015, **10**, e0144559.

304 J. Mendelsohn and J. Baselga, *Semin. Oncol.*, 2006, **33**, 369–385.

305 I. K. Mellinghoff, M. Y. Wang, I. Vivanco, D. A. Haas-Kogan, S. Zhu, E. Q. Dia, K. V. Lu, K. Yoshimoto, J. H. Y. Huang, D. J. Chute, B. L. Riggs, S. Horvath, L. M. Liau, W. K. Cavenee, P. N. Rao, R. Beroukhim, T. C. Peck, J. C. Lee, W. R. Sellers, D. Stokoe, M. Prados, T. F. Cloughesy, C. L. Sawyers and P. S. Mischel, *N. Engl. J. Med.*, 2005, **353**, 2012–2024.

Chapter II.

Antitumor Efficacy of Doxorubicin-Loaded Laponite®/Alginate Hybrid Hydrogels

Abstract

Degradable hybrid hydrogels with improved stability are prepared by incorporating nanodisks of biocompatible Laponite® (LP) in alginate (AG) hydrogels using calcium cations (Ca^{2+}) as a crosslinker. The DOX-loaded hybrid hydrogels give a controlled doxorubicin (DOX) release at physiological environment in a sustained manner. Under conditions that mimic the tumour environment, both the sustainability in DOX release (up to 17d) and the release efficiency from LP/AG-DOX hydrogels are improved. The *in situ* degradation of these hybrid hydrogels gives rise to nanohybrids that might serve as vehicles for carrying DOX through the cell membrane and diminish the effect of DOX ion-trapping in the acidic extracellular environment of the tumour and/or in the endo-lysosomal cell compartments.

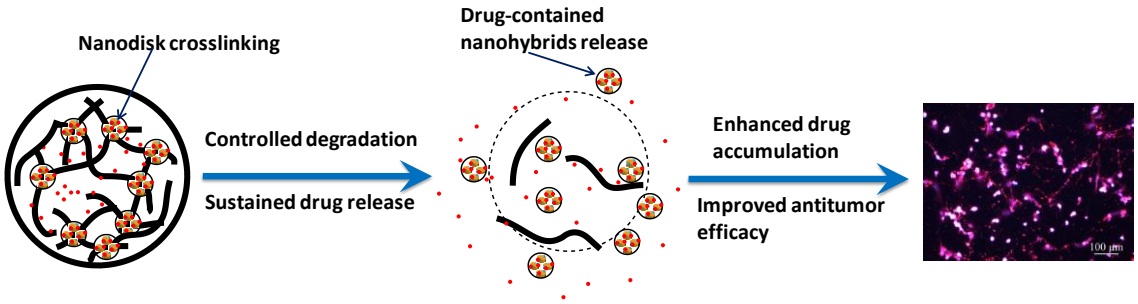

This Chapter is based on the following publication:

M. Gonçalves, P. Figueira, D. Maciel, J. Rodrigues, X. Shi, H. Tomás and Y. Li, Antitumor efficacy of doxorubicin-loaded laponite/alginate hybrid hydrogels, *Macromol. Biosci.*, 2014, 14, 110–120.

1. Introduction

Although DOX has been widely used in the treatment of different types of cancers[1–4], the development of resistance to its action is still one of the major obstacles for its successful application.[5] Similar to what happens with other anticancer drugs, DOX resistance may be associated with the decreased drug uptake (e.g., ion trapping inside acidic compartments), increased drug efflux (due to the over-expression of efflux pumps), activation of detoxifying or DNA repair mechanisms, etc.[6,7] As such, to overcome this problem, high DOX concentrations are needed to kill cancer cells[5]. However, free DOX is diffusive and easily penetrate and accumulate into normal cells and tissues, which causes severely, dose-limiting side-effects such as hypersensitivity and cardiotoxicity, thus limiting its clinical applications.[8–10] Therefore, there is an urgent need to develop safe DOX release systems, which cannot only locally and spatiotemporally deliver DOX into the tumour site, but also effectively transport DOX into the cell interior, leading to DOX accumulation and, ultimately, to cancer cell death.[11] Recently, injectable hydrogels have been employed as carriers for delivery of antitumor therapeutics, because they can exhibit targeted drug delivery in a localized area with prolonged bioactivity periods and improved biocompatibility.[12–14] Drugs and/or cells may be mixed with a hydrogel precursor, and form a hydrogel *in vitro* or after *in vivo* injection, thus allowing for easy drug loading and simple administration procedures and site-specificity.[15,16] It is well known that hydrogels contain high water content, and are usually appropriate for the delivery of hydrophobic small molecular drugs or water-soluble macromolecular drugs, instead of hydrophilic small molecular drugs.[17,18] Meanwhile, hydrogels often display low stability and an uncontrolled drug release behaviour, which not only shortens the efficacy of the drugs used, but also leads to big harmful side-effects. On the other hand, pH is one important environmental factor in the body. The extracellular environment of some tumours have a pH around 6.5[19,20], and the endosomal/lysosomal compartments have pH values in the range of 5.0–6.0.[20] How to endow biomaterials with pH sensitivity is very important but still a major challenge in the field of controlled drug delivery.[21,22]

Alginate (AG) is a linear and anionic polysaccharide consisting of α-*L*-guluronate and β-*D*-mannuronate residues, which can be ionically crosslinked by divalent cations, like calcium cations (Ca^{2+}). AG has been widely used in a high variety of biomedical applications, e.g., as carriers for encapsulation of cells[23], and delivery of proteins[24,25], and drugs.[26] AG has been reported as an injectable material for tissue engineering in minimally invasive surgeries using calcium chloride as a crosslinker.[27] However, conventional Ca^{2+}-AG gels can be easily dissolved due to the rapid exchange of Ca^{2+} with other cations present in phosphate-buffered saline (PBS) solution, which together with their high porosity leads to burst drug release.[28] Stable AG systems that have sustained drug release profile in a prolonged time are still required.

Clays and clay minerals have been effectively used to modify drug delivery systems.[29] Clay minerals can be classified as 1:1 sheets which consist of one tetrahedral sheet and one octahedral sheet, or 2:1 sheets which have an octahedral sheet sandwiched between two tetrahedral sheets. Compared with 1:1 clays like kaolinite, and other 2:1 clays like talc, pyrophyllite, illite, vermiculite, etc., smectite unit structure consists of two tetrahedral silica sheets sandwiching an octahedral sheet containing metal cations such as Al^{3+} or Mg^{2+}, and often has a relatively weak negative surface charge, allowing the easy delamination of individual layers and exchangeability with other cations.[30]

Laponite® (LP), a synthetic layered silicate belonging to the smectites class, with the empirical formula $Na^{+0.7}[(Si_8Mg_{5.5}Li_{0.3})O_{20}(OH)_4]^{-0.7}$, is pure, and can avoid side effects caused by possible impurities of natural clays such as montmorillonite.[31] LP has a disk shape and a large aspect ratio (25 nm in diameter and 0.92 nm in thickness), which can dissociate into non-toxic products [Na^+, $Si(OH)_4$, Mg^{2+}, Li^+], similar to the degradation products of bioactive glasses [Na^+, $Si(OH)_4$, Ca^{2+}, PO_4^{3-}].[32,33] The large surface area (330 m^2/g) and negative charged surface of LP enables the encapsulation of guest compounds, especially of cationic molecules.[34] LP also exhibits pH sensitivity through its edge surface charge.[33] These advantages together with its good biocompatibility[35], and osteoinductivity[36] make LP act as an ideal inorganic nanomaterial for drug delivery[35,37] and tissue engineering.[36] In our previous report[38], LP was incorporated into AG hydrogels, which exhibited improved properties, including a high encapsulation efficiency (EE) for methylene blue (MB, a cationic hydrophilic model drug), as well as its sustained and pH sensitive release. A member of the present team reported that doxorubicin can be encapsulated into the interlayer space of LP to form LP/DOX nanosized hybrids, which display an acid-triggered DOX release and enhanced cellular uptake and anticancer cytotoxicity.[35] Our earlier success in the design of the LP/AG hybrid hydrogels led us to hypothesize that by doping AG bulk hydrogels with the LP/DOX nanohybrids, an improved sustained release behaviour (for long-term therapeutic efficacy), stability and pH sensitivity could be obtained. Indeed, taking advantage of these properties, pH-triggered drug-delivery hydrogels are able to be developed and potentially exert a localized-drug delivery.[21,39]

In the present work, we aimed to develop a new type of DOX-loaded hybrid hydrogel system with improved stability and sustained DOX release behaviour. The hydrophilic drug DOX hydrochloride salt was first homogeneously mixed with LP-doped AG aqueous solution, and then hydrogels were formed via physical interaction using Ca^{2+} as a crosslinker. Along time, the LP/AG-DOX hydrogels suffered degradation and gave a sustained *in vitro* release (in an almost zero-order manner, in 11 d) of DOX. The excellent behaviour of the hybrid hydrogels as DOX delivery vehicles with the ability to release DOX during a long period of time is believed to confer therapeutic efficacy to the developed systems. To the best of our knowledge, this is the first report on the development and antitumor activity evaluation of LP-doped AG bulk hydrogels for the delivery of DOX. This study is expected to

contribute for the design of more effective and safe hydrogel-based drug carrier systems which may be used in a wide range of biomedical applications.

2. Experimental Section

2.1. Materials

Laponite® RDS (LP) was a generous offer from Rockwood Additives Limited (UK). Alginate acid sodium salt (AG, from brown Algae, Mw from 12 to 58 kDa, cell culture tested) was bought from Sigma (USA). Doxorubicin hydrochloride (DOX) was obtained from Aldrich (USA). Dulbecco's PBS powder (without Ca^{2+} and Mg^{2+}) was purchased from Invitrogen Corporation (USA).

2.2. Preparation of Hydrogels

AG hydrogels and LP/AG nanocomposite hydrogels with or without DOX were prepared by dropping 5 mL aqueous solutions of LP/AG/DOX [x/2/y (wt%), x = 0 and 0.2, y = 0 and 0.04] into 50 mL of 0.05 M/0.05 M calcium chloride/calcium sulphate solution under gently magnetic stirring. The formed hydrogels were allowed to crosslink with Ca^{2+} overnight for equilibration. The Ca^{2+}-crosslinked hydrogels were rinsed with distilled water three times (total 100 mL) to remove unencapsulated DOX and unreacted calcium chloride/calcium sulphate, and dried in an oven at 45 ºC to get AG, LP/AG, AG-DOX, and LP/AG-DOX hydrogels, respectively.

2.3. Swelling/Erosion Behaviour Study

In order to check the stability of hydrogels, the swelling/erosion behaviour of the AG-DOX and LP/AG-DOX hydrogels was determined by immersing hydrogels into the corresponding volume of PBS solution at pH = 7.4, 6.5, and 5.5 (the concentration of gels in the PBS solution was constant and equal to 0.2 mg/mL). At specific time intervals, the samples were removed from the swelling medium and were blotted with a piece of paper towel to absorb the excess of water on the surface. The fractional swelling (F_s) of the hydrogels was determined as follows:

$$F_s = \frac{m_t}{m_\infty} \qquad \text{Equation 1}$$

where m_t and m_∞ are the mass of hydrogels at time t and the stage with maximum weight, respectively.[40] All experiments were conducted in triplicate.

2.4. *In vitro* Drug Release Studies

1 mg of each sample was immersed in 5 mL of PBS solution at 37 ºC (studies were performed at pH values of 7.4, 6.5, and 5.5). At different intervals, the solution was taken out and the concentration of released DOX was determined spectrophotometrically at 475 nm. The cumulative release (C_r) of DOX against time was obtained by the following equation,

$$C_r = \frac{Abs_t}{Abs_0} \times 100 \qquad \text{Equation 2}$$

where Abs_t and Abs_0 are the cumulative amount of drug released at time t and the initial amount of drug used, respectively. All experiments were conducted in triplicate.

2.5. Biological Experiments

CAL-72 cells (an osteosarcoma cell line) were cultured in Dulbecco's modified Eagle medium (D-MEM) containing 10% fetal bovine serum (FBS, Gibco) and 1% of an antibiotic/antimycotic 100x solution (AA, Gibco, with penicillin, streptomycin, and amphotericin B). The medium was supplemented with 1% of L-glutamine 100x solution (Gibco) and 1% of insulin/transferin/selenium 100x solution (ITS, Gibco). Cells were grown at 37ºC in a humidified atmosphere with 5% carbon dioxide. Afterwards, the cells were harvested at 70–80% confluence, using trypsin/EDTA solution (Gibco) for the enzymatic detachment of the cells from the plastic substrate.

To prove if LP/AG-DOX hydrogels are therapeutically active, CAL-72 cells were first plated in 24-well plates for 24 h, with a seeding density of 15 x 10^3 cells per well. AG-DOX and LP/AG-DOX hydrogels (1 mg) were soaked in 5 mL of sterilized PBS solution at pH = 7.4 for 24, 48, and 72 h, respectively. The release media were kept for subsequent cell culture. It has to be noted that the total DOX concentration in the hydrogels (unreleased) was used for comparison with that of the free DOX used to treat cells. In the day after, DOX in PBS solution, and the release media from AG-DOX or LP/AG-DOX hydrogels, were added to the cells and then incubated for 48 h, at 37 ºC, before cell viability evaluation. Control experiments with DOX-free AG and LP/AG hydrogels were also performed using an equivalent mass concentration of that used in AG-DOX and LP/AG-DOX hydrogels.

The cell viability was quantified by the measurement of the metabolic activity of the cells in culture through the resazurin reduction assay. Briefly, after the 48 h incubation time, the cell culture medium was replaced with fresh medium containing resazurin at a concentration of 0.1 mg/mL, and then cells were kept at 37 ºC in the cell incubator for 3 h. Afterward, aliquots of the cell supernatant were transferred to 96-well opaque plates and the resorufin fluorescence (λ_{ex} = 530 nm, λ_{em} = 590 nm) was measured using a microplate reader (model Victor^3 1420, Perkin-Elmer). For fluorescence

microscopy studies, cells were plated 24 h before the incubation with the test solutions, to allow their attachment to the plastic surface. Freshly prepared DOX solutions and the release media of AG-DOX or LP/AG-DOX hydrogels were diluted in PBS solution in order to test different DOX concentrations. Cells were then further incubated at 37 ºC for 1 and 48 h. After that, the cells were washed with sterilized PBS solution and fixed with 3.7% glutaraldehyde and stained with 4',6-diamidino-2-phenylindole (DAPI, Sigma) for 30 min. After fixing, the cells were washed with PBS solution and ultrapure water for analysis by optical fluorescence microscopy (Nikon Eclipse TE 2000E inverted microscope).

3. Results and Discussion

3.1. DOX Loading and Swelling/Erosion Behaviour of the DOX-Loaded Alginate and LP/AG Hydrogels

As illustrated in Figure 19a, both AG and LP/AG hydrogels were prepared at an approximate size of 1mm. After DOX encapsulation, the AG and LP/AG hydrogels acquired a red colour, indicating the successful loading of DOX. To be used as injectable materials for biomedical applications, after injection, the hydrogels should effectively hold drugs in order to prevent their leakage, and thus decrease their side effects.[13] The encapsulation efficiency of DOX in AG and LP/AG gels is shown in Table 9. AG hydrogels had a high leakage of DOX after gel formation (the EE was only of 80 ± 11%), which may lead to high toxicity for normal tissues around. The incorporation of LP into alginate led to the capture of almost all DOX inside the hybrid hydrogels (the EE increased to 99 ± 1 wt% when 0.2 wt% of LP was present), which will be beneficial to avoiding the high toxicity caused by leaked DOX.

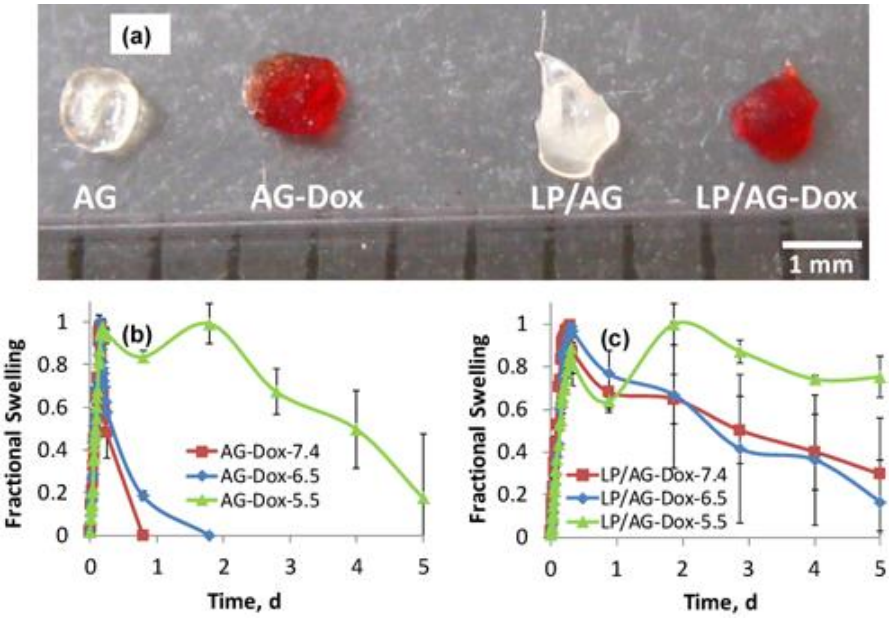

Figure 19. a) Photographs of AG and LP/AG hydrogels before and after DOX loading, b) the swelling/erosion behaviour of AG-DOX, and c) LP/AG-DOX hydrogels in PBS solution at the pH values of 7.4, 6.5, and 5.5.

Table 9. Encapsulation efficiency and loading capacity of AG-DOX and LP/AG-DOX hydrogels.

Sample	EE [a] [%]	Loading capacity [b] [%]
AG-DOX	80 ± 11	1.7 ± 0.3
LP/AG-DOX	99 ± 1	2.1 ± 0.0

a) EE = 100 × W_t/W_0, W_0, and W_t are the total DOX weight used for encapsulation and the weight of encapsulated DOX, respectively; b) Loading capacity = 100 × W_t/W, W_t and W denote the weight of encapsulated DOX and the weight of the DOX-loaded hydrogels, respectively.

As drug carriers, the swelling/erosion behaviour of hydrogels play an important role on their drug release property.[13] Therefore, the swelling/erosion behaviour of the AG-DOX and LP/AG-DOX hydrogels was investigated in PBS solution at pH = 7.4, 6.5, and 5.5 (Figure 19b, c). It has to be noted that the swelling/erosion experiments were stopped by day 5 because the hydrogels became too fragile to be handled. At pH = 7.4, the weight of AG-DOX hydrogels quickly increased (time of m_∞ is 3.8 h), followed by a rapid decrease (completely broken at 19 h). In comparison, the LP/AG-DOX hydrogels exhibited slower swelling rate (time of m_∞ is 7 h) with a gradual erosion process. Generally, swelling/erosion rate at earlier stage decreased when the pH value changed from 7.4 to 5.5 for both AG-DOX and LP/AG-DOX hydrogels. This is because AG tends to shrink at lower pH, which makes the hydrogels more difficult to deform at acid conditions.[41] Under all the pH values studied, the presence of LP in the hydrogels delayed the swelling and erosion processes. The above data indicate that the incorporation of LP in AG hydrogels increased their stability, probably because the LP nanodisks can act as physical crosslinkers and, as such, contribute to hampering the penetration of water into the gels due to its nanodisk shape with high aspect ratio and large surface area.

3.2. DOX Release Behaviour of the DOX-Loaded Alginate and LP/AG Hydrogels

For antitumor therapeutic applications, the encapsulated DOX should be released to exert its biological function. The release kinetics of DOX from the LP/AG-DOX hydrogels was studied in PBS solution using AG-DOX hydrogels as controls. As can be seen from Figure 20, under physiological conditions (pH = 7.4), the release of DOX from AG-DOX hydrogels was significantly faster than that from the LP/AG-DOX hydrogels. A burst release occurred in the AG-DOX hydrogels, with about 30 ± 1% DOX released in 1d, while only 14 ± 1% DOX was released from the LP/AG-DOX hydrogels in the same interval. The DOX release from AG hydrogels terminated at 1d, but the hybrid hydrogels exhibited a very sustainable DOX release up to 11d. The DOX release profile assumed a bimodal release mode, with a rapid release rate in the first 2d (almost zero-order) and a slow one (also almost zero-order) till 11d. The reason behind the sustained release of DOX from the LP/AG-DOX hydrogels may be related to the fact that DOX has strong physical interaction with LP with large surface area, which hampers the

diffusion of DOX from hydrogels, thereby avoiding the burst release effect. In contrast, for AG hydrogels, the hydrophilic DOX hydrochloride directly diffuses from the hydrogels into the release medium during the quick degradation of AG caused by the rapid exchange of Ca^{2+} with cations in the PBS solution (Figure 19b, c). More importantly, the final cumulative DOX release of LP/AG-DOX hydrogels (35 ± 1%) was higher than the corresponding AG-DOX hydrogels (30 ± 1%).

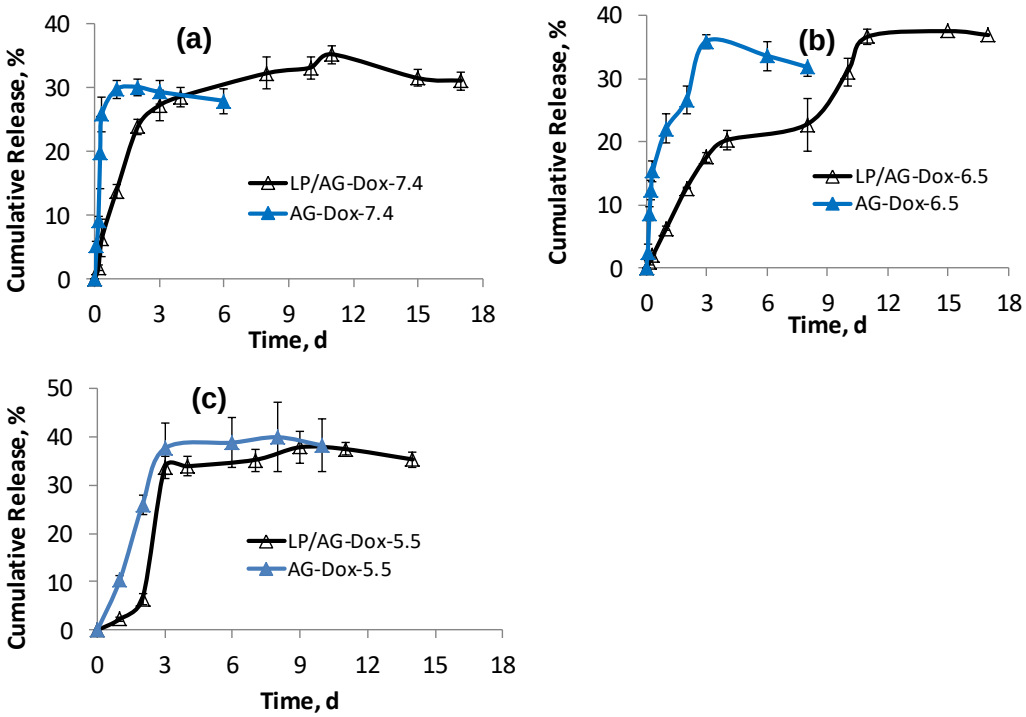

Figure 20. *In vitro* release of Dox from AG-DOX and LP/AG-DOX hydrogels in PBS solution at pH values of a) 7.4, b) 6.5, and c) 5.5.

Considering the quite acidic environment of the tumour site (pH = 6.5)[19,20] and endo/lysosomal compartments (pH = 5.0–6.0)[20], we also compared the release behaviours of DOX under both physiological (pH = 7.4) and acidic (pH = 6.5 and 5.5) conditions. As shown in Figure 20, both AG-DOX and LP/AG-DOX hydrogels displayed a slower DOX release rate at pH = 6.5 than at physiological pH (pH = 7.4). This was expected since alginate theoretically shrinks at low pH, which makes the release of the encapsulated drugs more difficult at acid conditions.[41] Also, the hybrid hydrogels gave a more sustained drug release than the corresponding pure AG-DOX hydrogels at pH = 6.5. For example, 36 ± 1% of DOX was released at day 3 for AG-DOX hydrogels (with a burst release), while only 17.6 ± 0.7% of DOX was released from the hybrid LP/AG-DOX hydrogels (linear release) during the same period. A maximum of DOX drug concentration (36 ± 1%) was achieved at day 3 in the release medium for the AG-DOX hydrogels, which rapidly decreased (to 32 ± 1% at day 8) probably due to the degradation of free DOX induced by acid-catalysed hydrolysis in PBS solution.[42,43] Differently, the hybrid hydrogels gave a continuous DOX release till day 15 (with a maximum DOX drug concentration 37.5 ± 0.2%),

keeping a high level drug concentration (36.9 ± 0.3%) at day 17. Their ability to release DOX in a sustained form will also avoid DOX leakage into the surrounding normal tissues which often occurs with injectable hydrogels, thus decreasing the DOX side effects in the body. Interestingly, with a further decrease of the pH value from 6.5 to 5.5, the DOX release rate of the AG-DOX hydrogels was reduced, while that of the LP/AG-DOX hydrogels was obviously accelerated, especially in the middle stage (LP/AG-DOX hydrogels displayed two distinct platform phases with an enhanced release rate in the middle stage). That is, LP/AG-DOX hydrogels display a higher pH sensitivity in DOX release, which could produce a better sustainable release at the pH = 6.5 (near the extracellular pH of a solid tumour), and an enhanced drug release at the pH = 5.5 (near the pH of the endo/lysosomal compartments). In order to better understand the mechanisms through which DOX is released from these systems, the release profiles were fitted by the exponential Korsmeyer–Peppas equation:[44]

$$F_r = \frac{Abs_t}{Abs_0} = kt^n \qquad \text{Equation 3}$$

where Abs_t and Abs_∞ correspond to the cumulative amount of drug released at time t and at equilibrium, respectively, k is the kinetic constant, and n is an exponent. n falls in the range 0.5–0.43 and 1.0–0.85 for spheres, when drug carriers are Fickian-diffusion-controlled systems and swelling/erosion-controlled ones, respectively[45,46]. The fitted data (Figure 21) indicate that, in the beginning stage, DOX was mainly released from both AG-DOX (n = 1.30) and LP/AG-DOX (n = 0.83) hydrogels at pH = 7.4 in a swelling/erosion-mediated mode, which is in agreement with their swelling/erosion profiles (Figure 19b, c).[47] The presence of LP in the nanocomposite hydrogels greatly decreased the k value from 111.2 (AG-DOX) to 13.6 (LP/AG-DOX). At all studied pH values (7.4, 6.5, and 5.5), AG-DOX hydrogels displayed higher k values (k is 111.2 at pH = 7.4, 50.4 at pH = 6.5, and 11.5 at pH = 5.5) in the first stage than the corresponding LP/AG-DOX hydrogels (k is 13.6 at pH = 7.4, 6.7 at pH = 6.5, and 2.3 at pH = 5.5), because of the quicker swelling/dissolution process of the former (Figure 19b, c). LP has a high surface area and nanodisk structure, which make it capable of diminishing the swelling/erosion process (in the first stage of release) of hydrogels by hampering penetration of water from outside. This, together with its strong interaction with DOX, can effectively decrease DOX diffusion rate from the hydrogels, and thus effectively sustain DOX release. At pH = 6.5, LP/AG-DOX hydrogels had an n value of 1.49 in the middle stage, and at pH = 5.5 they displayed even higher n values (1.48 at the earlier stage and 3.8 at the middle stage). The extraordinary increase in the n value at acid conditions may be caused by the protonation of DOX, which increases its hydrophilicity and thus the permeability across the hydrogels.[35] On the other hand, in the middle stage, the hydrogels suffer an erosion process which can release DOX aggregates formed between protonated cationic DOX

and anionic LP, AG, and/or LP/AG complexes, accelerating the DOX release rate.[48] The DOX release at the final stage may be caused by a diffusion and/or ion-exchange release process from nanocomplexes of AG-DOX, LP/DOX and/or LP/AG-DOX.[32,33,49]

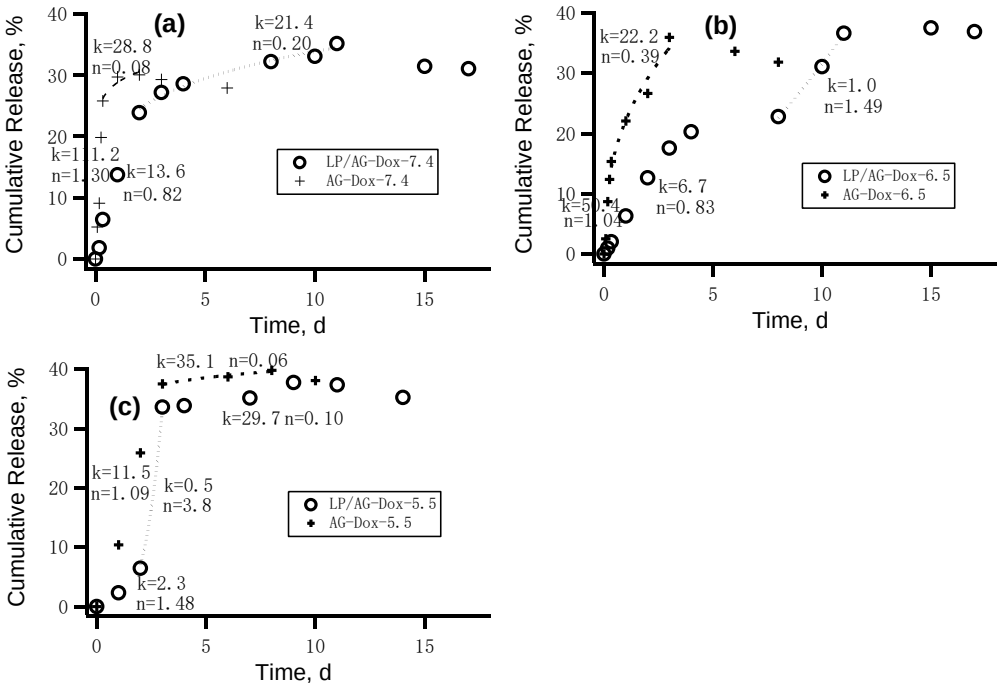

Figure 21. The release profiles of AG-DOX and LP/AG-DOX hydrogels at a) pH = 7.4, b) 6.5, and c) 5.5 were well fitted by Equation (1).

3.3. Antitumor Activity Assay

The antitumor activity of DOX upon release from the hybrid hydrogels was analysed by exposing CAL-72 cells to the release medium of LP/AG-DOX hydrogels and measuring cell metabolic activity using the resazurin reduction assay. As such, cell viability was indirectly evaluated based on the metabolic activity of cells in culture. As shown in Figure 22, compared to free DOX, the 72h-release medium of the AG-DOX and LP/AG-DOX hydrogels inhibited the growth of CAL-72 cells at all the tested DOX concentrations (cell viability results are expressed as a percentage of the control value). LP/AG-DOX hydrogels exhibited higher anticancer efficacy than the corresponding AG-DOX ones. For example, at a DOX concentration of 2.5 μM, almost all CAL-72 cells died after treatment with the release medium of the LP/AG-DOX hydrogels (11 ± 17% of cell viability), while about 32 ± 11% of cells were alive in the case of AG-DOX hydrogels.

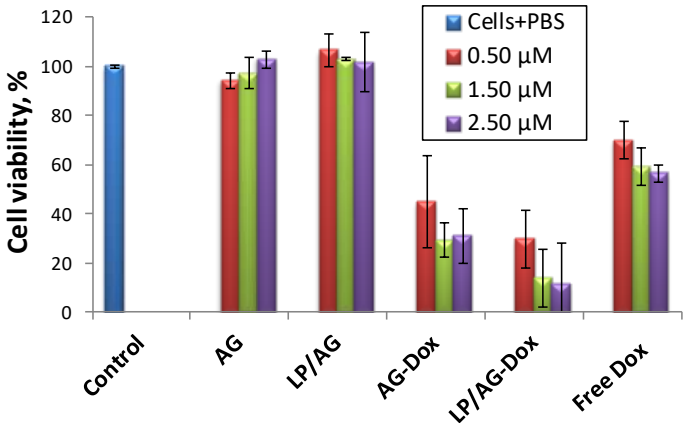

Figure 22. Cell viability of CAL-72 cells after 48h in culture. Cell viability was analysed in the presence of free DOX, and the 72h-release medium of AG-DOX and LP/AG-DOX hydrogels having different DOX concentrations. Untreated CAL-72 cells were used as a control. Control experiments were also done using AG and LP/AG hydrogels without DOX but at concentrations equivalent to those present in the AG-DOX and LP/AG-DOX hydrogels.

The DOX-free hydrogels (AG and LP/AG) did not display any cytotoxicity, showing cell viability similar to the untreated control cells. Our results indicate that the antitumor efficacy is solely related to the loaded drug within the hydrogels. In order to confirm the antitumor activity of the DOX loaded hybrid hydrogels, the morphology of cells treated with free DOX, the 72h-release medium of AG-DOX and LP/AG-DOX hydrogels was observed after 48 h incubation by optical microscopy (Figure 23). Cells in the control or cultured in the presence of the release medium from DOX-free AG and LP/AG hydrogels presented a healthy morphology, displaying a fusiform shape and being adherent to the cell culture dish surface. This indicates that AG and LP/AG hydrogels are quite cytocompatible. At a DOX concentration of 2.5 x 10^6 M, samples treated with free DOX and AG-DOX-release medium presented a mixture of fusiform (attached cells) and rounded (non-adherent cells or cells in a process of losing the adherence to the surface) cells, indicating a moderate level of cytotoxicity. However, at the same DOX concentration, almost all the cells cultured with LP/AG-DOX hydrogels died, as it can be observed by the lack of adherent cells and high quantity of cell debris present. The cell morphology results are in agreement with the metabolic activity quantitative data, indicating that DOX within the LP/AG-DOX hydrogels exert a higher antitumoral activity.

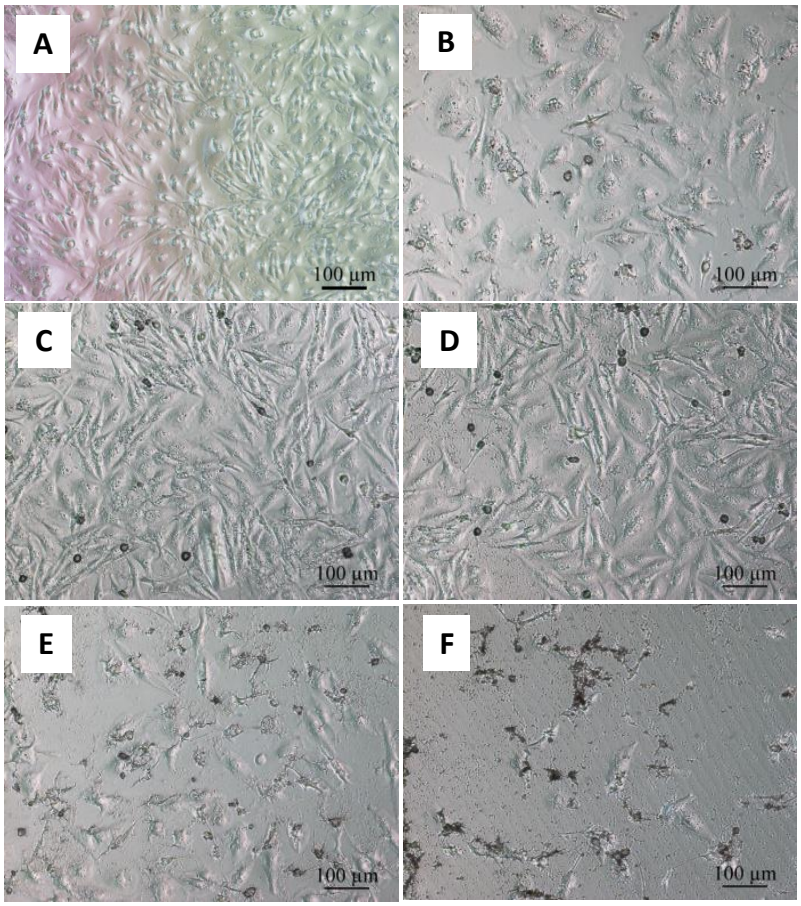

Figure 23. Cell morphology (optical microscopy) of CAL-72 cells after 48h incubation. a) Control (cells exposed to PBS solution); b) cells exposed to free DOX (2.5×10^{-6} M); c,d) cells exposed to the 72h-release media of AG and LP/AG unloaded hydrogels, respectively; e, f) cells exposed to the 72h-release media of AG-DOX and LP/AG-DOX hydrogels, respectively, at a 2.5×10^{-6} M DOX concentration.

The above drug release results showed that LP/AG-DOX hybrid hydrogels, compared to AG-DOX hydrogels, presented a more sustainable drug release behaviour and enhanced drug release efficiency, thus being expected to have long-term and better therapeutic efficacy. In order to check this hypothesis, the cytotoxicity of the 24, 48, and 72h release medium from AG-DOX and LP/AG-DOX hydrogels was also quantitatively studied using the resazurin reduction assay. As shown in Figure 24, the 24h-release medium of AG-DOX hydrogels with a DOX concentration of 1.5×10^{-6} M gave rise to a lower cell viability (27 ± 17%) than that obtained with LP/AG-DOX hydrogels (39 ± 7%). However, the 72h-release medium of AG-DOX hydrogels was much less effective than that released in the first 24 h, which was likely due to the fact that AG-DOX hydrogels stop releasing DOX after 24 h, simultaneously with the occurrence of DOX degradation (Figure 20). In contrast, the 48h-release of the LP/AG-DOX hydrogels led to lower cell viability (19 ± 9%) than the corresponding AG-DOX hydrogels (27 ± 7%). With the further increase of release time, the anticancer activity of AG-DOX hydrogels (cell viability: 29 ± 7% for the 72h-release medium) started to decrease, while the LP/AG-DOX hydrogels displayed a

continuously enhancement in the anticancer activity (cell viability: 14 ± 12% for the 72h-release medium). As previously seen, it is clear that AG and LP/AG hydrogels without DOX loading do not affect cell viability, indicating that the anticancer effect only results from the loaded DOX drug. The results clearly suggest that LP/AG-DOX hydrogels have a long-term anticancer activity, which may be very important in the clinical scenario.

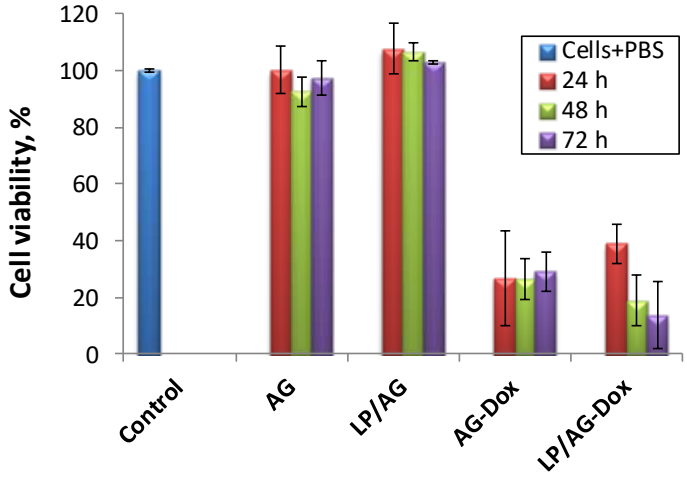

Figure 24. Cell viability of CAL-72 cells after 48h in culture and exposed to the 24, 48, and 72h-release media of AG-DOX and LP/AG-DOX hydrogels at a DOX concentration of 1.5×10^{-6} M. Untreated CAL-72 cells were used as a control. Control experiments were also done using AG and LP/AG hydrogels without DOX but at concentrations equivalent to those present in the AG-DOX and LP/AG-DOX hydrogels.

Since DOX is a fluorescent molecule, its accumulation in CAL-72 cells can be followed by fluorescence microscopy (Figure 25). A strong red fluorescence signal was visualized when cells were cultured in the presence of the 24 and 72h-release media of AG-DOX and LP/AG-DOX hybrid hydrogels. The results clearly show that DOX is spread not only in the cytoplasm but also in the nucleus of cells after 48 h of incubation. Compared to AG-DOX experiments, a higher density of red DOX can be seen inside the nucleus of cells when both 24 and 72h-release media of the hybrid LP/AG-DOX hydrogels were applied, and especially for the 72h-release medium. The 24h-release media of both AG-DOX and LP/AG-DOX hydrogels induced an obvious transformation of the cell shape (cells lost their fusiform shape) which indicates a death process. More fusiform shaped cells were found in the case of the 24h-release medium of LP/AG-DOX hydrogels because less DOX was released for these hydrogels in that short period (Figure 20). However, almost all the cells treated with the 72h-release medium of LP/AG-DOX hydrogels lost their fusiform shape, indicating the accelerated cell death process for this situation. The change in cell morphology was not so evident for the case of AG-DOX hydrogel released medium. A higher density of fusiform cells appeared for the 72h-release medium of AG-DOX than for the 24h-release medium, indicating that cancer cell growth can recover if no sufficient content of DOX is maintained in culture. These observations are in agreement with the quantitative data obtained in the

above cell viability assays. Interestingly, the drug release study (Figure 20) indicates that the amount of 72h-release DOX from LP/AG-DOX hydrogels is quite lower than that released from AG-DOX hydrogels. Therefore, the enhanced anticancer activity noticed for the 72h-release medium of LP/AG-DOX hydrogels must be attributed to the presence of LP, which probably helps deliver DOX through the cell membrane.

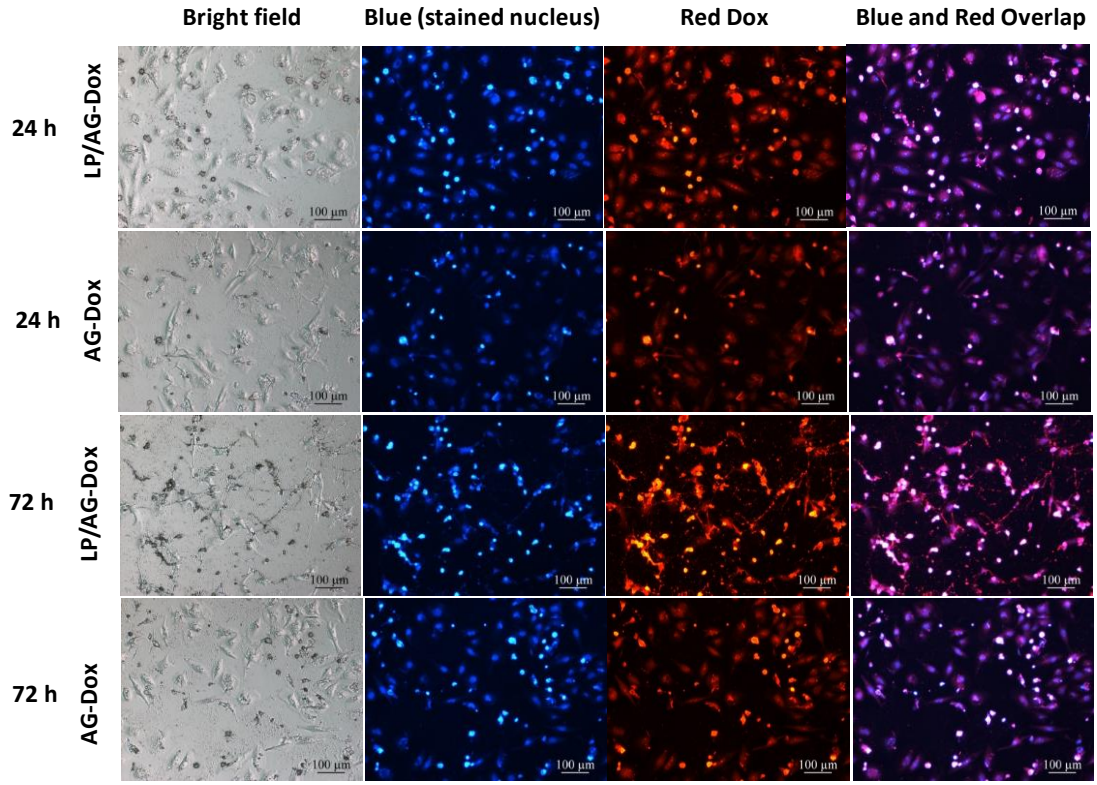

Figure 25. Bright field and fluorescence microscope images of CAL-72 cells after 48h culture with the 24h-release media and the 72h-release media of AG-DOX and LP/AG-DOX hydrogels with an equivalent DOX concentration (1.5×10^{-6} M). The cell nucleus (blue) is stained with DAPI; DOX emits a red fluorescent signal.

To better understand the role of LP on the DOX release from the hydrogels, the hydrogel released solutions were analysed by dynamic light scattering (DLS).

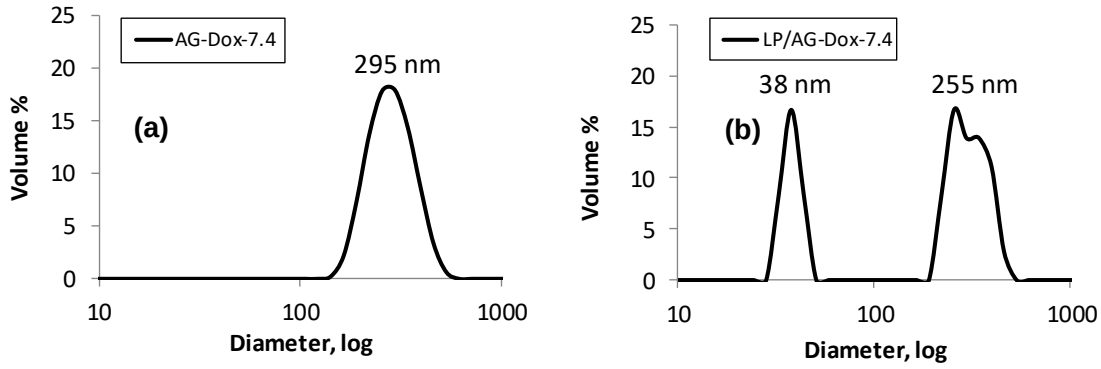

Figure 26. Dynamic light scattering (DLS) analysis of the release media from a) AG-DOX hydrogels and b) LP/AG-DOX hydrogels in PBS buffer, at a pH value of 7.4.

As can be seen in Figure 26, the AG-DOX-released medium contained nanoparticles (with a peak at 295 nm), probably consisting in AG-DOX nanoaggregates released from the hydrogels during their degradation. The LP/AG-DOX-released medium also revealed the presence of nanoparticles with a smaller size (with peaks at 38 and 255 nm), which is probably caused by more condensed complexation of LP with DOX through their strong physical interactions.[34] The average ζ-potential of these nanoaggregates was also measured, apparently decreasing from -25 ± 2 mV (AG-DOX hydrogels released-medium) to -27.8 ± 0.1 mV (LP/AG-DOX hydrogels released-medium), probably due to the successful incorporation of LP (-45.2 ± 3.1 mV, data not shown). The uptake of the drug by the cells is one of the key factors for the achievement of its therapeutic efficacy.[3] We hypothesized that, upon degradation, the bulk hydrogels release nanocarriers containing DOX, which are then taken up by cells and help the cellular internalization of the drug. Optical fluorescence microscopy was used to evaluate the extent of DOX internalization in CAL-72 cells, after 1 h of exposure to the drug, and using the 72h-release medium of AG-DOX and LP/AG-DOX hydrogels (Figure 27).

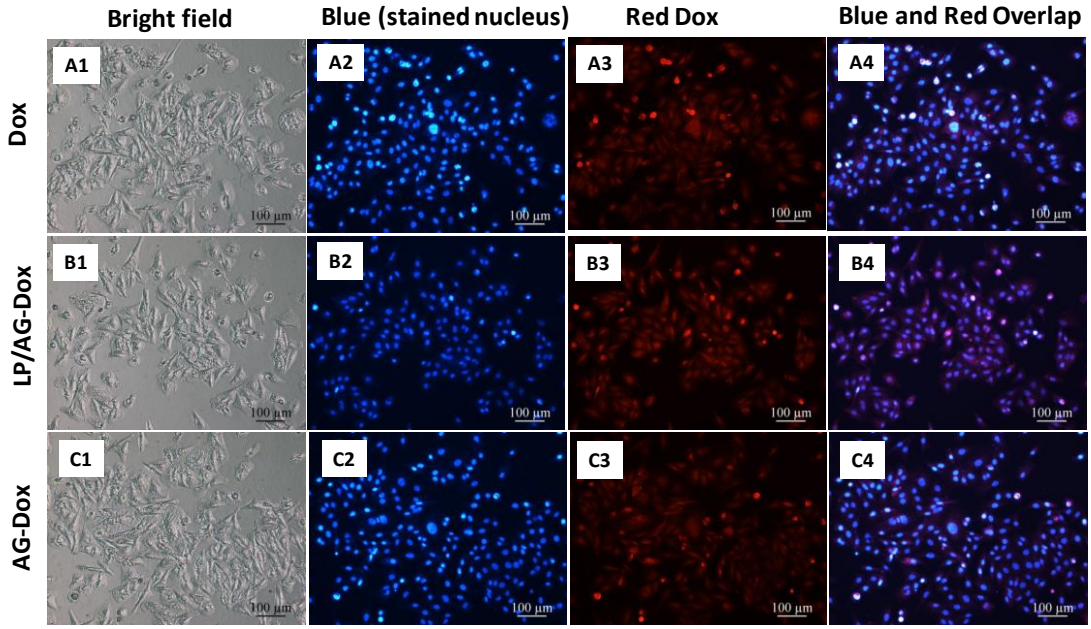

Figure 27. Images of CAL-72 cells incubated for 1h with free DOX (1.5×10^{-6} M, A1–A4) and the 72 h-release media from LP/AG-DOX (B1–B4) and AG-DOX (C1–C4) hydrogels containing an equivalent DOX concentration. The cell nucleus (blue) is stained with DAPI; DOX emits a red fluorescence signal.

A red fluorescence signal was observed in cell cytoplasm for all situations under study. However, compared to the other cases, cells cultured in the presence of the release medium of DOX-loaded LP/AG hydrogels displayed a stronger red fluorescence, suggesting that the presence of LP in the nanoaggregates accelerates the DOX uptake process. It is possible that nanocarriers resulting from the electrostatic interaction of DOX-loaded LP disks and AG were able to deliver a high dose of DOX into cancer cells in culture and help overcoming DOX ion-trapping in the acidic extracellular

environment of a solid tumour and the acidic endo-lysosomal compartment. The problem of DOX trapping inside the acidic endo-lysosomal compartment which is in part responsible for DOX resistance will, then, be circumvented. We believe that the nanoaggregates released from LP/AG-DOX hybrid hydrogels during their degradation process can act as DOX shuttles across the cell membrane and facilitating the internal release of the drug, leading to enhanced anticancer activity with a prolonged time. Due to their natural origin, biocompatibility and biodegradability, polysaccharides have been widely investigated as components for fabrication of various drug delivery systems. Although they can be crosslinked to form hydrogels for DOX delivery, these systems often lead to a burst release and quick drug release rate (in several hours), because of their high porosity and the hydrophilicity of the small DOX molecule.[17,18] For the chemically-crosslinked hydrogels, toxic small crosslinkers may be introduced, which together with their possible non-degradability could cause high *in vivo* cytotoxicity. Also the non-degradability may limit the drug release efficiency and lower therapeutic efficacy.[50] Our LP/AG-DOX nanocomposite hydrogels can effectively avoid DOX burst release and produce a sustainable release for up to 11d under physiological condition, by taking advantage of the strong interactions between LP and DOX. More importantly, during the degradation process, the hybrid hydrogels release LP/AG-DOX nanocomplexes, which serve as vehicles for DOX internalization into cancer cells, overcoming DOX resistance caused by ion trapping of DOX inside the tumour aggregates and/or in the endo-lysosomes. The DOX/free nanocomposite hydrogels are highly biocompatible. The sustainability in DOX release and their circumventing ion-trapping effect endow them with enhanced long term anticancer efficacy, with promising potential biomedical applications for delivery of various drugs beyond anticancer drugs.

4. Conclusion

In summary, we present a facile approach to prepare LP/AG-DOX hybrid hydrogels with a sustained DOX release profile and enhanced DOX antitumor activity. The incorporation of LP within the AG hydrogels improved the gel stability and the drug EE, avoiding the initial burst release of the drug. More importantly, the hybrid hydrogels degrade along the time, giving rise to a new type of nanohybrids, which serve as vehicles for DOX internalization into cancer cells and, possibly, help diminishing endo-lysosome DOX trapping. Furthermore, the LP/AG-DOX hydrogels release DOX in a sustained mode (almost zero-order) under the acidic conditions of a tumour extracellular environment (pH = 6.5). The good cytocompatibility of these hybrid hydrogels, together with their drug release and delivery properties, make us think that LP-based hydrogel drug carriers may also be helpful for other therapeutic applications.

References

1 H. T. Ta, C. R. Dass, I. Larson, P. F. M. Choong and D. E. Dunstan, *Biomaterials*, 2009, **30**, 3605–3613.

2 J. H. Maeng, D.-H. Lee, K. H. Jung, Y.-H. Bae, I.-S. Park, S. Jeong, Y.-S. Jeon, C.-K. Shim, W. Kim, J. Kim, J. Lee, Y.-M. Lee, J.-H. Kim, W.-H. Kim and S.-S. Hong, *Biomaterials*, 2010, **31**, 4995–5006.

3 C. Zhang, W. Wang, T. Liu, Y. Wu, H. Guo, P. Wang, Q. Tian, Y. Wang and Z. Yuan, *Biomaterials*, 2012, **33**, 2187–2196.

4 K. C. Weng, C. O. Noble, B. Papahadjopoulos-Sternberg, F. F. Chen, D. C. Drummond, D. B. Kirpotin, D. Wang, Y. K. Horn, B. Hann and J. W. Park, *Nano Lett.*, 2008, **8**, 2851–2857.

5 D. Kim, E. S. Lee, K. T. Oh, G. Z. Gao and Y. H. Bae, *Small*, 2008, **4**, 2043–2050.

6 J.-P. Gillet and M. M. Gottesman, in *Methods in Molecular Biology (Methods and Protocols)*, Humana Press, 2010, vol. 596, pp. 47–76.

7 J. W. Wojtkowiak, D. Verduzco, K. J. Schramm and R. J. Gillies, *Mol. Pharm.*, 2011, **8**, 2032–2038.

8 S. Wang, E. A. Konorev, S. Kotamraju, J. Joseph, S. Kalivendi and B. Kalyanaraman, *J. Biol. Chem.*, 2004, **279**, 25535–25543.

9 F. Gao, L. Li, T. Liu, N. Hao, H. Liu, L. Tan, H. Li, X. Huang, B. Peng, C. Yan, L. Yang, X. Wu, D. Chen and F. Tang, *Nanoscale*, 2012, **4**, 3365–3372.

10 P. K. Working, M. S. Newman, T. Sullivan and J. Yarrington, *J. Pharmacol. Exp. Ther.*, 1999, **289**, 1128–1133.

11 J. Shen, Q. He, Y. Gao, J. Shi and Y. Li, *Nanoscale*, 2011, **3**, 4314–4322.

12 J. Choi, T. Konno, M. Takai and K. Ishihara, *Biomaterials*, 2012, **33**, 954–961.

13 Y. Li, J. Rodrigues and H. Tomás, *Chem. Soc. Rev.*, 2012, **41**, 2193–2221.

14 A. M. Al-Abd, K.-Y. Hong, S.-C. Song and H.-J. Kuh, *J. Control. Release*, 2010, **142**, 101–107.

15 C. He, S. W. Kim and D. S. Lee, *J. Control. Release*, 2008, **127**, 189–207.

16 J. Kopeček and J. Yang, *Acta Biomater.*, 2009, **5**, 805–816.

17 F. Brandl, F. Kastner, R. M. Gschwind, T. Blunk, J. Teßmar and A. Göpferich, *J. Control. Release*, 2010, **142**, 221–228.

18 E. M. Pritchard, C. Szybala, D. Boison and D. L. Kaplan, *J. Control. Release*, 2010, **144**, 159–167.

19 M. Oishi, S. Sumitani and Y. Nagasaki, *Bioconjug. Chem.*, 2007, **18**, 1379–1382.

20 J. Yang, H. Chen, I. R. Vlahov, J.-X. Cheng and P. S. Low, *J. Pharmacol. Exp. Ther.*, 2007, **321**, 462–468.

21 N. Bhattarai, J. Gunn and M. Zhang, *Adv. Drug Deliv. Rev.*, 2010, **62**, 83–99.

22 Y. L. Chiu, S. C. Chen, C.-J. Su, C.-W. Hsiao, Y.-M. Chen, H.-L. Chen and H.-W. Sung, *Biomaterials*, 2009, **30**, 4877–4888.

23 Y.-S. Hwang, J. Cho, F. Tay, J. Y. Y. Heng, R. Ho, S. G. Kazarian, D. R. Williams, A. R. Boccaccini, J. M. Polak and A. Mantalaris, *Biomaterials*, 2009, **30**, 499–507.

24 A. W. Chan and R. J. Neufeld, *Biomaterials*, 2010, **31**, 9040–9047.

25 S. M. Jay, B. R. Shepherd, J. W. Andrejecsk, T. R. Kyriakides, J. S. Pober and W. M. Saltzman, *Biomaterials*, 2010, **31**, 3054–3062.

26 D.-H. Kim and D. C. Martin, *Biomaterials*, 2006, **27**, 3031–3037.

27 L. Zhao, M. D. Weir and H. H. K. Xu, *Biomaterials*, 2010, **31**, 6502–6510.

28 K. Y. Lee, K. H. Bouhadir and D. J. Mooney, *Biomaterials*, 2004, **25**, 2461–2466.

29 C. Viseras, P. Cerezo, R. Sanchez, I. Salcedo and C. Aguzzi, *Appl. Clay Sci.*, 2010, **48**, 291–295.

30 J. I. Dawson and R. O. C. Oreffo, *Adv. Mater.*, 2013, **25**, 4069–4086.

31 N. Negrete-Herrera, J. L. Putaux and E. Bourgeat-Lami, *Prog. Solid State Chem.*, 2006, **34**, 121–137.

32 L. L. Hench, *J. Am. Ceram. Soc.*, 1991, **74**, 1487–1510.

33 D. W. Thompson and J. T. Butterworth, *J. Colloid Interface Sci.*, 1992, **151**, 236–243.

34 BYK Additives & Instruments, *LAPONITE - Perform. Addit.*, 2014, 1–24.

35 S. Wang, Y. Wu, R. Guo, Y. Huang, S. Wen, M. Shen, J. Wang and X. Shi, *Langmuir*, 2013, **29**, 5030–5036.

36 A. K. Gaharwar, S. M. Mihaila, A. Swami, A. Patel, S. Sant, R. L. Reis, A. P. Marques, M. E. Gomes and A. Khademhosseini, *Adv. Mater.*, 2013, **25**, 3329–3336.

37 H. Jung, H.-M. Kim, Y. Bin Choy, S.-J. Hwang and J.-H. Choy, *Int. J. Pharm.*, 2008, **349**, 283–290.

38 Y. Li, D. Maciel, H. Tomás, J. Rodrigues, H. Ma and X. Shi, *Soft Matter*, 2011, **7**, 6231–6238.

39 A. Khdair, H. Handa, G. Mao and J. Panyam, *Eur. J. Pharm. Biopharm.*, 2009, **71**, 214–222.

40 F. Siepmann, K. Eckart, A. Maschke, K. Kolter and J. Siepmann, *J. Control. Release*, 2010, **141**, 216–222.

41 S.-C. Chen, Y.-C. Wu, F.-L. Mi, Y.-H. Lin, L.-C. Yu and H.-W. Sung, *J. Control. Release*, 2004, **96**, 285–300.

42 K. Wassermann and H. Bundgaard, *Int. J. Pharm.*, 1983, **14**, 73–78.

43 J. H. Beijnen, O. A. G. J. van der Houwen and W. J. M. Underberg, *Int. J. Pharm.*, 1986, **32**, 123–131.

44 R. W. Korsmeyer, R. Gurny, E. Doelker, P. Buri and N. A. Peppas, *Int. J. Pharm.*, 1983, **15**, 25–35.

45 F. Van de Manakker, K. Braeckmans, N. El Morabit, S. C. De Smedt, C. F. Van Nostrum and W. E. Hennink, *Adv. Funct. Mater.*, 2009, **19**, 2992–3001.

46 K. Kosmidis, E. Rinaki, P. Argyrakis and P. Macheras, *Int. J. Pharm.*, 2003, **254**, 183–188.

47 H. Abdelkader, O. Youssef Abdalla and H. Salem, *AAPS PharmSciTech*, 2008, **9**, 675–83.

48 Y. Li, J. L. Santos, D. Maciel, H. Tomás and J. Rodrigues, *J. Control. Release*, 2011, **152**, e55–e57.

49 H. Jung, H.-M. Kim, Y. Bin Choy, S.-J. Hwang and J.-H. Choy, *Appl. Clay Sci.*, 2008, **40**, 99–107.

50 L. Zhao, L. Zhu, F. Liu, C. Liu, Shan-Dan, Q. Wang, C. Zhang, J. Li, J. Liu, X. Qu and Z. Yang, *Int. J. Pharm.*, 2011, **410**, 83–91.

Chapter III.

pH-sensitive Laponite®/Doxorubicin/Alginate Nanohybrids with Improved Anticancer Efficacy

Abstract

The efficacy of the anticancer drug doxorubicin (DOX) is limited by an insufficient cellular uptake and drug resistance, which is partially due to ion trapping in acidic environments such as the extracellular environment of solid tumours and the interior of endolysosome vesicles. Herein, we describe the preparation and *in vitro* evaluation of a new type of nanohybrid for anticancer drug delivery which is capable of carrying a high load of the cationic DOX through the cell membrane. In addition, the nanohybrids use the acidic environment of the endolysosomes to release the drug, simultaneously helping to disrupt the endolysosomes and diminishing endolysosome DOX trapping. Furthermore, as the nanohybrid carriers are capable of sustained drug delivery, those that remain in the cytoplasm and still contain DOX are expected to exert a prolonged anticancer activity. Briefly, DOX is loaded onto biocompatible anionic Laponite® (LP) nanodisks with a high aspect ratio (25 nm in diameter and 0.92 nm in thickness) through strong electrostatic interactions to get DOX-loaded LP disks. Alginate (AG), a biocompatible natural polymer, is then coated onto the DOX-loaded LP disks (LP/DOX/AG nanohybrids) to prevent the burst release of the drug. The results demonstrate that the nanohybrids have a high encapsulation efficiency (80.8 ± 10.6%), are sensitive to pH and display a sustained drug release behaviour. Cell culture experiments indicate that the LP/DOX/AG nanohybrids can be effectively internalized by CAL-72 cells (an osteosarcoma cell line) and exhibit a remarkable higher cytotoxicity to cancer cells than the free DOX. The merits of LP/AG nanohybrids, such as biocompatibility, high loading capacity and stimulus responsive release of cationic chemotherapeutic drugs, render them as excellent platforms for drug delivery.

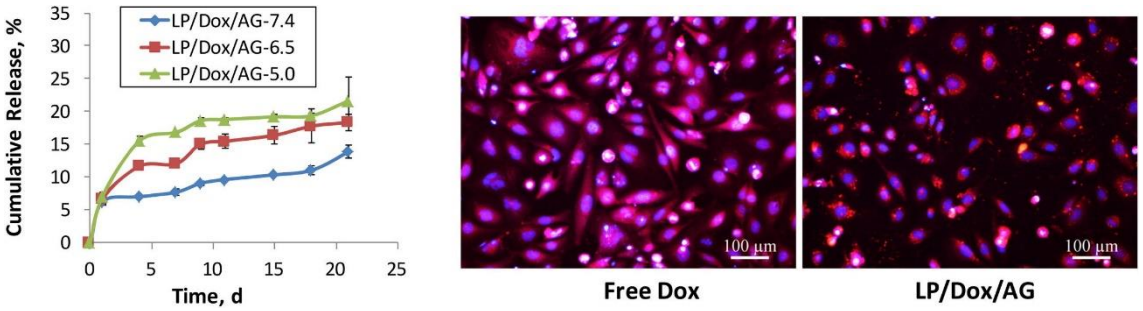

This Chapter is based on the following publication:

M. Gonçalves, P. Figueira, D. Maciel, J. Rodrigues, X. Qu, C. Liu, H. Tomás and Y. Li, pH-sensitive Laponite®/doxorubicin/alginate nanohybrids with improved anticancer efficacy, Acta Biomater., 2014, 10, 300–307.

1. Introduction

Nanomaterials may have a significant impact on the diagnosis and treatment of important diseases that affect mankind, such as cancer. In particular, nanomaterials can be designed to carry drugs and nucleic acids, releasing them inside the target cells in a controlled and efficacious way.[1–3] Doxorubicin (DOX) is one of the most widely used chemotherapeutic drugs for the treatment of cancer, including bone cancer[4], liver cancer[5] and breast cancer.[6,7] It is a weak base, with a pK_a of 8.30, and has been previously reported to undergo ion trapping in acidic conditions such as those present in the extracellular microenvironment of solid tumours (pH 6.5–6.9) and in the internal milieu of endolysosomes (pH 5.0–6.0).[8,9] Whereas uncharged DOX can freely permeate membranes, the protonated DOX has a lower membrane permeability, becoming trapped inside acidic compartments. It has also been shown that DOX may be pumped out of the cells by p-glycoprotein, which is a drug exporter molecule with enhanced activity in acidic environments.[10] Both these situations limit the therapeutic bioactivity of free DOX, and a large dosage or an increased number of injections may be needed to keep the desirable therapeutic efficacy, which often leads to adverse side effects in normal tissues, especially in the heart and kidneys.[11,12] Various drug delivery systems, including liposomes[13], dendrimers[14] and micro- and nanoparticles[15,16], have been developed for DOX administration, which improved its antitumor activity.[17] However, a great challenge still exists in the development of well-controlled drug release systems with the ability of increasing DOX cellular uptake and, triggered by environmental stimuli, of releasing the drug within the cytoplasm so that DOX can reach the nucleus to achieve the desired therapeutic effects.[18–20]

Clays and clay minerals have been effectively used to modify drug delivery systems.[21] LP, a kind of synthetic silicate nanoparticle, has a disk shape and a large aspect ratio (AR) (25 nm in diameter and 0.92 nm in thickness), which can degrade into non-toxic products (Na^+, $Si(OH)_4$, Mg^{2+}, Li^+), similar to the degradation products of bioactive glasses (Na^+, $Si(OH)_4$, Ca^{2+}, PO_4^{3-}).[22,23] As a physical crosslinker, LP has been hybridized with various polymers, such as polyethylene oxide (PEO) and PEO/chitosan, to improve cell adhesion, proliferation and differentiation.[24–27] LP has a large surface area (330 m^2/g), and can establish strong interactions with guest compounds.[28,29] The charges on the LP surfaces are negative and the edge charges are pH dependent.[23] In our previous studies, LP was incorporated into alginate bulk hydrogels, which greatly increased the loading capacity and the pH sensitivity in the release of a cationic model drug.[29–31] Also, it was reported that nanoparticles with a large AR can be more effectively taken up by cells compared to small AR nanoparticles.[32] We thus hypothesized that LP-based nanocarriers could be adequate systems to be used in the delivery of anticancer drugs such as DOX.

In the present work, we developed a new type of LP-based nanohybrid with pH sensitivity in the sustained release of DOX and improved antitumor activity. The process involved two steps: first, DOX was loaded onto the surface of LP via electrostatic interactions; second, the DOX-loaded LP was mixed with a solution of alginate (a biocompatible polymer[33,34]) to get DOX-loaded nanohybrids (LP/DOX/AG). It was found that the LP/DOX/AG nanohybrids presented a high DOX encapsulation efficiency, were effectively taken up by the osteosarcoma cell line CAL-72 and exhibited higher toxic activity than free DOX. Beyond the controlled release of DOX achieved by the nanohybrids at different pH values, it was found that the amount of released DOX increased by decreasing the pH (pH-triggered release) until a value similar to that existing inside the endolysosomal compartments.

It is known that cationic polymers, such as polyethylenimine, possess a high buffering capacity below physiological pH, due to the protonation of amines.[35] This process can occur inside cells upon fusion of the endosomes with the lysosomes (pH 5.0–6.0), resulting in more protons being pumped into these compartments with the concurrent influx of chloride ions (to maintain charge neutrality). This effect may increase the osmotic pressure and make the vesicles swell and disrupt (the so-called the "proton-sponge effect").[35–37] Taking advantage of this property, many cationic polymers have been use for gene delivery to improve the gene transfection efficiency.[36–39] However, their application is limited by the high cytotoxicity associated with cationic polymers, which tend to induce membrane disruption via nanohole formation, membrane thinning and erosion.[40,41] As the nanohybrids displayed a high buffer capacity (adsorption/absorption of protons), we hypothesize that they may also have the "proton-sponge effect".[35–37] The DOX resistance associated with DOX trapping inside the acidic endolysosomes will then be overcome. In addition, the nanohybrids were prepared using an environmental friendly method, without using any organic solvents and surfactants.

2. Material and methods

2.1. Materials

Laponite® RDS (LP) was kindly offered from Rockwood Additives Limited, UK. Alginate acid sodium salt (AG, from brown algae, MW from 12 to 58 kDa, cell culture tested) was purchased from Sigma. DOX was obtained from Aldrich. Triethylamine was obtained from Acros. Dulbecco's phosphate-buffered saline (PBS, without Ca^{2+} and Mg^{2+}) solution was bought from Invitrogen. All other reagents were from Sigma, unless otherwise indicated.

2.2. Preparation and characterization of the AG/DOX/LP nanohybrids

The LP/DOX/AG nanohybrids were prepared by dropping 5 mL of a 0.1 wt.% DOX aqueous solution into 25 mL of a 0.2 wt.% LP aqueous solution under 400 rpm magnetic stirring overnight. Then

10 mL of a 0.1 wt.% AG solution was dropped into the above mixture under magnetic stirring overnight, followed by the addition of 0.1 mL of trimethylamine under 400 rpm magnetic stirring overnight. The mixture was precipitated by a centrifuge (Sigma 3K30) under 19,872 g force for 5 min to remove unencapsulated DOX and free AG. The DOX content of the supernatants was determined spectrophotometrically at 490 nm using an ultraviolet–visible spectrometer (Perkin Elmer Lambda 2) for calculation of DOX encapsulation efficiency. The precipitate was kept at 4 °C for further study. The solid content of the LP/DOX/AG precipitate was 6 wt.% as determined by weight difference before and after drying. The hydrodynamic diameter and the surface charge of the LP/DOX/AG nanohybrids and the LP disks were measured at room temperature using a Zetasizer Nano ZS (Malvern Instruments, UK). The hydrodynamic diameters were determined with a detection angle of 173°. Zeta potential measurements were performed with a detection angle of 17° and calculated using the Smoluchowsky model for aqueous suspensions. Before measurement, the LP/DOX/AG or the LP were dispersed in ultrapure water and sonicated (BRANSON 2510, 100 W) for 15 min. The morphology of the LP and the LP/DOX/AG was examined on a transmission electron microscope (JEOL JEM-200CX). Before measurement, the samples were dispersed in ultrapure water under sonication (Branson 2510, 100 W) for 15 min. Aqueous suspensions of the samples (0.06 mg/mL) were dropped onto a 100-mesh formvar-coated copper grid and then air dried before imaging.

2.3. *In vitro* drug release studies

A stock solution of the nanohybrids was prepared by dispersing 30 mg of the LP/DOX/AG precipitate (solid content: 6 wt.%) in 1 mL of ultrapure water, followed by sonication (Branson 2510, 100 W) for about 15 min. In triplicate, 0.1 mL of the stock solution was transferred to 1.9 mL of PBS at 37 °C at pH values of 7.4, 6.5, 5.0, 3.0 and 1.0. At different intervals of time, the solutions were centrifuged at 13,845g for 5 min at room temperature. The DOX content released into the supernatants was determined spectrophotometrically as previously described. As a control, the release of free DOX in PBS solution at pH 7.4 was studied at equivalent DOX mass concentrations to those used for LP/DOX/AG. Briefly, 0.5 mL of a DOX solution inside a dialysis membrane (MW cutoff 14,000 Da, Green Bird, Shanghai Green Bird Science & Technology Development Co., Ltd.) was added to 9.5 mL of PBS solution at 37 °C. At different time intervals, 2 mL of solution was taken out for the DOX release analysis and renewed with 2 mL of fresh PBS buffer. The released DOX content in the released medium was determined spectrophotometrically as previously described. The cumulative release (C_r) of DOX against time was obtained according to the equation:

$$C_r = \frac{Abs_t}{Abs_{tot}} \times 100$$

where Abs_t and Abs_{tot} are the cumulative amount of drug released at time t and the total drug contained in the nanohybrids used for drug release, respectively.

2.4. Acid–base titration

The buffering capacity of the LP and LP/DOX/AG nanohybrids was determined by an acid–base titration assay over the pH range from 12.0 to 2.0. First, the two kinds of samples were diluted to a final concentration of 0.0775 mg/mL in 5 mL of NaCl (100 mM) aqueous solution. The pH values of the sample solutions as well as NaCl (100 mM) aqueous solution (control) were adjusted to 12.0 by 1 M NaOH, before 25 µL aliquots of 0.1 M HCl were successively added to the above solutions until the pH value reached 2.0, the changes in pH being monitored by a pH meter (model 744, Metrohm).

2.5. Biological assays

CAL-72 cells (an osteosarcoma cell line) were cultured in Dulbecco's modified Eagle's medium containing 10 vol.% fetal bovine serum (FBS, Gibco) and 1 vol.% of an antibiotic–antimycotic 100x solution (AA, containing penicillin, streptomycin and amphotericin B; Gibco). The medium was also supplemented with 1 vol.% of L-glutamine 100x solution (Gibco) and 1 vol.% of insulin–transferrin–selenium 100x solution (ITS, Gibco). Cells were grown at 37 °C in a humidified atmosphere with 5% of carbon dioxide. Afterwards, the cells were harvested at 70–80% confluence, using a trypsin–ethylenediaminetetraacetic acid solution. To determine whether the LP/DOX/AG nanohybrids were therapeutically active, the cells were first plated in 24-well plates for 24 h, with a seeding density of 1.5×10^4 cells per well. One day later, free DOX or LP/DOX/AG nanohybrid solutions (with equivalent DOX concentrations) were prepared in ultrapure water, filtered, added to the cell cultures and then incubated for 48 h at 37 °C, before performing the resazurin reduction assay to check cell viability. Note that LP was used as a control at equivalent mass concentrations to those used for LP/DOX/AG.

The cell viability was quantified by the measurement of the metabolic activity of the cells in culture through the resazurin reduction assay. Briefly, after the 48 h incubation period, the cell culture medium was replaced with fresh medium containing resazurin at a concentration of 0.1 mg/mL and kept at 37 °C in the cell incubator for 3 h. Afterwards, aliquots of the cell supernatant were transferred to 96-well opaque plates and the resorufin fluorescence (λ_{ex} = 530 nm, λ_{em} = 590 nm) was measured using a microplate reader (model Victor3 1420, PerkinElmer).

For the cell uptake study, cells were plated for 24 h before the incubation with freshly prepared DOX or LP/DOX/AG solutions (diluted in PBS) at 37 °C for 48 h. Subsequently, the cells were washed with sterilized PBS buffer and simultaneously fixed with 3.7 vol.% glutaraldehyde solution and stained with 4',6-diamidino-2-phenylindole (DAPI; Sigma) for 30 min. The cells were then washed with PBS

solution for further analysis by optical fluorescence microscopy (Nikon Eclipse TE 2000E inverted microscope).

3. Results and discussion

3.1. Preparation and physical characterization of DOX-loaded Laponite®/alginate nanohybrids (LP/DOX/AG)

LP/DOX/AG nanohybrids were prepared according to the procedure depicted in Figure 28. Schematic illustration for the formation and drug release of DOX-loaded LP/AG nanohybrids.

First, an aqueous solution of LP was mixed with an aqueous solution of DOX (under magnetic stirring, overnight) to load the anionic LP with the cationic DOX via electrostatic interactions. This was followed by coating with AG, a biocompatible and degradable natural polymer.[33,34] As such, the design of the nanohybrids included an inner part consisting of LP disks to confer on them pH sensitivity and serve as a temporarily drug reservoir, as well as an outer layer made of AG for improvement of their stability and controlled release properties. This strategy also enabled us to sandwich a toxic cationic anticancer drug between two biocompatible materials (Figure 28).

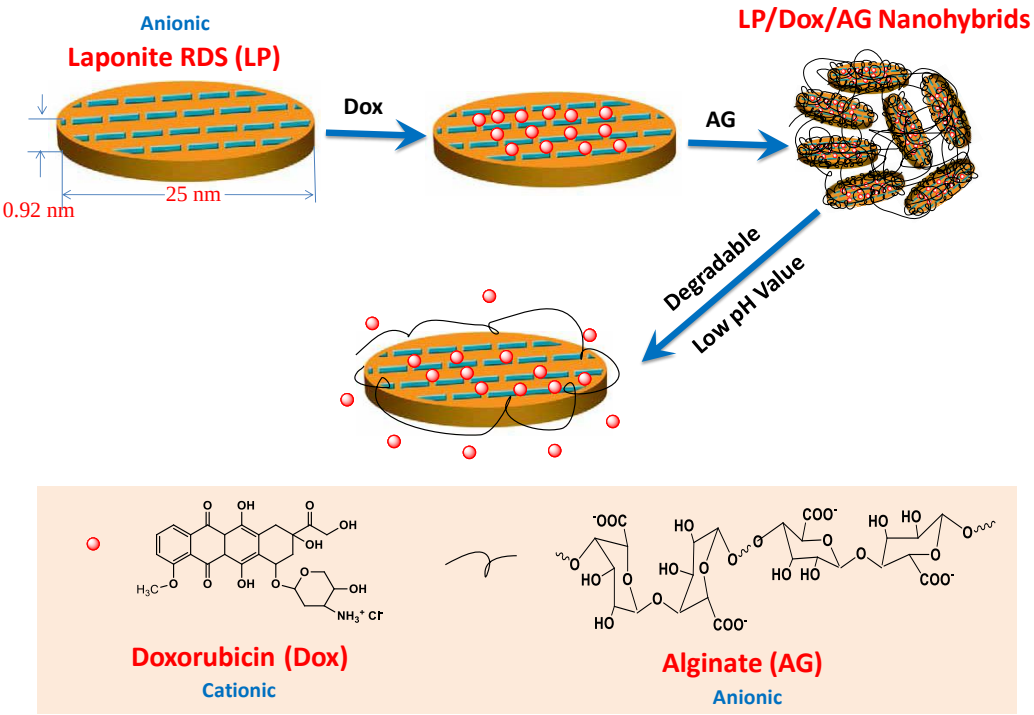

Figure 28. Schematic illustration for the formation and drug release of DOX-loaded LP/AG nanohybrids.

After the coating step, unbound polyelectrolyte and free DOX were removed by centrifugation. The encapsulation efficiency of the drug was determined by monitoring the concentration of drug in the supernatants by UV–visible spectrophotometry at 490 nm (Table 10). It should be noted that the

precipitate cannot be obtained from the mixture of LP/DOX in the absence of AG or from AG/DOX without LP by using the similar centrifugation process. Results demonstrated that DOX was effectively loaded in the nanohybrids with high encapsulation efficiency (80.8 ± 10.6%). Figure 29 shows the hydrodynamic diameter (size) of the nanohybrids analysed by dynamic light scattering (DLS) and the correspondent ζ-potentials. The Z-average size of LP was 28 ± 4 nm, indicating that LP was well dispersed in the aqueous solution, while the size of LP/DOX/AG gave a bimodal distribution with Z-average size of 142 ± 4 nm, suggesting the formation of the nanohybrids. The ζ-potential apparently increased from −45.2 ± 3.1 mV (LP) to −18.4 ± 0.5 mV (LP/DOX/AG nanohybrids), revealing the successful loading of the cationic drug and electrostatic binding to alginate.

Table 10. Encapsulation efficiency and loading capacity of DOX-loaded LP/AG nanohybrids.

Sample	Encapsulation efficiency (%)[a]	Loading capacity (%)[b]
LP/DOX/AG	80.8 ± 10.6	7.5 ± 0.9

a) Encapsulation efficiency = $100*W_t/W_0$, W_0 and W_t being the total DOX weight used for encapsulation and the weight of encapsulated DOX, respectively; b) Loading capacity = $100*W_t/W$, W_t and W being the weight of encapsulated DOX and the weight of DOX-loaded nanohybrids, respectively.

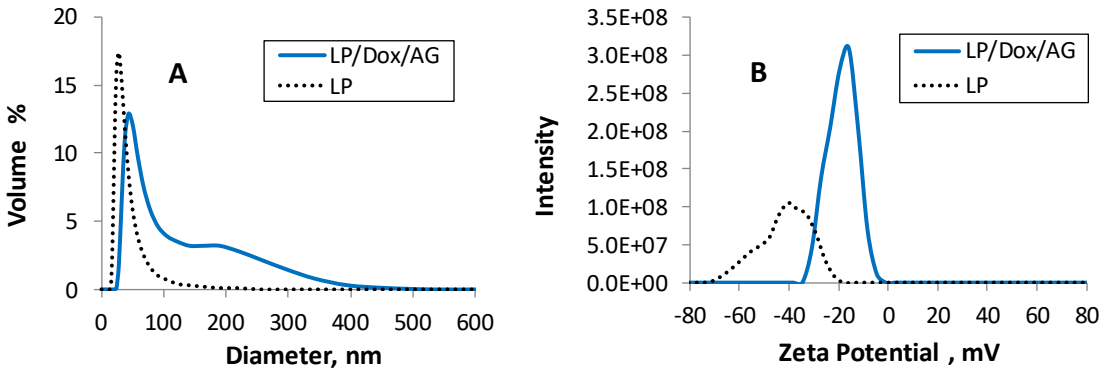

Figure 29. Hydrodynamic diameter (A) and zeta potential (B) of blank LP and DOX-loaded LP/AG nanohybrids in water (representative experiment).

Transmission electron microscopy (TEM) was also used to characterize LP and LP/DOX/AG nanohybrids. As shown in Figure 30, TEM images indicate that the LP ranged in size from 20 to 50 nm, while the LP/DOX/AG particles were around 200 nm. The TEM results are in agreement with those obtained by DLS analysis. The larger diameter of the LP/DOX/AG nanohybrids when compared to that of LP obtained by TEM again confirmed the formation of the nanohybrids.

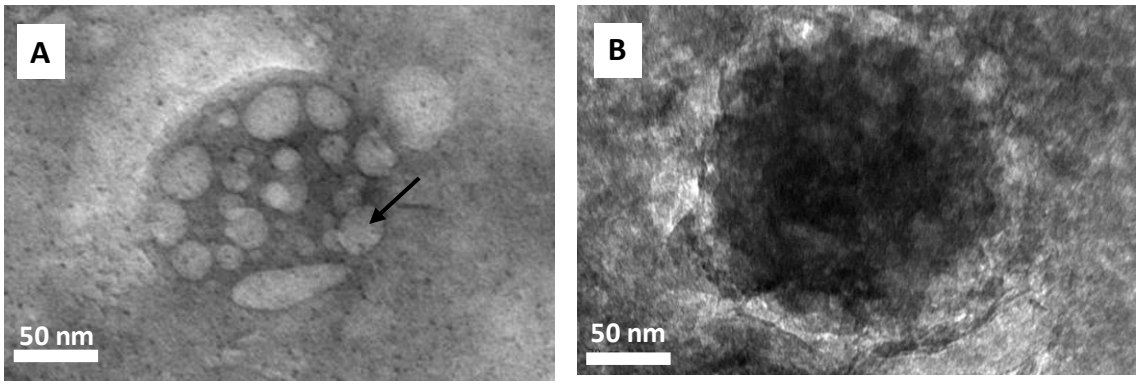

Figure 30. TEM images of LP (A) and LP/DOX/AG nanohybrids (B). The black arrow indicates the individual LP nanodisk.

3.2. Drug release from LP/DOX/AG nanohybrids

For antitumor therapeutic applications, the encapsulated DOX should be released into the cytoplasm and reach the nucleus, where it will exert its biological activity. The release kinetics of DOX from LP/DOX/AG nanohybrids was investigated *in vitro* in PBS solution at different pH values (Figure 31A). As can be seen, at the physiological pH value (pH 7.4), the cumulative release of DOX from the LP/DOX/AG hybrids was 6.2 ± 0.5 wt.% within 1 day. After that time, the DOX was released almost in zero-order mode till 21 days with a final cumulative release of 13.8 ± 1.0 wt.%. As a comparison, free DOX in PBS solution gave a rapid release in 3 h. These results indicate that the nanohybrids could effectively avoid a burst release of DOX at the beginning and give a sustained release of the drug over time.

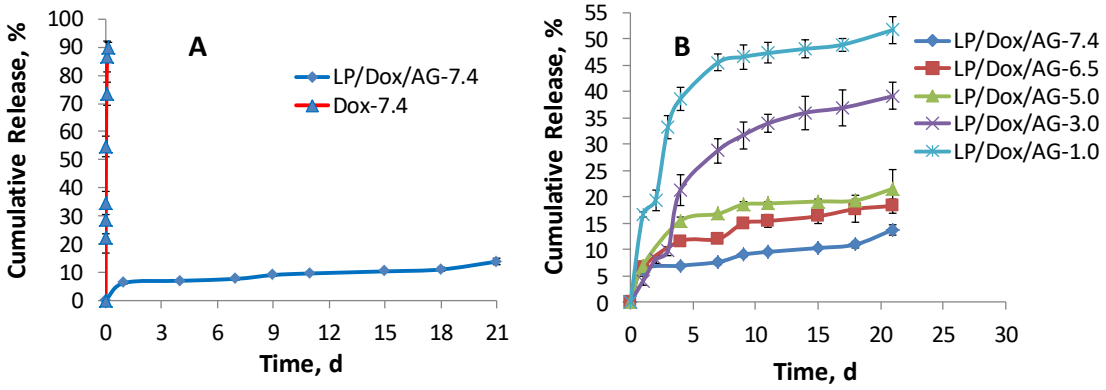

Figure 31. The release profiles for free DOX and LP/DOX/AG nanohybrids at pH 7.4 (A), and for LP/DOX/AG nanohybrids at different pH values (7.4, 6.5, 5.0, 3.0 and 1.0) (B) in PBS solution as a function of soaking time.

The kinetics of drug release was also studied under acidic pH conditions that resembled the extracellular environment of a solid tumour (pH 6.5), the endolysosome internal milieu (pH 5.0)[8,9] and the microenvironment of the stomach (pH 1.0–3.0).[42] During the initial time period, the DOX release rate was significantly faster under acid conditions than at physiological pH, revealing that the

nanohybrids were pH sensitive (Figure 31B). The lower the pH, the higher the rate of drug release. For example, the DOX cumulative release at day 7 was 7.6 ± 0.5 wt.% at pH 7.4, 12.0 ± 0.6 wt.% at pH 6.5, 16.8 ± 0.1 wt.% at pH 5.0, 28.8 ± 2.3 wt.% at pH 3.0 and 45.5 ± 1.6 wt.% at pH 1.0. Since alginate theoretically shrinks at low pH, its presence in the nanohybrids would make the release of the encapsulated drugs more difficult under acid conditions.[43] Therefore, the accelerated drug release effect induced by decreasing the pH should be mainly caused by an acid-induced LP degradation and/or an ion-exchange release process in PBS buffer.[22,23] This pH sensitivity in DOX release means that, even if DOX release is limited under physiological conditions (less toxicity to normal tissues), the nanohybrids will release more of their drug cargo in the solid tumour extracellular environment (pH 6.5) and in the endolysosomal vesicles (pH 5.0) (enhanced anticancer activity). Importantly, the DOX cumulative release in equilibrium (till 21 days) was 13.8 ± 1.0 wt.% for pH 7.4, 18.3 ± 1.3 wt.% for pH 6.5, 21.6 ± 3.6 wt.% for pH 5.0, 39.1 ± 2.5 wt.% at pH 3.0 and 51.7 ± 2.6 wt.% at pH 1.0 (Figure 31B). Therefore, the nanohybrids gave a sustained release profile at all studied pH values, meaning that DOX's anticancer activity is expected to be maintained over a long period of time, which should further increase the drug's therapeutic efficacy. It should be noted that a sustained release of DOX from the nanohybrids may be important in achieving long-term therapeutic results, and thus could be beneficial in reducing side effects by decreasing the dose and/or the number of drug administrations.

3.3. Buffering capacity of LP/DOX/AG nanohybrids

The buffering capacity of LP/DOX/AG nanohybrids was studied by acid–base titration. From the titration curves in Figure 32, we can conclude that a significant higher volume of acid is necessary to achieve the same pH value when the LP or the LP/DOX/AG nanohybrids are present, revealing the buffering action of LP. Indeed, LP has a negatively charged surface and pH-dependent charged edges, which may contribute to its buffering capacity.[23] Furthermore, the nanohybrids displayed a slightly higher buffering capacity than pure LP, which is probably related to the presence of alginate. In fact, the pKa of AG is 3.49 (corresponding to the carboxylic groups of the mannuronic (3.38) and guluronic acid monomers (3.65)), but its protonation process starts around pH 7.0.[44] Based on these results and on the explanations that can be found in the literature for nanomaterials with similar buffering behaviour, we raise the hypothesis that the high buffer capacity of LP and the nanohybrids may lead to the disbalance of the endolysosomal compartments and accelerate their rupture to release DOX (this is known by the "proton-sponge effect").[35–37] Indeed, the adsorption/absorption of protons by LP may lead to an additional pumping of protons into the endolysosomal vesicles followed by an influx of chloride anions (to maintain electric neutrality), an increase in osmotic pressure and finally a disruption of the vesicles. Therefore, the problem of DOX trapping inside the acidic endolysosomal compartment, which is in part responsible for DOX resistance, may be overcome.[8,9]

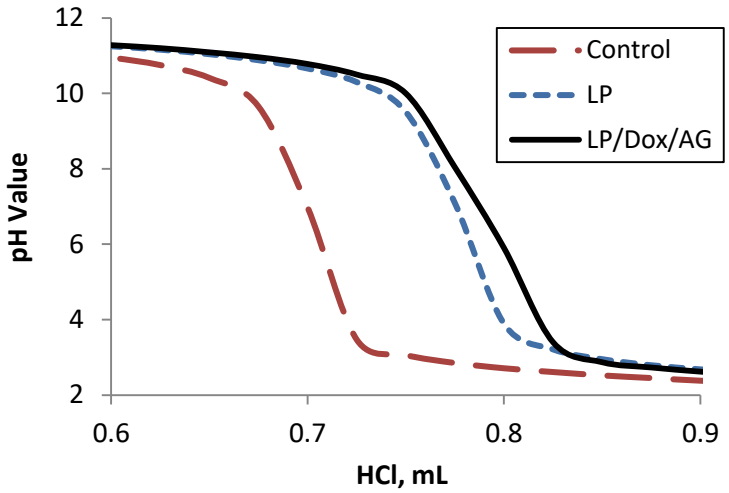

Figure 32. Acid–base titration profiles for LP and LP/DOX/AG nanohybrids in 100 mM NaCl solution (titrated using 0.1 M HCl). A control experiment was done in the absence of LP and LP/DOX/AG.

3.4. Cytotoxicity and cellular internalization of LP/DOX/AG nanohybrids

The antitumor bioactivity of the DOX upon its release from LP/DOX/AG nanohybrids was evaluated using CAL-72 cells (an osteosarcoma cell line). The cells were cultured in the presence of free DOX and LP/AG/DOX nanohybrids at increasing DOX concentrations (from 0.05 to 1.50 µM), and cell metabolic activity was quantified by the resazurin reduction assay. The cell metabolic activity was used as an indirect measure of cell viability, and PBS solution was used as a control. As shown in Figure 33, both free DOX and LP/DOX/AG nanohybrids were able to effectively inhibit cell growth. At DOX concentrations of 0.28 µM or higher, the cytotoxicity induced by LP/DOX/AG nanohybrids was always significantly higher than the corresponding free DOX solutions. It should be mentioned that LP alone did not affect cell viability. Therefore, the therapeutic efficacy is only due to the drug loaded within the nanohybrids.

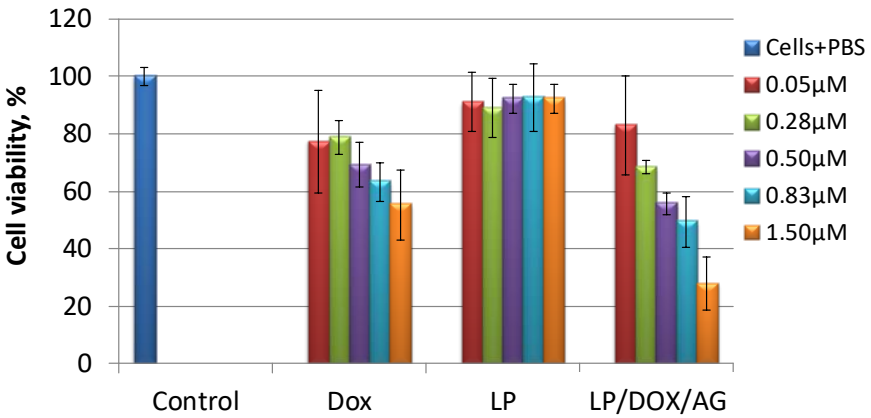

Figure 33. Cytotoxicity of free DOX, LP/DOX/AG nanohybrids (with equivalent DOX concentration) and LP (with equivalent weight concentration of the corresponding LP/DOX/AG) after 48 h of cell culture using the CAL-72 cell line (± standard deviation).

In order to confirm the antitumor activity of the DOX-loaded nanohybrids, the morphology of cells treated with free DOX and LP/DOX/AG nanohybrids was observed after 48 h by optical microscopy (Figure 34). Cells in the control or cultured in the presence of LP disks present a healthy morphology, displaying a fusiform shape and being adherent to the cell culture dish surface. This indicates that LP is quite cytocompatible. At a DOX content of 1.5 μM, samples treated with free DOX presented a mixture of fusiform (attached cells) and rounded (non-adherent cells or cells in a process of losing the adherence to the surface) cells, indicating a moderate level of cytotoxicity. However, at the same DOX concentration, most of the cells cultured with LP/DOX/AG nanohybrids died, and only some round cells could be observed using the optical microscope. The cell morphology results are in agreement with the metabolic activity quantification data, indicating that DOX within the LP/DOX/AG nanohybrids exerts a higher antitumor activity.

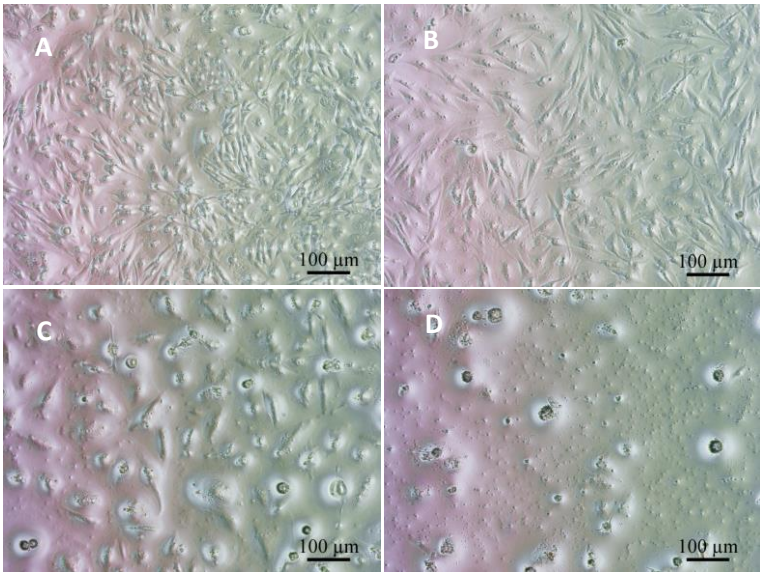

Figure 34. Cell morphology (optical microscopy) (CAL-72 cell line) after 48 h in culture with (A) PBS, (B) LP with an equivalent amount of LP/DOX/AG, (C) free DOX (1.5 μM) and (D) LP/DOX/AG with an equivalent amount of DOX (1.5 μM).

The extent of cell uptake of the drug delivery systems plays an important role in the achievement of the required therapeutic efficacy.[45] As DOX is a fluorescent molecule, its internalization by CAL-72 cells can be followed using fluorescence microscopy (Figure 35). A strong red fluorescence signal was visualized when cells were cultured in the presence of free DOX, and also when LP/DOX/AG nanohybrids were used. The results clearly show that DOX is spread not only in the cytoplasm but also in the nucleus of cells after 48 h of incubation. Compared to free DOX experiments, a higher density of red dots can be seen inside the nucleus of cells when the nanohybrids were applied. Also, DOX-loaded LP/AG nanohybrids led to an obvious transformation of the cell shape (cells lost their fusiform shape), which indicates an accelerated death process. The change in cell morphology was not so evident in the

case of free DOX assays. These observations are in agreement with the quantitative data obtained in the previous cell viability assays and can be attributed to a high rate of DOX internalization promoted by the nanohybrids, as well as to the facilitated release of DOX from the endolysosomal compartments which can more easily reach the nucleus. Overall, the fluorescence microscopy analysis also shows that the anti-tumour efficacy of DOX-loaded LP/AG nanohybrids is higher than that of an equivalent concentration of free DOX.

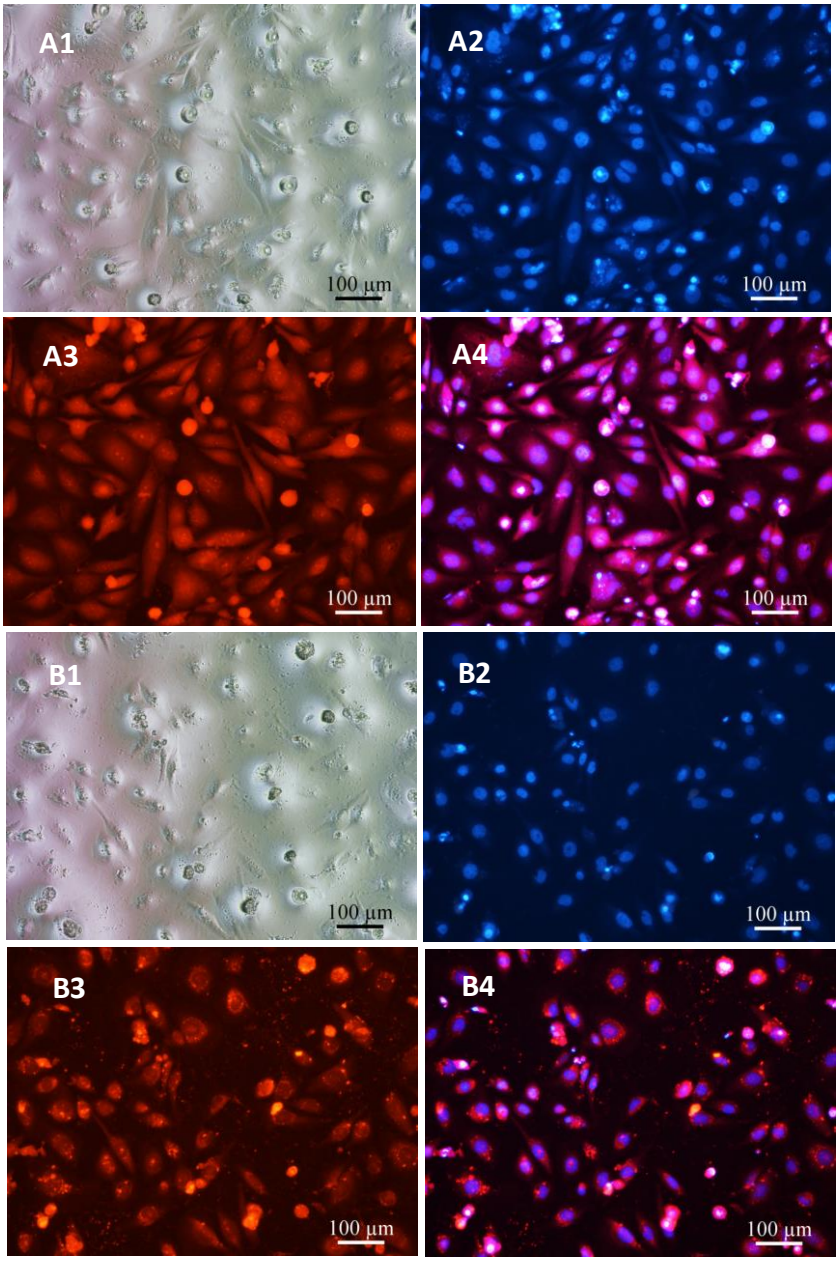

Figure 35. Images of CAL 72 cells incubated for 48 h with free DOX (0.83 µM, A1–A4) and DOX-loaded LP/AG nanohybrids containing an equivalent DOX concentration (B1–B4). (A1, B1) Bright-field images; (A2, B2) fluorescence images with nucleus staining (DAPI, blue); (A3, B3) fluorescence images from DOX (Red); (A4, B4) merged images.

4. Conclusions

In summary, we developed an easy approach to encapsulate DOX within LP/AG nanocarriers. The formed LP/DOX/AG nanohybrids presented a high drug loading capacity and displayed drug release pH sensitivity, with a sustained release profile of the drug (important for biomedical applications requiring a prolonged antitumor therapy). Furthermore, the nanohybrids exhibited a significantly higher cytotoxicity than free DOX used at the same concentration. Overall, the LP/DOX/AG nanohybrids are able to overcome the physiological DOX resistance due to ion trapping inside acidic compartments. They can effectively transport DOX across the cell membrane (counteracting the effect of the acidic extracellular microenvironment in solid tumours). Second, the presence of LP/AG in the nanohybrids may lead to an accelerated disruption of the acidic endolysosomal vesicles with release of DOX into the cytoplasm (non-encapsulated or still encapsulated DOX). These new nanohybrids are very promising vectors for the delivery of other weak base chemotherapeutics and, due to their acidic pH sensitivity, may be even useful for the delivery of oral drugs for the treatment of stomach diseases (pH 1.0–3.0).[42]

References

1 S. Vrignaud, J.-P. Benoit and P. Saulnier, *Biomaterials*, 2011, **32**, 8593–8604.

2 S. Luo, E. Zhang, Y. Su, T. Cheng and C. Shi, *Biomaterials*, 2011, **32**, 7127–7138.

3 K. C. Barick, S. Singh, N. V. Jadhav, D. Bahadur, B. N. Pandey and P. A. Hassan, *Adv. Funct. Mater.*, 2012, **22**, 4975–4984.

4 H. T. Ta, C. R. Dass, I. Larson, P. F. M. Choong and D. E. Dunstan, *Biomaterials*, 2009, **30**, 3605–3613.

5 J. H. Maeng, D.-H. Lee, K. H. Jung, Y.-H. Bae, I.-S. Park, S. Jeong, Y.-S. Jeon, C.-K. Shim, W. Kim, J. Kim, J. Lee, Y.-M. Lee, J.-H. Kim, W.-H. Kim and S.-S. Hong, *Biomaterials*, 2010, **31**, 4995–5006.

6 K. C. Weng, C. O. Noble, B. Papahadjopoulos-Sternberg, F. F. Chen, D. C. Drummond, D. B. Kirpotin, D. Wang, Y. K. Horn, B. Hann and J. W. Park, *Nano Lett.*, 2008, **8**, 2851–2857.

7 F. P. Seib, E. M. Pritchard and D. L. Kaplan, *Adv. Funct. Mater.*, 2013, **23**, 58–65.

8 B. P. Mahoney, N. Raghunand, B. Baggett and R. J. Gillies, *Biochem. Pharmacol.*, 2003, **66**, 1207–1218.

9 J. W. Wojtkowiak, D. Verduzco, K. J. Schramm and R. J. Gillies, *Mol. Pharm.*, 2011, **8**, 2032–2038.

10 L. Bao, A. Haque, K. Jackson, S. Hazari, K. Moroz, R. Jetly and S. Dash, *Am. J. Pathol.*, 2011, **178**, 838–852.

11 S. Wang, E. A. Konorev, S. Kotamraju, J. Joseph, S. Kalivendi and B. Kalyanaraman, *J. Biol. Chem.*, 2004, **279**, 25535–25543.

12 R. Erttmann, N. Erb, A. Steinhoff and G. Landbeck, *J. Cancer Res. Clin. Oncol.*, 1988, **114**, 509–513.

13 J. Park, P. M. Fong, J. Lu, K. S. Russell, C. J. Booth, W. M. Saltzman and T. M. Fahmy, *Nanomedicine Nanotechnology, Biol. Med.*, 2009, **5**, 410–418.

14 L. M. Kaminskas, B. D. Kelly, V. M. McLeod, G. Sberna, D. J. Owen, B. J. Boyd and C. J. H. Porter, *J. Control. Release*, 2011, **152**, 241–248.

15 M. L. Tan, A. M. Friedhuber, D. E. Dunstan, P. F. M. Choong and C. R. Dass, *Biomaterials*, 2010, **31**, 541–551.

16 S. Park, H. S. Kim, W. J. Kim and H. S. Yoo, *Int. J. Pharm.*, 2012, **424**, 107–114.

17 K. E. Uhrich, S. M. Cannizzaro, R. S. Langer and K. M. Shakesheff, *Chem. Rev.*, 1999, **99**, 3181–3198.

18 Z. Teng, X. Zhu, G. Zheng, F. Zhang, Y. Deng, L. Xiu, W. Li, Q. Yang and D. Zhao, *J. Mater. Chem.*, 2012, **22**, 17677–17684.

19 J.-Z. Du, X.-J. Du, C.-Q. Mao and J. Wang, *J. Am. Chem. Soc.*, 2011, **133**, 17560–17563.

20 M. Shi, K. Ho, A. Keating and M. S. Shoichet, *Adv. Funct. Mater.*, 2009, **19**, 1689–1696.

21 J. I. Dawson and R. O. C. Oreffo, *Adv. Mater.*, 2013, **25**, 4069–4086.

22 L. L. Hench, *J. Am. Ceram. Soc.*, 1991, **74**, 1487–1510.

23 D. W. Thompson and J. T. Butterworth, *J. Colloid Interface Sci.*, 1992, **151**, 236–243.

24 A. K. Gaharwar, P. Schexnailder, V. Kaul, O. Akkus, D. Zakharov, S. Seifert and G. Schmidt, *Adv. Funct. Mater.*, 2010, **20**, 429–436.

25 Q. Jin, P. Schexnailder, A. K. Gaharwar and G. Schmidt, *Macromol. Biosci.*, 2009, **9**, 1028–1038.

26 P. J. Schexnailder, A. K. Gaharwar, R. L. Bartlett, B. L. Seal and G. Schmidt, *Macromol. Biosci.*, 2010, **10**, 1416–1423.

27 A. K. Gaharwar, P. J. Schexnailder, B. P. Kline and G. Schmidt, *Acta Biomater.*, 2011, **7**, 568–577.

28 T. Takahashi, Y. Yamada, K. Kataoka and Y. Nagasaki, *J. Control. Release*, 2005, **107**, 408–416.

29 Y. Li, D. Maciel, H. Tomás, J. Rodrigues, H. Ma and X. Shi, *Soft Matter*, 2011, **7**, 6231–6238.

30 Y. Li, J. L. Santos, D. Maciel, H. Tomás and J. Rodrigues, *J. Control. Release*, 2011, **152**, e55–e57.

31 M. Gonçalves, P. Figueira, D. Maciel, J. Rodrigues, X. Shi, H. Tomás and Y. Li, *Macromol. Biosci.*, 2014, **14**, 110–120.

32 H. Meng, S. Yang, Z. Li, T. Xia, J. Chen, Z. Ji, H. Zhang, X. Wang, S. Lin, C. Huang, Z. H. Zhou, J. I. Zink and A. E. Nel, *ACS Nano*, 2011, **5**, 4434–4447.

33 Y. Li, J. Rodrigues and H. Tomás, *Chem. Soc. Rev.*, 2012, **41**, 2193–2221.

34 D. Maciel, P. Figueira, S. Xiao, D. Hu, X. Shi, J. Rodrigues, H. Tomás and Y. Li, *Biomacromolecules*, 2013, **14**, 3140–3146.

35 O. Boussif, F. Lezoualc'h, M. A. Zanta, M. D. Mergny, D. Scherman, B. Demeneix and J.-P. Behr, *Proc. Natl. Acad. Sci.*, 1995, **92**, 7297–7301.

36 A. E. Nel, L. Mädler, D. Velegol, T. Xia, E. M. V. Hoek, P. Somasundaran, F. Klaessig, V. Castranova and M. Thompson, *Nat. Mater.*, 2009, **8**, 543–557.

37 D. W. Pack, A. S. Hoffman, S. Pun and P. S. Stayton, *Nat. Rev. Drug Discov.*, 2005, **4**, 581–593.

38 A. Nouri, R. Castro, V. Kairys, J. L. Santos, J. Rodrigues, Y. Li and H. Tomás, *J. Mater. Sci. Mater. Med.*, 2012, **23**, 2967–2980.

39 N. D. Sonawane, F. C. Szoka and A. S. Verkman, *J. Biol. Chem.*, 2003, **278**, 44826–44831.

40 K. Jain, P. Kesharwani, U. Gupta and N. K. Jain, *Int. J. Pharm.*, 2010, **394**, 122–142.

41 M. R. Park, H. W. Kim, C. S. Hwang, K. O. Han, Y. J. Choi, S. C. Song, M. H. Cho and C. S. Cho, *J. Gene Med.*, 2008, **10**, 198–207.

42 S.-H. Cheng, W.-N. Liao, L.-M. Chen and C.-H. Lee, *J. Mater. Chem.*, 2011, **21**, 7130–7137.

43 M. Davidovich-Pinhas and H. Bianco-Peled, *Carbohydr. Polym.*, 2010, **79**, 1020–1027.

44 C. Lamelas, F. Avaltroni, M. Benedetti, K. J. Wilkinson and V. I. Slaveykova, *Biomacromolecules*, 2005, **6**, 2756–2764.

45 J. L. Santos, H. Oliveira, D. Pandita, J. Rodrigues, A. P. Pêgo, P. L. Granja and H. Tomás, *J. Control. Release*, 2010, **144**, 55–64.

Chapter IV.

Polyester Dendrimers Based on bis-MPA for Doxorubicin Delivery

Abstract

Doxorubucin (DOX) is an anticancer drug often used in clinical practice because of its efficacy against a wide group of cancer types. However, it presents severe side effects and, as such, research is ongoing trying to find adequate nanoscale systems for its delivery that can help to surpass this problem without compromising its efficacy. Polyester dendrimers based on the monomer 2,2-bis(hydroxymethyl)propionic acid (bis-MPA) are very promising systems for biomedical applications due to their biodegradability properties. In the present study, bis-MPA-based dendrimers were, for the first time, evaluated as vehicles for the delivery of DOX in cancer cells. Generations 4 and 5 bis-MPA-based dendrimers with hydroxyl groups at the surface were used (B-G4-OH, B-G5-OH), together with dendrimers partially-functionalized with amine groups at their surface (B-G4-NH_2, B-G5-NH_2). The idea was to compare the effect of different functional groups on dendrimers' behaviour without increasing too much their cytotoxicity. Generations 4 and 5 poly(amidoamine) (PAMAM) dendrimers were also tested for comparison.

Results confirmed the cytocompatibility of bis-MPA-based dendrimers, independently of the surface groups that were present. The B-G4-NH_2 and B-G5-NH_2 dendrimers were the ones that retained a higher number of DOX molecules during the loading process. However, as accessed by *in vitro* drug release studies in complete cell culture medium, drug release was more faster in these systems. These results were consistent with the cytotoxicity studies done using several models of cancer cell lines (CAL-72, A2780 and MCF-7 cells) and human mesenchymal stem cells (hMSCs) since the dose-response profile presented by these dendrimers was very similar to the one shown by the free drug. On the contrary, the B-G4-OH and B-G5-OH dendrimers had a lower loading capacity but were able of delivering the drug in a sustained manner, thus showing a lower cytotoxicity behaviour for equivalent periods of time. Overall, results show that it is possible to tune the drug delivery properties of bis-MPA-based dendrimers by modification of their surface functional groups.

1. Introduction

The main goal of nanomedicine is to improve the healthcare system by the development of nanomaterials for the diagnosis, treatment and follow-up of diseases, as well as other medical conditions. Since cancer is an increasing problem worldwide, there is big interest in applying nanomedicine solutions to minimize it and, in fact, most of the nanomaterials that are being developed envisage applications in this field.[1–3]

Nanomaterials can be made of different materials and shapes.[2] At the moment, polymers are the most studied materials for nanomedicine purposes.[4] They gathered scientists' attention due to the easiness in tuning their properties, such as chemical composition, morphology, size and biodegradability.[2] Despite of this, classical polymers possess a big disadvantage which is the difficulty in controlling their molecular size with accuracy, a requirement needed for nanomaterials aimed at moving from the bench to the bedside. This difficulty does not apply, however, to all polymer's classes. In fact, amongst polymer classes, dendrimers stand out due to their unique properties and architecture. Dendrimers are monodisperse molecules with structural perfection, being this an important characteristic that distinguish them from the classical polymers. Indeed, they are branched molecules that polymerize starting in a central core, growing towards the periphery. With each repeated branching cycle, the generation of the dendrimer increases, also increasing its molecular weight and number of peripheral terminal groups. Indeed, this last aspect is responsible for dendrimers' multivalency, another important feature of these molecules. In the biomedical field, dendrimers are regarded as interesting platforms for drug delivery since they can transport small drugs inside their structural voids (encapsulation), by adsorption or by covalent conjugation to their terminal functionalities.

The poly(amidoamine) (PAMAM) dendrimers, introduced by Tomalia *et al.*[5], are the most studied type of dendrimers, also for drug delivery, probably due to their early commercial availability. Several works have shown that PAMAM dendrimers can be loaded with anticancer drugs and serve as vehicles for their delivery inside tumours cells. However, PAMAM dendrimers may present toxicity associated with their surface functional groups, namely the ones that have amine groups at the periphery, since they display a high positive charge at the physiological pH. This toxicity increases with the generation number (G_x).[6,7] In order to overcome this issue, a few strategies have been employed, such as the acetylation of the amine groups or the conjugation of polymers (for example, polyethylene glycol) at the surface.[6,8–11]

One type of dendrimers that is not so extensively explored for drug delivery is the 2,2-bis(hydroxymethyl)propionic acid (bis-MPA)-based polyester family.[12] These dendrimers are biodegradable and, nowadays, also commercially available with different surface functional groups

and generations.[13,14] In fact, the existent studies on the use of bis-MPA-based dendrimers for drug and/or gene delivery[15–21] refer that they can be an excellent choice as delivery vehicles since they exhibit a very good biocompatibility *in vitro* and *in vivo*, a high water solubility and an easy surface functionalization. The non-cytotoxic behaviour of these systems was also confirmed by Feliu *et al.* using a library of bis-MPA-based dendrimers with hydroxyl and carboxyl surface groups.[22]

Doxorubicin (DOX) is considered one of the first-line treatments in chemotherapy, being used for a variety of cancer types. However, although DOX exhibits a broad spectrum of activity, it also has associated severe side effects, namely cumulative cardiotoxicity and myelosuppression.[23,24] As such, the need to overcome this concern is of major importance and, in this sense, researchers all over the world are trying to develop new nanoscale systems suitable for DOX delivery that will help diminish its secondary effects, as well as improve its biodistribution and efficacy. Although there are already a few DOX-based nanotherapeutics in the market (liposomal systems), they still present limitations, and the need to search for new solutions persist.

The aim of this work was to evaluate the performance of bis-MPA based dendrimers for the delivery of DOX into cancer cells. Several cell lines were used as cancer cell models - an osteosarcoma cell line (CAL-72), a breast adenocarcinoma cell line (MCF-7), and an ovarian carcinoma cell line (A2780). The cytotoxicity effect of the DOX-loaded dendrimers was also evaluated using human mesenchymal stem cells (hMSCs) as recent evidences show that they may have a role in tumour development.[25–27] Indeed, some reports reveal that hMSCs are recruited to tumour sites, supporting its development – e.g., by suppressing the immune response, enhancing angiogenesis, inhibiting apoptosis, and promoting epithelial to mesenchymal transition and thus metastasis formation. The study was focused on generations 4 and 5 of bis-MPA-based dendrimers with hydroxyl terminal groups (B-G4-OH, B-G5-OH), as such and partially-functionalized at the surface with amine groups (B-G4-NH_2, B-G5-NH_2). The objective was to compare the effect of different surface functional groups on dendrimers' performance, without increasing too much their cytotoxicity behaviour. Experiments with PAMAM dendrimers were also done for comparison purposes. As far as we know, this is the first work reporting the use of bis-MPA based dendrimers as scaffolds for DOX loading and delivery.

2. Experimental section

2.1. Reagents and materials

Generation 4 (G4) PAMAM dendrimers with amine and hydroxyl surface groups (P-G4-NH_2 and P-G4-OH, respectively) were purchased from Dendritech (USA), as well as generation 5 (G5) PAMAM dendrimers (P-G5-NH_2 and P-G5-OH, respectively). All PAMAM dendrimers had an ethylenediamine core. G4 and G5 polyester dendrimers based on bis-MPA with hydroxyl surface groups and a

trimethylol propane core (B-G4-OH and B-G5-OH, respectively) were bought from Polymer Factory (Sweden). Regenerated cellulose dialysis membrane (molecular weight cutoff, MWCO = 1 kDa) was obtained from Spectrum Labs. Doxorubicin hydrochloride salt (DOX.HCl) was acquired from Zibo Ocean International Trade Co, Ltd. N, N'-dicyclohexylcarbodiimide (DCC, 99%) was bought from Alfa Aesar. 4-(Dimethylamino)pyridine (DMAP) was obtained from Acros Organics. Triethylamine (TEA) was purchased from Merck4Biosciences. N-(tert-Butoxycarbonyl) glycine (BOC-Gly-OH), *p*-Toluenesulfonic acid monohydrate (PTSA), and formaldehyde solution were purchased from Sigma-Aldrich. Hydrochloric acid (HCl, 37%), ethyl acetate (EtOAc, analytical grade 99.98%), tetrahydrofuran (THF, analytical grade 99,99%), dimethylformamide (DMF, HPLC grade, 99.99%) and dichloromethane (DCM, HPLC grade, 99.99%) were bought from Fisher Scientific. Water used for the experiments was HyClone™ Water (Molecular Biology Grade) obtained from GE Healthcare Life Sciences. Slide-A-Lyzer mini dialysis devices were purchased from Thermo Fisher Scientific.

2.1. Preparation and characterization of B-G4-NH_2 and B-G5-NH_2 dendrimers

2.1.1. Synthesis of 1,4-Dimethylpyridinium p-toluenesulfonate (DPTS)

DPTS was synthesized as described in the literature[28,29] by mixing saturated solutions of DMAP and PTSA in THF at 1:1 equivalent molar ratio. For the first solution, 2.5 g (0.2 mol, 2 M) of DMAP were dissolved in THF, under stirring, at room temperature (RT). For the second solution, 3.9 g (0.2 mol, 2 M) of PTSA were dissolved in THF, under stirring, at RT. These two solutions were mixed under magnetic stirring, at RT, and a white precipitate was immediately formed. This precipitate was filtered, washed with THF and dried under vacuum. The structure of DPTS was confirmed by ^{1}H NMR.

2.1.2. Surface modification of B-G4-OH and B-G5-OH dendrimers

The surface modification of the polyester dendrimers based on bis-MPA and having hydroxyl end groups was made according the work developed by Movellan[20] and colleagues (Figure 36). Briefly, 1 eq of each dendrimer was dissolved in dry DCM followed by the addition of 2 eq of BOC-Gly-OH and 0.4 eq of DPTS (per hydroxyl surface group), under argon atmosphere.

Due to solubility difficulties, about 1.5 mL of DMF was added and left 1h30 at RT, under magnetic stirring, until complete dissolution. Afterwards, the reaction flask was cooled to 0 ^{o}C and a solution of 1.5 eq (per hydroxyl surface group) of DCC, in dry DCM, was added dropwise. The reaction was allowed to proceed for 24h, at RT, under argon atmosphere and magnetic stirring. Then, EtOAc was added and the reaction mixture was homogenised. In terms of product recovery, two different procedures were adopted depending on the dendrimer generation. First, in the case of the B-G4-OH dendrimer, a liquid-liquid extraction was used and, later, for the B-G5-OH dendrimer, vacuum filtration was used (Hirsch-

Type Funnel, pore number 4). In the first case, two liquid phases were obtained - on the top was the EtOAc with a white precipitate, and at the bottom a transparent DCM phase. The transparent DCM phase contained the final crude product which was collected after solvent evaporation and, later, re-dissolved in methanol. In the second method, used for the B-G5-OH dendrimer, the mixture was purified by filtration after EtOAc addition, separating the white precipitate from the crude product. The second procedure was considered more effective to get a product with higher purity. From this stage on, the procedure was the same for both generations of bis-MPA based dendrimers. The crude products, which were dissolved in liquids, were purified by dialysis (MWCO = 1 kDa) against methanol, for 24 h. On the following day, the solvent was evaporated and the BOC-protected dendrimer based on bis-MPA was obtained. For BOC removal, a typical procedure for deprotection of amine groups was used. Briefly, the product was dissolved in a 3 M solution of HCl in EtOAc and left stirring for 30 min at RT. Then, the solvent was evaporated and the product characterized by ^{1}H NMR.

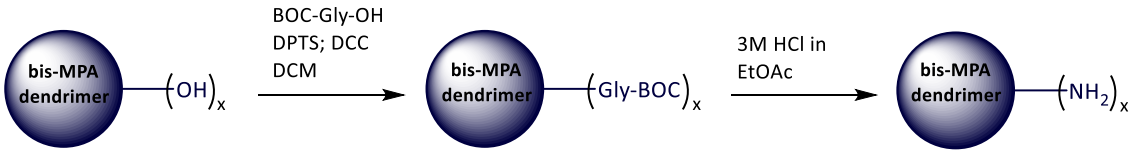

Figure 36. Simplified reaction scheme for the surface modification of the neutral bis-MPA dendrimers.

2.1.3. Characterization of the B-G4-NH_2 and B-G5-NH_2 dendrimers

Nuclear Magnetic Resonance Spectroscopy (NMR)

^{1}H NMR spectra were acquired in a Bruker Avance II^{+} 400 MHz equipment and used to confirm the surface modification of bis-MPA dendrimers. All the compounds were prepared in deuterium oxide (D_2O 99.99 atom % D, Sigma-Aldrich) before measurements.

Estimation of the primary amine group content of dendrimers by the TNBS assay

The 2,4,6-trinitrobenzenesulfonic acid (TNBS) reagent can be used to provide qualitative data regarding the number of free amine groups at the surface of dendrimers.[30] Basically, the TNBS reagent will react with the available primary amine groups resulting in a yellow product with maximum absorption peaks at 340 nm (trinitrophenyl amine) and 420 nm (Meisenheimer complex). At the same time, TNBS hydrolyses to picric acid, which exhibits overlapping peaks with the main product, trinitrophenyl amine.[31] The number of primary amine surface groups in bis-MPA and PAMAM dendrimers was estimated using ultraviolet-visible spectroscopy using TNBS reagent and glycine as standard. Essentially, serial dilutions of a glycine solution (400 µM) were performed to generate a calibration curve. The samples (2 mg/mL stock solution) and the standard solutions were diluted using sodium tetraborate (0.1 M, pH 9.3) solution to a final volume of 1 mL. Afterwards, 25 µL of TNBS

reagent (0.01 M), previously diluted with water, was added to each standard and sample and incubated, in the dark, at RT, for 30 min. After that, absorption scan measurements were performed using a GBC-Cintra 40, UV–Visible spectrophotometer.

2.2. Doxorubicin loading

DOX.HCl was loaded into PAMAM dendrimers (P-G4-OH and P-G4-NH_2; P-G5-OH and P-G5-NH_2) and bis-MPA based dendrimers (B-G4-OH and B-G4-NH_2; B-G5-OH and B-G5-NH_2) with different generations and end groups. First, dendrimers were dissolved in distilled water. After that, a stock solution of DOX.HCl (4 mg/mL) was prepared in methanol and then neutralized with TEA (the molar ratio TEA:DOX was 3.33:1). Then, the neutralized DOX was added dropwise to the dendrimer solution under magnetic stirring and protected from light. A DOX:dendrimer molar ratio of 5:1 was used. The reaction proceeded for 4 days, at RT, with the lid open to allow solvent evaporation. Later on, the mixture was centrifuged at 15,000 rpm for 5 min and the free DOX precipitate was washed with distilled water three times. The supernatant containing the DOX-loaded dendrimers was collected and lyophilized and the free DOX precipitate was dissolved in methanol and analysed by spectrophotometry. To calculate the loading efficiency (LE) and loading capacity (LC), a calibration curve of DOX in methanol was performed using UV-Vis scan measurements.

$$L.E.(\%) = \frac{mass\ of\ loaded\ DOX}{initial\ mass\ of\ DOX} \times 100 \qquad \text{Equation 1}$$

$$L.C.(\%) = \frac{mass\ of\ loaded\ DOX}{mass\ of\ DOX\ loaded\ dendrimers} \times 100 \qquad \text{Equation 2}$$

2.3. *In vitro* drug release

The release profile of DOX from bis-MPA based and PAMAM dendrimers was assessed *in vitro* using the dialysis cassette system (Slide-A-Lyzer mini dialysis system, MWCO = 2 kDa). Briefly, stock solutions of DOX and DOX-loaded dendrimers were prepared in HyClone™ Water at a final concentration of 0.5 mg/mL. Inside of the dialysis system a total volume of 0.3 mL was placed which corresponded to 0.1 mL of dendrimer aqueous solution and 0.2 mL of supplemented cell culture medium, that is, DMEM medium (Sigma-Aldrich) containing 10% (v/v) foetal bovine serum (FBS, Gibco) and 1% (v/v) antibiotic-antimycotic (AA, 100x solution, Gibco). The dialysis system was submerged in 10 mL of supplemented media and incubated at 37 °C. All samples were prepared considering equivalent amounts of DOX (2.5 μg/mL). At predetermined time points, an aliquot of 0.1 mL of media was withdrawn and an equal amount of fresh medium was replenished. DOX concentrations were determined by fluorimetry using a microplate reader (model Victor^3 1420, PerkinElmer) and a standard

calibration curve. The cumulative release (C_r) of DOX over time was calculated according to the following equation[32]:

$$C_r\ (\%) = \frac{V_o C_n + V_t \times \sum_1^{n-1} C_i}{m_{DOX}} \times 100 \qquad \text{Equation 3}$$

Where V_o is the volume of release media, C_n is the measured concentration of DOX in a certain time point, and m_{DOX} is the initial mass of DOX; V_t is the volume of the aliquots previously removed and C_i the correspondent DOX concentrations in those aliquots. Replicates were performed for each experiment (n = 3) and the average was determined.

2.4. Cell culture and *in vitro* cell viability assays

Several cell lines were used as cancer cell models - an osteosarcoma cell line (CAL-72, DSMZ, Germany), a breast adenocarcinoma cell line (MCF-7, DSMZ, Germany), and an ovarian carcinoma cell line (A2780, European Collection of Cell Cultures, UK). The cytotoxicity effect of the DOX-loaded dendrimers was also evaluated using human mesenchymal stem cells (hMSCs). The hMSCs were collected from human trabecular bone samples obtained during surgery interventions in the sequence of traumatic events (only biological material that would have been discarded was used); all process was approved by the Ethics Committee of Dr. Nélio Mendonça Hospital (Madeira principal hospital). CAL-72 cells were cultured in DMEM medium containing 10% (v/v) foetal bovine serum FBS (Gibco), 1% (v/v) insulin-transferrin-sodium selenite (100× solution, Gibco), 2 mM L-glutamine (Gibco) and 1% (v/v) AA solution. MCF-7 cells were grown in RPMI 1640 medium (Sigma-Aldrich) supplemented with 20% (v/v) FBS, 1% (v/v) nonessential amino acids (NEAA, 100× solution, Gibco), 1 mM sodium pyruvate (Sigma-Aldrich), 3.3 µg/mL human insulin (Gibco) and 1% (v/v) AA solution. A2780 cells were cultured in RPMI 1640 medium supplemented with 10% (v/v) FBS, 2 mM L-glutamine and 1% (v/v) AA solution. The hMSCs were grown in α-MEM medium (Sigma-Aldrich) supplemented with 10% (v/v) FBS and 1% (v/v) AA solution. Initially, cells were cultured at 37 °C, in a humidified atmosphere with 5% (v/v) carbon dioxide (CO_2), being harvested when 70 – 80% of confluency was reached. First, cells were washed with phosphate buffered saline (PBS, Sigma-Aldrich) solution, and then were detached from the bottom of the culture flask using trypsin-ethylenediaminetetraacetic acid solution (TE, 0.05% w/v, Gibco). The cells were then seeded in 24-well plates at a cell density of 10,000 cells per well. One day after, aqueous solutions of free DOX, DOX-loaded bis-MPA based dendrimers and PAMAM dendrimers (with equivalent DOX concentrations) and, also, of the empty dendrimers (used as controls with equivalent dendrimer mass concentrations) were prepared. The cells were further incubated with these systems for 48 h. Cell viability was indirectly measured through the resazurin reduction assay

which relies on the metabolic activity of cells. Briefly, after 48 h of incubation time, the cell medium was removed and replenished with fresh medium containing resazurin (Sigma-Aldrich) with a final concentration of 0.1 mg/mL. Afterwards, the cells were kept in the incubator for 3 h. At the end, aliquots of the media were transferred to an opaque 96-well plate and resorufin fluorescence was measured in the microplate reader (model Victor^3 1420, Perkin–Elmer). The results are presented as a percentage of the metabolic activity relative to the control and correspond to the mean of 3 replicates.

Cells were observed using fluorescence microscopy after 48 h in contact with the test solutions. For this, cells were washed with sterilized DPBS solution and fixed with 3.7% formaldehyde (Sigma-Aldrich). After removing the fixative solution, the cell nucleus was stained using 4',6-diamidino-2-phenylindole dilactate (DAPI, Sigma-Aldrich) for 30 min. To conclude the process, the cells were washed two times with DPBS solution and finally washed with ultrapure water (Milli-Q system, Millipore). Pictures were taken using an optical fluorescence microscope (Nikon Eclipse TE 2000E inverted microscope).

2.5. Statistics

Statistical analyses were performed using the GraphPad Prism 7. One-way ANOVA with Tukey Post Hoc test was used to assess the statistical difference between group means using as comparison the non-loaded dendrimer and DOX-loaded dendrimer. A probability level of $p<0.05$ was considered to be significant.

3. Results and discussion

Poly(amidoamine) (PAMAM) dendrimers are, by far, the most studied dendrimers for biomedical applications, and particularly for drug delivery purposes. However, although presenting very interesting properties as carriers for a wide range of therapeutic molecules, such as anticancer drugs, their use *in vivo* is being limited by their inherent toxicity and poor degradability under physiological conditions. Polyester dendrimers, as those based on the 2,2-bis(hydroxymethyl)propionic acid (bis-MPA) monomer, on the contrary, were described as having a high biocompatibility and degradability. In the present work, and as far as we know for the first time, bis-MPA based dendrimers are investigated *in vitro* as vehicles for doxorubicin. Starting from bis-MPA dendrimers (generations 4 and 5) with hydroxyl end groups, bis-MPA dendrimers partially-functionalized with amine termini (Figure 37 and Figure 38) were first prepared and characterized using suitable physicochemical techniques. Then, all hydroxyl-terminated and amino-terminated dendrimers based on bis-MPA were loaded with DOX and their *in vitro* drug release profile, as well as their cytotoxic behaviour were studied. For comparative purposes, the experiments were also done

with PAMAM dendrimers. All results are presented and discussed in more detail in the following sections.

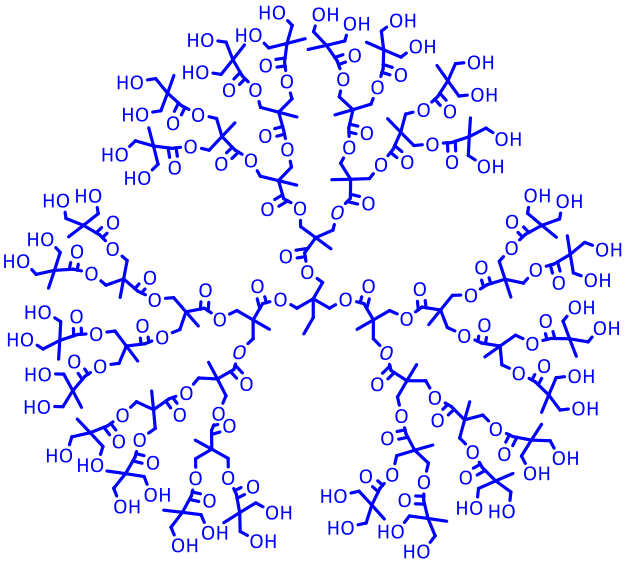

bis-MPA dendrimer generation 4 hydroxyl-terminated: $C_{231}H_{374}O_{138}$

MW = 5359.40 g/mol

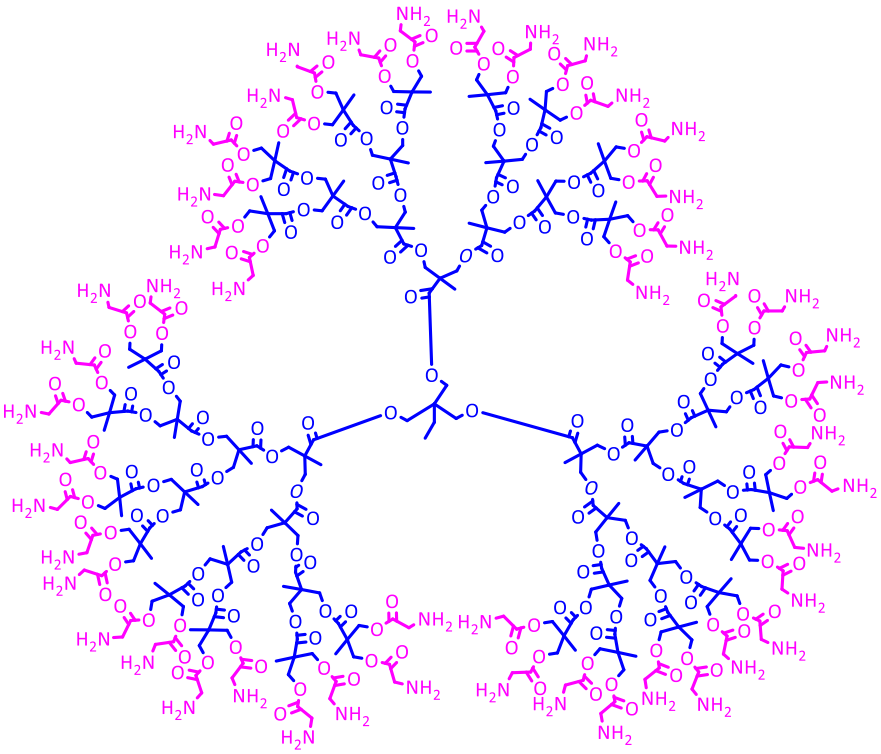

bis-MPA dendrimer generation 4 amino-terminated: $C_{327}H_{518}N_{48}O_{186}$

MW = 8097.89 g/mol

Figure 37. Schematic representation of generation 4 bis-MPA-based dendrimers with hydroxyl and amine termini. Note that, in the present work, the dendrimers were only partially functionalized at the surface with amine groups.

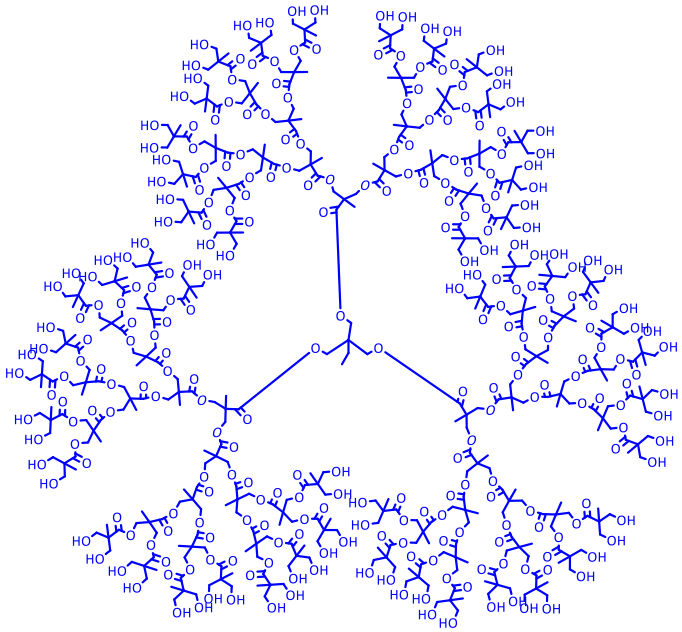

bis-MPA dendrimer generation 5 hydroxyl-terminated: $C_{471}H_{758}O_{282}$

MW = 10932.96 g/mol

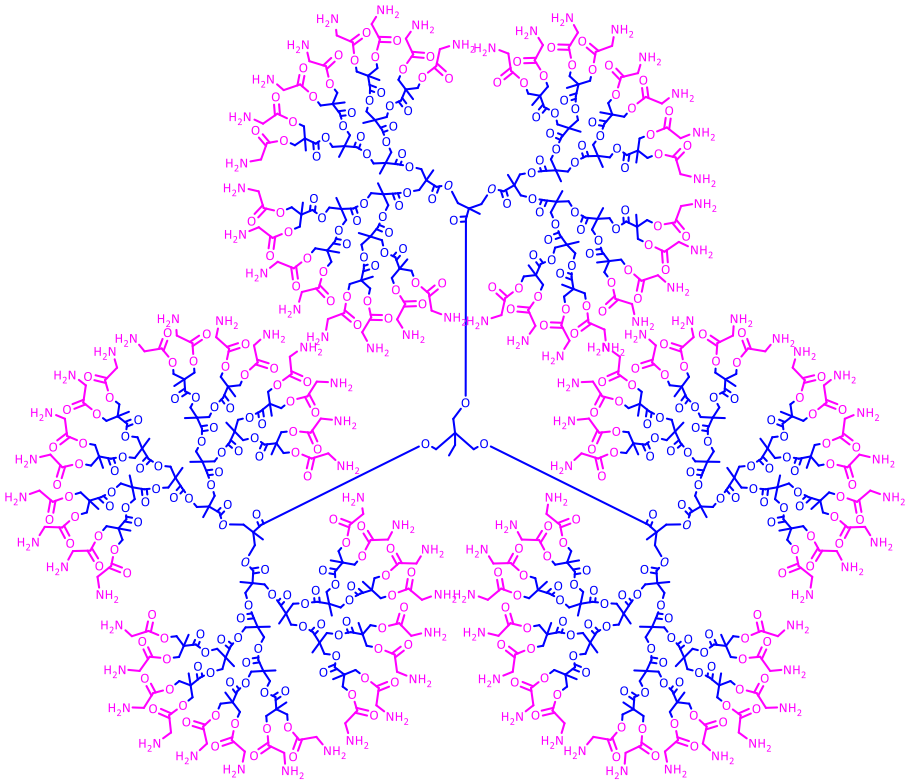

bis-MPA dendrimer generation 5 amino-terminated: $C_{663}H_{1046}N_{96}O_{378}$

MW = 16409.96 g/mol

Figure 38. Schematic representation of generation 5 bis-MPA-based dendrimers with hydroxyl and amine termini. Note that, in the present work, the dendrimers were only partially functionalized at the surface with amine groups.

3.1. Preparation and characterization of partially-functionalized B-G4-NH_2 and B-G5-NH_2 dendrimers

Generation 4 and generation 5 bis-MPA dendrimers with hydroxyl surface groups were modified to obtain dendrimers with amine termini through a two-step reaction. In a first stage, the dendrimers were conjugated to BOC-Gly-OH and afterwards deprotected in acid conditions. The partially-modified bis-MPA dendrimers with amine termini were characterized by ^{1}H NMR (400 MHz), using D_2O as solvent (spectra are shown in Figure 39 and Figure 40). In the ^{1}H NMR spectra, the solvent peak was identified at δ = 4.79 ppm and multiple peaks were attributed to bis-MPA-based dendrimer protons. The peak integration was made considering the characteristic proton peaks of the -C*H*$_2$O- group (δ ≈ 4.46 to 4.28) that corresponds to 90 protons (in generation 4) or 186 protons (in generation 5) in both the bis-MPA-based dendrimers with hydroxyl termini and the bis-MPA-based dendrimers with amine termini. For both dendrimer generations, the successful surface modification with amine groups is represented by the appearance of a new proton signal at δ = 4.04 ppm (-C*H*$_2$NH$_2$). Additionally, other peaks could be identified in the spectra which were related with the solvent (δ ≈ 3.04 and 2.88 ppm) and the starting material DCC (δ ≈ 3.23 ppm).

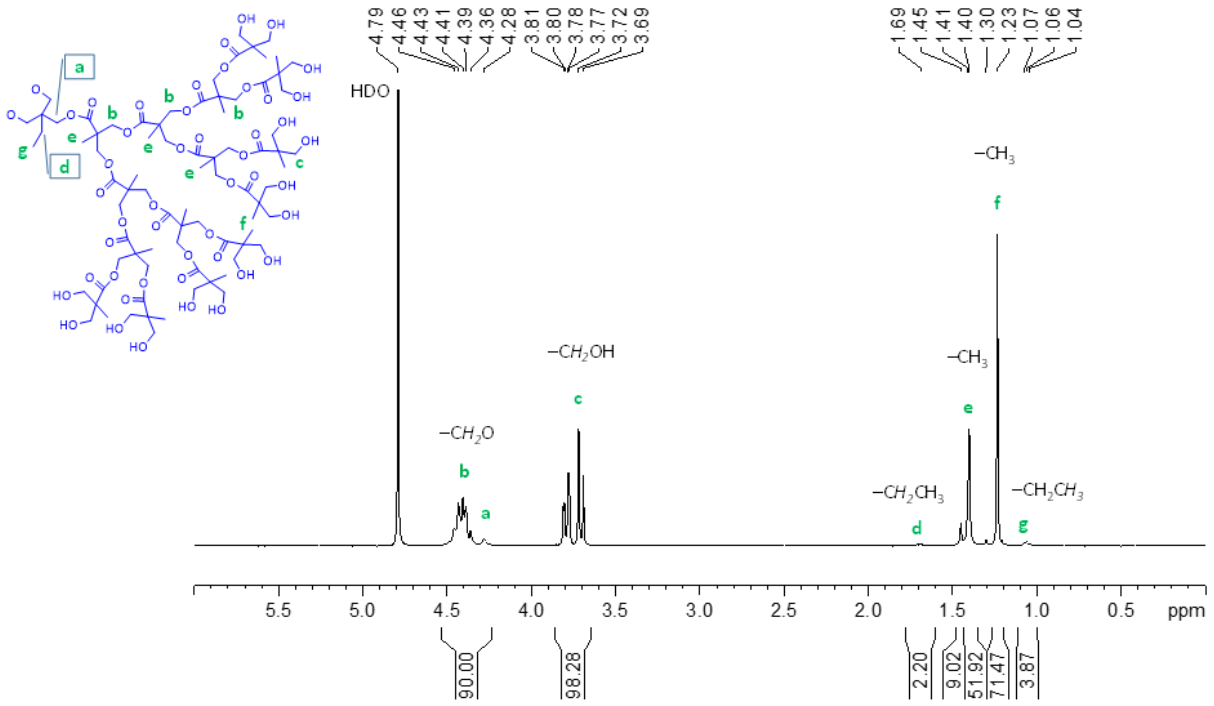

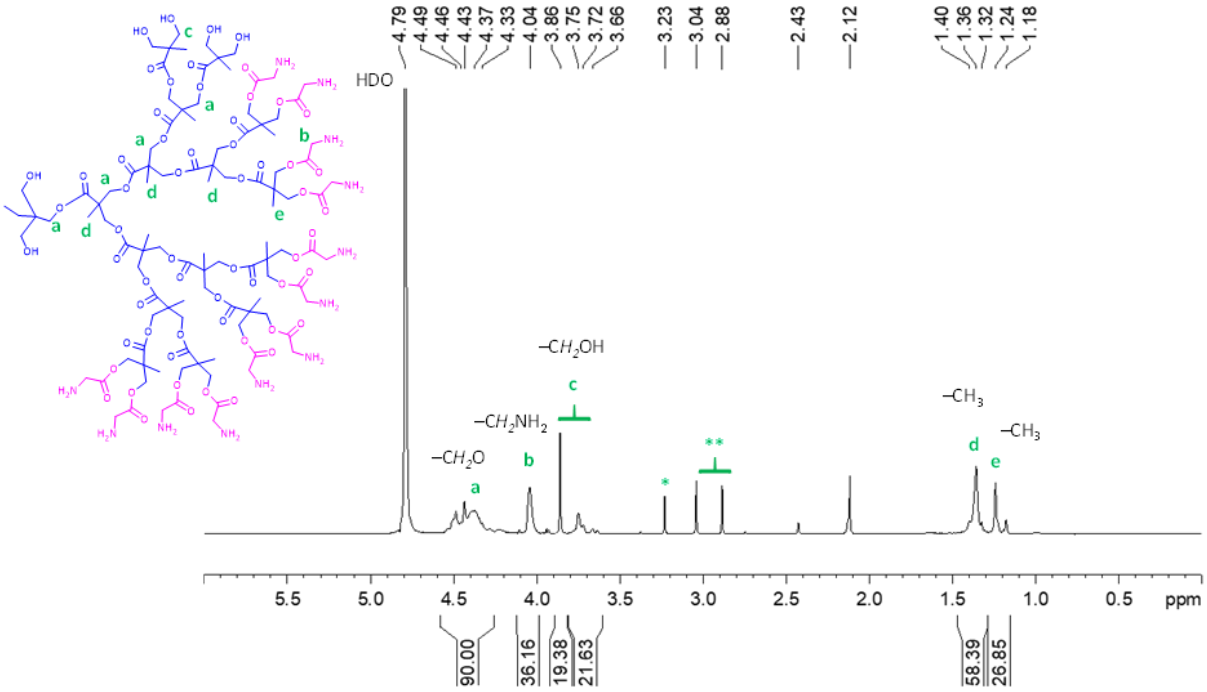

Figure 39. ^{1}H NMR spectra (400 MHz, in D_2O) of B-G4-OH and B-G4-NH_2 dendrimers (results are consistent with eighteen amine termini per dendrimer).

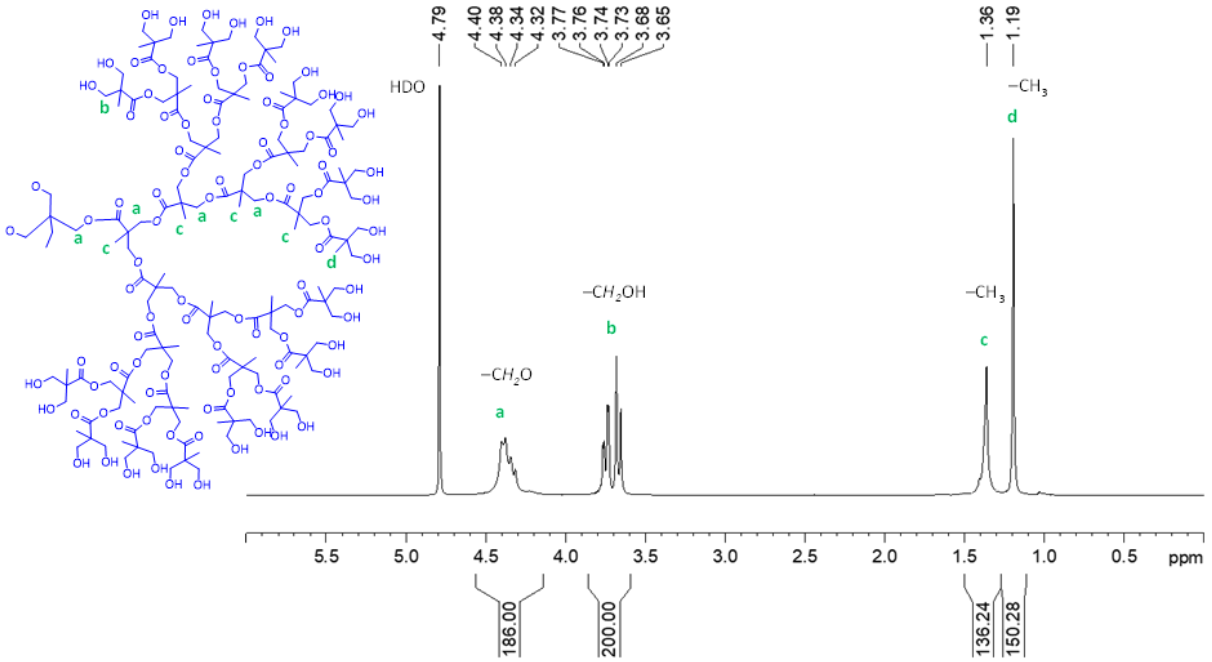

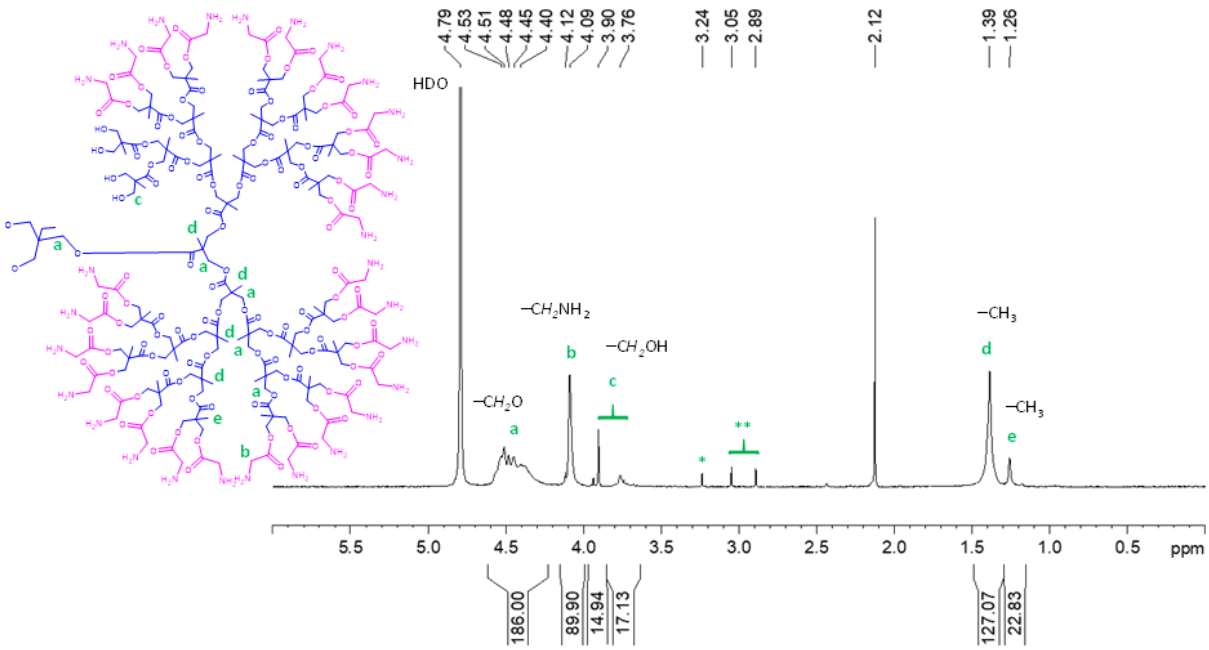

Figure 40. ^{1}H NMR spectra (400 MHz, in D_2O) of B-G5-OH and B-G5-NH_2 dendrimers (results are consistent with forty five amine termini per dendrimer).

According with the ^{1}H NMR spectra, the surface modification of the dendrimers was not fully complete, that is, partially-modified bis-MPa-based dendrimers were obtained which was the initial objective. The full surface modification of the generation 4 dendrimer, would result in a total of 48 amine surface groups. However, a total of 18 amine termini were achieved, corresponding to 38% of surface modification. For generation 5, a complete modification would correspond to a total of 96 amine surface groups and, in this case, a total of 45 amine termini were obtained which corresponds to 47% of surface modification.

The TNBS assay was further used to assess the functionalization degree of the surface of bis-MPA dendrimers with amine groups. Essentially, the assay consists in measuring the complexation degree of the TNBS reagent with the dendrimers through light absorption measurement. Based on a calibration curve, the surface modification degree was determined for both generations of the amine-terminated bis-MPA dendrimers, being 49% for the B-G4-NH_2 (24 amine groups) and 51% for the B-G5-NH_2 (49 amine groups). For the B-G5-NH_2, the results of the ^{1}H NMR analysis are in good agreement with those of the TNBS assay. For the B-G4-NH_2, there is a bigger difference in the results obtained from the two methods used to access the functionalization degree but, still, it was possible to confirm that the B-G4-NH_2 dendrimers were successfully partially modified (one should have in mind that the TNBS assay is not as accurate as the NMR analysis).

3.2. Doxorubicin loading in dendrimers

The loading of DOX into the dendrimers was performed by adapting a protocol previously reported.[33–40] Both bis-MPA-based dendrimers and PAMAM dendrimers were loaded with DOX. Essentially, a stock solution of DOX was prepared in methanol and added dropwise to the dendrimer aqueous solution. Few days after, the DOX-loaded dendrimers were obtained by centrifugation and freeze-dried. The free DOX precipitate was kept and later dissolved in methanol for DOX quantification by UV-Vis spectrophotometry and indirect determination of the amount of DOX retained in the dendrimers. Results regarding the Loading Efficiency (LE) and the Loading Capacity (LC) are present in Table 11. LE corresponds to the percentage (w/w) of drug used in the loading process that was retained inside dendrimers. LC corresponds to the percentage (w/w) of DOX in the loaded dendrimer.

Table 11. Loading Efficiency (LE) and Loading Capacity (LC) for PAMAM and bis-MPA-based dendrimers (both generations 4 and 5).

Sample	LE (% w/w)	LC (% w/w)
P-G4-OH/DOX	61	13
P-G4-NH_2/DOX	42	8
B-G4-OH/DOX	37	17
B-G4-NH_2/DOX	100	26
P-G5-OH/DOX	44	9
P-G5-NH_2/DOX	75	7
B-G5-OH/DOX	35	9
B-G5-NH_2/DOX	100	13

As shown in Table 11, the loading capacity increased for bis-MPA-based dendrimers after partial functionalization with amine groups at the surface. The LC values were 17%, 9%, 26%, and 13% for B-G4-OH, B-G5-OH, B-G4-NH_2 and B-G5-NH_2, respectively. Interestingly, the lower generation dendrimers (B-G4-OH and B-G4-NH_2) achieved bigger LC values than the higher generations (B-G5-OH and B-G5-NH_2). Loading efficiencies were about 100% for bis-MPA-based dendrimers after partial functionalization with amine groups at the surface, meaning that practically all the initial mass of DOX was complexed to these dendrimers. When comparing the loading capacity of bis-MPA-based dendrimers and PAMAM dendrimers, it can be observed that, for the same generation, the amine-terminated bis-MPA-based dendrimers exhibit higher cargos, especially for generation 4 dendrimers. It should be noticed that bis-MPA-based dendrimers have lower molecular weights and less number of surface functional groups than PAMAM dendrimers, which should be an advantage in practical terms. Also, bis-MPA-based dendrimers are biodegradable. From all the dendrimers under study, the B-G4-NH_2 dendrimer was the one that achieved a higher loading capacity (26%).

A panoply of works reported the use of PAMAM dendrimers as potential vehicles for DOX encapsulation.[35,39,41–43] However, as previously mentioned and as far as we know, this work is the first to report the use of bis-MPA dendrimers as potential delivery vehicles for doxorubicin. Zeng *et al.*[18,44] used bis-MPA-based polymers for DOX delivery too but the design of the carrier systems was different. They prepared copolymer micelles made of poly(ethylene glycol) (PEG)-modified hyperbranched polyester Boltorn® H30 and H40 polymers (that are polymers of bis-MPA) for doxorubicin delivery. These micelles were also able to be loaded with DOX molecules presenting a loading efficiency ranging from 31 to 43%.

3.3. *In vitro* drug release

One of the main goals of an ideal drug carrier is to release the encapsulated drug in a sustained manner. The *in vitro* drug release behaviour of B-G4-OH, B-G5-OH, B-G4-NH_2 and B-G5-NH_2 dendrimers was studied in cell culture medium (supplemented with 10% FBS and 1% AA), at pH 7.4 and 37ºC (Figure 41). The idea was to use a medium that simulates the fluid in the physiological environment and, simultaneously, that will allow a direct correlation of the obtained results with the cytotoxicity ones obtained in *in vitro* cell culture experiments. For comparative purposes, *in vitro* DOX release studies were also done in parallel with DOX-loaded PAMAM dendrimers.

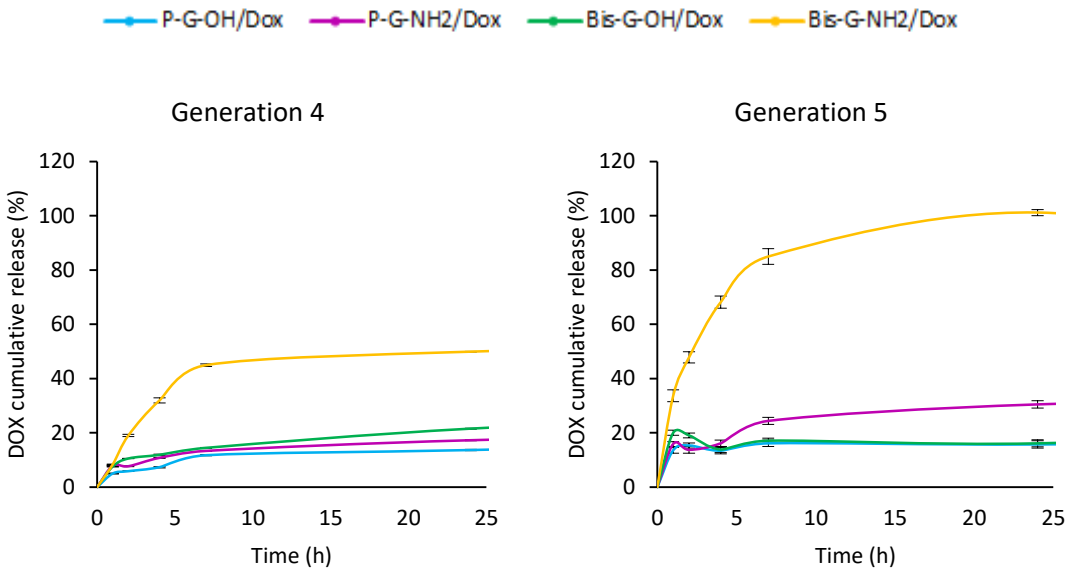

Figure 41. Cumulative release of DOX from bis-MPA-based and PAMAM dendrimers in cell culture media supplemented with 10% FBS and 1% AA (pH 7.4) at 37 ºC. Free DOX was dissolved in HyClone™ Water and released under the same conditions giving a burst release (not shown). All the samples presented the same DOX content. Data is expressed as a percentage of the total amount of DOX content in the samples, mean ± SD (n = 3).

The observation of Figure 41 shows that all the materials presented sustained DOX release profiles, although release was faster in the first hours of the experiments. B-G5-NH_2/DOX dendrimers have a faster release of drug in the first 4 h (~70%) followed by a slow release, achieving about 100% of release after 24 h. The B-G4-NH_2/DOX dendrimers present a more sustained release of DOX as, after a 4 h incubation period, only about 30%, of the drug was released (2.3 times less). All the other dendrimers (B-G4-OH, B-G5-OH, and PAMAM dendrimers) presented similar drug release profiles achieving very low DOX cumulative release values after 24h (between 10 and 25%).

3.4. Cell culture and *in vitro* cell viability assays

The cytotoxicity of the DOX-loaded bis-MPA-based dendrimers and PAMAM dendrimers was assessed by *in vitro* cell culture experiments. For that purpose, the cells were exposed to non-loaded and DOX-loaded dendrimers at increasing DOX concentrations (from 0.1 to 5 µM). After 48h exposure, cell viability was evaluated by measuring their metabolic activity using the resazurin reduction assay. The results are shown in Figure 42 and Figure 43, being expressed as a percentage of cell viability in relation to the control, that is, cells which were not exposed to DOX. Different cell lines were used as cancer cell models, namely an osteosarcoma cell line (CAL-72), a breast adenocarcinoma cell line (MCF-7), and an ovarian carcinoma cell line (A2780). The effect of DOX release over hMSCs was also evaluated since, as mentioned before, these cells have been implicated in supporting tumour growth.[25,26]

In general, the non-loaded bis-MPA-based dendrimers were not cytotoxic for all concentrations studied and for all cell types used. Cytotoxic effects were only observed for generation 5 bis-MPA-based dendrimers when using CAL-72 cells. This is not surprising since it is known that dendrimer cytotoxicity is also dependent on cell type.[6] As widely reported in the literature, the PAMAM dendrimers presented generation and surface functional group-dependent toxicity.[45–50] The PAMAM dendrimers possessing amine groups at the surface, due to their strong cationic nature, were especially cytotoxic, being clear that cell viability decreased with increasing dendrimer concentration. Like the bis-MPA-based dendrimers, in most experiments, the PAMAM dendrimers with hydroxyl terminal groups were not cytotoxic.

As expected, the toxic effect caused by the free drug increased with its concentration. The ovarian cancer cell line A2780 was particularly sensitive to DOX presence. When bis-MPA-based dendrimers were loaded with DOX, the results showed a good correlation with their drug release profiles. The B-G4-NH_2/DOX and the B-G5-NH_2/DOX dendrimers led to a higher cytotoxicity then the B-G4-OH/DOX and the B-G5-OH/DOX dendrimers for which drug was released at a lower rate. So, the bis-MPA-based dendrimers partially functionalized with amine groups at the surface were not intrinsically toxic (due to the reduced number of amine groups) but, when loaded with DOX, led to a

level of toxicity similar to that caused by the free drug. Likely, as good drug carriers, they facilitate the entrance of doxorubicin inside cells. At a long term, however, B-G4-OH/DOX and the B-G5-OH/DOX dendrimers could act as better DOX delivery vectors because of their slow release profile. Also for these loaded dendrimers, toxicity increases with DOX concentration.

Regarding the PAMAM dendrimers, in general, the cytotoxic behaviour of P-G4-OH/DOX and P-G5-OH/DOX was lower than for all other DOX loaded dendrimers. On the contrary, the P-G4-NH_2/DOX and the P-G5-NH_2/DOX dendrimers showed dose-dependent cytotoxicity that should be related with their strong cationic nature, and not to the drug itself, since the extension of DOX release was limited for these dendrimers (Figure 41).

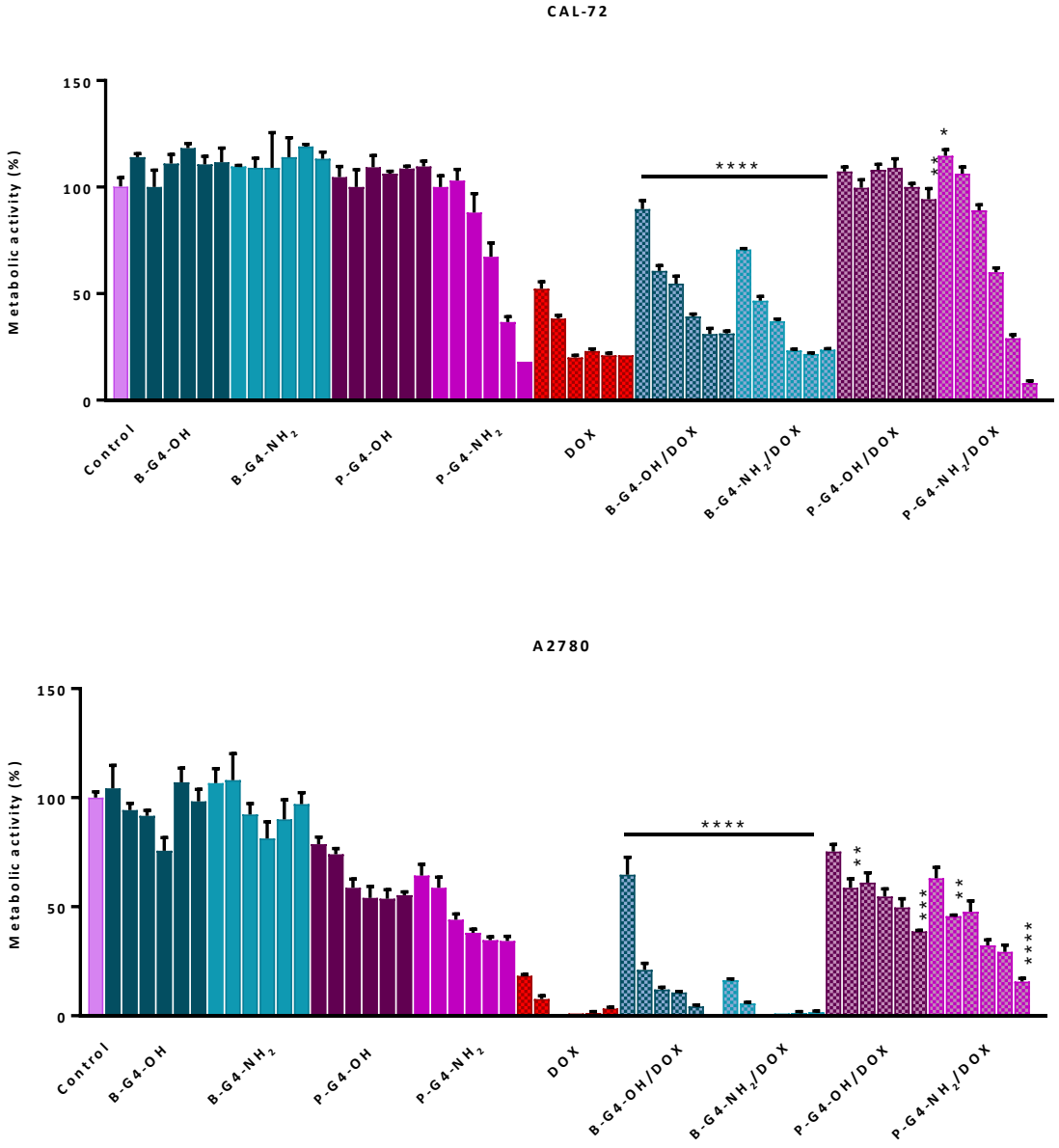

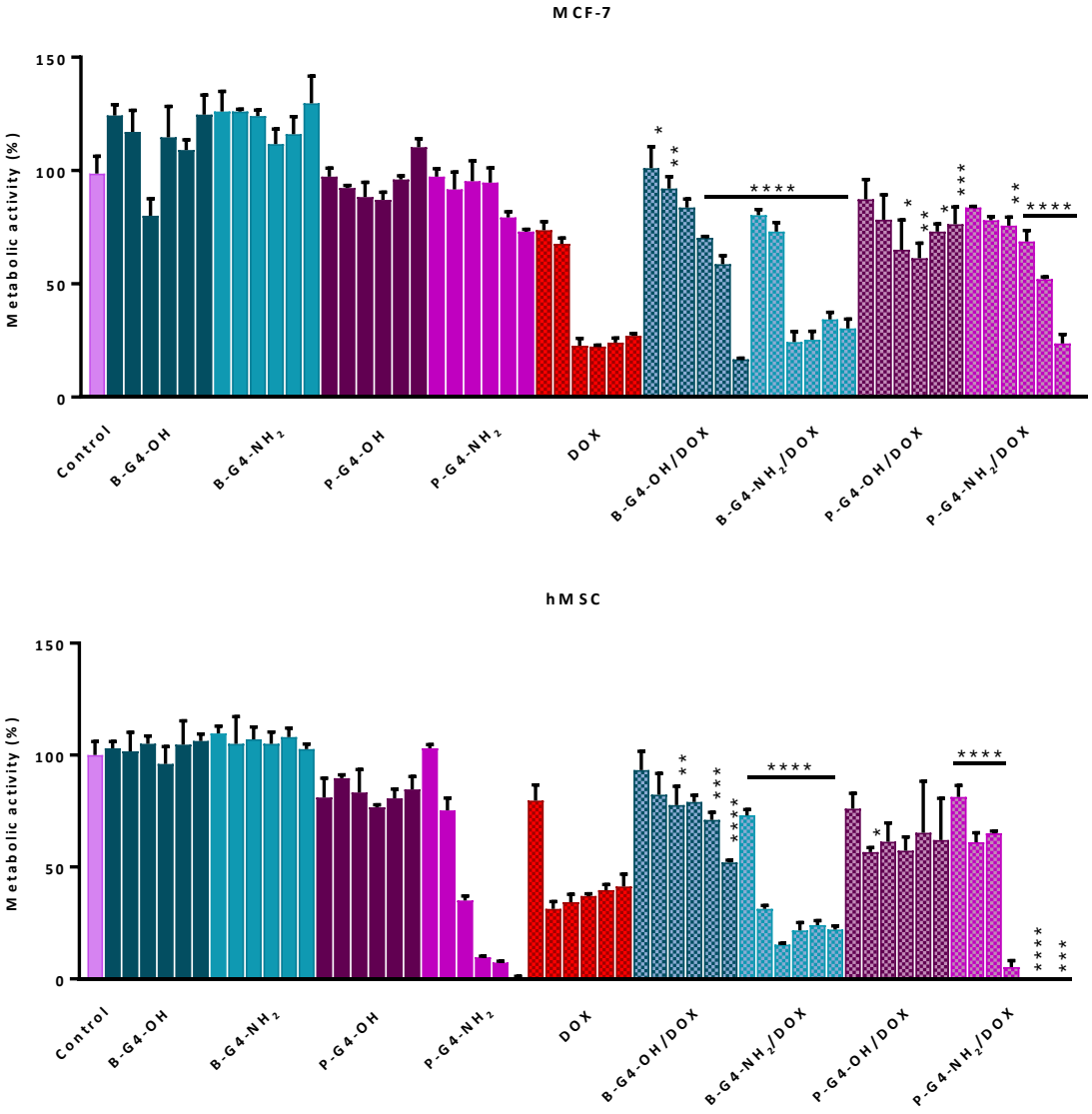

Figure 42. Cell viability of different cancer cell lines (MCF-7, A2780 and CAL-72) and human mesenchymal stem cells (hMSC) after 48 h exposure to the DOX-loaded dendrimers (generation 4, G4) to a range of DOX concentrations (0.1, 0.5, 1, 2, 3 and 5 µM). Free DOX and non-loaded dendrimers were used as controls. Data is expressed by mean ± SD (n = 3). One-way ANOVA with Tukey's Post Hoc test was used to assess the statistical difference between non-loaded dendrimer mean and DOX-loaded dendrimer mean (*p < 0.0332, **p < 0.0021, ***p < 0.002, ****p < 0.001).

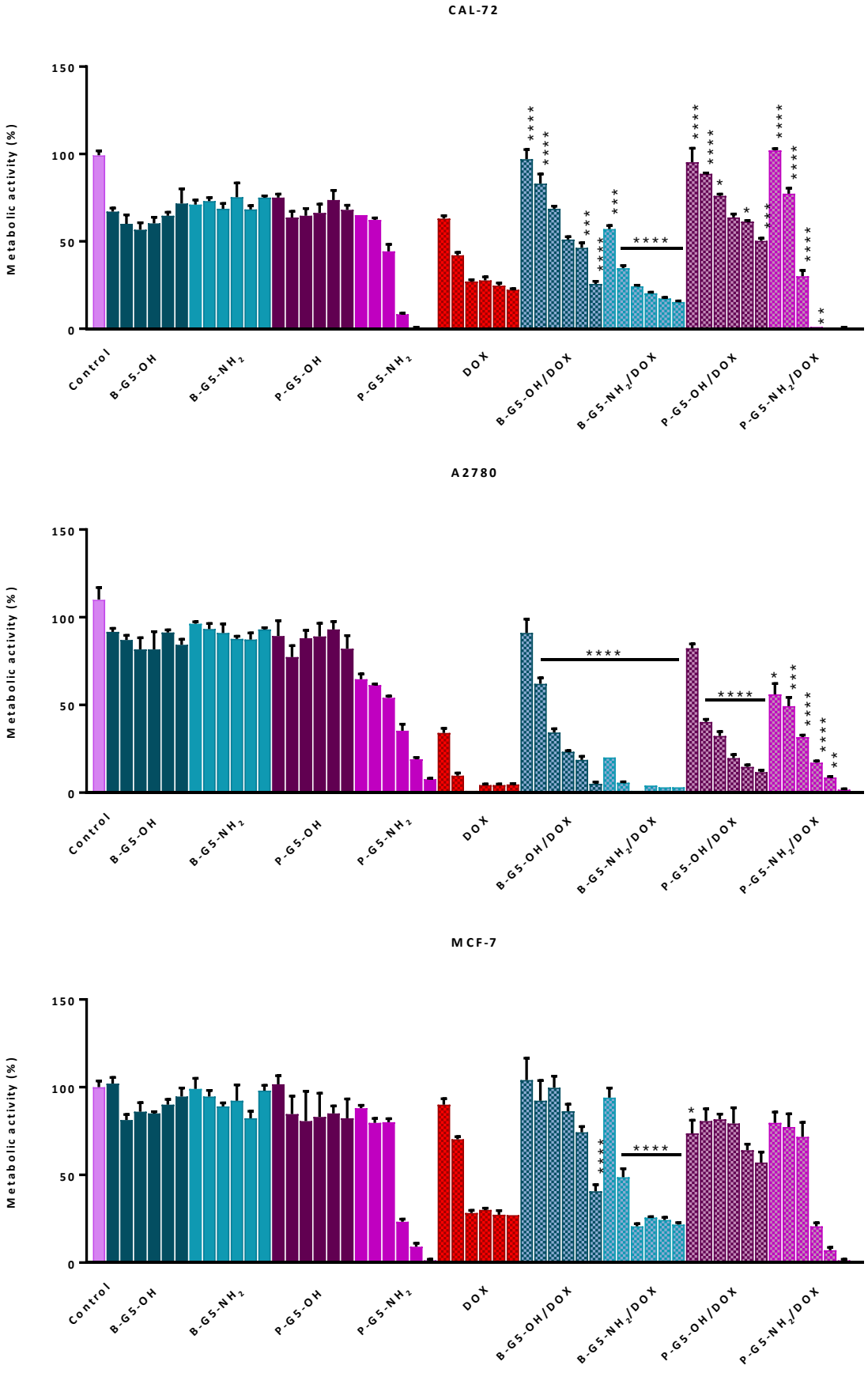
CAL-72
A2780
MCF-7
Metabolic activity (%)
150
100
50
0
Control
B-G5-OH
B-G5-NH2
P-G5-OH
P-G5-NH2
DOX
B-G5-OH/DOX
B-G5-NH2/DOX
P-G5-OH/DOX
P-G5-NH2/DOX

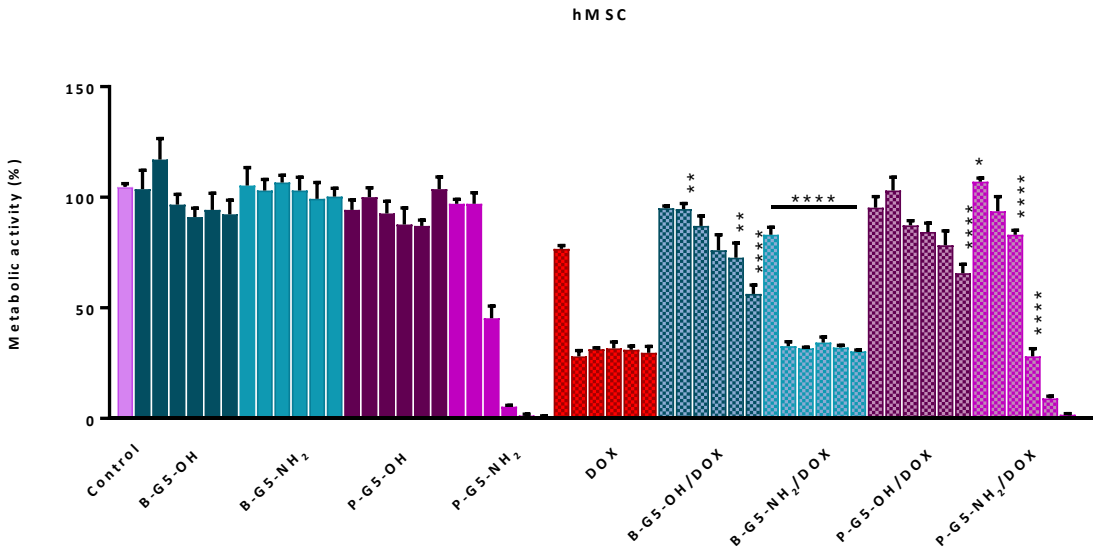

Figure 43. Cell viability of different cancer cell lines (MCF-7, A2780 and CAL-72) and human mesenchymal stem cells (hMSC) after 48 h exposure to the DOX-loaded dendrimers (generation 5, G5) to a range of DOX concentrations (0.1, 0.5, 1, 2, 3 and 5 µM). Free DOX and non-loaded dendrimers were used as controls. Data is expressed by mean ± SD (n = 3). One-way ANOVA with Tukey's Post Hoc test was used to assess the statistical difference between non-loaded dendrimer mean and DOX-loaded dendrimer mean (*p < 0.0332, **p < 0.0021, ***p < 0.002, ****p < 0.001).

The antitumor efficacy of the DOX-loaded dendrimers was further validated by optical fluorescence microscopy. Cell morphology is one of the factors to consider when assessing the effects of drugs (that is, to evaluate if the cells remained healthy or have undergone a death process). Thus, the morphology of the tested cell lines was observed in the inverted microscope after the fixation and staining process. As an example, Figure 44 shows the aspect of the CAL-72 cells after 48 h exposure to DOX-loaded dendrimers. Cells treated with HyClone™ Water and with the non-loaded dendrimers were used as controls. When healthy, cells exhibit a fusiform shape and are adherent to the bottom of the plate. Regarding Figure 44, it is possible to verify that these features were preserved in cells treated with water (Figure 44, A) and also in the ones exposed to the neutral dendrimers. After checking the DOX-treated cells, it is clear that they lost their normal shape, becoming more rounded, starting to detach from the bottom of the well producing cell debris. These findings suggest that probably cells underwent apoptosis.

Since DOX is a fluorescent molecule, its cellular localization can be observed by fluorescence microscopy. After the 48 h incubation period, the cell nuclei were stained with a fluorescent probe (DAPI) and fluorescence pictures were captured. Figure 44 show different intensities of DOX fluorescence according to DOX concentration and uptake. Comparing the cells exposed to the free DOX with the ones exposed to the cationic dendrimers, it is possible to verify that the ones exposed to the

amine-terminated bis-MPA dendrimers exhibit a higher toxicity which suggests an improved therapeutic effect. Moreover, even at the lower concentration, it is possible to observe that the amine-terminated bis-MPA dendrimers exert a much higher effect over the cells. This effect is probably due to the quick release of DOX and also due to the superior DOX cargo carried by the dendrimers.

In general, bringing together the cell morphological results and the quantitative metabolic activity results, it is possible to say that bis-MPA-based dendrimers are promising vehicles for DOX delivery into cancer cells. First, when not loaded with doxorubicin, these dendrimers do not affect the viability of most of the cell types used in these studies. Second, when loaded with the drug, they can efficiently transport the drug to the interior of the cells. After 48h, the B-G4-NH_2/DOX and B-G5-NH_2/DOX dendrimers were the most efficient regarding antitumor activity. However, B-G4-OH/DOX and B-G5-OH/DOX dendrimers show a slower release profile and, likely, will be better drug delivery systems for *in vivo* applications. Previous reports had already evaluated the biodegradability capacity of bis-MPA-based dendrimers when compared to the PAMAM dendrimer family, which is considered an advantage in terms of safety for the human body.[22] In this work, it is further shown that bis-MPA-based dendrimers, independently of containing hydroxyl groups at the surface or be partially surface functionalized with amines, can actually act as DOX delivery vectors.

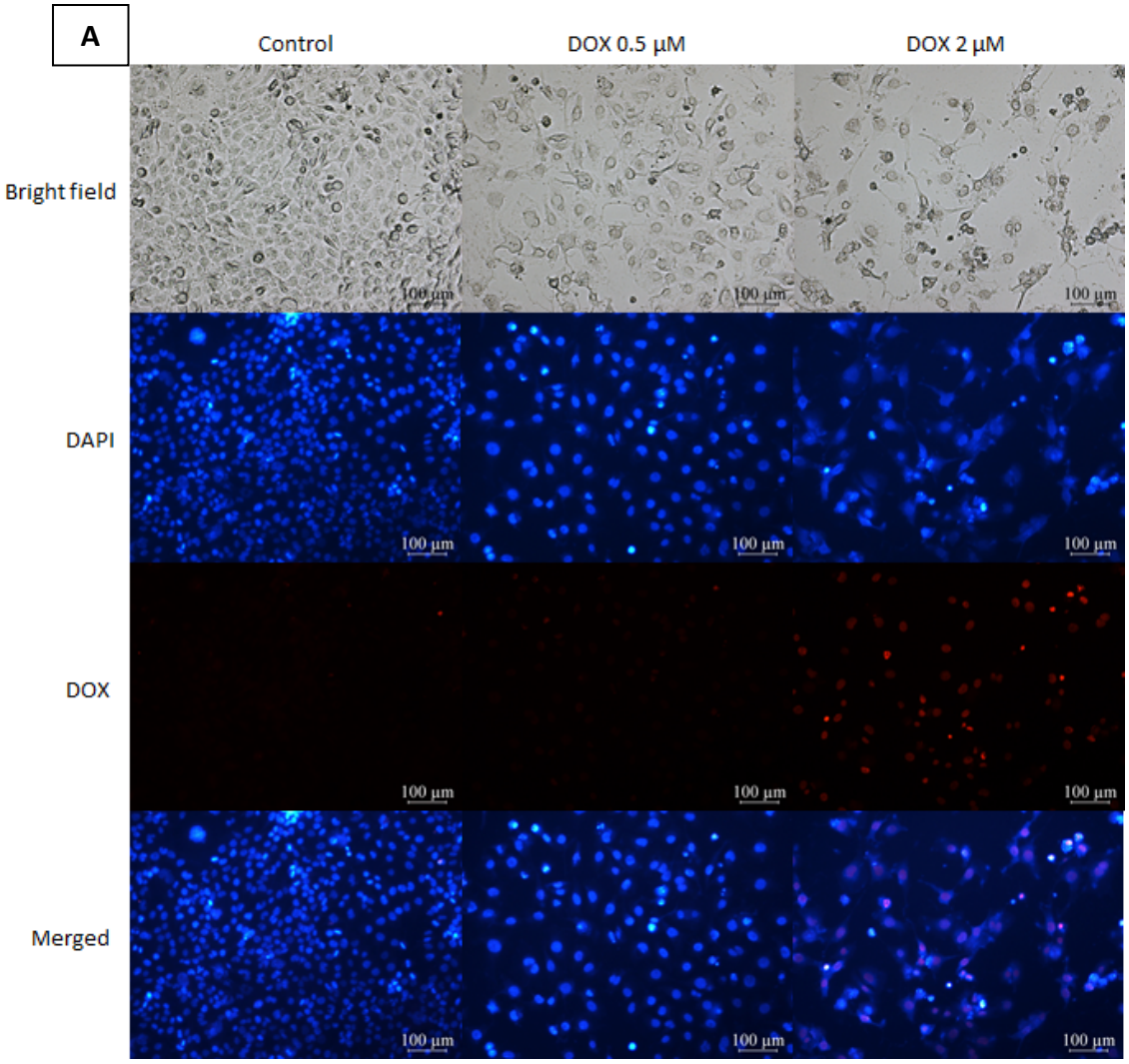
A
Control
DOX 0.5 µM
DOX 2 µM
Bright field
DAPI
DOX
Merged
100 µm

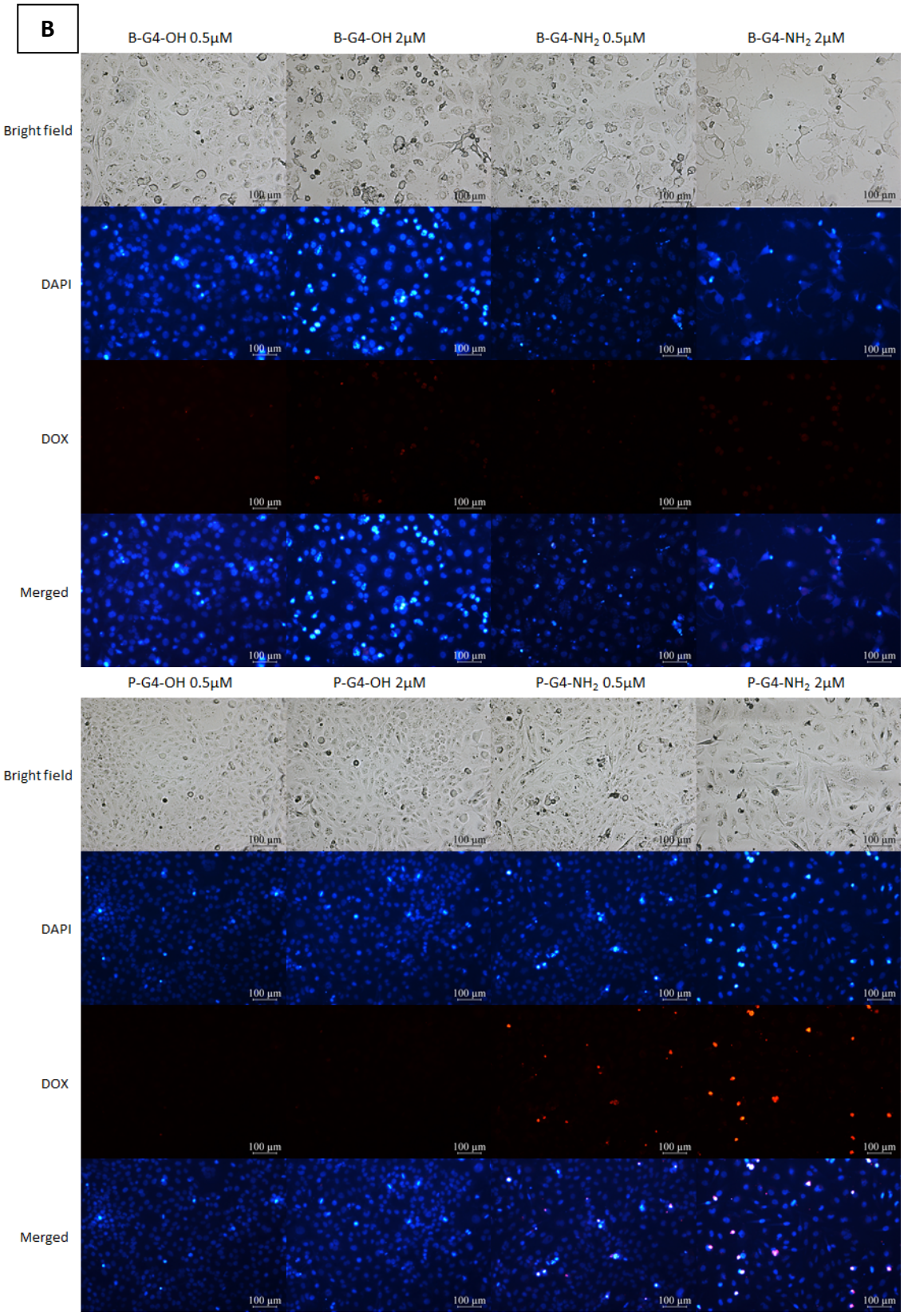
B
B-G4-OH 0.5μM
B-G4-OH 2μM
B-G4-NH2 0.5μM
B-G4-NH2 2μM
Bright field
DAPI
DOX
Merged
P-G4-OH 0.5μM
P-G4-OH 2μM
P-G4-NH2 0.5μM
P-G4-NH2 2μM
Bright field
DAPI
DOX
Merged
100 μm

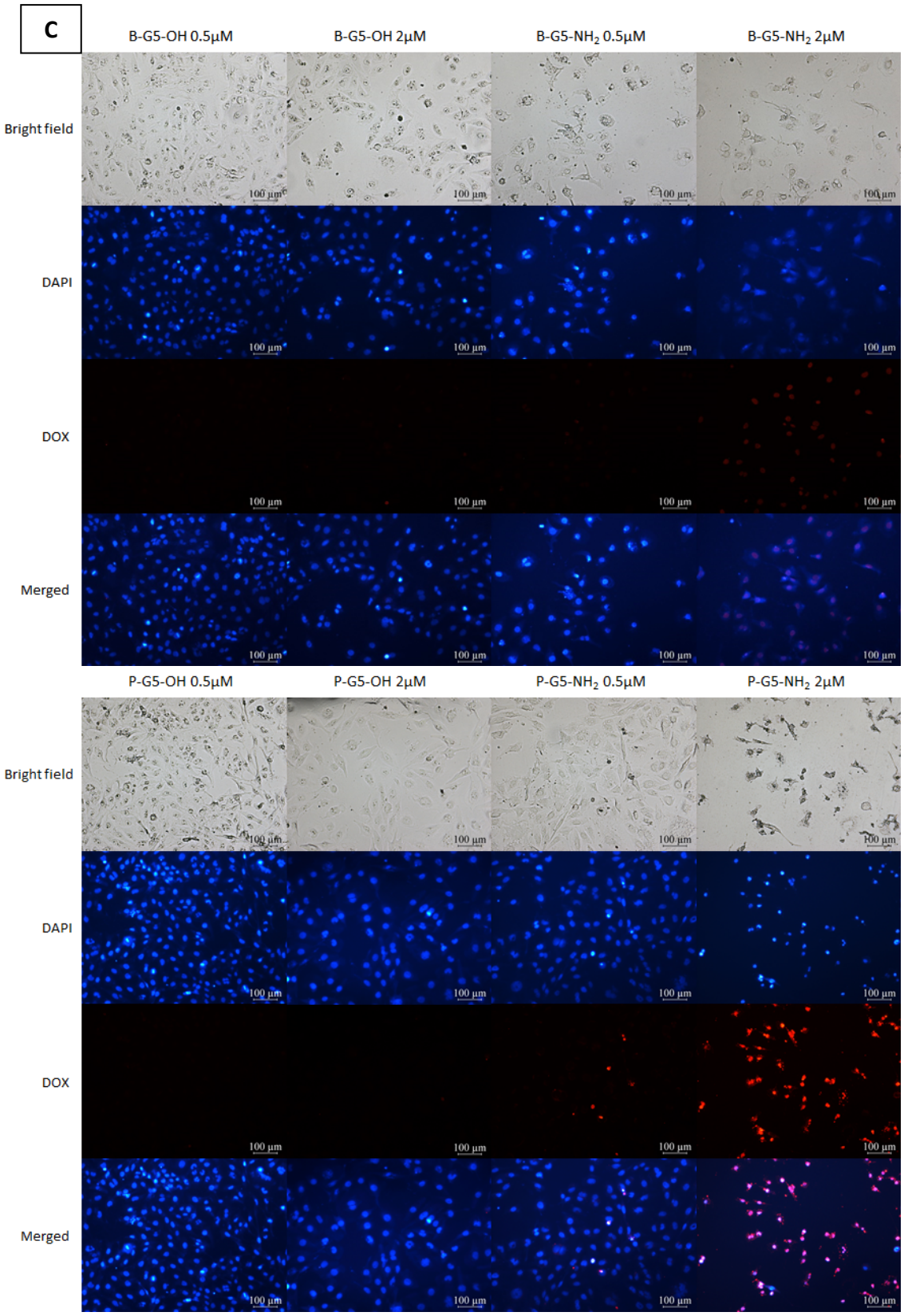

Figure 44. Bright field and fluorescence microscope images of CAL-72 cancer cells after 48 h culture with: A) HyClone™ Water and free DOX (controls); B) DOX-loaded PAMAM and bis-MPA dendrimers (generation 4) and C) DOX-loaded PAMAM and bis-MPA dendrimers (generation 5). The cell nucleus is stained with DAPI (blue fluorescence); DOX gives a red fluorescence signal.

4. Conclusions

Bis-MPA-based dendrimers are becoming popular due to their biodegradability, biocompatibility and commercial availability. The main idea of this work was to study the behaviour of bis-MPA-based dendrimers as doxorubicin delivery vehicles after surface functionalization with amine groups without significantly increasing their cytotoxicity that is, controlling the extent of the functionalization. So, in summary, generation 4 and generation 5 bis-MPA-based dendrimers were, respectively, functionalized at the surface with 38% and 47% of amine groups (as accessed by ^{1}H NMR spectroscopy). When compared with bis-MPA-based dendrimers with hydroxyl surface groups and with PAMAM dendrimers, these dendrimers exhibited higher drug loading capacities but, also, faster initial drug release rates. Indeed, results showed that, when loaded with the drug, after 48h, they were as cytotoxic as the free drug in solution, probably because they facilitate the entrance of doxorubicin inside cells. Nevertheless, the *in vitro* drug release experiments suggested that doxorubicin could be released in a sustained manner using all the evaluated nanocarriers. Indeed, the hydroxyl-terminated bis-MPA dendrimers were considered the most promising candidates for DOX delivery *in vivo* due to their more prolonged and sustained release profile.

Overall, this work suggests that the bis-MPA-based dendrimer family can be used in drug delivery applications. Results also point out that, likely, the drug loading capacity and drug release rate of these dendrimers can be modulated based on the degree of functionalization of the surface with amine groups. More work will be done in a near future to better understand this behaviour, as well as the type of interactions that are established between doxorubicin molecules and bis-MPA-based dendrimers.

References

1 V. S. Saji, H. C. Choe and K. W. K. Yeung, *Int. J. Nano Biomater.*, 2010, **3**, 119–139.

2 G. Chen, I. Roy, C. Yang and P. N. Prasad, *Chem. Rev.*, 2016, **116**, 2826–2885.

3 J. Shi, P. W. Kantoff, R. Wooster and O. C. Farokhzad, *Nat. Rev. Cancer*, 2017, **17**, 20–37.

4 K. E. Uhrich, S. M. Cannizzaro, R. S. Langer and K. M. Shakesheff, *Chem. Rev.*, 1999, **99**, 3181–3198.

5 D. A. Tomalia, H. Baker, J. Dewald, M. Hall, G. Kallos, S. Martin, J. Roeck, J. Ryder and P. Smith, *Polym. J.*, 1985, **17**, 117–132.

6 R. Duncan and L. Izzo, *Adv. Drug Deliv. Rev.*, 2005, **57**, 2215–2237.

7 J. B. Wolinsky and M. W. Grinstaff, *Adv. Drug Deliv. Rev.*, 2008, **60**, 1037–1055.

8 V. K. Yellepeddi, A. Kumar and S. Palakurthi, *Expert Opin. Drug Deliv.*, 2009, **6**, 835–850.

9 V. Mishra, U. Gupta and N. K. Jain, *J. Biomater. Sci.*, 2009, **20**, 141–166.

10 M. A. Mintzer and M. W. Grinstaff, *Chem. Soc. Rev.*, 2011, **40**, 173–190.

11 L.-P. Wu, M. Ficker, J. B. Christensen, P. N. Trohopoulos and S. M. Moghimi, *Bioconjug. Chem.*, 2015, **26**, 1198–1211.

12 H. Ihre, A. Hult and E. Söderlind, *J. Am. Chem. Soc.*, 1996, **118**, 6388–6395.

13 A. Carlmark, E. Malmström and M. Malkoch, *Chem. Soc. Rev.*, 2013, **42**, 5858–5879.

14 J. A. K. Twibanire and T. B. Grindley, *Polymers (Basel).*, 2014, **6**, 179–213.

15 O. L. Padilla De Jesús, H. R. Ihre, L. Gagne, J. M. J. Fréchet and F. C. Szoka, *Bioconjug. Chem.*, 2002, **13**, 453–461.

16 H. R. Ihre, O. L. Padilla de Jesús, F. C. Szoka and J. M. J. Fréchet, *Bioconjug. Chem.*, 2002, **13**, 443–452.

17 R. Reul, J. Nguyen and T. Kissel, *Biomaterials*, 2009, **30**, 5815–5824.

18 X. Zeng, Y. Zhang, Z. Wu, P. Lundberg, M. Malkoch and A. M. Nyström, *J. Polym. Sci. Part A Polym. Chem.*, 2012, **50**, 280–288.

19 J. Movellan, P. Urbán, E. Moles, J. M. de la Fuente, T. Sierra, J. L. Serrano and X. Fernàndez-Busquets, *Biomaterials*, 2014, **35**, 7940–7950.

20 J. Movellan, R. González-Pastor, P. Martín-Duque, T. Sierra, J. M. De La Fuente and J. L. Serrano, *Macromol. Biosci.*, 2015, **15**, 657–667.

21 A. Lancelot, R. González-Pastor, A. Concellón, T. Sierra, P. Martín-Duque and J. L. Serrano, *Bioconjug. Chem.*, 2017, **28**, 1135–1150.

22 N. Feliu, M. V. Walter, M. I. Montañez, A. Kunzmann, A. Hult, A. Nyström, M. Malkoch and B. Fadeel, *Biomaterials*, 2012, **33**, 1970–1981.

23 C. F. Thorn, C. Oshiro, S. Marsh, T. Hernandez-Boussard, H. McLeod, T. E. Klein and R. B. Altman, *Pharmacogenet. Genomics*, 2011, **21**, 440–446.

24 O. Tacar, P. Sriamornsak and C. R. Dass, *J. Pharm. Pharmacol.*, 2013, **65**, 157–170.

25 M. R. Reagan and D. L. Kaplan, *Stem Cells*, 2011, **29**, 920–927.

26 A. I. Chang, A. H. Schwertschkow, J. A. Nolta and J. Wu, *Curr. Cancer Drug Targets*, 2015, **15**, 88–98.

27 K.-J. Rhee, J. I. Lee and Y. W. Eom, *Int. J. Mol. Sci.*, 2015, **16**, 30015–30033.

28 B. P. Khanal and E. R. Zubarev, *Angew. Chemie - Int. Ed.*, 2007, **46**, 2195–2198.

29 H. Wu, H. Zhu, J. Zhuang, S. Yang, C. Liu and Y. C. Cao, *Angew. Chemie - Int. Ed.*, 2008, **47**, 3730–3734.

30 S. L. Snyder and P. Z. Sobocinski, *Anal. Biochem.*, 1975, **64**, 284–288.

31 B. Gyarmati, N. Hegyesi, B. Pukánszky and A. Szilágyi, *Express Polym. Lett.*, 2015, **9**, 154–164.

32 H. Deng, X. Zhao, J. Liu, J. Zhang, L. Deng, J. Liu and A. Dong, *Nanoscale*, 2016, **8**, 1437–1450.

33 D. Maciel, P. Figueira, S. Xiao, D. Hu, X. Shi, J. Rodrigues, H. Tomás and Y. Li, *Biomacromolecules*, 2013, **14**, 3140–3146.

34 S. Wang, Y. Wu, R. Guo, Y. Huang, S. Wen, M. Shen, J. Wang and X. Shi, *Langmuir*, 2013, **29**, 5030–5036.

35 H. Liao, H. Liu, Y. Li, M. Zhang, H. Tomás, M. Shen and X. Shi, *J. Appl. Polym. Sci.*, 2014, **131**, 40358–40368.

36 M. Gonçalves, P. Figueira, D. Maciel, J. Rodrigues, X. Shi, H. Tomás and Y. Li, *Macromol. Biosci.*, 2014, **14**, 110–120.

37 M. Gonçalves, P. Figueira, D. Maciel, J. Rodrigues, X. Qu, C. Liu, H. Tomás and Y. Li, *Acta Biomater.*, 2014, **10**, 300–307.

38 G. Wang, D. Maciel, Y. Wu, J. Rodrigues, X. Shi, Y. Yuan, C. Liu, H. Tomás and Y. Li, *ACS Appl. Mater. Interfaces*, 2014, **6**, 16687–16695.

39 X. He, C. S. Alves, N. Oliveira, J. Rodrigues, J. Zhu, I. Bányai, H. Tomás and X. Shi, *Colloids Surf B Biointerfaces*, 2015, **125**, 82–89.

40 S. Xiao, R. Castro, D. Maciel, M. Gonçalves, X. Shi, J. Rodrigues and H. Tomás, *Mater. Sci. Eng. C*, 2016, **60**, 348–356.

41 A. J. Khopade and F. Caruso, *Biomacromolecules*, 2002, **3**, 1154–1162.

42 Y. Wang, X. Cao, R. Guo, M. Shen, M. Zhang, M. Zhu and X. Shi, *Polym. Chem.*, 2011, **2**, 1754–1760.

43 M. Gonçalves, D. Maciel, D. Capelo, S. Xiao, W. Sun, X. Shi, J. Rodrigues, H. Tomás and Y. Li, *Biomacromolecules*, 2014, **15**, 492–499.

44 X. Zeng, Y. Zhang and A. M. Nyström, *Biomacromolecules*, 2012, **13**, 3814–3822.

45 J. C. Roberts, M. K. Bhalgat and R. T. Zera, *J. Biomed. Mater. Res.*, 1996, **30**, 53–65.

46 N. Malik, R. Wiwattanapatapee, R. Klopsch, K. Lorenz, H. Frey, J. W. Weener, E. W. Meijer, W. Paulus and R. Duncan, *J. Control. Release*, 2000, **65**, 133–148.

47 R. B. Kolhatkar, K. M. Kitchens, P. W. Swaan and H. Ghandehari, *Bioconjug. Chem.*, 2007, **18**, 2054–2060.

48 T. C. King Heiden, E. Dengler, W. J. Kao, W. Heideman and R. E. Peterson, *Toxicol. Appl. Pharmacol.*, 2007, **225**, 70–79.

49 M. Goncalves, R. Castro, J. Rodrigues and H. Tomás, *Curr. Med. Chem.*, 2012, **19**, 4969–4975.

50 L. Bodewein, F. Schmelter, S. Di Fiore, H. Hollert, R. Fischer and M. Fenske, *Toxicol. Appl. Pharmacol.*, 2016, **305**, 83–92.

Supplementary material

Table S1. Quantities of materials and reagents used for bis-MPA dendrimer surface modification.

Materials	MW, g/mol	n, mol	mass, g
B-G4-OH	5338.3	4.35E-05	0.2321
BOC-Gly-OH	175.18	4.17E-03	0.7351
DPTS	294.37	8.35E-04	0.2494
DCC	206.33	3.13E-03	0.6642
B-G5-OH	10932.9	2.31E-05	0.2527
BOC-Gly-OH	175.18	4.44E-03	0.7977
DPTS	294.37	8.88E-04	0.2889
DCC	206.33	3.33E-03	0.7100

Table S2. Quantities of dendrimers and DOX used for the loading process.

Sample	Dendrimer		DOX	
	n, mol	**Final Conc., mM**	**n, mol**	**Final Conc., mM**
P-G4-OH	1.751E-06	0.318	8.755E-06	1.592
P-G4-NH_2	1.759E-06	0.320	8.794E-06	1.599
B-G4-OH	4.683E-06	0.851	2.342E-05	4.258
B-G4-NH_2	3.087E-06	0.561	1.544E-05	2.807
P-G5-OH	1.209E-06	0.300	6.044E-06	1.501
P-G5-NH_2	9.922E-07	0.302	4.961E-06	1.508
B-G5-OH	3.659E-06	0.803	1.829E-05	4.015
B-G5-NH_2	2.217E-06	0.529	1.108E-05	2.647

Characterization of B-G4-NH_2 and B-G5-NH_2 dendrimers

The partially-modified bis-MPA dendrimers with amine termini were characterized by ^{1}H NMR (400 MHz), using D_2O as solvent. The peak integration was made considering one of the characteristic proton peaks of the bis-MPA dendrimer (δ ≈ 4.46 to 4.28). For both dendrimer generations, the successful surface modification with amine groups is represented by the appearance of a new proton signal at δ = 4.04 ppm (-C*H*$_2$NH$_2$).

- B-G4-OH

^{1}H NMR (D_2O, 400 MHz) δ (ppm): 4.46-4.28 (90.00 H), 3.81-3.69 (98.28 H), 1.69 (2.20 H), 1.45-1.40 (60.94 H), 1.23 (71.47 H) and 1.07-1.04 (3.87 H).

- B-G4-NH_2

^{1}H NMR (D_2O, 400 MHz) δ (ppm): 4.49-4.33 (90.00 H), 4.04 (36.16 H), 3.86 (19.38 H), 3.75-3.66 (21.63 H), 1.40-1.32 (58.39 H) and 1.24-1.18 (26.85 H).

- B-G5-OH

^{1}H NMR (D_2O, 400 MHz) δ (ppm): 4.40-4.32 (186.00 H), 3.77-3.65 (200.00 H), 1.36 (136.24 H) and 1.19 (150.28 H).

- B-G5-NH2

^{1}H NMR (D_2O, 400 MHz) δ (ppm): 4.53-4.40 (186.00 H), 4.12-4.09 (89.90 H), 3.90 (14.94 H), 3.76 (17.13 H), 1.39 (127.07 H) and 1.26 (22.83 H)

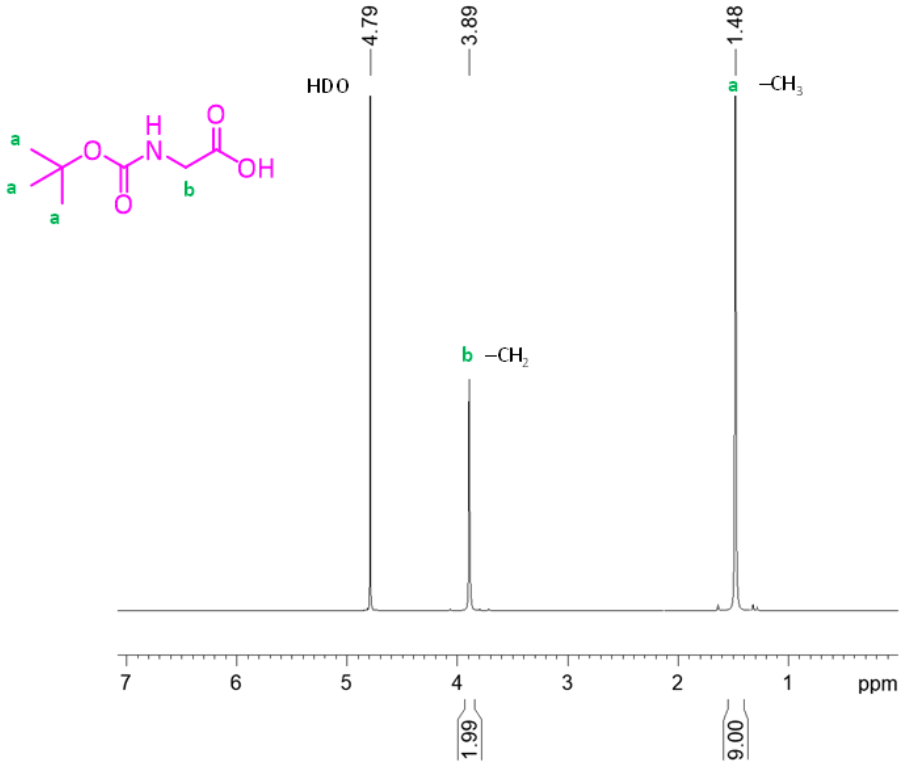

Figure S1. ^{1}H NMR spectra (400 MHz, in D_2O) of BOC-Gly-OH.

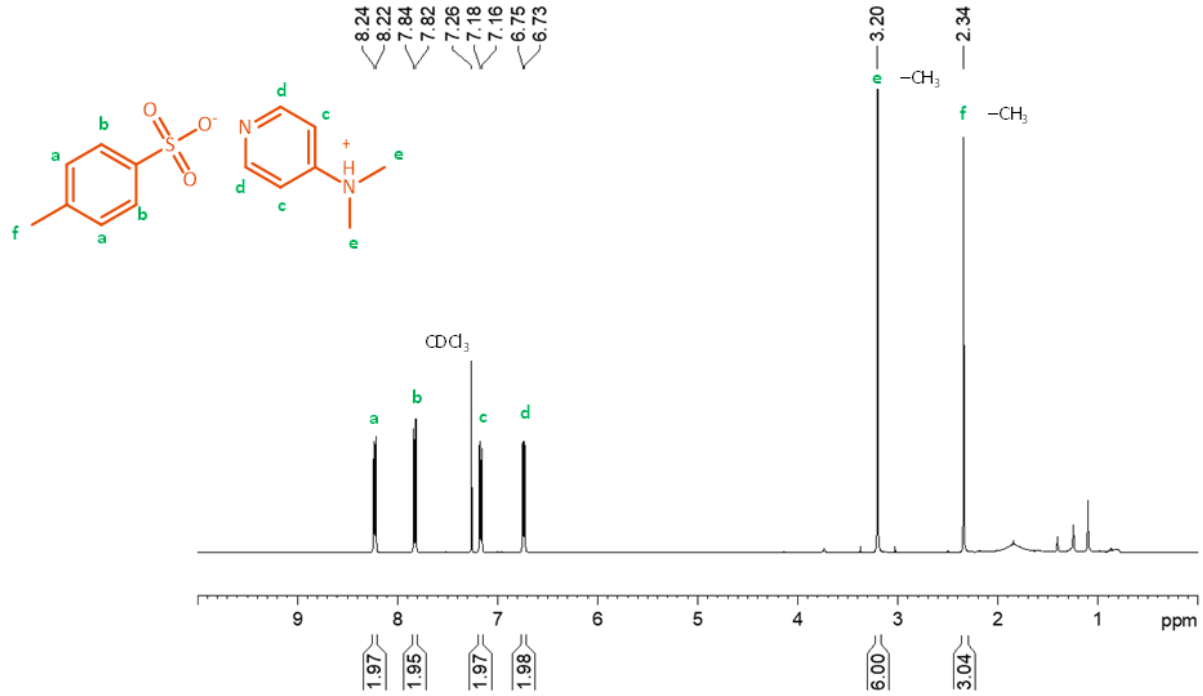

Figure S2. ^{1}H NMR spectra (400 MHz, in D_2O) of DPTS.

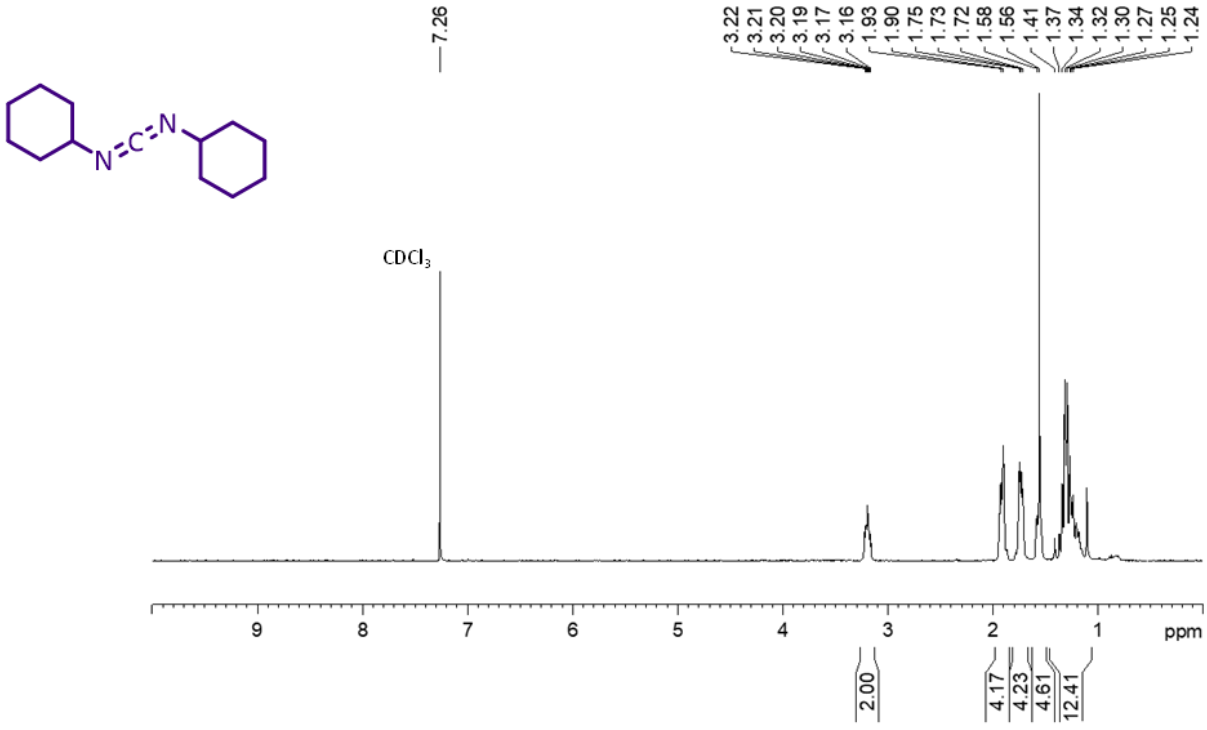

Figure S3. ^{1}H NMR spectra (400 MHz, in D_2O) of DCC.

Conclusions

Nowadays much of cancer nanomedicine research is focused on the design of new drug delivery systems for the transport and delivery of conventional anticancer drugs, thus improving their efficacy and reducing their side effects. Doxorubicin is an antitumor drug widely used as first-line treatment due to its broad spectrum of activity. Also, this drug is associated with several secondary effects, being cardiac failure the most common. Several strategies are thus currently under laboratory and clinical investigation in order to suppress these weaknesses. Currently, there are a few doxorubicin-based nanotherapeutics already in the market (in clinical use), some under clinical trials and numerous still in laboratory research.

The main goal of this thesis was to design new nanocarrier systems based on different nanomaterials with the purpose of delivering the anticancer drug doxorubicin.

In a first approach, a macroscale hybrid hydrogel based on Laponite® and alginate crosslinked with calcium cations was prepared and loaded with doxorubicin. Throughout the degradation process, this hybrid hydrogel gives rise to new nanohybrids, which serve as shuttles for doxorubicin cell uptake. Overall, results show that the incorporation of Laponite® leads to an increase in gel stability, and also to a more controlled and sustained drug release. The *in vitro* cytotoxicity revealed that there is no toxicity associated with the material itself being this effect just related with the therapeutic effect of doxorubicin.

Subsequently, based on previous works of our group, we have developed a new type of Laponite®-based nanohybrids. Fundamentally, the doxorubicin was loaded onto the Laponite® disks by electrostatic interactions and, later on, these complexes were coated with alginate. According to the results, this system presents a high sustainable and controlled drug release with pH sensitivity. Moreover, the *in vitro* cytotoxicity was superior to the equivalent concentration of free doxorubicin and not related to the material itself.

Finally, biodegradable dendrimers based on 2,2-bis(hydroxymethyl) propanoic acid (bis-MPA) were studied as drug delivery systems for doxorubicin. It was demonstrated that bis-MPA-based dendrimers partially functionalized at the surface with amine groups exhibit a high capacity to accommodate doxorubicin molecules (high drug cargo) but presented a faster initial drug release rate. Likely, due to their more sustained drug release profile, bis-MPA-based dendrimers constitute better

systems to be used *in vivo*. Very important, the *in vitro* cell culture results proved that the bis-MPA dendrimer family is quite biocompatible, including the dendrimers partially functionalized at the surface with amine groups.

In conclusion, several nanocarriers were developed in the scope of this thesis that showed good cytocompatibility, capacity to be loaded with doxorubicin and sustained/controlled drug release profiles. Using *in vitro* cell culture experiments, they served as efficient shuttles for doxorubicin and were able to kill cancer cells. For the future, it will be necessary to test these systems *in vivo* to evaluate their actual feasibility as doxorubicin nanocarriers.

CENTRO DE QUÍMICA DA MADEIRA

UNIVERSIDADE da MADEIRA

FCT Fundação para a Ciência e a Tecnologia
MINISTÉRIO DA CIÊNCIA, TECNOLOGIA E ENSINO SUPERIOR

PEst-OE/QUI/UI0674/2013
PTDC/CTM-NAN/116788/2010
Ph.D. grant SFRH/BD/88721/2012 (M. Gonçalves)

arditi agência regional para o desenvolvimento da investigação tecnologia e inovação

Project M1420-01-0145-FEDER-000005-CQM+

MADEIRA 14-20 REGIÃO AUTÓNOMA DA MADEIRA PORTUGAL 2020 UNIÃO EUROPEIA Fundo Social Europeu

Project PROEQUIPRAM - M1420-01-0145-FEDER-000008

A Nossa Universidade

Colégio dos Jesuítas
Rua dos Ferreiros - 9000-082, Funchal

Tel: +351 291 209400
Fax: +351 291 209410
Email: gabinetedareitoria@uma.pt

FCT
Fundação para a Ciência e a Tecnologia
MINISTÉRIO DA EDUCAÇÃO E CIÊNCIA